



# MONASH University

***On the carbon dynamics of Australian subalpine grasslands***

*Ian McHugh*

*BSc (hons)*

A thesis submitted for the degree of *Doctor of Philosophy* at

Monash University in 2016

(School of Earth, Atmosphere and Environment)

## Copyright notice

© Ian McHugh (2016). Except as provided in the Copyright Act 1968, this thesis may not be reproduced in any form without the written permission of the author.

*I certify that I have made all reasonable efforts to secure copyright permissions for third-party content included in this thesis and have not knowingly added copyright content to my work without the owner's permission.*

## Abstract

Grasslands in the alpine and subalpine tracts of the Australian southeast occupy a small area but store substantial quantities of soil carbon, which is likely to be affected as climate change shifts the balance between processes of ecosystem carbon import and export. In order to investigate the effects of differences in climate on carbon balance in subalpine grassland ecosystems, eddy covariance instrumentation was established at two climatologically contrasting sites during 2007/08: a cooler, wetter site that sustains winter snow cover (Dargo), and a warmer, drier site that does not (Nimmo). Both were substantial carbon sinks in 2007 and 2008;  $93.0$  and  $111.4 \text{ gC m}^{-2} \text{ a}^{-1}$  for Dargo, respectively, and  $203.8$  and  $322.0 \text{ gC m}^{-2} \text{ a}^{-1}$  for Nimmo. Differences in annual carbon uptake were mainly contributed by photosynthetic rather than respiratory fluxes, largely in association with temperature differences, which had two main effects. First, the retention of snow (and associated cessation of photosynthesis) reduced winter gross primary production (GPP) at Dargo. Second, since both sites showed effectively the same temperature-normalised bulk canopy photosynthetic response, GPP was generally lower at the cooler Dargo. Both sites were also subject to drought (severe regional drought conditions during 2006 continued into early 2007), resulting in the observed lower carbon uptake in 2007. The cross-year NEE difference was reduced at Dargo because increased GPP during the wetter summer of 2008 (also observed at Nimmo) was offset by decreased GPP during the cooler winter – and associated longer, later-lying snow season – of 2008. Since the co-occurrence of warm, dry or cool, wet conditions are characteristic of the dominant mode of regional climate variability, ENSO, this suggests that snow cover may moderate the interannual amplitude of NEE variability in these ecosystems. Superimposed on this, however, are expected longer-term changes in carbon storage. Consistent with globally observed soil carbon / climate relationships, soil carbon storage was almost 50% higher at Dargo ( $19.4 \text{ kgC m}^{-2}$ ) relative to Nimmo ( $13.4 \text{ kgC m}^{-2}$ ). On the basis of such relationships, warming and drying would be expected to result in reductions in soil carbon, particularly at Dargo, where the cool, moist conditions presently limit decomposition and thus maximise storage of labile soil carbon. While losses of soil carbon may be partially offset by the effects of warming on plant growth, both structural limitations on carbon sequestration in grassland vegetation and the slow expected rate of succession towards woody functional plant groups suggest that net carbon losses are likely in coming decades.

## Declaration

This thesis contains no material which has been accepted for the award of any other degree or diploma at any university or equivalent institution and that, to the best of my knowledge and belief, this thesis contains no material previously published or written by another person, except where due reference is made in the text of the thesis.



---

Ian McHugh



## Acknowledgements

I would like to thank my main supervisor, Professor Jason Beringer for his academic guidance, general support and friendship during what has been a long and difficult process, and for his faith in me when I lacked it in myself. I would also like to thank my secondary supervisors, Professors Nigel Tapper and Marks Adams for their academic contribution and support. I also owe a great debt to project technician Michael Kemp, who was crucial to the establishment and maintenance of the research sites that form the basis of this work. His role was often conducted under difficult conditions (sub-zero temperatures, snow storms, thunderstorms, marauding bovines) but always with good humour (and occasional bad language). I would also like to acknowledge the provision of financial support for this project by the Bushfire CRC (now Bushfire and Natural Hazards CRC).

For her tireless emotional support, and also for her faith in me when I lacked it in myself, I am forever thankful to my partner and now wife, Matthia Dempsey. Even if academia has sometimes been difficult during the day, it has always been a pleasure to go home at night. Only more so with the arrival of my children.

# Table of Contents

<b>LIST OF FIGURES.....</b>	<b>VIII</b>
<b>LIST OF TABLES .....</b>	<b>XII</b>
<b>1. INTRODUCTION .....</b>	<b>1</b>
1.1 PRELUDE .....	1
1.2 RESEARCH CONTEXT .....	1
1.2.1 <i>Mountain ecosystems in a changing climate</i> .....	1
1.2.2 <i>Ecosystem function, carbon dynamics and climate</i> .....	3
1.2.3 <i>Ecosystem carbon balance and climate change</i> .....	5
1.2.4 <i>The Australian High Country and Climate Change</i> .....	7
1.3 RATIONALE, AIMS AND APPROACH .....	9
1.3.1 <i>Rationale</i> .....	9
1.3.2 <i>Research focus and aims</i> .....	10
1.3.3 <i>Approach</i> .....	12
1.4 SCOPE .....	14
1.4.1 <i>Temporal scale</i> .....	14
1.4.2 <i>Spatial scale</i> .....	14
1.5 LINKAGES .....	15
1.5.1 <i>HighFire and the High Country Fuels and Ecosystem Function (HCFEF) Project</i> .....	15
1.5.2 <i>Fluxnet and Ozflux</i> .....	15
1.6 THESIS OUTLINE .....	16
1.7 CONVENTIONS .....	16
<b>2. LITERATURE REVIEW .....</b>	<b>17</b>
2.1 INTRODUCTION .....	17
2.2 SUBALPINE GRASSLAND ECOSYSTEMS .....	17
2.2.1 <i>Definition</i> .....	17
2.2.2 <i>Geography</i> .....	18
2.2.3 <i>Climate</i> .....	19
2.2.4 <i>Vegetation</i> .....	21
2.2.5 <i>Soils</i> .....	23
2.3 ECOSYSTEM CARBON STORAGE .....	24
2.3.1 <i>Vegetation</i> .....	25
2.3.2 <i>Soils</i> .....	27
2.4 ECOSYSTEM CARBON BALANCE .....	31

2.4.1	<i>Conceptual overview</i> .....	31
2.4.2	<i>Primary controls of gross primary production (GPP)</i> .....	34
2.4.3	<i>Primary controls of ecosystem respiration (<math>R_e</math>)</i> .....	39
2.4.4	<i>Estimates of annual carbon balance among alpine grassland ecosystems</i> .....	43
2.4.5	<i>Interactive controls on carbon balance of alpine grassland ecosystems</i> .....	48
2.5	THE EDDY COVARIANCE TECHNIQUE .....	55
2.5.1	<i>Basic theory</i> .....	55
2.5.2	<i>Key Assumptions</i> .....	57
2.5.3	<i>Corrections</i> .....	60
2.5.4	<i>Uncertainties</i> .....	64
2.6	SUMMARY .....	71
<b>3.</b>	<b>SITE SELECTION AND METHODOLOGY .....</b>	<b>72</b>
3.1	INTRODUCTION .....	72
3.2	SITE DESCRIPTIONS .....	73
3.2.1	<i>Dargo</i> .....	75
3.2.2	<i>Nimmo</i> .....	77
3.3	SITE INSTRUMENTATION .....	79
3.3.1	<i>Micrometeorological installation</i> .....	79
3.3.2	<i>Chamber system</i> .....	83
3.4	POST-PROCESSING OF EDDY COVARIANCE DATA .....	86
3.4.1	<i>Raw data processing</i> .....	87
3.4.2	<i>Quality assurance</i> .....	91
3.4.3	<i>Passive evaluation</i> .....	98
3.5	IMPUTATION OF FLUX AND METEOROLOGICAL DATA .....	99
3.5.1	<i>CO<sub>2</sub> fluxes</i> .....	99
3.5.2	<i>Meteorological drivers</i> .....	103
3.6	FLUX UNCERTAINTY ANALYSIS .....	105
3.6.1	<i>Systematic error</i> .....	105
3.6.2	<i>Model error</i> .....	106
3.6.3	<i>Random error</i> .....	107
3.7	FLUX PARTITIONING AND DATA ANALYSIS .....	109
3.7.1	<i>Ecosystem respiration model</i> .....	109
3.7.2	<i>Gross primary production model</i> .....	111
3.7.3	<i>Growing season index model</i> .....	113
3.8	VEGETATION AND SOIL SAMPLING .....	115
3.8.1	<i>Vegetation</i> .....	115
3.8.2	<i>Soils</i> .....	115

<b>4.</b>	<b>DATA QUALITY ANALYSIS .....</b>	<b>117</b>
4.1	INTRODUCTION .....	117
4.1	DATA RETENTION .....	118
4.2	SYSTEMATIC MEASUREMENT ERROR .....	120
4.2.1	<i>Surface energy balance closure .....</i>	<i>121</i>
4.2.2	<i>Nocturnal CO<sub>2</sub> flux underestimation .....</i>	<i>134</i>
4.3	RANDOM ERROR .....	144
4.4	MODEL ERROR .....	147
4.5	UNCERTAINTY ANALYSIS .....	150
4.6	SUMMARY .....	152
<b>5.</b>	<b>SITE METEOROLOGICAL CHARACTERISTICS.....</b>	<b>154</b>
5.1	INTRODUCTION .....	154
5.2	SOLAR RADIATION.....	155
5.3	TEMPERATURE .....	158
5.3.1	<i>Air temperature.....</i>	<i>158</i>
5.3.2	<i>Soil temperature.....</i>	<i>161</i>
5.4	MOISTURE AVAILABILITY.....	165
5.4.1	<i>Precipitation.....</i>	<i>165</i>
5.4.2	<i>Humidity.....</i>	<i>168</i>
5.4.3	<i>Evapotranspiration.....</i>	<i>169</i>
5.4.4	<i>Soil moisture.....</i>	<i>170</i>
5.5	SUMMARY .....	173
<b>6.</b>	<b>ECOSYSTEM CARBON STORAGE.....</b>	<b>174</b>
6.1	INTRODUCTION .....	174
6.2	SOILS .....	175
6.3	VEGETATION .....	180
6.4	TOTAL ECOSYSTEM CARBON STORAGE .....	183
6.5	SUMMARY .....	184
<b>7.</b>	<b>ECOSYSTEM CARBON EXCHANGE .....</b>	<b>187</b>
7.1	INTRODUCTION .....	187
7.2	ANNUAL CARBON BALANCE .....	188
7.2.1	<i>NEE .....</i>	<i>188</i>
7.2.2	<i>Ecosystem respiration (<math>R_e</math>) and gross primary production (GPP) .....</i>	<i>190</i>
7.3	SEASONAL CARBON BALANCE DYNAMICS .....	194
7.3.1	<i>Summer (JFM) .....</i>	<i>194</i>
7.3.2	<i>Autumn (AMJ) .....</i>	<i>199</i>

7.3.3	Winter (JAS).....	200
7.3.4	Spring (OND) .....	204
7.4	CONTROLS ON CARBON BALANCE DYNAMICS.....	206
7.4.1	Ecosystem respiration ( $R_e$ ) .....	206
7.4.2	Gross Primary Production (GPP).....	215
7.5	SUMMARY .....	234
<b>8.</b>	<b>RECONCILING PATTERNS OF CARBON STORAGE AND EXCHANGE .....</b>	<b>236</b>
8.1	EFFECTS OF CLIMATE VARIABILITY.....	237
8.2	SYSTEMATIC MEASUREMENT ERROR .....	241
8.3	UNMEASURED COMPONENTS OF ECOSYSTEM CARBON BALANCE .....	242
8.3.1	Emission of non-CO <sub>2</sub> carbon species .....	242
8.3.2	Non-atmospheric transfer.....	242
8.3.3	Grazing effects .....	243
8.3.4	Low-frequency / high-impact events .....	244
8.4	CLIMATE CHANGE .....	245
8.5	SUMMARY .....	246
<b>9.</b>	<b>CONCLUSIONS .....</b>	<b>247</b>
9.1	RECAPITULATION OF OBJECTIVES AND FINDINGS .....	247
9.2	IMPLICATIONS OF FUTURE CLIMATE CHANGE .....	250
9.3	RELEVANCE, LIMITATIONS AND SCOPE FOR FURTHER INVESTIGATION .....	252
<b>10.</b>	<b>REFERENCES .....</b>	<b>255</b>

# List of Figures

---

Figure 2.1: distribution of Australia's alpine and sub-alpine regions .....	18
Figure 2.2: zonation and physical characteristics of the mainland Australian High Country .....	19
Figure 2.3: generalised east-west topographic/precipitation cross section at approximately S36°30' .....	20
Figure 2.4: subalpine grassland on Dargo High Plains. ....	21
Figure 2.5: daytime land surface temperatures across a Swiss Alps elevational transect .....	22
Figure 2.6: typical landscape / vegetation association and vertical structure of Australian alpine humus soils..	23
Figure 2.7: contours of soil organic carbon density superimposed on Holdridge (1947) world life zones .....	27
Figure 2.8: ecosystem carbon balance .....	33
Figure 2.9: a) relationship between published values of ecosystem respiration ( $R_e$ ) and gross primary production (GPP); b) impact of length of growing season on NEE from published values.....	46
Figure 2.10: relationship between annual NEE and mean annual temperature among primarily temperature- limited ecosystems in the Fluxnet database.....	47
Figure 2.11: relationship between annual $R_e$ and soil temperature.....	47
Figure 2.12: annual average change in global ambient CO <sub>2</sub> concentration (black series) superimposed on variations in Southern Oscillation Index (SOI; brown represents negative phase and blue represents positive phase) .....	51
Figure 2.13: Cartesian control volume over homogeneous terrain.....	58
Figure 2.14: undamped (solid line) and damped (dashed line) cospectra, indicating progressively increasing losses for higher frequency distributions corresponding to decreasing measurement height .....	61
Figure 2.15: schematic representation of error categories .....	66
Figure 3.1: locations of Dargo and Nimmo study sites. ....	74
Figure 3.2: topographic representation of Dargo High Plains site.....	76
Figure 3.3: topographic representation of Nimmo Plain site.....	78
Figure 3.4: general instrument deployment .....	79
Figure 3.5: deployment of sensors to measure soil heat flux .....	81
Figure 3.6: manual portable chamber system and permanent collars 1-14 at Dargo. ....	84
Figure 3.7: sample chamber incubation .....	85

Figure 3.8: flux data processing and quality assurance procedure .....	86
Figure 3.9: flow chart of EdiRe processing procedure to generate raw half-hourly flux estimates .....	87
Figure 3.10: ideal orientation of sonic anemometer relative to prevailing wind .....	95
Figure 3.11: generic 5-6-1 multi-layer perceptron (MLP) neural network architecture .....	101
Figure 4.1: seasonal distribution of data coverage .....	118
Figure 4.2: Percentage of available and acceptable raw C flux data remaining after application of QC criteria	119
Figure 4.3: energy balance closure at Dargo.....	122
Figure 4.4: mean diurnal energy balance ( $\pm$ SE) for Dargo site .....	123
Figure 4.5: relative and absolute energy balance closure as a function of friction velocity ( $u^*$ ) at Dargo. ....	125
Figure 4.6: Ogive plots of kinematic heat flux.....	127
Figure 4.7: a) half-hourly composite absolute energy balance residual as a function of available energy; b) comparison of hysteresis and approximated magnitude of biomass enthalpy change .....	129
Figure 4.8: a) Dargo site regression of cumulative daily sensible and latent heat fluxes on available energy; b) mean diurnal half hourly average and cumulative energy fluxes .....	130
Figure 4.9: diurnal average ( $\pm$ SE) for Dargo of: a) soil heat flux (G) and absolute EB deficit; b) soil heat flux components.....	131
Figure 4.10: friction velocity ( $u^*$ ) and applicable thresholds for six temperature classes .....	136
Figure 4.11: a) 2007/08 time series of nocturnally- and daytime-derived ecosystem respiration ( $R_e$ ) for Dargo site; b) least squares regression of LRF- on nocturnal- $R_e$ .....	137
Figure 4.12: comparison of Lloyd and Taylor temperature response functions fitted to nocturnal- and LRF- $R_e$ for Dargo site. ....	138
Figure 4.13: monthly mean diurnal respiration calculated from L&T function and soil temperatures using daytime and nocturnal best-fit parameters .....	139
Figure 4.14: comparison of $R_e$ from chamber measurements with $R_e$ estimated from Lloyd and Taylor (L&T) function parameterised using 2008 nocturnal eddy covariance data from Dargo site .....	141
Figure 4.15: a) frequency distribution of random error ( $\delta$ ) at Dargo; b) random error variance as a function of $CO_2$ flux magnitude for both sites. ....	145
Figure 4.16: Monte Carlo-simulated cumulative random uncertainty estimates for Dargo 2007/08 .....	146
Figure 4.17: comparison of observed $CO_2$ fluxes with artificial neural network output.....	148
Figure 4.18: effects of decreasing random error on correlation between noiseless artificial neural network $CO_2$ flux time series and the same series with artificial noise imposed .....	149

Figure 4.19: cumulative model uncertainty for Dargo 2007/08.....	151
Figure 5.1: cross-site comparison of 2007/08 daily photosynthetically active radiation components .....	157
Figure 5.2: cross-site comparison of 2007/08 air temperatures .....	159
Figure 5.3: a) potential temperature ( $T_0$ ) and wind speeds for Dargo and Nimmo.....	161
Figure 5.4: cross-site comparison of 2007/08 soil temperatures.....	163
Figure 5.5: Australian Water Availability Project annual precipitation percentile maps .....	166
Figure 5.6: seasonal precipitation totals.....	167
Figure 5.7: 2007/08 daily mean site albedo.....	167
Figure 5.8: cross-site comparison of 2007/08 humidity .....	168
Figure 5.9: cumulative precipitation (P) and evapotranspiration (ET) for sites in 2007/08. ....	169
Figure 5.10: a) average bulk surface resistance ( $\pm 95\%$ confidence interval for mean) during daylight hours for all available data during study period, and; b) average aerodynamic resistance during daylight hours. ....	170
Figure 5.11: a) average bulk surface resistance during daylight hours.....	170
Figure 5.12: 2007/08 volumetric soil moisture .....	171
Figure 6.1: layer average (a) and cumulative (b) depth profiles of soil organic carbon density.....	177
Figure 6.2: extrapolated cumulative soil organic carbon (SOC) density curve for Dargo and Nimmo sites.....	179
Figure 6.3: allocation of carbon to above- and belowground phytomass carbon pools.....	181
Figure 6.4: relative magnitudes of ecosystem (soil + phytomass) carbon storage for Dargo and Nimmo. ....	184
Figure 7.1: comparison of annual NEE (this study) with primarily temperature-limited ecosystems in the Fluxnet global database .....	189
Figure 7.2: relationship between annual ecosystem respiration and mean annual temperature for European grasslands.....	191
Figure 7.3: relationship between GPP and $R_e$ for international Fluxnet sites.....	193
Figure 7.4: 2007/08 cross-site comparison of net ecosystem exchange (NEE), gross primary production (GPP) and ecosystem respiration ( $R_e$ ).....	196
Figure 7.5: relationship between MODIS 1km LAI product (collection 5, TERRA product MOD15A2) and 10-day running mean of Nimmo site daily total GPP for 2007/08. ....	198
Figure 7.6: 2006-08 log-linear regression-estimated GPP (from MODIS LAI) and Nimmo site daily total GPP. .	199
Figure 7.7: winter mean daily NEE ( $\pm SE$ ) for snow-covered and snow-free conditions at Dargo.....	201
Figure 7.8: cross-site winter diurnal NEE ( $\pm SE$ ) comparison .....	202



Figure 7.9: ideal temperature response curves derived from temperature response function parameters .....	207
Figure 7.10: soil moisture response of $R_e$ .....	211
Figure 7.11: cross-site comparison of photosynthetic light response .....	217
Figure 7.12: light response function estimates of GPP for sites using observed and crossed light conditions and response parameters .....	218
Figure 7.13: a) comparison of 2007/08 LAI and $A_{opt}$ for Nimmo site; b) relationship between MODIS LAI and $A_{opt}$ at Nimmo site. ....	219
Figure 7.14: daily GPP as a function of air temperature ( $T_a$ ) and photosynthetically active radiation (PAR) ....	221
Figure 7.15: comparison of time series of $A_{opt}$ with surface temperature and photoperiod.....	222
Figure 7.16: mean ( $\pm 95\%CI$ ) $A_{opt}$ binned by $1^\circ C$ temperature increments for Dargo and Nimmo .....	225
Figure 7.17: 2007/08 comparison of Dargo normalised $A_{opt}$ ( $A_{opt} / A_{opt\_max}$ ) with growing season index and associated ramp function scalars.....	227
Figure 7.18: 2007/08 comparison of Nimmo normalised $A_{opt}$ ( $A_{opt} / A_{opt\_max}$ ) with growing season index and associated ramp function scalars.....	228
Figure 7.19: coefficient of determination ( $r^2$ ) between GSI and $A_{opt}$ for model and data years .....	230
Figure 7.20: comparison of GSI model temperature response scalars for $A_{opt}$ with sigmoid response scalar for $R_e$ at Dargo.....	231
Figure 7.21: GSI model temperature response scalars for $A_{opt}$ at Dargo and Nimmo derived from response parameters in Table 7.7.....	232
Figure 8.1: a) winter/spring mean temperature deciles for twelve El Niño events; b) winter/spring mean rainfall deciles for twelve El Niño events (BOM, 2014).....	239

---

# List of Tables

---

Table 2.1: peak phytomass C storage values reported in the literature. ....	26
Table 2.2: soil organic carbon (SOC) density values reported in the literature. ....	29
Table 2.3: alpine grassland NEE values reported in the literature .....	44
Table 3.1: general attributes of field sites .....	74
Table 3.2: site instrumentation. ....	80
Table 3.3: flux data quality classification scheme .....	96
Table 3.4: suggested combined data quality classes of Foken <i>et al.</i> (2004). ....	96
Table 3.5: control variables used as inputs for artificial neural networks. ....	102
Table 3.6: data sources for imputation of meteorological drivers. ....	104
Table 4.1: linear best fit regression parameters of turbulent energy fluxes on available energy .....	122
Table 4.2: measured mass quantities ( $\pm 95\%$ CI of sample mean) and thermal properties of soil constituents .	131
Table 4.3: seasonal and annual friction velocity ( $u^*$ ) thresholds for Dargo and Nimmo. ....	135
Table 4.4: Lloyd and Taylor temperature response function parameter estimates .....	137
Table 4.5: linear regression coefficients for random error variance as a function of CO <sub>2</sub> flux magnitude. ....	145
Table 4.6: Monte Carlo-simulated cumulative random uncertainty estimates for Dargo 2007/08. ....	147
Table 4.7: annual total uncertainty (sum of random and model error-derived uncertainties) in gCO <sub>2</sub> a <sup>-1</sup> for Dargo and Nimmo 2007/08 .....	151
Table 5.1: seasonal and annual average daily total incident photosynthetically active radiation .....	156
Table 5.2: 2007/08 seasonal and annual average daily, daytime and nocturnal site air temperatures .....	158
Table 5.3: 2007/08 seasonal and annual average daily soil temperatures .....	162
Table 5.4: annual precipitation totals for Dargo and Nimmo .....	166
Table 6.1: average ( $\pm$ SE) soil physical and chemical properties .....	176
Table 6.2: average ( $\pm$ SE) above- and belowground phytomass .....	181
Table 6.3: average ecosystem carbon storage ( $\pm$ SE) in soil and phytomass for Dargo and Nimmo .....	183

---

Table 7.1: annual sums ( $\text{gC m}^{-2}$ ) of ecosystem respiration ( $R_e$ ), gross primary production (GPP) and net ecosystem exchange (NEE) $\pm 95\%$ confidence intervals.....	188
Table 7.2: seasonal sums ( $\text{gC m}^{-2}$ ) of ecosystem respiration ( $R_e$ ), gross primary production (GPP) and net ecosystem exchange (NEE) $\pm 95\%$ confidence intervals.....	195
Table 7.3: 2007/08 comparison of fitted parameter values of Lloyd and Taylor (1994) temperature response function .....	207
Table 7.4: 2007/08 cross-site comparison of annual $R_e$ and potential $R_e$ .....	209
Table 7.5: 2007/08 comparison of fitted parameter values of sigmoid soil moisture response function. ....	211
Table 7.6: coefficient of determination ( $r^2$ ) for regression of $A_{\text{opt}}$ on driving variables above and below threshold temperature of $15^\circ\text{C}$ .....	223
Table 7.7: ramp function parameters for temperature ( $T$ , $^\circ\text{C}$ ) and photoperiod (PP, hours) minima and maxima for simplified GSI model (optimised using 2008 data). ....	231
Table 8.1: estimated annual leaching C losses .....	243

---

# 1. Introduction

---

## 1.1 Prelude

Climate change is expected to drive significant alteration to the function of terrestrial ecosystems, and temperature-limited mountain ecosystems are considered to be particularly sensitive. As a result, the carbon balance of these ecosystems is expected to be altered, with attendant implications for ecosystem carbon storage. This is in turn important because of the role of the carbon cycle in the regulation of climate. This thesis investigates the interactions between climate and carbon dynamics in subalpine grassland ecosystems of the south-eastern Australian mainland's mountainous regions (the so-called 'High Country'). While the study focuses on these linkages in the present day, its scientific relevance is in building insight into how these ecosystems may respond to expected changes in climate into the future.

## 1.2 Research Context

### 1.2.1 Mountain ecosystems in a changing climate

It is well established that the observed warming of the global climate since the middle of the 20th century (approximately 0.13°C per decade) is primarily associated with anthropogenic emission of greenhouse gases (largely CO<sub>2</sub>) via fossil fuel combustion and biomass burning (Meehl *et al.*, 2007; NRC, 2010). This warming has altered precipitation regimes through shifts in global circulation patterns and intensification of the hydrological cycle (Meehl *et al.*, 2007; Trenberth *et al.*, 2007).

In combination with the effects of changing atmospheric (and oceanic) chemistry, these physical changes in the earth system have profound implications for the functioning of the terrestrial biosphere<sup>1</sup> (Walker *et al.*, 1999a). Already there is strong evidence for climate-driven responses in

---

<sup>1</sup> The collective biotic component of the earth system (Chapin *et al.*, 2002).

ecosystems<sup>2</sup> all over the world (Rosenzweig *et al.*, 2008), which are expected to continue with future climatic change (Fischlin *et al.*, 2007). However, ecosystems vary in their vulnerability to climate change. Among those considered to be most vulnerable are mountain ecosystems (Beniston, 2003; Körner *et al.*, 2005; Laurance *et al.*, 2011), which are thus early indicators, or 'bellwethers', of change (Wookey *et al.*, 2009). Their potential vulnerability arises due to both rates of climatic change anticipated in mountain regions and the inherent sensitivity of ecosystems to a given rate of change.

With respect to rates of change, it has been hypothesised that warming-driven losses of snow and ice cover in alpine<sup>3</sup> regions may have a localised effect analogous to polar amplification, in which the loss of highly reflective snow and ice cover exposes the underlying low-albedo surface, with consequent enhancement of radiative absorption and thus warming (Giorgi *et al.*, 1997). Accordingly, a number of higher elevation climate records indicate enhanced warming in the past century relative to the observed global rates of change (Beniston *et al.*, 1997; Thompson *et al.*, 2000), particularly at the lower margins of current snow and ice cover (Pepin and Lundquist, 2008). Moreover, given the optical and thermal properties of snow, reduced spatial and temporal extent and thickness of snow cover result in profound changes in the microclimate experienced by plants (Körner, 2005).

The inherent sensitivity of mountain ecosystems is associated with a range of factors, including: i) the key role of low temperatures in shaping evolutionary adaptations / interactions of constituent species (Wookey *et al.*, 2009); ii) fundamental barriers to migration (i.e. the altitudinal limits of the mountains the ecosystems occupy) (Pittock, 2009); iii) limited geographical ranges dictated by the generally localised effects of – and correspondingly steep climatic gradients associated with – altitude and topography (Barry, 1994); iv) the short migratory distance required for potential competitors to colonise ecosystems (Walther *et al.*, 2005); v) the limited gene pools of characteristically small, isolated and often endemic populations (Theurillat *et al.*, 1998), and; vi) existing environmental resource pressures in mountain regions (Körner *et al.*, 2005). Three main responses are possible for mountain ecosystems and their constituent species: local persistence through adaptation, local extinction or, where possible, geographical migration (Aitken *et al.*, 2008).

---

<sup>2</sup> The total ecological system of an area comprised of the organisms and the physical environment with which they interact (Chapin *et al.*, 2002).

<sup>3</sup> Mountain regions are generally geographically subdivided into four major bioclimatic zones. The uppermost is the nival zone, which lies above the permanent snowline (absent in Australia); between the permanent snowline and (natural) treeline is the alpine zone; between treeline and the winter snowline is the subalpine zone, and; below the winter snowline but still at significant altitude in relation to the surrounding area is the montane zone (Körner, 2003).

Ecosystems at higher elevations are therefore particularly at risk due to limited or non-existent migratory capacity. Already, numerous international studies report recent altitudinal increases in alpine treeline in association with winter warming (see Harsch *et al.*, 2009 for a review). There is, however, some degree of inertia to upslope colonisation by species resulting from: i) limited seed dispersal ability of potential colonisers; ii) resilience of extant ecosystems, such that disturbance may be required to facilitate establishment of colonisers, and; iii) constraints potentially imposed by other (e.g. edaphic) environmental conditions (Walther *et al.*, 2005). These factors may thus allow ecosystems to persist – at least in terms of the dominant functional types that define them – despite moderate changes in climate; even at present, in many cases extant high-altitude plant species' may not be in equilibrium with what might be considered 'preferred' climate (Körner, 1998). Nonetheless, even in the absence of wholesale ecosystem replacement, significant habitat loss – and concomitant species loss – is expected at higher altitudes in the coming century (Thuiller *et al.*, 2005; Engler *et al.*, 2011).

Such changes are of concern not only for intrinsic reasons, but also because mountain ecosystems are valuable to humanity, through the provision of food and water resources, recreation and tourism destinations and natural (e.g. biodiversity) and aesthetic values (Körner *et al.*, 2005). Mountain regions generally have been described as 'water towers' for their role in the hydrological cycle (enhancement of precipitation associated with orographic uplift) and the consequent storage and release of water from glaciers, snowpacks, soils and groundwater (Körner *et al.*, 2005). Moreover, Schimel *et al.* (2002) have highlighted the potentially significant role of mountains in the sequestration of carbon. However, the sequestration potential of terrestrial ecosystems is in general expected to be affected by climate change (Cao and Woodward, 1998). Since the cycling of carbon between ecosystems and atmosphere is a direct manifestation of ecological function, it is among the most vulnerable ecosystems that changes in ecosystem carbon dynamics are expected to be most pronounced (Fischlin *et al.*, 2007).

### 1.2.2 Ecosystem function, carbon dynamics and climate

Carbon enters ecosystems via photosynthetic fixation – and subsequent assimilation into tissue - of organic compounds from atmospheric CO<sub>2</sub> by autotrophic organisms. The materials and chemical energy supplied by these compounds are exploited for maintenance, growth and movement across all trophic levels via the process of respiration, which is the primary pathway for

return of carbon (as CO<sub>2</sub>) to the atmosphere (Schlesinger, 1997). Assimilation and respiration are thus the basic elements of the ecosystem carbon cycle (see Chapter 2, section 2.4.1, for a more formal description of the carbon cycle components). Since carbon is the structural 'skeleton' of organic compounds, terrestrial ecosystems represent a large store of carbon both in the biota and as organic matter in soils (Chapin *et al.*, 2002).

The regulation of both assimilatory and respiratory processes is highly dependent on climate (Chapter 2, section 2.4). On hourly, daily and seasonal time scales assimilation is primarily controlled by solar radiation, temperature and moisture availability, and respiration is also primarily controlled by temperature and moisture availability (Baldocchi and Valentini, 2004). Over longer time periods, the balance between these processes determines the rate of accumulation of carbon within the ecosystem; in late-successional communities subject to stationary climatic conditions, internal feedback processes eventually draw rates of carbon import and export into approximate equilibrium (Lambers *et al.*, 2008). The amount of carbon stored by ecosystems in this quasi-equilibrium state is however highly variable among the world's ecosystems (Adams *et al.*, 1990). Climate is one of the key determinants of this variability (Schlesinger, 1997).

The pattern of allocation of carbon between ecosystem vegetation and soil reservoirs is also strongly dependent on climate. At low temperatures, short growing seasons and the microclimatological advantages of small stature result in relatively limited biomass production and retention (Grace, 1988; Körner, 2003). As such, the vegetation carbon reservoir is small in ecosystems in cold regions (such as those at higher latitudes and altitudes). On the other hand, large soil organic matter (and thus carbon) quantities are generally typical of cold region ecosystems (Post *et al.*, 1982). The accumulation of organic matter occurs because the rate of addition of biological detritus from litterfall and root mortality initially exceeds the rate of decomposition, which is strongly temperature-dependent (Lloyd and Taylor, 1994) and initially constrained more by low temperatures than production (Kirschbaum, 1995). Over time, the progressive immobilisation of nutrients in undecomposed soil organic matter and decreases in pH reduce substrate optimality for primary production, thus drawing the ecosystem towards approximate carbon neutrality (Körner, 2003). Colder climate ecosystems are therefore generally characterised by relatively small vegetation and large soil carbon pools (Post *et al.*, 1982; Olson *et al.*, 1983). As such, despite characteristically small amounts of biomass, the total storage of carbon (per unit area) is often comparable to that of far more productive terrestrial ecosystems (Adams *et al.*, 1990).

Moisture availability is also an important determinant of carbon accumulation in ecosystems. However, in contrast to the effects of temperature, dry conditions constrain production

processes more than decomposition processes (Schwalm *et al.*, 2010), such that dry regions are typified by small vegetation (Schlesinger, 1997) and soil carbon (Post *et al.*, 1982) reservoirs. As such, while cold or dry conditions both constrain amounts of biomass production and retention (resulting in small vegetation carbon reservoirs), they have opposing effects on soil organic matter (and thus soil carbon) retention.

### 1.2.3 Ecosystem carbon balance and climate change

A key implication of the climatic dependence of carbon storage is that climate change is expected to drive concomitant changes in carbon balance – and in turn carbon storage – as assimilatory and respiratory processes respond differently to changing climatic regimes. Low temperatures limit the length of growing seasons, and thus as the atmosphere warms, longer growing seasons are accompanied by enhanced assimilation of carbon by vegetation (Nemani *et al.*, 2003; Linderholm, 2006). In mountain ecosystems of Europe, spatial patterns of biomass production at present are strongly linked to temperature (Jonas *et al.*, 2008), and future warming is expected to enhance biomass production (Rammig *et al.*, 2010). However, there is also evidence to suggest that at lower temperatures, decomposition of soil organic matter – which as discussed above is often abundant in cold mountain regions - may be stimulated more by warming than net primary production, resulting instead in net carbon release (Kirschbaum, 1995; Kirschbaum, 2000; Davidson and Janssens, 2006). In addition to changes in temperature, the other profound effect of climatic change is the alteration of the hydrological cycle and thus soil moisture availability. As noted above, assimilation is more sensitive to drought conditions than decomposition (Schwalm *et al.*, 2010), and substantial drying may therefore also result in net release of carbon from ecosystems.

Thus the potential magnitude of change in carbon storage in ecosystems depends on both the specific nature of climatic change (i.e. region-specific changes in both temperature and hydrological regimes), as well as the relative sensitivities of vegetation and soil carbon pools to those changes. At present, there is clear evidence that terrestrial ecosystems globally represent a net sink for carbon, absorbing approximately 30% of the anthropogenic carbon contribution to the atmosphere. Between 2000-06, this represented a sink of approximately  $2.8\text{PgC a}^{-1}$  (Canadell *et al.*, 2007). A significant proportion of this sequestration is thought to be associated with vegetation responses both to a  $\text{CO}_2$ -enriched atmosphere, and - in boreal and temperate regions – the



stimulation of growth by warmer temperatures<sup>4</sup> (Foley and Ramankutty, 2004; Heimann and Reichstein, 2008). With respect to cold regions, the ecosystems of the Arctic are thought to have been a net carbon sink of 0-0.8PgC a<sup>-1</sup> in recent years (McGuire *et al.*, 2009). Comparable assessments for mountain ecosystems globally are lacking, but available analyses suggest that net uptake of carbon is currently occurring in most surveyed regions (e.g. Kato *et al.*, 2006; Koch *et al.*, 2008, but see Chapter 2, section 2.5.4 for a review).

Nonetheless, ongoing changes in climate into the future are projected to result in the transition of the terrestrial biosphere to a net carbon source during the 21<sup>st</sup> century (Cox *et al.*, 2000; Friedlingstein *et al.*, 2006), as increasing temperatures stimulate decomposition (Davidson and Janssens, 2006) and – in combination with increased frequency of drought – reduce primary production (Matthews *et al.*, 2007). Current climatic variability provides an analogue for these possible future effects. The El Niño Southern Oscillation (ENSO) is strongly correlated with the rate of increase in atmospheric CO<sub>2</sub>; El Niño events (i.e. generally warmer, drier conditions) are associated with large anthropogenically-driven increases in atmospheric CO<sub>2</sub> due to the weakening of the biospheric sink, while smaller increases occur in association with La Niña (i.e. generally cooler, wetter conditions) due to strengthening of the sink (Rödenbeck *et al.*, 2003; Heimann and Reichstein, 2008). In cold (e.g. Arctic) regions, it is also expected that ecosystems will transition from carbon sink to carbon source later in this century in response to continued warming, as the carbon cycle effects of warming-enhanced growth are overwhelmed by warming-enhanced decomposition (Schuur *et al.*, 2008). Artificial warming experiments suggest similar responses may occur in alpine ecosystems (Egli, 2004; Hagedorn *et al.*, 2010).

One of the key reasons for concern about changes in the carbon balance of the terrestrial biosphere is potential feedbacks<sup>5</sup> to climate. As a net carbon sink, the biosphere currently provides negative feedback to climate change, but as detailed above the transition to carbon source could potentially occur during this century, resulting in positive feedback. Unfortunately, there are significant deficiencies in our understanding of both production (Matthews *et al.*, 2007) and decomposition (Trumbore and Czimczik, 2008) processes. These deficiencies translate to uncertainties in coupled carbon cycle-climate models, contributing approximately 40% of the current model uncertainty (Huntingford *et al.*, 2009), which rank second only to anthropogenic emissions

---

<sup>4</sup> It is also thought to be partly associated with vegetation regrowth from historical land clearing activity in some regions, as well as the effects of inadvertent global nitrogen deposition (Schimel, 1995).

<sup>5</sup> Carbon cycle-climate feedbacks may be positive or negative. Positive feedbacks are those which move the system towards a new equilibrium state by amplifying initial perturbation, and negative feedbacks act to return the system to its previous equilibrium state by dampening initial perturbation (Kump *et al.*, 2004).

pathways in contributing to uncertainties in climate change projections (Raupach and Canadell, 2010). Given these uncertainties, there is a need to improve our understanding of ecosystem carbon cycle responses to climate.

#### 1.2.4 The Australian High Country and Climate Change

The Australian High Country (herein High Country) covers approximately 11,000km<sup>2</sup>, and encompasses forest, heath and grassland ecosystems as well as other more specialised assemblages in the alpine zone (Williams and Costin, 1994). Despite their relatively small spatial extent, the scientific (Good, 1989), cultural (Lennon, 1999), economic (primarily tourism) (Mules *et al.*, 2005) and resource (particularly water) (Crabb, 2003) significance of the Australian Alps are today well recognised. Yet the ecosystems of the High Country face a range of environmental pressures, including cattle grazing, exotic species invasion, hydroelectric development, tourism (and associated infrastructure) and climate change. In the long term, climate change is potentially both the most damaging and the least understood (Williams and Wahren, 2005).

The southeast region in which they are located has seen substantial changes in climate in recent decades. While few formal analyses of recent observed changes in temperatures in the High Country are available, Gallagher *et al.* (2009) report temperature increases of an estimated 0.7°C at altitudes above 1500m between 1950 and 2007, comparable to those reported for Australia and the southern hemisphere in recent years (Cai *et al.*, 2007; Trenberth *et al.*, 2007). Weak mid-winter and moderate late-season declines in snow pack depth have been reported across multiple alpine sites (Hennessy *et al.*, 2008), with reductions in springtime snow depths of up to 40% attributable primarily to temperature increases (Nicholls, 2005). While historical precipitation patterns have not been documented for the High Country specifically, precipitation has decreased significantly in the Australian south-east in the past 50 years (Murphy and Timbal, 2008).

Substantial ongoing changes are also expected into the future. While detailed regional estimates are not available for the High Country, model projections indicate (scenario-dependent) warming of 0.3-2.7°C by 2050 (relative to 1990) in near-coastal (i.e. <400km inland) areas in southern Australia, accompanied by declines in rainfall (0 to -15%) and snow cover (10-39% by 2020 and 22-85% by 2050) (Suppiah *et al.*, 2007; Hennessy *et al.*, 2008). Large losses of snow cover are related to the fact that mild Australian climatic conditions provide marginal conditions for the presence of snow cover (Slatyer *et al.*, 1985). Warmer temperatures (and correspondingly increased

evapotranspiration) and lower rainfall are also expected to further increase the recurrence of drought in the broader south-eastern Australian region (Nicholls, 2004; CSIRO, 2010). In turn, this raises the spectre of probable corresponding increases in wildfire frequency (Hennessy *et al.*, 2005). Wildfire is historically rare among the alpine ecosystems of the High Country (due to limited fuel – i.e. phytomass and litter - availability and moist conditions), with return frequencies of large fires of approximately 50-100 years (Williams *et al.*, 2008a).

Drought and wildfire are nonetheless a natural and historically recurrent feature of the ecology of the High Country, and ecosystems are substantially resilient to their effects (Williams, 1990; Scherrer and Pickering, 2005; Williams *et al.*, 2008b). Ongoing changes in the frequency of such events are however expected to impact significantly on the ecosystems of the High Country (Williams and Wahren, 2005). Moreover, in addition to the direct effects on ecosystems of changes in air temperature (Jarrad *et al.*, 2008; Jarrad *et al.*, 2009), one of the indirect effects expected to have a profound ecological impact is the projected loss of snow cover (Edmonds *et al.*, 2006; Green and Pickering, 2009). As previously noted, this may be more important than changes in ambient air temperatures because the loss of snow cover radically alters the microclimate adjacent to the surface; this is particularly important among low statured ecosystems, which often experience sustained and complete coverage for some period of the year (Körner, 2005).

As a result of these factors, in common with the situation globally, the ecosystems of the Australian High Country are among those likely to be most substantially affected by climate change (Hughes, 2003; Pickering *et al.*, 2008; Laurance *et al.*, 2011). But despite a rich heritage of ecological research in the Australian High Country - focusing in particular on linkages between environmental parameters (e.g. climate, soils, disturbance) and patterns of distribution of vegetation communities (Williams and Wahren, 2005) - the nature of these impacts on ecosystems of the High Country are, as noted above, not well understood. While recent research has begun to focus on potential growth effects of warming (Byars *et al.*, 2007; Jarrad *et al.*, 2008; Gallagher *et al.*, 2009; Jarrad *et al.*, 2009; Green, 2010) and drought (Griffin and Hoffmann, 2011) on a number of plant species in the High Country, there is a dearth of research addressing the potential carbon cycle implications of climatic change in the Australian High Country.

## 1.3 Rationale, Aims and Approach

### 1.3.1 Rationale

A crucial first step in developing insights into how changes in carbon status (i.e. in terms of both carbon stores and balances) of High Country ecosystems may proceed with climate change in future is to build an understanding of this status at present.

With respect to storage, similarly to global observations of large stores of soil carbon in cold regions globally (e.g. Post *et al.*, 1982), the high organic matter (and corresponding carbon) content of Australian alpine soils has been widely documented (Costin *et al.*, 1952; Spain *et al.*, 1983; Jenkins and Adams, 2010). However, published estimates of typical ecosystem carbon densities for the High Country are generally lacking in the literature. Such information would provide insight into the potential future evolution of the carbon balance with climate, for two reasons. First, the potential for ecosystems to become a source of carbon to the atmosphere in future is fundamentally constrained by the amount of carbon stored at present. And second, differences in carbon storage across climatic gradients may indicate potential carbon storage under different climatic states – in other words, current climatically-determined spatial variability can be used as a partial analogue of the effects of changing climate over time.

With respect to carbon balance, several recent studies have been undertaken that begin to address the responses of High Country ecosystem carbon balance to climate at present (for example, Jenkins and Adams, 2010; Warren and Taranto, 2011). Despite the value of these studies in elucidating linkages between soil carbon dynamics and climate, they focus on the respiratory component of the carbon balance alone. However, it is vitally important to understand both the assimilatory and respiratory components of the ecosystem carbon cycle, since the net carbon balance (i.e. the magnitude of the ecosystem carbon source or sink) depends on the magnitudes of both terms. It is also important to understand how these components of the carbon balance respond to meteorological controls, since this information is critical in beginning to understand how future changes in climate may affect the carbon balance. Since snow cover is expected to decline so dramatically, it is also important to understand the effects of snow cover on the carbon balance at present, since northern hemisphere studies have documented its profound effect upon ecosystem carbon cycling (Walker *et al.*, 1999b; Brooks *et al.*, 2011).

A more comprehensive understanding of ecosystem-scale carbon status at present also has further benefits. With respect to the assimilatory component of the carbon balance, it provides information about the growth responses of vegetation communities to climatic controls as well as revealing thresholds of vulnerability to extremes of, for example, temperature and moisture availability, thus complementing existing species-level analyses with ecosystem-scale *in situ* observational research. An understanding of growth responses to climate also furthers our knowledge about how amounts of aboveground vegetation may change. In the absence of rapid successional changes in plant functional type, increases in aboveground vegetation may result in modest gains in carbon storage. However, such changes may nevertheless further contribute to changes in fire frequency by altering the available fuel load (Cary *et al.*, 2012). Changes in fire frequency have the potential to significantly alter the carbon balance of ecosystems (Williams *et al.*, 2012).

Moreover, it also provides data that can be used to validate models of ecosystem carbon cycle dynamics that are vital to efforts to extend our knowledge of ecosystem – and corresponding carbon cycle - responses to climate in time and space (e.g. Reichstein *et al.*, 2007). In this sense, ecosystems at the ends of the bioclimatic spectrum provide a stringent test for the capabilities of such models. Finally, the inherent vulnerability of mountain ecosystems to changes in climate potentially makes them an ideal early warning system for climate-driven changes in the biosphere, and changes in carbon cycle dynamics provide a fingerprint of underlying changes in ecosystem function that may not otherwise be readily (e.g. visually) apparent.

### 1.3.2 Research focus and aims

This study therefore takes as its major focus the investigation of current levels of carbon storage as well as carbon balance in one of the common ecosystems of the Australian High Country: the sod tussock grassland (herein simply grassland - see Chapter 2 for a more formal definition) communities of the subalpine tracts. These grassland ecosystems are somewhat unique at the continental level given that, whereas the distributions of most grasslands are related to water availability (Sala, 2001), the presence of the grassland biome in the Australian Alps is due to the exclusion of other plant functional types at low temperatures (Moore and Williams, 1976). Temperature-limited grasslands are both common in the Australian Alps (Costin *et al.*, 2000) and among the most common of ecosystems at medium altitudes globally (Körner, 2003). While

numerous observations of elevation increases in treeline have been noted around the world (Harsch *et al.*, 2009), the pace of such changes is expected to be slow in Australia due to the poor dispersal ability of the sole treeline species, *Eucalyptus pauciflora* (Green, 2009), and the necessity of substantial disturbance to provide opportunities for colonisation (Ferrar *et al.*, 1988). As such, in the near future, the spatial extent of grasslands in the High Country is expected to remain stable or even possibly to increase (Pickering, 2004).

In order to gain insight into potential carbon cycle effects of future climate change, the investigation takes a comparative approach utilising two climatologically contrasting sites: a cooler, wetter site subject to a consistent winter snowpack and a warmer, drier site with more sporadic snow cover. There are two key reasons for this approach. First, while the study is limited to observation of the current carbon cycle in these grassland ecosystems, as alluded to previously, insight into potential effects of future climate change on ecosystem carbon dynamics can be gained by substituting temporal and spatial dimensions. The differences in climate between the sites are thus broadly analogous to changes that might plausibly be expected to occur in the region during this century (though caveats - e.g. the effects of non-climatic local factors on ecosystem carbon dynamics – necessarily apply). The general lack of snow cover at the second site is particularly important, since as previously discussed, the effects of changes in snow cover are expected to have profound effects on seasonally snow-covered ecosystems.

The second (related) reason is associated with the potential for generalisation of knowledge about the carbon cycle dynamics of individual ecosystems to the biome<sup>6</sup> level. In order to apply ecosystem knowledge at the biome level it is necessary to understand the mechanisms that drive variations in these dynamics across ecosystems within the biome. These variations may arise as a result of contrasts in either external abiotic forcing or the internal biotic response to this forcing. Understanding the relative contributions of these factors to similarities and differences in ecosystem carbon dynamics is an important aid in the development of parsimonious models that can effectively capture the behaviour of the system. Such models are, as noted above, critical tools in the effort to investigate potential climate-driven changes in carbon cycle dynamics.

The overarching aim of the comparative analysis is thus to assess the role of climate in shaping contrasts in ecosystem carbon storage and ecosystem / atmosphere carbon exchange between two climatically contrasting Australian subalpine grasslands. The specific objectives undertaken at each site in order to achieve this aim are as follows:

---

<sup>6</sup> A general class of ecosystems (Chapin *et al.*, 2002).

1. Quantify carbon storage in soil and vegetation reservoirs;
2. Quantify net exchange of carbon between ecosystem and atmosphere;
3. Quantify assimilatory and respiratory components of net carbon exchange;
4. Quantify the effects of climatic controls on these components.

### 1.3.3 Approach

While comprehensive descriptions of the research sites and the precise methodological details of the measurement campaign are provided in Chapter 3, here a brief overview of the general approach is provided.

With respect to the quantification of carbon storage in soil and vegetation reservoirs (Objective 1), given the relatively short time scale of the field component of this investigation (two years), it was possible to treat the soil storage of carbon at the research sites as static, such that a single set of survey measurements were considered appropriate for quantification of soil carbon. The vegetation carbon quantity reported in this investigation represents the maximum phytomass quantity observed during the peak of the growing season.

Measurement of carbon exchange between ecosystems and atmosphere (Objective 2) was undertaken using the eddy covariance technique, the theoretical details of which are discussed in Chapter 2. In brief, the technique involves measurement of high-frequency (10Hz) covariances of eddy velocities and mass concentration of carbon in the atmosphere approximately normal to and above the vegetation canopy, from which mean transfer or ‘flux’<sup>7</sup> between the surface and the atmosphere can be resolved by application of theory and a number of key simplifying assumptions. These automated measurements operate continuously, and allow a high resolution continuous record of carbon exchange to be obtained.

Partitioning of the net ecosystem / atmosphere exchange of carbon between assimilatory and respiratory components (Objective 3) involves first ascertaining the respiratory component by taking advantage of the fact that in the absence of photosynthetic activity, nocturnal carbon exchange consists entirely of respiration. Empirical relationships expressing the dependence of respiration on meteorological controls developed for nocturnal conditions (see Chapter 3,

---

<sup>7</sup> Flux or flux density refers to the unit quantity of a given entity through unit surface area per unit time (Oke, 1987).

section 3.7) can then be used to estimate respiration during all times, and gross ecosystem assimilation is in turn calculated as the difference between net carbon exchange and ecosystem respiration.

Linking the assimilatory and respiratory exchanges to meteorological controls (Objective 4) requires measurement of the relevant meteorological variables. These measurements were made concurrently with those of the eddy covariance system. As described above, empirical relationships were then developed to express the response of the individual component exchanges to these controls. It is then possible to link any differences in carbon balance that may arise between sites to external drivers and / or internal responses.



## 1.4 Scope

### 1.4.1 Temporal scale

The investigation of ecosystem / atmosphere carbon exchange is limited to two full years of analysis (2007 and 2008), although both sites continue to be operational up to the present. At least one complete year was required to provide meaningful estimates of carbon balance, which is highly seasonally variable. The primary rationale for two years was that, given the strong interannual variability imposed by ENSO in south-eastern Australia, it may be possible to gain some insight into potential future climate response of ecosystem carbon balance by comparing carbon dynamics across climatologically contrasting years.

### 1.4.2 Spatial scale

While the reasons for the selection of two sites in this study were discussed previously, the choice of the ecosystem as the scale of study was motivated by several considerations. While environmental research can potentially be undertaken at a number of levels (i.e. cellular, individual, species, ecosystem, biome, biosphere), the ecosystem is considered to be the '*... first unit in the molecule-to-ecosphere levels of organisation that is complete, that is, has all of the components, biological and physical, necessary for survival*' (Sala *et al.*, 2000, p.1). It is characterised by strong ecological interactions within its boundaries but weak interactions across them (Fischlin *et al.*, 2007). This has two implications that make ecosystem-scale measurements advantageous. First, ecological interactions critical in shaping the whole system response to external stimuli, while far too complex and too numerous to be explicitly mapped via a bottom-up approach, are implicitly included in ecosystem-integrated measurement approaches such as eddy covariance. And second, the ecosystem scale is such that the response of the biosphere to global perturbations (e.g. climate change) can – when scaled appropriately - potentially be estimated from the sum of ecosystem responses (Baldocchi *et al.*, 2001).

## 1.5 Linkages

### 1.5.1 HighFire and the High Country Fuels and Ecosystem Function (HCFEF) Project

This investigation is part of the High Country Fuels and Ecosystem Function (HCFEF) project, a subcomponent of the HighFire project funded through the Bushfire Cooperative Research Centre. HCFEF is a collaborative effort that brings together members of the Bushfire CRC, UNSW, Ensis, the University of Melbourne, Monash University, the Institute for Atmospheric Research, Garmisch (IFU) and Albert-Ludwigs University, Freiburg. It aims to improve understanding of the dynamics of carbon, water and energy in Australia's alpine and sub-alpine vegetation and how this relates to fuel accumulation, a vital component in determining risks and behaviour of bushfire. The findings of this investigation will contribute to the understanding of interactions between bushfire and climate change in the country by advancing our understanding of how climatic conditions affect biomass production in grassland ecosystems at present.

### 1.5.2 Fluxnet and Ozflux

The sites established for this investigation are also part of a global network of sites providing continuous high resolution monitoring of ecosystem / atmosphere exchanges of carbon (and other trace gases), water and energy. This network, known as Fluxnet<sup>8</sup> (Baldocchi *et al.*, 2001), currently has 576 active sites internationally, with 28 sites – including both of those established for this project - active in Australia under the auspices of Ozflux<sup>9</sup>, the Australian regional network. Among the primary purposes of the Fluxnet are to '*... underpin the interpretation of regional CO<sub>2</sub> source-sink patterns, CO<sub>2</sub> flux responses to forcings, and predictions of the future terrestrial [carbon] balance,*' (Friend *et al.*, 2007, p610) and thus to act as '*... a canary in the coalmine with respect to quantifying how the terrestrial biosphere's metabolism is responding to global change*' (Baldocchi, 2007, p547). The establishment of the sites for this project thus also provide further support for this broader aim, and extends the Australian arm of the network ('OzFlux') to encompass ecosystems of Australia's coldest bioclimatic zone.

---

<sup>8</sup> <http://fluxnet.ornl.gov/>

<sup>9</sup> <http://www.ozflux.org.au/>

## 1.6 Thesis Outline

Chapter 2 reviews and summarises the current literature relevant to the above-stated aims. A thorough description of the methodology used is found in Chapter 3. In Chapter 4, a brief summary of findings related to issues of data quality and underlying uncertainties associated with critical assumptions is provided. A summary comparison of relevant climatic conditions between sites is presented in Chapter 5. Chapter 6 discusses the research findings with respect to carbon storage (Objective 1), and the research findings for Objectives 2, 3 and 4 are found in Chapter 7. Concluding remarks are in Chapter 8, followed by a complete bibliography.

## 1.7 Conventions

The standard micrometeorological sign convention - used here and throughout this study – references the carbon flux sign to the atmosphere i.e. net surface carbon influx (efflux) represents a loss (gain) of carbon with respect to the atmosphere and is thus denoted with a negative (positive) sign. Where the convention (or units) has differed for reported literature values, they have been converted for consistency. Energy fluxes reported in this work are positive when directed away from the surface and negative when directed towards the surface.

The analysis compares carbon fluxes between sites at both annual and seasonal time scales, but since the measurement period extended from January 2007 to December 2008, an altered convention is used for the seasonal analysis, as follows:

- Summer: January, February, March (JFM)
- Autumn: April, May, June (AMJ)
- Winter: July, August, September (JAS)
- Spring: October, November, December (OND)

## 2. Literature Review

---

### 2.1 Introduction

This chapter reviews the available literature relevant to the research questions investigated in this study, as outlined in Chapter 01. It begins with a comprehensive description of the grasslands that form the focus of this study. It then proceeds to a discussion of the available research literature detailing carbon storage in subalpine grasslands and analogous ecosystems internationally, including linkages to environmental factors that determine amounts and patterns of allocation of carbon within the ecosystem. This is followed by a conceptual overview of the ecosystem / atmosphere carbon balance and the key environmental controls that drive the major processes of carbon import to and export from the ecosystem, and a survey of the available international literature detailing ecosystem / atmosphere carbon exchanges in analogous ecosystems. The chapter concludes with a brief technical discussion outlining the theoretical underpinnings, assumptions, corrections and uncertainties associated with eddy covariance, the primary methodological technique used in this study.

### 2.2 Subalpine Grassland Ecosystems

#### 2.2.1 Definition

The term grassland here simply refers to ecosystems in which herbaceous species represent the overwhelmingly dominant vegetation functional group (Jones and Donnelly, 2004). The subalpine designation refers to the fact that the sites are below the so-called *climatic* treeline (i.e. the uppermost altitude of treeline). While the altitude of the climatic treeline (conventionally cited as approximately 1800m on mainland Australia, depending on aspect) is primarily determined by the temperature lapse rate, the presence of tracts of treeless vegetation below this boundary (demarcated by so-called *inverted* or 'hanging' treelines) arises due to localised topographically-induced climatic variability (Slatyer, 1989; Williams *et al.*, 2003). However, whether alpine or

subalpine, the treeless regions occur due to fundamentally similar climatic constraints (i.e. low temperatures)<sup>10</sup>, and it is therefore deemed appropriate to make comparisons with, and draw on the literature from, both alpine and subalpine grasslands generally.

## 2.2.2 Geography

As noted in Chapter 1, alpine and subalpine regions represent approximately 11,000km<sup>2</sup>, or 0.15% of Australian land area (Williams and Wahren, 2005). Their geographic character is one of a distinctly scattered suite of relatively small 'islands', the most spatially contiguous among them being the Snowy Mountains in NSW and the Central Plateau in Tasmania (Figure 2.1) (Costin, 1983; Williams and Costin, 1994).

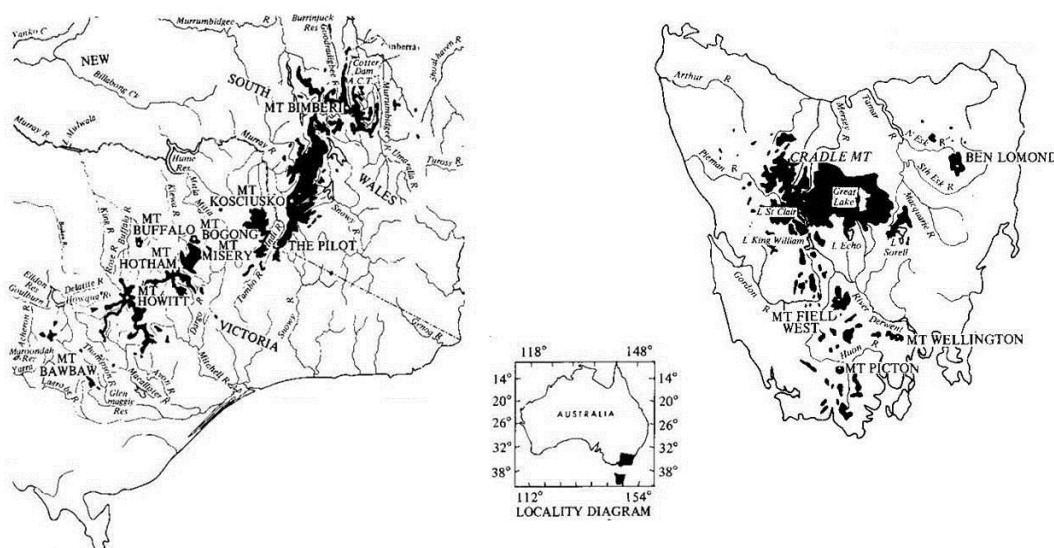


Figure 2.1: distribution of Australia's alpine and sub-alpine regions (from Williams and Costin, 1994; p468).

The zonation of the Australian High Country – including indicative altitudinal thresholds of each zone as well as general physical characteristics - is depicted in Figure 2.2. The subalpine zone occurs between approximately 1300-1800m, and is characterised by moderate topography, a mosaic of woodlands interspersed with treeless vegetation, and snow cover persisting for a month or more

<sup>10</sup> Some researchers thus instead designate any natural, climatically-induced treeless vegetation communities in mountain regions as alpine by definition (Ashton and Williams, 1989).

(Mason and Williams, 2008b). Grassland ecosystems occur both above and below climatic treeline and dominate flatter areas (0-5°) (Williams *et al.*, 2003). In combination with the closely associated tall alpine herbfields, they represent more than 50% of vegetation cover in the Kosciuszko region's alpine zone (Costin *et al.*, 2000).

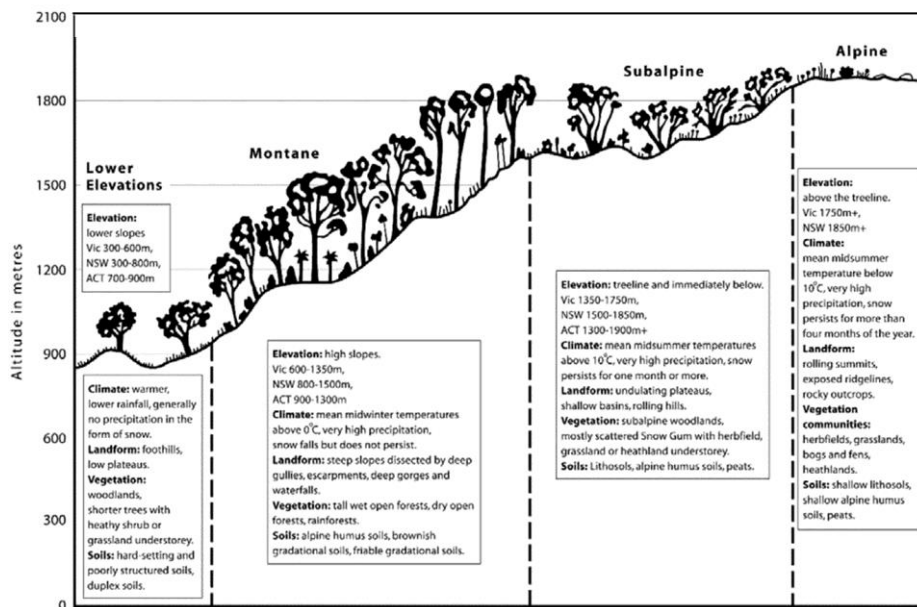


Figure 2.2: zonation and physical characteristics of the mainland Australian High Country (from Mason and Williams, 2008b, p2).

### 2.2.3 Climate

While the climate of the Australian High Country is broadly classified as temperate, it is distinguished by the lack of a very distinct dry season and a typically cool summer (Stern *et al.*, 2000). In part, this reflects the maritime character of the Australian Alps due to their proximity to the coast, resulting in relatively moderate climatic conditions. Frosts are frequent (>100/yr) and can occur at any time of year, and temperatures below -20°C occur at higher elevations (Brown and Millner, 1989; Williams *et al.*, 2003). Annual precipitation varies between 1000-4000mm (Williams *et al.*, 2003) and generally increases with elevation (Brown and Millner, 1989). The spatial and temporal extent of snowpack increases with elevation from the winter snowline: in the Snowy Mountains, approximately 1200km<sup>2</sup> sustains snow cover for more than 60 days (Slatyer *et al.*, 1985).

Strong spatial variability in precipitation arises in the High Country due to the effects of altitude and the orientation of the ranges on the air mass properties of the prevailing synoptic weather systems that deliver rainfall to the region. The principal sources of precipitation over the Alps are depressions in the mid-latitude westerlies, and less commonly intrusions of moist air masses from the tropics or in association with depressions off the east coast (Brown and Millner, 1989). Winter precipitation thus tends to dominate over much of the Alps. It is also particularly marked along the western slopes, whereas the rain shadow thereby created results in progressively reduced winter precipitation towards the east (Figure 2.3). The easterly slopes instead receive a much larger proportion of precipitation during summer, when the weakening of the westerlies allows intrusion of moist air masses and occasional thunderstorm activity, though average precipitation is much lower (Brown and Millner, 1989).

Relative to heath and woodland communities, grassland communities generally occur in locations where exposure to the elements is high i.e. low temperatures and snow depth and persistence, high winds, and frequent occurrence of frosts (Williams, 1987). Huber *et al.* (2011) report minimum and maximum monthly mean temperatures of approximately 0 and 15°C for subalpine grasslands, and also note higher seasonal amplitude of air temperature in comparison to heath or woodland communities.

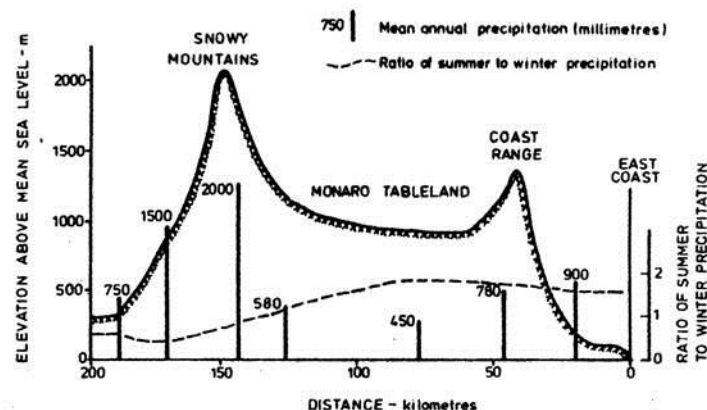


Figure 2.3: generalised east-west topographic/precipitation cross section at approximately S36°30' (from Brown and Millner, 1989, p301).

#### 2.2.4 Vegetation

Australian alpine grassland ecosystems are characterised by a low-statured (generally less than 20cm), dense canopy of stiff-leaved, predominantly tussock-forming grasses (Figure 2.4) which include *Poa* spp. (including *P. hiemata*, *P. costiniana*, *P. fawcettiae*, *P. gunnii*), with lesser representations of *Rytidosperma* spp. (*nudiflorum*, *nivicola*) (Williams *et al.*, 2003). Other herbaceous species (mainly forbs) are also common, including representatives of *Celmisia*, *Craspedia* and *Brachyscome* genera (Costin *et al.*, 2000; Williams *et al.*, 2003).

Relative to other ecosystems, the amount of biomass in alpine grasslands is low. Typical global aboveground biomass quantities for temperate grasslands are 250g m<sup>-2</sup> (Chapin *et al.*, 2002) and for alpine grasslands 100-400g m<sup>-2</sup> (Körner, 2003). While few specific reports of Australian biomass quantities are available, Bear and Pickering (2006) report much higher aboveground dry mass totals for alpine grasslands of over 1000g m<sup>-2</sup> in Kosciuszko National Park. However, alpine grasses generally retain large quantities of necromass in order to insulate the growing part of the plant, resulting in very dense tussocks (Körner, 2003). Necromass often represents the majority (60-70%) of the standing phytomass in the canopy (Hofstede *et al.*, 1995; Ni, 2004). The estimates of Bear and Pickering (2006) above are thus thought to represent aboveground phytomass rather than biomass.



Figure 2.4: subalpine grassland on Dargo High Plains.



The very small quantity of biomass in alpine grasslands is thought to relate primarily to the microclimatic advantages of small stature (Körner, 1998). Specifically, the dense, prostrate growth form reduces the efficiency of aerodynamic coupling with the planetary boundary layer by minimising the drag imposed by the relatively smooth surface (relative to aerodynamically ‘rough’ forest canopies) and thus dampening shear-induced turbulent mixing<sup>11</sup>. As such, daytime surface temperatures are more closely coupled to the radiative environment than to air temperature above the canopy (Grace, 1988). Therefore, when radiation is plentiful, temperatures are elevated in grasslands relative to taller, more open forest canopies, as dramatically illustrated in Figure 2.5. This effectively extends the length of the growing season by elevating surface temperatures relative to ambient conditions.

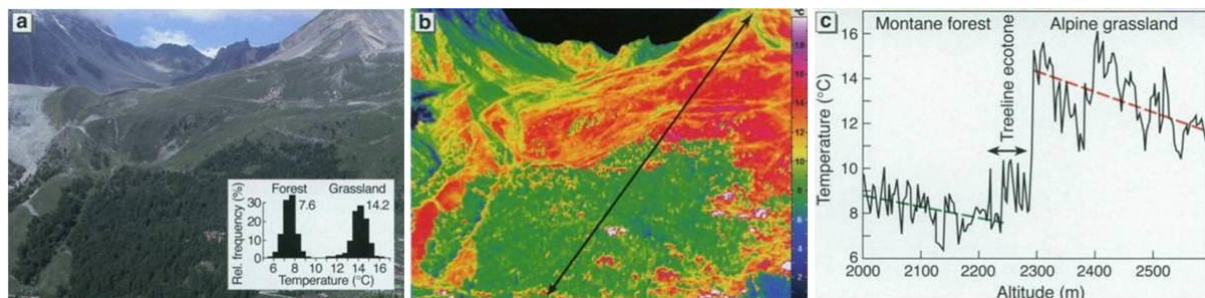


Figure 2.5: daytime land surface temperatures across a Swiss Alps elevational transect (from Körner, 2007, p322).

However, the majority of plant matter in grasslands broadly and in alpine grasslands in particular (Körner, 2003; Mokany *et al.*, 2006) is stored belowground. This is thought to reflect the fact that a relatively large proportion of plant resources must be invested in belowground biomass in order to maximise the capture of nutrients, since alpine soils are relatively nutrient-poor (see section 2.3.2 below) (Billings, 1974a). Moreover, plants may also have belowground structures for storage of resources that allow a more rapid response to moderation of climatic conditions at the onset of the growing season (Billings, 1974b). Although no published estimates were available for Australian subalpine grasslands, Jackson *et al.* (1996) report that belowground biomass in grasslands globally is generally less than  $1.5\text{kg m}^{-2}$ , with the ratio of above- to belowground biomass generally decreasing with colder and/or drier conditions (Gill *et al.*, 2002).

<sup>11</sup> Short stature also confers a number of additional advantages, including: i) avoidance of low temperatures and desiccation in winter by being under snow; ii) protection from wind damage; iii) reduced structural tissue requirement (Grace, 1988).

## 2.2.5 Soils

While a wide range of soil types occurs across the Australian Alps, the soils associated with alpine grasslands are generally friable, coarse-textured, organic-rich, nutrient-poor, acidic, and often poorly drained (Williams, 1987). These 'alpine humus soils' (Figure 2.6) are widespread and occur across a range of parent material types and floristic communities (Costin, 1986). Since alpine humus soils tend to be found more commonly on flat or gently sloping terrain, soil mantles are generally relatively deep (up to 1m) in the context of alpine regions (Costin *et al.*, 1952). This well-developed mantle also owes to the fact that, in contrast to other alpine areas of the globe that were ice-covered during the last glacial maximum (Poulenard and Podwojewski, 2006), glaciation was confined to a very small proportion of the Australian alpine landscape (Galloway, 1989).

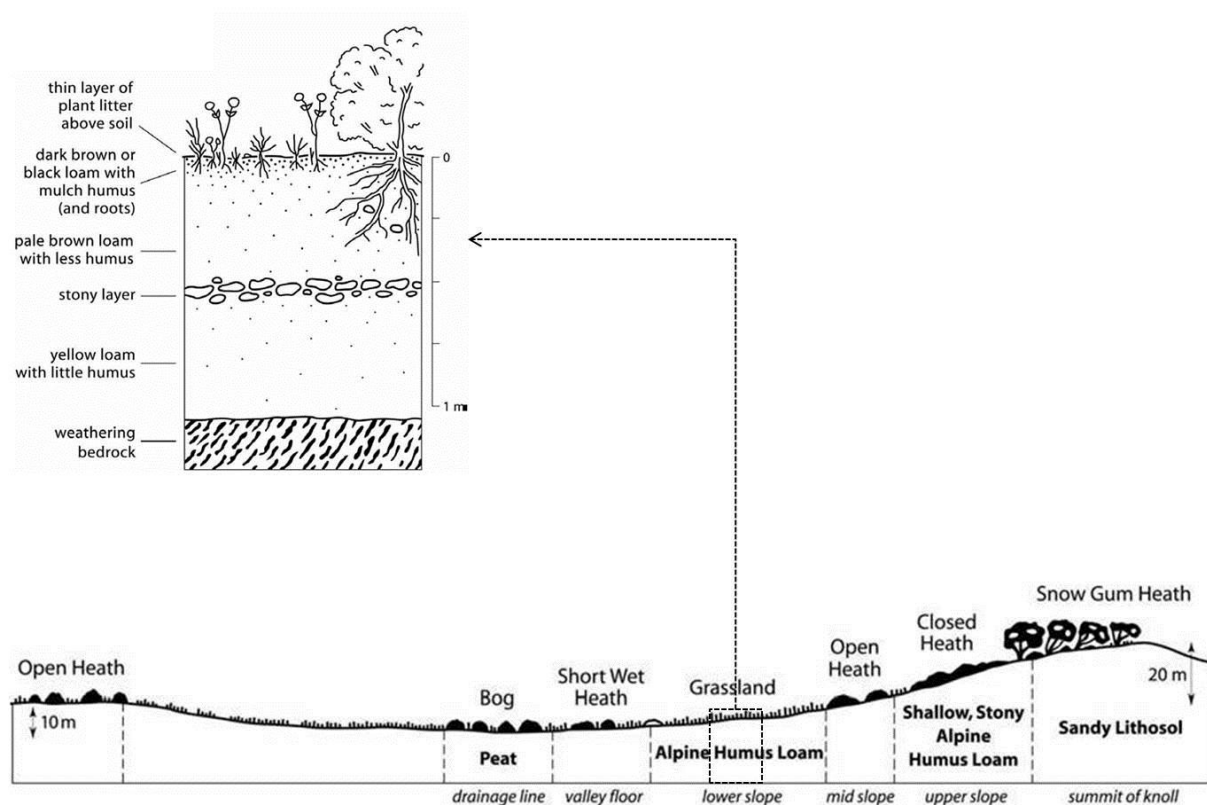


Figure 2.6: typical landscape / vegetation association and vertical structure of Australian alpine humus soils (modified from Mason and Williams, 2008a p3-4).

Large quantities of soil organic matter (SOM<sup>12</sup>) is a typical property of alpine soils (Poulenard and Podwojewski, 2006), reflecting the long-term balance between inputs of biological detritus primarily from litterfall and root mortality and its decomposition by the soil microbial community, as well as the secondary processes of leaching, fire and erosion (Torn *et al.*, 2009). Accumulation of SOM occurs because of the differential effects of climatic factors on these primary processes (Torn *et al.*, 2009). While low temperatures limit both production and decomposition (see sections 2.4.2 and 2.4.3), decomposition is more sensitive to low temperatures than production (Kirschbaum, 1995), and thus gradual accumulation of soil organic matter occurs. Similarly, high soil moisture is more limiting to decomposition than to production due to limitation of oxygen supply to aerobic soil microorganisms (Chapin *et al.*, 2002). The system is brought into equilibrium by negative feedback when SOM accumulation begins to reduce substrate optimality for production, for example via the progressive immobilisation of nutrients in the undecomposed SOM pool or decreases in pH (Körner, 2003). Strongly acid soils are common in alpine regions due to a combination of high rainfall and the effects of SOM itself. Acidification is facilitated both by the leaching of non-acid nutrient cations (e.g. Ca<sup>2+</sup> and Mg<sup>2+</sup>) with which organic matter forms soluble complexes, and the dissociation of H<sup>+</sup> ions from acid functional groups present in organic matter. The combination of leaching of nutrients and slow rates of decomposition and mineralisation (due to the effects of low temperatures on decomposer activity – see section 2.4.3.1) in turn typically results in low nutrient availability in alpine soils (Billings, 1974a; Brady and Weil, 2002).

## 2.3 Ecosystem Carbon Storage

The amount of carbon stored in different ecosystems – and the manner of its partitioning between vegetation and soil pools – is highly geographically variable, depending primarily on the climate and dominant plant functional type of the ecosystem (Post *et al.*, 1982; Schlesinger, 1997). While a specific ranking for ‘alpine grasslands’ is not available in the literature, Adams *et al.* (1990) report that the amount of carbon stored per unit area in ‘temperate and montane grasslands’ is slightly greater than the average for the terrestrial biosphere. Specifically, while the estimated area of this classification is approximately 5.9% of ecosystem coverage, it represents approximately 7.2% of the terrestrial biosphere’s carbon storage. In alpine grasslands, the pattern of storage of carbon is different to both lowland grasslands and lowland ecosystems in general in the sense that the vast

---

<sup>12</sup> A heterogeneous mixture of organic compounds in both chemical and particulate forms (Torn *et al.*, 2009).

majority of carbon stored in the ecosystem is in the organic matter of the soil rather than in vegetation, a pattern typical of cold, relatively moist ecosystems. The following discussion summarises the sizes of these pools reported in the literature for alpine grasslands (and closely analogous ecosystem classifications).

### 2.3.1 Vegetation

As discussed in section 2.2.4, in comparison to other ecosystems, the amount of phytomass is low in alpine grasslands, and the vegetation carbon pool is correspondingly small. Adams *et al.* (1990) report a total vegetation (i.e. above- and belowground phytomass) carbon pool of  $1\text{ kg m}^{-2}$  for temperate and montane grasslands, compared to over 20 to  $40\text{ kg m}^{-2}$  for various forest types, although amounts in some tropical forests may be up to 200 times higher (Schlesinger, 1997).

Literature estimates of pythomass carbon are presented in Table 2.1, and while varying substantially, aboveground carbon is generally less than  $0.5\text{ kgC m}^{-2}$ , and belowground quantities generally exceed those of aboveground. The variation reflects local differences not only in climatic factors but also in edaphic, ecological and human (management activity including grazing, harvesting *etc.*) factors. In general, however, colder and / or dryer sites generally have lower carbon quantities than climatically milder sites. In the moderate temperate climate of the European Alps (e.g. see Tappeiner *et al.*, 2008, in Table 2.1 below), reported values are similar to those cited by Adams *et al.* (1990) above. More recent estimates from the Tibetan Plateau report very low quantities of carbon in aboveground vegetation (Ni, 2004; Fan *et al.*, 2008; Ma *et al.*, 2010b). There are also apparent progressive decreases in aboveground vegetation carbon storage associated with increasingly cold and/or dry sites (eg. from mountain meadow to alpine meadow to alpine steppe to alpine desert, as observed in Ni, 2004). Correspondingly, where estimates are available, evidence suggests that a much larger proportion of phytomass (and thus carbon) is stored belowground on the Tibetan Plateau, most likely reflecting the effects of limited belowground resources (and thus higher investment in belowground structures to capture those resources) and extreme aboveground climates. In contrast to the very low quantities of carbon stored in phytomass in alpine grasslands, the soil carbon pool is much larger, as detailed below.

**Table 2.1: peak phytomass C storage values reported in the literature.**

Site	Source	Ecosystem classification	Method	Aboveground carbon (kg C m <sup>-2</sup> )	Belowground carbon (kg C m <sup>-2</sup> )	Total (kg C m <sup>-2</sup> )
Global	Adams <i>et al.</i> (1990)	Temperate and montane grasslands	Literature review	-	-	1
Global	Lambers <i>et al.</i> (2008)	Tundra and alpine meadow	Literature review	0.3	-	-
China	Ni (2004)	Mountain meadow	Direct survey data	0.074	-	-
		Alpine meadow		0.04	-	-
		Alpine steppe		0.013	-	-
		Alpine desert		0.005	-	-
Tibetan Plateau	Fan <i>et al.</i> (2008)	Alpine meadow	Direct survey data	0.103	2.063	2.166
		Alpine meadow-steppe	Direct survey data	0.041	1.74	1.78
Swiss Alps	Tappeiner <i>et al.</i> (2008)	Alpine meadow (acid soil)	Literature review	0.321	0.795	1.116
		Alpine meadow (calcareous soil);		0.271	0.595	0.865
Tibetan Plateau	Fang <i>et al.</i> (2010)	Alpine & temperate grasslands	Literature review	-	-	0.215-1.287
Tibetan Plateau	Ma <i>et al.</i> (2010a)	Mountain meadow	Direct survey data	0.11	0.53	0.64
		Alpine meadow	Direct survey data	0.048	0.29	0.34

### 2.3.2 Soils

As previously discussed, alpine soils are typically rich in organic matter, and thus are correspondingly a large store of carbon. A strong relationship between climate and soil carbon is observed globally, with soil carbon stocks directly correlated with rainfall and inversely correlated with temperature (Post *et al.*, 1982). As such, some of the highest soil carbon stocks are observed in ecosystems with cold, moist climates, including those of high-latitude (e.g. Tarnocai *et al.*, 2009) and high-altitude regions (Körner, 2003), as illustrated in Figure 2.7.

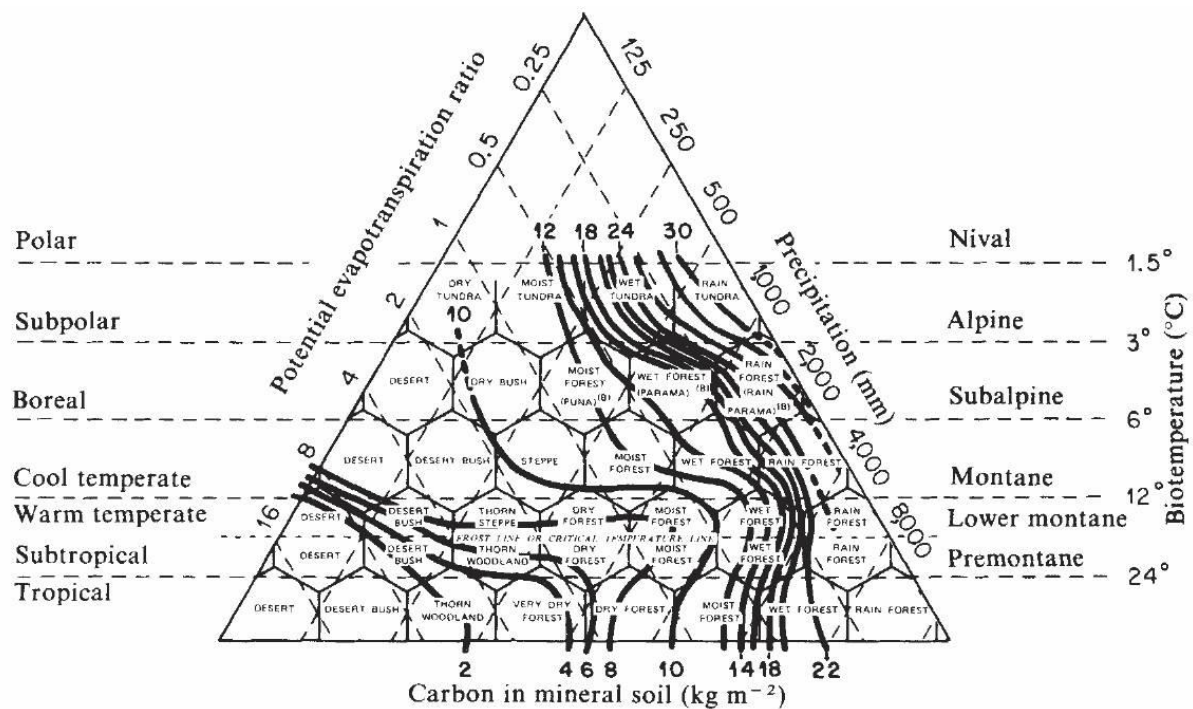


Figure 2.7: contours of soil organic carbon density superimposed on Holdridge (1947) world life zones (from Post *et al.*, 1982, p158).

Literature estimates of soil organic carbon density (SOCD<sup>13</sup>) in alpine and subalpine ecosystems are presented in Table 2.2. Schlesinger (1977) reports average SOCD values for ecosystems designated as 'alpine and tundra' of 21kgC m<sup>-2</sup>, with included estimates from profiles generally sampled either to bedrock or to 1m. Given the relatively shallow soil profiles often present in mountain soils, this implies that such estimates capture the bulk of total soil carbon. Adams *et al.* (1990) report SOCD of 13kgC m<sup>-2</sup> for temperate and alpine grasslands. Post *et al.* (1982) offer SOCD estimates for tundra only, but characterise tundra as occurring in both subpolar and alpine landscapes, citing 10.9, 22.2 and 36.6kgC m<sup>-2</sup> for moist, wet and rain tundra, respectively (tundra mean = 21.8kgC m<sup>-2</sup>). For sub/alpine soils generally, Körner gives a far broader range of 5-51kgC m<sup>-2</sup>; however, the largest values are reported to occur under dwarf shrub-dominated ecosystems at relatively low altitudes, and values of 4-22kgC m<sup>-2</sup> are nominated as being more typical of alpine conditions.

The estimates in Table 2.2 illustrate a great degree of variability between sites, reflecting the effects of both climatic and non-climatic (e.g. edaphic, management) factors. In China, grassland soils store a similar quantity of C to those of forests (Xie *et al.*, 2007), but meadow ecosystems in the colder climates of the high-elevation Tibetan Plateau have the highest grassland SOC (Wang *et al.*, 2003). Nonetheless, estimates for sites on the Tibetan Plateau (typically less than 10kgC m<sup>-2</sup>) are generally lower than those for sites in other parts of the world (e.g. Europe, New Zealand, US, with wide variation in values but generally between 10-20kgC m<sup>-2</sup>). This in part relates to the fact that much of the Tibetan Plateau is also extremely dry, and Yang *et al.* (2008) report a direct correlation between soil organic carbon and precipitation across the Plateau. Correspondingly, Yang *et al.* (2010b) report higher values in wetter sites (e.g. mountain meadow) and lower values in dryer sites (e.g. alpine steppe). However, it has also been consistently observed internationally (Garcia-Pausas *et al.*, 2007) and in Australia (Costin *et al.*, 1952) that at the highest elevations and lowest temperatures, the trend towards increasing SOCD reverses.

Since the quantities and patterns of allocation of carbon to vegetation and soil carbon pools are highly climatically dependent, changes in climate are – as detailed in Chapter 1 - likely to drive changes in carbon storage. This change in storage arises due to the different effects of a changing climate on the dynamic balance between processes of carbon import to and export from the ecosystem, to which the discussion now turns.

---

<sup>13</sup> Whole-profile integrated gravimetric soil carbon content per square metre.

**Table 2.2: soil organic carbon (SOC) density values reported in the literature.**

Site	Ecosystem classification	Source	Method	Depth of profile (cm)	Mean SOC density (kg C m <sup>-2</sup> )
Global	Alpine ecosystems	Schlesinger (1977)	Literature review	Variable	4-27
Global	Tundra	Post <i>et al.</i> (1982)	Literature review	Variable	10.9-36.6
Global	Temperate / montane grasslands	Adams <i>et al.</i> (1990)	Literature review	Variable	13
Global	Alpine ecosystems	Körner (2003)	Literature review	Variable	5-51
Scotland	Alpine ecosystems	Grieve (2000)	Direct survey	Variable (complete profile)	4-22
USA	Subalpine meadow	Prichard <i>et al.</i> (2000)	Direct survey	Variable (complete profile)	6.7-12.4
New Zealand	Montane tussock grassland	Tate <i>et al.</i> (2000)	Direct survey	Variable (complete profile)	19.9
China (Tibet)	Alpine meadow	Ni (2002)	Survey / review	Variable	18.2
China (Tibet)	Alpine meadow	Wu <i>et al.</i> (2003)	Meta-analysis of survey data	Variable (complete profile)	9.47
	Subalpine meadow			Variable (complete profile)	16.65
France	Montane grasslands	Garcia-Pausas <i>et al.</i> (2007)	Direct survey	Variable (complete profile)	5.9-29.9
China (Tibet)	Alpine meadow	Ohtsuka <i>et al.</i> (2008)	Direct survey	0-30	2.6 (4400m ASL)
			Direct survey		13.7 (4950m ASL)
China (Tibet)	Mountain meadow	Yang <i>et al.</i> (2008)	Direct survey and satellite NDVI / vegetation-soil C regressions	0-30 / 0-50 / 0-100	6.17 / 7.51 / 9.05
	Mountain steppe			0-30 / 0-50 / 0-100	4.43 / 5.43 / 6.52
Switzerland	Montane grassland	Leifeld <i>et al.</i> (2009)	Direct survey	0-30	5.3-11.6
China (Tibet)	Alpine meadow	Yang <i>et al.</i> (2009)	Satellite NDVI / vegetation-soil C regressions	0-30	5.48
	Alpine steppe			0-30	2.54

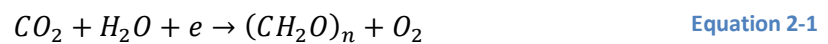


Switzerland	Alpine grassland	Djukic <i>et al.</i> (2010)	Direct survey	Variable (complete profile)	26 (1700m ASL) 13 (1900m ASL)
China (Tibet)	Alpine meadow	Yang <i>et al.</i> (2010b)	Direct survey	0-30 / 0-100	8.44 / 12.72
	Alpine steppe			0-30 / 0-100	3.11 / 5.17
	Mountain meadow			0-30 / 0-100	12.02 / 20.13
	Mountain steppe			0-30 / 0-100	9.43 / 13.4

## 2.4 Ecosystem Carbon Balance

### 2.4.1 Conceptual overview

At the ecosystem scale, the time-dependent carbon balance - or net ecosystem production (NEP) – represents the dynamic balance between continual processes of carbon import to and export from the system. Carbon enters ecosystems via photosynthesis, in which plants reduce atmospheric CO<sub>2</sub> to yield a carbohydrate molecule in the presence of water (with oxygen as a by-product), an endergonic reaction driven by solar radiation in the 400-700nm waveband (Campbell and Norman, 1998). A simplification of this process is as follows (where  $e$  represents energy in the form of solar photons) (Schlesinger, 1997):



Essentially the reverse process occurs (i.e. Equation 2-1 proceeds from right to left) when respiration occurs – harvesting the energy thereby liberated for work - and CO<sub>2</sub> is released back to the atmosphere. In terrestrial ecosystems, multicellular plants are thus the dominant means by which carbon is imported into the ecosystem from the atmosphere. The aggregate gross photosynthetic fixation of carbon by plants per unit ecosystem area is gross primary production (GPP) (Figure 2.8). Approximately half of GPP is generally returned to the atmosphere by plants via autotrophic respiration ( $R_a$ ). Heterotrophic respiration ( $R_h$ ) of soil microbes and saprophytic fungi - as well as multicellular animals - also transfers carbon from ecosystem to atmosphere. The sum of  $R_a$  and  $R_h$  constitutes ecosystem respiration ( $R_e$ ). Thus net ecosystem production (NEP) represents the difference between these assimilatory and respiratory processes, as follows (Chapin *et al.*, 2006):

$$NEP = GPP - R_e$$
Equation 2-2

Net ecosystem exchange (NEE) is similar (although of opposite sign<sup>14</sup>) to NEP, but differs in that NEE includes only the ecosystem / atmosphere exchange of carbon. It thus may include non-

---

<sup>14</sup> As noted in Chapter 1, 1.7, the sign convention used for carbon fluxes references the flux sign to the atmosphere i.e. net surface carbon influx (efflux) represents a loss (gain) of carbon with respect to the atmosphere and is thus denoted with a negative (positive) sign.

respiratory carbon effluxes such as photo-oxidation of organic carbon and exclude respiratory carbon effluxes not transferred via the atmosphere (for example hydrologic transfer of dissolved inorganic carbon) (Chapin *et al.*, 2006). The actual rate of carbon accumulation in an ecosystem thus ultimately depends on influxes and effluxes of non-CO<sub>2</sub> carbon compounds – both via the atmosphere (e.g. volatile organic compounds [VOC], carbon monoxide [CO] and methane [CH<sub>4</sub>]) and other transfer pathways (e.g. aquatic exchanges of dissolved organic and inorganic carbon [DIC and DOC, respectively]). Over long (e.g. multi-decadal) timescales it also depends on the effects of disturbances (including for example fire, insect attack, grazing by animals or harvesting by humans) that – while an important term in the carbon balance - may not occur concurrently with the measurement period. The long-term net accumulation of carbon in an ecosystem is thus represented by the net ecosystem carbon balance (NECB; Chapin *et al.*, 2006):

$$NECB = -NEE + F_{CO} + F_{CH_4} + F_{VOC} + F_{DIC} + F_{DOC} + F_{PC} \quad \text{Equation 2-3}$$

Where F represents ‘flux’ and F<sub>PC</sub> represents the flux of particulate carbon via disturbance. Since NECB is also highly spatially variable, spatial and temporal integration of NECB over a heterogeneous landscape is termed net biome productivity (NBP). Given the associated methodological difficulties, measurement of the additional terms of NECB – and extrapolation to NBP - is beyond the scope of this investigation. However, when the additional terms in Equation 2-3 are small, NEE can be considered a useful approximation of NECB.

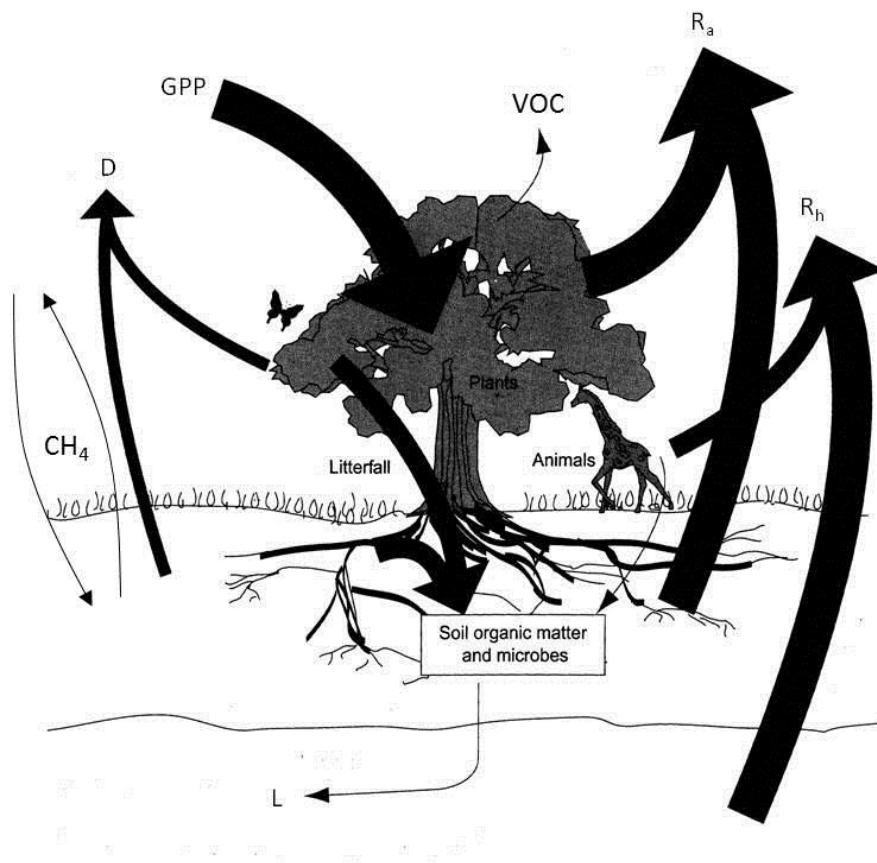


Figure 2.8: ecosystem carbon balance (GPP = gross primary production;  $R_a$  = autotrophic respiration;  $R_h$  = heterotrophic respiration; D = disturbance; L = leaching; VOC = volatile organic compounds;  $CH_4$  = methane; adapted from Chapin *et al.*, 2002, p.124).

Under stationary climatic conditions in late successional ecosystems, the carbon balance is *on average* likely to be approximately in equilibrium (Lambers *et al.*, 2008). However, over short periods NEE is rarely zero. It fluctuates in response to diurnal and seasonal cycles, as well as interannual climatic variability. This fluctuation occurs because of the distinct responses of the biotic processes of GPP and  $R_e$  to abiotic climatic drivers. Sustained imbalances in NEE may thus also occur in response to long term changes in climate. A first step in developing insight into potential responses of ecosystem carbon balance to future changes in climate is to understand how climatic drivers control ecosystem carbon balance at present. A discussion of ecosystem responses to these drivers – with specific reference to alpine grassland ecosystems – follows.

## 2.4.2 Primary controls of gross primary production (GPP)

On hourly, daily and seasonal time scales GPP is primarily controlled by solar radiation, temperature and moisture availability (Baldocchi and Valentini, 2004). While the nature of the response of GPP to these abiotic drivers in reality differs greatly among species, the discussion below focuses on the ecosystem-scale response, consistent with the scale of analysis in this study.

### 2.4.2.1 *Solar radiation*

As discussed in section 2.4.1, solar radiation is the energy source for photosynthesis, and as such the radiation environment is a primary driver of GPP. Photosynthetic responses to light are approximately hyperbolic; efficiency is highest at low insolation, gradually declines until light saturation and is eventually inhibited under high insolation (Jones, 1992). Among alpine plants, saturation generally occurs at relatively high levels, an evolutionary response to the reduced atmospheric optical depth and correspondingly higher insolation periodically experienced at higher altitudes (Billings, 1974b). However, high-elevation ecosystems may also be subject to increased orographic cloud, and thus may experience high insolation infrequently (Barry, 2008). The isotropic radiation field under cloudy skies allows increased photon penetration of the canopy and thus exposure of leaves that are partially or fully shaded under direct beam radiation (Campbell and Norman, 1998). This may be of particular relevance in alpine tussock grassland ecosystems because of the short, dense tussock form. Thus at low insolation under cloudy skies light use efficiency is often substantially enhanced in tussock grasslands (Chen *et al.*, 2009).

Photoperiod is also an important factor determining the length of the growing season, but its effects are seasonally variable (Körner, 2003). Since temperatures generally lag insolation by 1-2 months, photoperiod is more likely to limit growth in autumn, when temperatures are high relative to photoperiod, and is less influential during spring, when temperatures are low relative to photoperiod and snow often persists (Ram *et al.*, 1988; Van Wijk and Williams, 2003; Migliavacca *et al.*, 2011).

#### 2.4.2.2 *Temperature*

As with all chemical reactions, the biochemical reactions involved in photosynthesis are highly temperature-dependent, increasing exponentially as a function of temperature. Because the low kinetic energy of molecules at low temperatures reduces rates of chemical reaction (Jones, 1992), alpine plants adjust catalytic enzyme levels to increase photosynthetic reaction rates at low temperatures (Billings, 1974a). However, while this adaptation broadens the range over which alpine plants can maintain photosynthetic response, peak temperature optima for photosynthesis among alpine plants are broadly comparable to those of lowland species (Körner, 2003). It is instead the previously discussed decoupling effect of the morphological characteristics of the canopy (see section 2.2.4) that allow continued activity at lower ambient air temperatures. The temperatures actually experienced by the plant are instead strongly linked to the radiant environment, such that when radiation is available to drive photosynthesis, temperatures tend to be correspondingly warm (Körner, 2003). However, there is an inevitable trade-off that arises in relation to this morphological cold adaptation: the risk of high temperature photosynthetic constraint during warmer periods. This occurs primarily due to increased photorespiration, and in extreme cases, enzyme inactivation and photo-oxidative destruction of pigments (Jones, 1992).

Nevertheless, ambient air temperature does not generally exert a strong influence on alpine plant productivity at shorter (i.e. hourly to daily) timescales (Körner, 2003). However, at very low temperatures continued plant activity is constrained by both the biochemical limitation imposed on metabolic and photosynthetic processes and the potential for chilling or freezing injury to vital organs (Jones, 1992). Alpine plants therefore undergo a dormancy period during the coldest conditions (Billings, 1974b; Körner, 2005). This typically occurs at temperatures close to freezing (Larcher, 2012). Because of the correspondingly truncated growing season, annual primary production is relatively low in alpine ecosystems, despite the fact that it is on average approximately comparable to that of lowland ecosystems during the growing season. Thus growing season length is a primary determinant of annual alpine plant primary production (Körner, 2003).

Low temperature also has indirect effects on plant growth via its effects on rates of both nutrient mineralisation (Billings, 1974a) and uptake by plants (Chapin, 1978). In effect, a trade-off between production and the resources required to support production arises. In order to optimise capture of vital – and limited – nutrients (for example, nitrogen, which is vital to leaf photosynthetic activity), a large proportion of assimilated carbon must be allocated to non-productive belowground biomass, which correspondingly reduces the availability of resources for investment in productive

leaf tissue (therefore limiting leaf area and in turn photosynthetic uptake of carbon). Therefore low temperatures indirectly limit productivity via nutrient supply.

#### 2.4.2.3 *Moisture availability*

Water fulfils essential biochemical, transport, structural and thermoregulatory roles in the functioning of plants (Lambers *et al.*, 2008). Evaporation from stomata drives water movement along a hydrostatic gradient from the soil through the plant and acts as a cooling agent by dissipating surplus energy via latent heat release; however, it is also a major pathway for water loss among ecosystems. Plant moisture stress may be induced by low supply (i.e. low soil moisture) and/or high demand (i.e. high leaf – atmosphere vapour pressure deficit), and plants thus act to regulate water potential by varying stomatal aperture in response to these signals. Because stomata are also the conduit for carbon uptake from the atmosphere, water loss is an inevitable consequence of photosynthesis; correspondingly, reductions in stomatal conductance in response to water status alter the supply of CO<sub>2</sub> and thus rates of carbon assimilation (Jones, 1992).

However, while water limitation is, as previously stated, common in lowland grasslands, it is less commonly the case in alpine regions because altitude-driven reductions in temperature (and thus atmospheric demand) often accompany orographically-induced increases in rainfall (although xeric mountain environments occur in some regions) (Barry, 2008). Moreover, the low leaf area of the vegetation, often dense canopy and low aerodynamic conductance (and thus decoupling, as discussed in relation to temperature in section 2.2.4) associated with the relatively smooth surface in alpine ecosystems all combine to limit rates of evapotranspiration (Körner, 2003). Additionally, reductions in stomatal aperture have more effect on transpirational losses than on carbon gains (Chapin *et al.*, 2002).

For these reasons, reports of strong control of plant production by moisture availability in alpine grasslands are relatively infrequent in the literature. Transpiration rates are largely insensitive to soil moisture availability until approximately 75% of available soil water is depleted (Chapin *et al.*, 2002), and Wieser *et al.* (2008) report that evapotranspiration is largely insensitive to interannual rainfall variability in Swiss Alpine grasslands. Therefore, soil moisture variability above a given threshold is unlikely to have a significant impact on transpiration and thus – via stomatal regulation of moisture loss - GPP. For relatively moist sites (i.e. high precipitation and / or low evapotranspiration), soil moisture may remain above this threshold even in dry years. Vegetation

productivity may however be much more sensitive to drought at lower rainfall sites. In sites where soil moisture is periodically limiting, productivity responses are strongly tied to the seasonality of rainfall: in particular, summer rather than winter rainfall is the crucial determinant of productivity (Gilgen and Buchmann, 2009). Long dry periods during summer, when atmospheric demand is increased by warm temperatures, result in lower soil moisture than at other times of year, with corresponding effects on plant growth (Griffin and Hoffmann, 2011).

#### 2.4.2.4 *CO<sub>2</sub> partial pressure*

In addition to causing changes in climate, the increasing concentration of CO<sub>2</sub> in the earth's atmosphere also has significant biochemical effects with corresponding ramifications for the carbon balance of many terrestrial ecosystems (Körner *et al.*, 2007; Ziska and Bunce, 2007). Given that: i) alpine plants generally endure low CO<sub>2</sub> partial pressures (pCO<sub>2</sub>) by virtue of high altitude, and; ii) pCO<sub>2</sub> experienced at sea level prior to the industrial revolution today occurs above 2600m, a marked response of alpine plants might be expected. The possible effects of increasing atmospheric CO<sub>2</sub> are nonetheless not addressed in this study, since multi-year CO<sub>2</sub>-enrichment experiments have elicited effectively no positive growth response in alpine grasslands (Körner *et al.*, 1997).



#### 2.4.2.5 Biotic controls

The temporal dynamics of carbon assimilation reflect variations in both the abiotic factors described above as well as the corresponding biotic response to those factors. One of the key measures of biotic response that determines the ecosystem carbon balance at the ecosystem scale is the leaf area of the canopy (the standard measure of which is leaf area index, or LAI<sup>15</sup>) (Chapin *et al.*, 2002). Since the leaf surface is the site of photosynthetic uptake of CO<sub>2</sub>, photosynthetic activity depends directly on the amount of leaf area deployed by the vegetation. Since LAI varies in response to abiotic factors, it can be argued that it is a *proximate* control of photosynthetic activity whereas the abiotic factors discussed above represent *ultimate* controls. Despite large variation in ecosystem-scale GPP across biomes and corresponding environmental conditions, when scaled by leaf area and length of growing season it is maintained within a relatively small range (1-3gC m<sup>-2</sup> leaf d<sup>-1</sup>) (Chapin *et al.*, 2002). Since growing season length is in turn a function of the abiotic factors discussed above, an empirical model may therefore theoretically capture the ecosystem carbon balance without explicit inclusion of biotic variables such as leaf area; biotic response (including the effects of leaf area) is instead captured in the parameters of the model functions.

However, leaf area is often required as an additional explanatory variable in ecosystem models because the specific response of the canopy to abiotic factors may not be a priori known or may be too complex to be adequately captured by an empirical model. For example, the phenological responses of the canopy to abiotic factors may be threshold-driven; in the case of alpine ecosystems, this is often related to photoperiodic or thermal cues (Körner, 2003). Moreover, large external (e.g. management) impacts may also result in step changes in ecosystem function; for example, cutting of pasture grasses for hay causes a step change in leaf area that is reflected in the carbon balance (Rogiers *et al.*, 2008; Wohlfahrt *et al.*, 2008; Schmitt *et al.*, 2010).

---

<sup>15</sup> Unit area leaf per unit area ground, typically expressed in m<sup>2</sup> m<sup>-2</sup> (Chapin *et al.*, 2002).

### 2.4.3 Primary controls of ecosystem respiration ( $R_e$ )

As discussed in section 2.4.1, ecosystem respiration ( $R_e$ ) is the sum of autotrophic (above- and belowground) and heterotrophic (largely soil microbial) components. Since these components both involve fundamentally similar biochemical reactions, they are expected to respond in broadly similar ways to environmental stimuli. Moreover, separation of these components is an ongoing research challenge, and was beyond the scope of this study; as such, the discussion below primarily summarises the literature addressing  $R_e$ .

#### 2.4.3.1 *Temperature*

Autotrophic respiration increases exponentially with temperature in the short term (Lambers *et al.*, 2008), while at longer time scales it is thought to be maintained at a relatively constant fraction of GPP (approximately 60% in grassland ecosystems) (Amthor and Baldocchi, 2001). Nonetheless, transient extreme high temperatures may occur, in which case respiration may be constrained by enzyme inactivation (which also occurs at low temperatures) or death of cells, organs or individuals (Jones, 1992; Lambers *et al.*, 2008). Similarly, heterotrophic respiration also increases approximately exponentially with temperature (Fang and Moncrieff, 2001), although there is also an apparent acclimation response with temperature sensitivities decreasing with increasing temperature (Kirschbaum, 1995; Kirschbaum, 2000).

In alpine grasslands an exponential relationship between temperature and  $R_e$  is correspondingly generally reported (e.g. Cao *et al.*, 2004; Kato *et al.*, 2004; Kato *et al.*, 2006; Bahn *et al.*, 2008). In contrast to lowland grassland ecosystems, where soil moisture may exert the dominant control over  $R_e$ , temperature is generally reported to be the dominant control over  $R_e$  in alpine grasslands (e.g. Koch *et al.*, 2008; Fu *et al.*, 2009; Warren and Taranto, 2011). It should also be noted that respiration rates also depend on a large number of other factors, including substrate quality (although this is in turn indirectly related to temperature by its influence on the distribution of vegetation functional groups that contribute litter to the soil), the composition of the decomposer

community, soil physical and chemical properties and disturbance regimes (e.g. fire)<sup>16</sup> (Hobbie *et al.*, 2000; Davidson and Janssens, 2006).

#### 2.4.3.2 *Moisture availability*

It has long been established that soil heterotrophic respiration is sensitive to soil moisture levels (Orchard and Cook, 1983). When soils are close to saturation, reduced rates of diffusion of oxygen through the soil limit respiration rates; at very low soil moisture, diffusion of substrate to microbes via water films on soil particles is reduced, thereby also limiting respiration (Davidson and Janssens, 2006). The level of autotrophic respiration is regulated by the requirements of other processes (primarily growth and maintenance) for its products (Amthor and Baldocchi, 2001). As such, under conditions of sustained dessication, respiration decreases in concert with the general decline in carbon assimilation and overall metabolism associated with the slower growth resulting from these conditions (Lambers *et al.*, 2008). Under saturated conditions, aerobic root respiration may also be reduced (Lambers *et al.*, 2008).

Thus both autotrophic and heterotrophic respiration are generally sensitive to very dry or very moist conditions; this is reflected in  $R_e$ , which is relatively insensitive at intermediate values, with little response of soil respiration to changes in soil moisture between 20-50% by volume (Fang and Moncrieff, 2001), a result also broadly replicated in alpine soils (Suh *et al.*, 2009). Therefore wetting of very dry soils and drying of very wet soils may both produce increases in soil respiration (Koch *et al.*, 2008). Soil moisture is therefore an important determinant of  $R_e$  during summer at some alpine grassland ecosystems (Li *et al.*, 2008; Wohlfahrt *et al.*, 2008), although this is generally at drier sites. For example, Wohlfahrt *et al.* (2008) report that while at more moist (alpine) grassland sites, temperature was the primary control on  $R_e$ , at drier (lowland or drought-affected) sites soil moisture was more important. Low soil moisture has also been observed to reduce  $R_e$  in Australian subalpine grasslands during both summer and autumn (Warren and Taranto, 2011). On the other hand, at more moist sites, periodic saturation of soil may also cause inhibition of  $R_e$  (Hu *et al.*, 2008).

---

<sup>16</sup> These factors (and the complex interplay between them) are extremely important in determining the temperature dependence of respiration, since they may give rise to different (similar) apparent temperature sensitivities that mask similar (different) intrinsic sensitivities (Davidson and Janssens, 2006). This may explain the often contradictory results of temperature dependence studies in the literature (von Lützow and Kögel-Knabner, 2009).

The effects of dry soils thus appear to be qualitatively similar for  $R_e$  and GPP: both are relatively insensitive above a given soil moisture threshold, but become increasingly sensitive below this threshold (Reichstein *et al.*, 2007). Crucially, however, recent multisite analyses indicate that GPP is approximately 50% more sensitive to drought than  $R_e$  across a range of different ecosystem types (Schwalm *et al.*, 2010). It is for this reason that sustained drought conditions generally coincide with large net losses of carbon from ecosystems (e.g. Ciais *et al.*, 2005). On the other hand,  $R_e$  is more constrained by moist conditions than is GPP (Chapin *et al.*, 2002).

#### 2.4.3.3 *Biotic controls*

As was previously noted with respect to GPP, while the magnitude of  $R_e$  represents the biotic response to abiotic factors, it may be necessary to invoke additional biotic factors to explain this response. In the case of GPP, this was related to the fact that either the underlying response of GPP to abiotic factors was poorly understood, or that other factors – such as disturbance in the form of, for example, agricultural cultivation, confounded the ecological response. Because the feedstock of  $R_e$  is labile carbon compounds generated by photosynthetic assimilation,  $R_e$  is inevitably tied to primary production.

Autotrophic respiration ( $R_a$ ) is directly dependent on photosynthetic assimilate supply (Amthor and Baldocchi, 2001), while the labile carbon pool available in the soil matrix for heterotrophic respiration ( $R_h$ ) depends on both exudation of assimilates from the roots and, over longer time scales, addition of detritus through litterfall (Davidson and Janssens, 2006). Cross-site comparative analyses have thus identified spatial variation in productivity as an important (Reichstein *et al.*, 2003) or even dominant (Janssens *et al.*, 2001) control on  $R_e$ . Recent analysis has thus demonstrated that  $R_e$  is strongly correlated with GPP ( $r^2=0.89$ ) across the global network of flux sites (Baldocchi, 2008). Single site studies have similarly identified the importance of GPP in explaining temporal variations in  $R_e$  in grasslands (Xu and Baldocchi, 2004; Chimner and Welker, 2005; Aires *et al.*, 2008; Bahn *et al.*, 2008; Hussain *et al.*, 2011), while experimental studies in which assimilate supply was interrupted by tree girdling (Hogberg *et al.*, 2001) or clipping of herbaceous vegetation (Craine *et al.*, 1999; Bahn *et al.*, 2006) have highlighted the importance of assimilate supply in controlling  $R_e$ .

While the above discussion implies a linkage in which  $R_e$  is dependent on GPP, the mineralisation of nutrients required to mobilise nutrients in plant-available (i.e. inorganic) forms

occurs as a result of heterotrophic respiratory activity. Without this activity, nutrients sequestered in organic matter would remain unavailable and plant production would quickly halt, since, next to water, nutrient supply is the most important factor limiting biological production (Lambers *et al.*, 2008). The linkage between GPP and  $R_e$  is therefore ultimately *interdependent*. Detailed discussion of these issues is however beyond the scope of this study.

#### 2.4.4 Estimates of annual carbon balance among alpine grassland ecosystems

As discussed in Chapter 1, at present the terrestrial biosphere is acting as a net carbon sink, as confirmed both by top down accounting methods (Canadell *et al.*, 2007) and bottom up ecosystem-scale measurements (Baldocchi, 2008). The available literature indicates that mountain and alpine grassland ecosystems are – on average – also net carbon sinks. It should be emphasised that the data summarised below almost exclusively represent estimates of NEE (derived using the eddy covariance technique – see section 2.5), and as such may be slightly different from estimates of whole ecosystem carbon accumulation (i.e. NECB), as previously discussed.

While no published reviews of aggregate global estimates of NEE are available in the literature for alpine grasslands as a biome, the available site values of cumulative annual NEE, GPP and  $R_e$  are summarised in Table 2.3. The mean NEE ( $\pm$ SD) of the included site estimates is approximately  $-69 \pm 146 \text{ gC m}^{-2} \text{ a}^{-1}$ . Some of the data included represent NEE of intensively managed grasslands (e.g. Zeeman *et al.*, 2010); where authors have provided estimates of the magnitudes of non-atmospheric or non- $\text{CO}_2$  carbon exchanges, a more representative estimate of net carbon uptake can be obtained. When these estimates are used (for applicable sites) instead of NEE, the mean uptake decreases to  $-55 \pm 126 \text{ gC m}^{-2} \text{ a}^{-1}$ , with a range of -290 to  $256 \text{ gC m}^{-2} \text{ a}^{-1}$ .

The results for alpine grasslands are similar to those reported by Novick *et al.* (2004) for a range of different lowland grasslands (rangelands, steppe, prairie) in the USA with a mean ( $\pm$ SD) of  $-53 \pm 157 \text{ gC m}^{-2} \text{ a}^{-1}$ , although a much larger range of +400 to  $-800 \text{ gC m}^{-2} \text{ a}^{-1}$ . Despite the similar mean to that reported here, the broader range most likely reflect the effects of rainfall variability, as previously discussed. A more recent analysis of a range of European grasslands (including dry semi-natural pastures, intensively managed near-coastal grasslands and cool, moist subalpine grasslands) by Gilmanov *et al.* (2007) reports a slightly smaller NEE range of +160 to  $-650 \text{ gC m}^{-2} \text{ a}^{-1}$ , with stronger (though still highly variable) mean ( $\pm$ SD) uptake of  $-150 \pm 200 \text{ gC m}^{-2} \text{ a}^{-1}$ . The higher mean partly relates to the relatively high carbon uptake of the managed grasslands; Schmitt *et al.* (2010) report that among mountain grasslands, NEE as well as its component fluxes tend to decrease with decreasing levels of management. This is thought to be associated with the fact that the managed sites have higher soil fertility due to fertiliser addition. Thus among managed grasslands, Gilmanov *et al.* (2007) report NEE of up to  $-2400 \text{ gC m}^{-2} \text{ a}^{-1}$ , and GPP and  $R_e$  of up to -6900 and  $6000 \text{ gC m}^{-2} \text{ a}^{-1}$ , respectively.

**Table 2.3: alpine grassland NEE values reported in the literature (for sites where disturbance factors and non-CO<sub>2</sub> carbon exchanges were explicitly accounted for, NEP is given).**

Site	Ecosystem classification	Source	Period	Peak daily NEE (gC m <sup>-2</sup> d <sup>-1</sup> )	Annual NEE (gC m <sup>-2</sup> a <sup>-1</sup> )	Annual GPP (gC m <sup>-2</sup> a <sup>-1</sup> )	Annual R <sub>e</sub> (gC m <sup>-2</sup> a <sup>-1</sup> )
Haibei, Qinghai	Alpine meadow	Gu <i>et al.</i> (2003)		-15.9	-	-	-
Haibei, Qinghai	Alpine meadow	Kato <i>et al.</i> (2004)	2001-02	-3.9	-	-	-
Haibei, Qinghai	Alpine meadow	Gu <i>et al.</i> (2005b)	2001-02	-	-290	-	-
Haibei, Qinghai	Alpine meadow	Kato <i>et al.</i> (2006)	2002	-	-78.5	575.1	496.6
			2003	-	-91.7	647.3	555.6
			2004	-	-192.5	681.1	488.5
Monte Bondone, Italian Alps	Alpine meadow	Bahn <i>et al.</i> (2008)	2002-04	-	-	1358	1743
Stubai, Austrian Alps	Mountain meadow		2002-06	-	-	1697	1792
Ötztal Range, Tyrol, Austria	Alpine meadow	Koch et al. (2008)	2003	-	-120	-	-
			2004	-	-109	-	-
Mount Rigi, Central Switzerland	Subalpine grassland	Rogiers <i>et al.</i> (2008)	2002-03	-	+120	1201	1321
			2003-04	-	+256	1358	1614
			2004-05	-	+116	1253	1371
Haibei, Qinghai	Alpine meadow	Zhao <i>et al.</i> (2005)	2004	-	-282	-	-
Haibei, Qinghai	Alpine shrub meadow	Fu <i>et al.</i> (2009)	2004	-	-85.3	501.5	416.2
			2005	-	-51.7	553.9	502.2
Damxung, Tibet	Alpine steppe meadow		2004	-	+37.4	238.0	278.3
			2005	-	+54.8	173.7	229.4
Continued below							

Table 2.3 continued

Site	Ecosystem type	Source	Period	Peak daily NEE (gC m <sup>-2</sup> d <sup>-1</sup> )	Annual NEE (NEP) (gC m <sup>-2</sup> a <sup>-1</sup> )	Annual GPP (gC m <sup>-2</sup> a <sup>-1</sup> )	Annual R <sub>e</sub> (gC m <sup>-2</sup> a <sup>-1</sup> )
Qilian Mountains, Tibet	Alpine meadow, 3 sites:	Zhang <i>et al.</i> (2009)	2006				
	<i>Kobresia pygmaea</i>			0.919	-76.9	799	722
	<i>K. humilis</i>			1.446	-149.4	1053	914
	<i>K. tibetica</i>			1.550	-147.6	1158	1011
Monte Bondone, Italian Alps	Alpine meadow	Marcolla <i>et al.</i> (2011)	2003	-	+50	-	-
			2004	-	-29	-	-
			2005	-	+15	-	-
			2006	-	-75	-	-
			2007	-	-110	-	-
			2008	-	-28	-	-
			2009	-	+112	-	-



However, there is a second reason that carbon uptake in alpine grasslands is expected to be lower than in other ecosystems. The terrestrial biosphere carbon sink implies that assimilatory carbon gain by ecosystems exceeds respiratory carbon loss, and data from Fluxnet eddy covariance sites indicates that this imbalance is remarkably consistent:  $R_e$ :GPP is approximately 0.77 (earlier estimates by Law *et al.*, 2002 yielded an estimate of 0.83), with GPP explaining 89% of cross-site variation in  $R_e$  (Figure 2.9a) (Baldocchi, 2008). Given this imbalance, as GPP increases, the magnitude of NEE must also on average increase. Thus because variations in growing season length account for much of the variation in ecosystem primary production (Chapin *et al.*, 2002), this implies that sites with longer growing seasons are on average expected to have larger carbon uptake. One of the key insights drawn from meta-analysis of data across Fluxnet sites is that the length of the growing season is a strong predictor of annual NEE; each additional day of season length increases annual net ecosystem carbon uptake by approximately  $5.6\text{gC m}^{-2}$  among temperate and boreal deciduous forests and  $3.7\text{gC m}^{-2}$  among deciduous and evergreen savannah (Figure 2.9b) (Baldocchi, 2008).

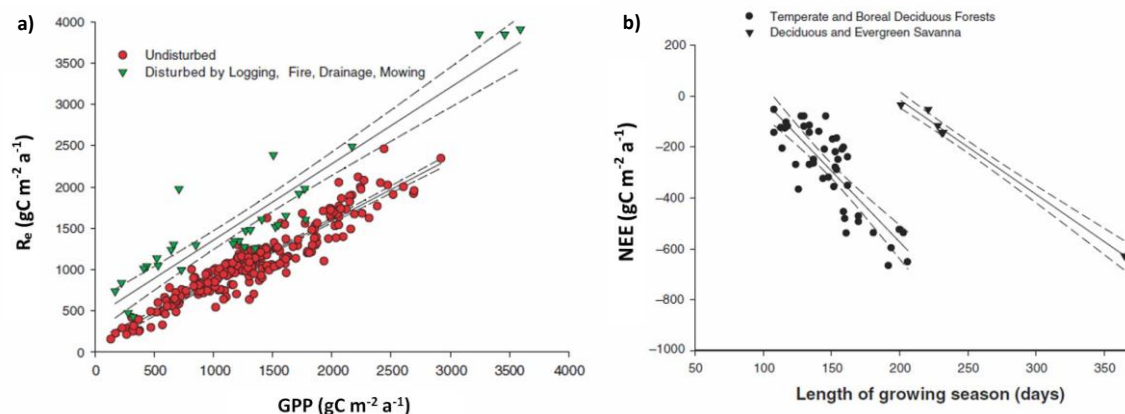


Figure 2.9: a) relationship between published values of ecosystem respiration ( $R_e$ ) and gross primary production (GPP); b) impact of length of growing season on NEE from published values (from Baldocchi, 2008, pp9-10).

While the growing seasons have been lengthened by planetary warming in recent decades (Linderholm, 2006), as discussed in (section 2.4.2.2), the growing season in alpine ecosystems nonetheless remains limited to periods of sufficiently high temperatures. Therefore, among primarily temperature-limited ecosystems generally, NEE scales with mean annual temperature (Figure 2.10) (Yi *et al.*, 2010). As such, the previously-cited average ecosystem carbon sink for alpine grasslands is considerably less than that of the Fluxnet mean ( $\pm\text{SD}$ ) of approximately

$-181 \pm 269 \text{ gC m}^{-2} \text{ a}^{-1}$  (Baldocchi, 2008). Since  $R_e$  is generally strongly related to GPP,  $R_e$  also increases with increasing temperature (Figure 2.11) (Janssens *et al.*, 2003; Bahn *et al.*, 2008).

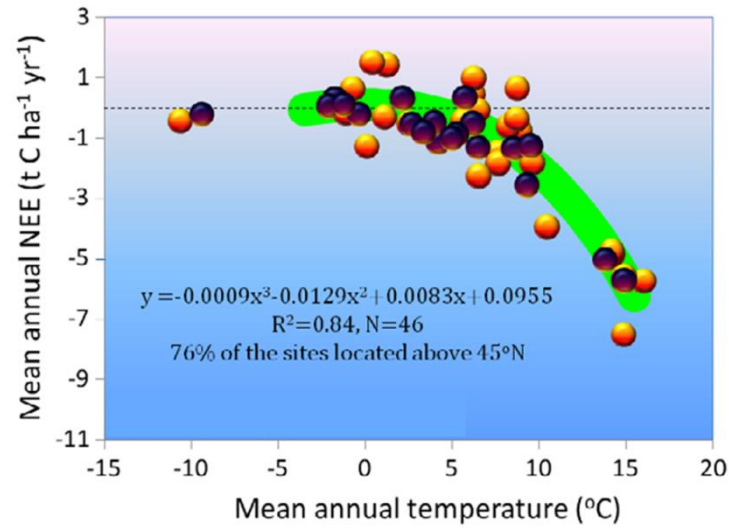


Figure 2.10: relationship between annual NEE and mean annual temperature among primarily temperature-limited ecosystems in the Fluxnet database (Yi *et al.*, 2010, p7).

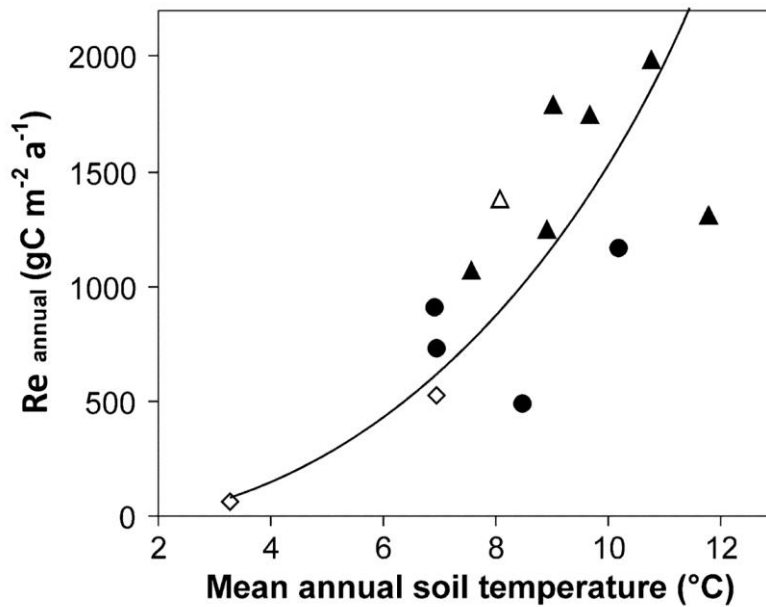


Figure 2.11: relationship between annual  $R_e$  and soil temperature (Bahn *et al.*, 2008, p1358).

#### 2.4.5 Interactive controls on carbon balance of alpine grassland ecosystems

While the key abiotic controls of the ecosystem carbon balance have been discussed in isolation above, in reality the dynamics of this balance over time represent the emergent behaviour of the ecosystem responding to these controls simultaneously. The relative importance of these controls depends on the temporal scale in question, and is discussed separately for short-term (sub-annual) and long-term (inter-annual) below.

##### 2.4.5.1 *Short-term controls*

Given that the entire ecosystem carbon cycle is underpinned by the capacity of the ecosystem to capture carbon from the atmosphere, it is not surprising that insolation – the energy source for photosynthesis – is a dominant short-term driver of the carbon balance of ecosystems in general (Ruimy *et al.*, 1995) and grasslands in particular (Gilmanov *et al.*, 2007). Wohlfahrt *et al.* (2008) conclude that insolation is the most important abiotic factor influencing NEE in European mountain grasslands, explaining 50-75% of the variation in NEE on average. However, they also document a strong and highly site-dependent seasonal pattern in the relative importance of insolation. Among the cooler (high altitude/latitude) grasslands, insolation was the key driver of NEE during the summer, explaining a much lower proportion of NEE variance in cool and wet spring and autumn conditions. At the warmer sites (lower altitude/latitude), the reverse was observed, with insolation most important during spring and autumn, but not during summer, when soil moisture was limiting.

The above example underscores the importance of secondary modulating factors in influencing the ecosystem carbon balance. As noted above, among drier ecosystems, soil moisture may exert an important influence, and is commonly the dominant control on primary production and concomitantly ecosystem carbon dynamics in lowland grassland ecosystems (for example, Flanagan *et al.*, 2002; Suyker *et al.*, 2003; Jaksic *et al.*, 2006; Nagy *et al.*, 2007; Aires *et al.*, 2008). However, this is less common among alpine grasslands due to the high orographic rainfall and low atmospheric moisture demand that often characterises mountain regions. Nonetheless, Fu *et al.* (2009) report that soil moisture was an important control on NEE in a dry alpine meadow ecosystem on the Tibetan Plateau. In Australia, while the High Country is characterised by relatively moist conditions in general (see section 2.2.3), the periodic occurrence of drought – as well as its

consequences for alpine plant growth – is well documented (Williams, 1990; Griffin and Hoffmann, 2011). Given that drought conditions are expected to become more common across the region in future (see previous discussion in section 1.2.4), this may have significant implications for the carbon balance of High Country ecosystems.

More commonly, temperature is reported to be a key control on NEE in alpine ecosystems. For example, in the study by Fu *et al.* (2009) cited above, in an alpine grassland that retained relatively high soil moisture throughout the growing season, temperature was reported to be a dominant control – via its effect on leaf area - of ecosystem carbon exchange. Even in the moisture-limited ecosystem, temperature nonetheless exerted an important influence on NEE. This inferred influence was based primarily on the strong correlation observed between temperature and maximum canopy photosynthetic capacity; it should be emphasised that there are difficulties in comprehensively disentangling the effects of air temperature and insolation given the strong autocorrelation between them (Körner, 2003). This may be accentuated in alpine grasslands since the decoupling effect of canopy structure ensures that PPFD is a strong driver of the temperature actually experienced by the plants.

However, Saito *et al.* (2009) concluded that both soil temperature and PPFD were independently important drivers of NEE of an alpine meadow during the growing season. While temperature may have a strong effect on NEE via its control of  $R_e$ , in this case the net uptake of carbon increased with both insolation and temperature, implying that the stimulatory effect of temperature on GPP overrode its effect on  $R_e$ . During the non-growing season, however, soil temperature was the main control on NEE; since GPP was low or negligible during the non-growing season, net carbon loss from the ecosystem occurred with increasing temperature as a result of increasing  $R_e$ . Below 0°C, NEE was approximately neutral because GPP and  $R_e$  were close to zero. Between 0-8°C,  $R_e$  – controlled by soil temperature - dominated GPP such that the ecosystem was a net source of carbon during these periods (i.e. NEE +ve), generally during the early or late growing season. Above 5°C, in response to increasing temperature and PPFD, GPP increased more rapidly than  $R_e$ , such that at approximately 8°C, the ecosystem transitioned from net carbon source to sink, reaching maximum uptake at approximately 15°C. At this site, the authors also reported that soil moisture was not an important control on NEE or its component fluxes, since plentiful rainfall occurred during the growing season.

Similarly, Fu *et al.* (2006) report that at constant light levels, carbon uptake of an alpine shrub meadow increased with temperature, indicating that the response of GPP to temperature exceeds that of  $R_e$ . However, at higher light levels, this effect was eventually reversed with

increasing temperatures, because GPP reached light saturation (Gu *et al.* (2003) report saturation in an alpine meadow at photosynthetic photon flux density (PPFD) of approximately  $1800\mu\text{mol m}^{-2} \text{s}^{-1}$ ), while further increases in temperatures resulted in higher  $R_e$ , such that carbon uptake was reduced. Thus while the temperature optimum for ecosystem carbon uptake partially reflects the effects of temperature on  $R_e$ , there is also a temperature optimum for photosynthetic activity of the canopy (Körner, 2003).

While the discussion above has focused on the abiotic controls on carbon balance, it must also be emphasised that biotic controls such as LAI also explain some variation in ecosystem carbon balance (Koch *et al.*, 2008; Wohlfahrt *et al.*, 2008). This may apply due to the direct effects of LAI on GPP, particularly where changes in GPP are not explained by *a priori* known functions of abiotic variables, or step changes in LAI are imposed by disturbance (Wohlfahrt *et al.*, 2008). This may also indirectly affect  $R_e$ , as discussed in section 2.4.3.3, since the supply of assimilates for respiration depends on GPP and thereby leaf area (Bahn *et al.*, 2008).

#### 2.4.5.2 *Inter-annual controls*

While the above discussion establishes the important controls on NEE, with respect to expected changes in ecosystem carbon balance in future, the information that can be gained from carbon cycle responses to abiotic and biotic controls at diurnal and seasonal time scales is of limited use because these controls are statistically non-stationary and their respective influences vary with time. As such, with the exception of brief seasonal transitions, the carbon balance is rarely in equilibrium at these time scales. While a given carbon cycle control may be an important or dominant determinant at diurnal and season time scales, it may be less important over longer time scales. For example, while insolation is a dominant driver of NEE over diurnal and seasonal time scales (Baldocchi and Valentini, 2004), over inter-annual time scales moisture availability and temperature assume increasingly important roles. At the scale of the terrestrial biosphere, this is reflected in the strong inter-annual variations superimposed on the background anthropogenically-induced rate of change of atmospheric  $\text{CO}_2$  concentration (Figure 2.12) (Heimann and Reichstein, 2008). These variations are primarily ENSO-driven, with larger increases in atmospheric  $\text{CO}_2$  during warm *El Niño* years when drought affects large regions of the terrestrial biosphere, and much lower increases during cool *La Niña* years. Moreover, temperature and moisture availability are the two climatic variables expected to change systematically in future, such that inter-annual linkages

between these variables and ecosystem carbon cycle can provide some insight into the implications of future climate change.

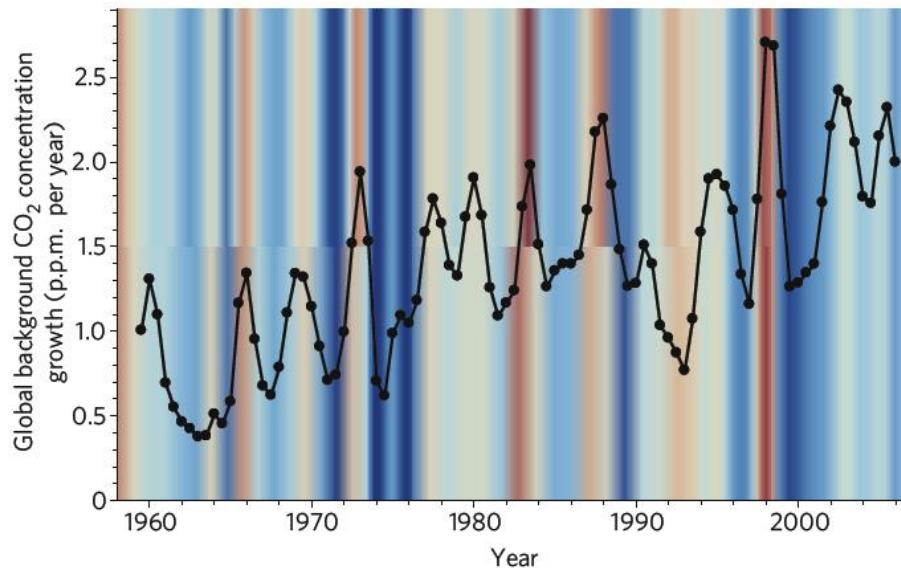


Figure 2.12: annual average change in global ambient CO<sub>2</sub> concentration (black series) superimposed on variations in Southern Oscillation Index (SOI; brown represents negative phase and blue represents positive phase) (from Heimann and Reichstein, 2008, p289).

A relatively small number of studies have reported multi-annual results for ecosystem carbon balance in alpine grasslands. However, those that are available generally report that temperature is a key control. For a three-year period (2002-04), Kato *et al.* (2006) report that temperature was the dominant control on inter-annual differences in NEE in a Tibetan alpine meadow. The year with the largest net uptake of carbon (i.e. more negative NEE) was characterised by warm spring temperatures but relatively cool summer temperatures. The result of this was that the longer growing season increased GPP but the cool summer temperatures suppressed  $R_e$ , while having little effect on GPP. The effect of warmer spring temperatures on  $R_e$  was not sufficient to offset the effect of reduced summer temperatures.

On the other hand, while Fu *et al.* (2009) also report that inter-annual variation in NEE in a Tibetan alpine meadow was largely controlled by temperature, the temporal dynamics of temperature variation – and correspondingly the effect on the annual carbon balance - were different to the above study. While warmer temperatures resulted in earlier increases of LAI and

larger GPP as reported above, higher summer temperatures enhanced  $R_e$  more, such that the year with the longer growing season had reduced uptake. This effect has also been reported for the northern hemisphere as a whole: warmer spring temperatures have resulted in stronger net carbon uptake by the terrestrial biosphere in recent years, but this has been counterbalanced by reduced carbon uptake due to hotter and drier summer conditions in the same period (Angert *et al.*, 2005). This underscores the fact that the response of the carbon cycle depends on the temporal characteristics of temperature changes, as well as the superimposed effects of changed moisture variability.

Temperature also has a crucial effect on another variable that influences both GPP and  $R_e$ : snow cover. Snow is an excellent insulator, and therefore soils are generally far warmer under snow than in its absence, effectively decoupling the soil from the atmosphere (Edwards and Cresser, 1992). With respect to climate change, it is therefore possible that warming could result in periodically colder soil conditions during winter (Groffman *et al.*, 2001; Hardy *et al.*, 2001) due to the expected loss of snow cover (Hayhoe *et al.*, 2008; Hennessy *et al.*, 2008). On the other hand, during warmer snow-free periods, soils remain closely coupled with the air and would thus be expected to warm.

In either case, given the sensitivity of  $R_e$  to temperature, such changes have significant implications for winter carbon balance, since  $R_e$  during winter remains significant under snowpack in alpine (Brooks *et al.*, 2005) and arctic (Zimov *et al.*, 1993) environments. In tundra and boreal ecosystems, winter  $R_e$  may account for 10-30% of annual  $R_e$ . Nobrega and Grogan (2007) experimentally increased snow depth to examine its effect on carbon cycling in a birch hummock tundra ecosystem, and report that moderate increases in snow depth caused increases in temperature and corresponding increases in both autotrophic and heterotrophic respiration. The increase in winter  $R_e$  (relative to control plots) was approximately  $16\text{gC m}^{-2}$ , approximately 50% of the estimated growing season carbon sink of  $29\text{-}37\text{g C m}^{-2}$ .

The effects of snow cover on  $R_e$  – and thus NEE – in alpine grasslands have been documented by a number of authors. In a two year period, Zeeman *et al.* (2010) report that during the warmer year, NEE increased relative to the cooler year not primarily due to the longer growing season and consequently larger GPP, but due to decreased  $R_e$  associated with lower soil temperatures resulting from reduced snow pack. Similarly, Rogiers *et al.* (2008) report that in a three year period (across 2002-05), while an intensively-managed mountain grassland was a carbon source in all three years, it was a much larger source during the year with the longest period of snow cover.

Such data for ecosystems in Australia are largely lacking, but as reported in Chapter 01 (section 1.2.4), snow cover is thought to be in decline and this is expected to continue into the future (Nicholls, 2005; Hennessy *et al.*, 2008). Warren and Taranto (2011) provide some of the few data on carbon cycling available for the Australian High Country, and report that  $R_e$  during the snow-covered period in subalpine grasslands represented approximately 5% of annual  $R_e$ . However, snow cover had a relatively modest effect on soil temperature in the Australian environment because air temperatures were close to zero. This suggests that snow cover may have a relatively modest effect on  $R_e$  in Australia.

Although as noted above, several authors have reported soil moisture effects on short term carbon balance (or components thereof) in mountain grasslands (Li *et al.*, 2008; Wohlfahrt *et al.*, 2008), no studies were found reporting soil moisture as a control on inter-annual variations in ecosystem carbon balance in alpine grasslands. This reflects the fact that most alpine ecosystems are generally primarily energy- rather than water-limited. Because both GPP and  $R_e$  are relatively unresponsive to soil moisture variation above a give threshold, moist sites may not reach such thresholds even when ostensibly in drought (Gilgen and Buchmann, 2009). For example, despite large losses of carbon across ecosystems of western Europe in response to the 2003 drought and concomitant heatwave (Ciais *et al.*, 2005), alpine grassland sites in Switzerland appear to have been broadly unaffected (Wohlfahrt *et al.*, 2008). In contrast, high inter-annual variability in ecosystem carbon balance linked to stochastic variability in precipitation (Sala, 2001; Chou *et al.*, 2008; Yi *et al.*, 2012) is characteristic of lowland grassland ecosystems (see, for example: Flanagan *et al.*, 2002; Suyker *et al.*, 2003; Jaksic *et al.*, 2006; Nagy *et al.*, 2007; Aires *et al.*, 2008; Yi *et al.*, 2012). For this reason, primary production in grasslands is among the most inter-annually variable of any ecosystem (Yi *et al.*, 2012). Given the relatively mild climate of Australian alpine and subalpine regions in combination with strong ENSO-induced inter-annual climatic variability, it is possible that soil moisture may have more influence on the carbon balance than in similar ecosystems elsewhere.

A single study from an alpine meadow research site with seven years of available data (Marcolla *et al.*, 2011) also indicated that over such time periods, the effect of inter-annual climatic variation on the carbon cycle was partially attenuated by changing ecosystem response; that is, inter-annual variation in NEE was damped because variations in climate were counteracted by variations in ecosystem response. This phenomenon, whereby variability in the long-term carbon balance induced by climatic variability is reduced by compensating ecosystem response, indicates some acclimatising capacity of the ecosystem, and is also observed in other ecosystems (e.g. forests) (Richardson *et al.*, 2007).



Finally, a number of studies also address agricultural disturbance effects on NEE (which may affect leaf area index, as well as soil chemistry, structure, temperature and moisture content), with variable results. While Zeeman *et al.* (2010) report that grasslands subject to lower management intensity were stronger carbon sinks on an annual basis, the reverse finding was reported by Schmitt *et al.* (2010). Since management interventions may take a range of forms, it is not surprising that the effects on NEE may be variable. Reports of the effects of grazing on the carbon balance in alpine grassland ecosystems are also variable, with some finding relatively little response to grazing (Lin *et al.*, 2011), some reporting large losses of carbon from grazed versus ungrazed sites (Welker, 2004), and some even reporting lower losses of carbon from more heavily grazed sites (Cao *et al.*, 2004). In Australia, the High Country has historically been (and in some locations continues to be) subject to cattle grazing (Wahren *et al.*, 1994), as well as periodic fire (Williams *et al.*, 2008a). The carbon cycle impacts of these factors have not been documented. While the sites in the current investigation were subject to summertime grazing, given the equivocal nature of the results in the literature, the difficulties involved in experimentally quantifying the effects of grazing, and the very low grazing intensity involved, the topic of grazing-related disturbance is largely beyond the scope of this study.

The interacting effects of environmental controls on NEE at seasonal to multi-annual timescales are thus complex. Insolation is clearly the main driver of seasonal variation in NEE, and temperature appears to exert control both directly (e.g. by reaction rates for photosynthesis and respiration) and indirectly (via controls on leaf area). Inter-annually, the effects of temperature vary depending on seasonal timing, with higher spring temperatures increasing carbon uptake (often indirectly, by causing earlier snowmelt) and higher summer temperatures generally having the reverse effect. Soil moisture is less likely to be limiting in alpine grasslands generally, but in drier regions it is clearly important. The discussion now turns to a review of the measurement techniques used in this study.

## 2.5 The Eddy Covariance Technique

As discussed, in Chapter 1, the primary methodological tool used in this study was the eddy covariance technique. A brief introduction to the technique – basic theory, assumptions, corrections and uncertainties – is provided below.

### 2.5.1 Basic theory

Turbulent eddies are primarily responsible for the exchange of mass and energy between the surface and the atmosphere (Arya, 2001). When imperfectly mixed, a given atmospheric entity (herein denoted by  $C$ , given this study's focus on carbon) – which may be any of the scalar properties contained or transported by an eddy (mass or energy) - thus shows short-term fluctuations around its long-term average (Oke, 1987). This can be expressed (using Reynolds decomposition) thus:

$$C = \bar{C} + C' \quad \text{Equation 2-4}$$

Where overbar and prime denote the time average and the instantaneous deviation from the time average, respectively. With respect to the mean vertical flux density<sup>17</sup> (herein simply 'flux',  $F$ ) of the constituent, the relevant properties are the vector component of the eddy normal to the surface ( $w$ ), the density of the air ( $\rho$ ) and the mixing ratio of the constituent (here  $C$ , since the focus of this study is carbon).  $F_c$  represents the time average of the instantaneous products of these properties (decomposed as above), as follows:

$$F_c = \overline{(\bar{\rho} + \rho')(\bar{w} + w')(C + C')} \quad \text{Equation 2-5}$$

On expansion this yields eight terms (see Oke, 1987). However, those involving a single primed quantity are neglected because the average of their fluctuations around the mean is by definition zero; quantities involving fluctuations in  $\rho$  can be ignored because air density remains

---

<sup>17</sup> Flux density represents the time rate of flow of an entity per unit space (Oke, 1987).

virtually constant close to the surface, and; terms containing  $\bar{w}$  can be ignored because mass conservation dictates that over sufficient time vertical velocity is close to zero. The remaining term is the basis of the eddy covariance (herein EC) technique (so-called because F is equal to the time-averaged covariance of instantaneous fluctuations in the vertical velocity and C), as follows (assuming time-invariant density):

$$F_c = \rho \overline{w' C'} \quad \text{Equation 2-6}$$

Fast response instrumentation is used to measure these quantities at a point above the surface. A sonic anemometer is used to measure three-dimensional wind vectors and temperature, and an infra-red gas analyser (IRGA) to measure molar densities of water vapour and CO<sub>2</sub>. While these measurements are made at a single point in space, since flux estimates derive from time averages, Taylor's Hypothesis can be invoked: as long as an eddy evolves over a time scale significantly longer than the time taken to advect past the measurement point, it can be considered 'frozen', and thus point measurements of atmospheric turbulence as a function of time can be interpreted as representative of the turbulent field in space (Stull, 1997). This equally applies to the scalar properties of those eddies, such that the measured flux is interpreted as a spatial average.

Thus while exchanges of carbon occur via innumerable microscopic point sources and sinks heterogeneously arranged in three-dimensional space throughout the ecosystem, eddy covariance measurements estimate the flux integrated over a large area. Under ideal conditions (see below), this surface or 'footprint' area is considered representative of fluxes across the surface/atmosphere interface. Its size is a function of measurement height, wind speed, atmospheric stability and surface roughness (Marcolla and Cescatti, 2005). In order to ensure that measurements are representative of a given ecosystem, it must be larger than within-ecosystem scales of heterogeneity and smaller than the spatial extent of the ecosystem.

As such, the appropriate measurement height is a function of the upwind extent of the ecosystem in question. Furthermore, measurements must be made within the internal boundary layer, in which flux magnitude is nearly constant with height (Lenschow, 1995). This layer constitutes the lower 10% of the atmospheric boundary layer<sup>18</sup>. However, close to the canopy, wake turbulence and thermal effects enhance eddy diffusivities such that theoretical scaling approximations and

---

<sup>18</sup> The atmospheric boundary layer represents the '... lower part of the atmosphere that interacts with the biosphere and is closely coupled to the surface by turbulent exchange processes' (Lenschow, 1995, p127).

assumptions implicit in the use of eddy covariance cannot reliably be applied. This roughness sublayer extends to a height of approximately three times the canopy (Kaimal and Finnigan, 1994). Reliable flux measurements are made in the overlying inertial sublayer, in which wind speeds under neutral conditions conform to a logarithmic profile and fluxes are approximately constant with height (Moncrieff *et al.*, 2000).

### 2.5.2 Key Assumptions

The above discussion alluded to the reliance of the eddy covariance technique on a number of simplifying assumptions. Three of these were explicitly stated: i) time averaged point measurements can be interpreted as spatial averages; ii) fluxes are measured only within the area of interest, and; iii) measurements are made within the constant flux layer. However, careful site selection and setup can ensure that these assumptions are generally met. On the other hand, a number of implicit idealising assumptions with respect to the basic theory are also made, all of which are commonly violated under field conditions to some degree. In some cases the consequences for measurement may be severe.

The first assumption is associated with the previously outlined Reynolds averaging procedure used to calculate the flux itself. In defining the statistics of turbulent fluctuations in terms of time averages, it is assumed that the ergodic hypothesis – that time and ensemble averages are equivalent – is fulfilled (Stull, 1997). However, the ergodic assumption is strictly met only in the case of a stationary time series, and when the time series is non-stationary the rules of the Reynolds averaging procedure are violated (Kaimal and Finnigan, 1994). In practice, associated errors are negligible when the data are weakly non-stationary, with a ‘stationary’ time series generally defined on the basis of statistical thresholds (Foken and Wichura, 1996). However, under certain conditions – for example, stable nocturnal conditions during which turbulence is intermittent, or when source / sink strength of the relevant entity is changing rapidly – the time series may become strongly non-stationary (Aubinet, 2008).

The fact that the aim of EC is to ascertain fluxes between surface and atmosphere implies a second critical assumption: that fluxes at the measurement height are representative of those at the physical surface. As with the previously-discussed assumptions, in the strictest sense this condition is *never* met, but EC measurements can be considered valid when it is a reasonable approximation. Discussion of this point is facilitated by the introduction of the concept of a Cartesian control volume

(Figure 2.13). The true surface flux of an entity is balanced by the net fluxes of the entity across the upper (horizontal – defined by the instrument height) and side (vertical) boundaries of the volume and changes in storage within the volume itself, as expressed in the mass conservation equation below (Foken *et al.*, 2012a):

$$NEE = \underbrace{\overline{\rho w' C'}}_I(h_m) + \underbrace{\int_0^{h_m} \frac{\delta \overline{C}}{\delta t} dz}_{II} + \underbrace{\int_0^{h_m} \left[ \rho \bar{u} \frac{\delta \overline{C}}{\delta x} + \rho \bar{v} \frac{\delta \overline{C}}{\delta y} \right] dz}_{III} + \underbrace{\int_0^{h_m} \left[ \rho \bar{w} \frac{\delta \overline{C}}{\delta z} \right] dz}_{IV} \quad \text{Equation 2-7}$$

Where  $h_m$  represents time,  $x$ ,  $y$  and  $z$  define the Cartesian coordinates of the volume, and  $u$ ,  $v$  and  $w$  the longitudinal, lateral and vertical wind components, respectively. The upper boundary is defined by the measurement height of the EC instrumentation. Term I in Equation 2-7 represents the EC-derived flux as described above; term II is the time rate of change of storage of  $C$  within the volume; terms III and IV represent horizontal and vertical advection, respectively.

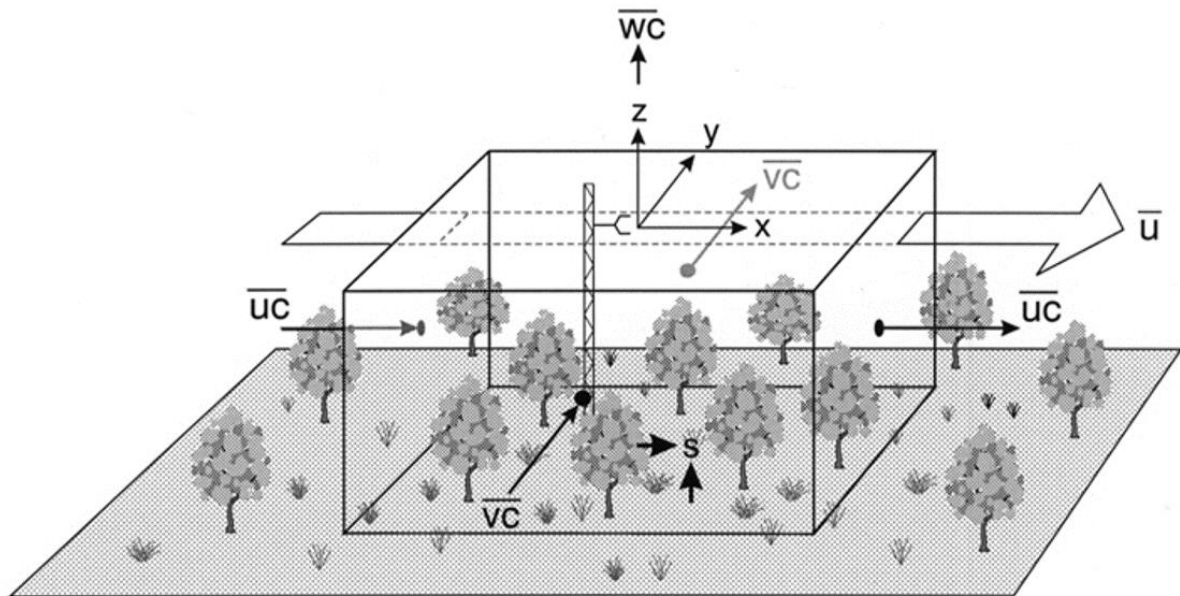


Figure 2.13: Cartesian control volume over homogeneous terrain ( $u$  = mean horizontal wind;  $\bar{u}C$  = mean horizontal transport of  $C$  parallel to mean horizontal wind;  $\bar{v}C$  = mean horizontal transport of entity  $C$  normal to mean horizontal wind;  $\bar{w}C$  = mean vertical transport of entity  $C$ ;  $s$  = source / sink term) (from Finnigan *et al.*, 2003, p3).

Because measurements are made at a point, only turbulent transfer through the lid of the control volume can be resolved using the eddy covariance technique. The remaining terms are unmeasured and largely unquantifiable without additional instrumentation. Term II is negligible under stationary conditions, but can be accounted for under non-stationary conditions if measurements of changes in concentration within the volume are made. Where the depth of the control volume is small, profile measurements can be replaced by the change in observed mean concentration at the measurement height without causing major error, though in practice the term is generally small (Aires *et al.*, 2008).

Horizontal advection (term III) is expected to be negligible if the spatial distribution of sources and sinks in the upwind direction is homogeneous at the necessary scale, and vertical advection (term IV) is expected to be negligible if there are no large-scale regions of preferred vertical motion within the landscape (Foken *et al.*, 2012a). However, there is increasing evidence that these advection terms may periodically be non-negligible. This is most likely to occur in very stable or unstable boundary layer conditions that develop under clear skies and light winds, such that the influence of surface features on the adjacent layer of the atmosphere may induce large scale atmospheric circulations in the landscape. For example: i) contrasting radiative and thermal properties of landscape surfaces (e.g. grassland versus adjacent forest) may generate localised 'hotspots' of preferred convective activity (Kanda *et al.*, 2004), and; ii) heating or cooling of the air adjacent to the surface in sloped terrain may induce up- or downslope flows (Aubinet, 2008). However, it may also be a consequence of the topographic characteristics of the landscape interacting with the synoptic flow, such that streamline divergence adjacent to the surface occurs regularly (Finnigan *et al.*, 2003).

Clearly, if unmeasured terms in the mass balance become significant in magnitude, then the measured turbulent flux at the top of the control volume (in combination with the storage change within the volume) can no longer be equated to the magnitude of the surface source or sink term. It is because these terms cannot be easily measured that sites with characteristics that are least likely to violate the implicit assumption of one-dimensional turbulent transfer are preferred; namely, flat, level terrain and surface homogeneity (Kaimal and Finnigan, 1994). Inevitably, field sites in the real world tend to diverge from these ideal conditions significantly. The consequences for measurement are discussed in further detail in section 2.5.4, which outlines key sources of potential systematic error associated with violation of the above assumptions. First however, a brief discussion of corrections required to account for known sources of error is provided.

### 2.5.3 Corrections

A number of corrections must also be applied to account for the known limitations of the measurement system. Here a brief conceptual description of these corrections is provided, while methodological details of their application in this study are provided in Chapter 3 (section 3.4).

#### 2.5.3.1 *Coordinate rotation*

Levelling of the sonic anemometer is problematic both because of the difficulty in establishing and maintaining a perfectly level experimental arrangement, and because the aim is to measure fluxes normal to a surface that is rarely locally perfectly horizontal (Finnigan *et al.*, 2003; Lee *et al.*, 2004a). It is thus necessary to rotate the orthogonal reference frame to prevent contamination of the vertical velocity vector ( $w$ ) by the horizontal vectors (i.e. mean  $[u]$  and cross  $[v]$  wind components) over an appropriate period of time (Rebmann *et al.*, 2012).

The traditional approach is to rotate into so-called natural wind coordinates (Lee *et al.*, 2004a). In this system, the first rotation aligns the x-axis with the time-averaged horizontal flow (such that the mean of the cross-wind vector  $[\bar{v}]$  is zero), and the second rotation sets the z-axis normal to (and increasing away from) the mean horizontal streamline (such that the mean of the vertical wind vector  $[\bar{w}]$  is zero). The assumption of  $\bar{w} \approx 0$  is reasonable if the terrain and surface properties are uniform (i.e. no regions of preferred vertical motion at the relevant measurement scale), since significant departures over sufficient time would violate mass conservation. However, as previously discussed, non-ideal landscape characteristics or topography may under specific conditions result in  $\bar{w} \neq 0$ , and explicit forcing of  $\bar{w}$  to zero may consequently yield highly unrealistic rotations (Lee *et al.*, 2004a).

The planar rotation method (Wilczak *et al.*, 2001) instead involves rotation into a mean streamline coordinate frame determined over a longer period (e.g. monthly) (Lee *et al.*, 2004a). The vertical axis of the coordinate frame is perpendicular to the mean streamline plane defined over the given period, while the x-axis is rotated into the mean flow for the averaging period as above. As such, this rotation method is generally favoured in conditions where complex landscape features may be expected to induce conditions in which the assumption of  $\bar{w} = 0$  is frequently not met (Finnigan *et al.*, 2003).

### 2.5.3.2 Frequency response corrections

Low-frequency flux attenuation stems primarily from choices in data treatment – as discussed previously, the choice of inappropriately short averaging periods (and subsequent rotation to force  $\bar{w}$  to zero) may result in low-frequency contributions being filtered out of flux estimates. In contrast, high frequency flux attenuation relates principally to specific instrumental limitations – namely, sampling rate limitations and sampling path-length averaging, the effects of electronic filters designed to reduce noise in sensor output signals, and the separation of sensors in space (Massman and Clement, 2004). The issue of high-frequency flux attenuation is pertinent to the current study, since the low measurement height of the instrumentation means that the contribution of high frequency eddies to the flux is increased (Figure 2.14) (Foken *et al.*, 2012a; Wohlfahrt *et al.*, 2012).

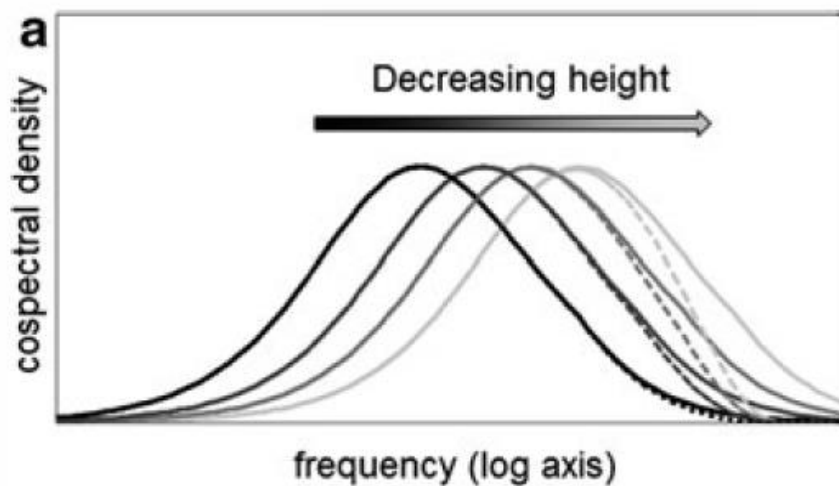


Figure 2.14: undamped (solid line) and damped (dashed line) cospectra, indicating progressively increasing losses for higher frequency distributions corresponding to decreasing measurement height (from Foken *et al.*, 2012a, p16).

The fractional error in flux estimates arising from dampening of the high-frequency component of the cospectral density (i.e. the Fourier transform of the covariance time series into the frequency domain) can be expressed as (Moncrieff *et al.*, 2000):



$$\frac{\Delta F_{\chi}}{F_{\chi}^{EC}} = 1 - \frac{\int_0^{\infty} T_{w\chi}(f) C_{w\chi}(f) df}{\int_0^{\infty} C_{w\chi}(f) df}$$

Where  $\Delta F_{\chi}$  and  $F_{\chi}^{EC}$  represent the ideal and measured flux of entity  $\chi$  (here  $\text{CO}_2$ ),  $f$  is cyclic frequency, and  $C_{w\chi}(f)$  and  $T_{w\chi}(f)$  are the idealised cospectral density and transfer function (collectively encompassing the above mentioned sources of error), respectively. Thus both the transfer function and idealised cospectra must be known before high-frequency flux attenuation can be corrected. For scalar cospectra, the forms of Kaimal *et al.* (1972) – developed from field measurements over flat terrain with short, homogeneous vegetation – are commonly used (Foken *et al.*, 2012b). In reality, observed cospectra are generally far less smooth than these idealised forms (Massman and Clement, 2004). Moreover, at some sites there may be systematic differences between idealised and observed cospectra arising from differences in field conditions relative to those under which the Kaimal forms were derived – for example over tall forest canopies (eg. Amiro, 1990).

Transfer functions are approximated using either theoretically- or analytically-based approaches. In the theoretical approach, a series of theoretically-derived frequency-dependent functions is used to approximate the effects of the various causes of flux attenuation (Moore, 1986). In the analytical method, it is assumed that the cospectrum of another quantity (generally  $\overline{w'\theta'}$ ) can be measured without error, and can thus – assuming proportionality between scalar cospectra – be used to correct the attenuated scalar flux accordingly (Foken *et al.*, 2012b). Because: i) the theoretical approach is more suited to open path systems, and; ii) the Kaimal cospectral forms are more suited to sites with short canopies, the theoretical approach was used in this study.

### 2.5.3.3 Density corrections for open path gas analysers

Changes in density of a given gaseous constituent of air within an open volume can occur due to gain / loss of the constituent, ‘dilution’ by the addition of another constituent or – most importantly - by thermally driven expansion of the air. A surface sensible or latent heat source or sink will thus result in updrafts and downdrafts of air near the surface having different densities. Consequently, as demonstrated by Webb *et al.* (1980), conservation of dry air under conditions in which the surface is a source or sink for sensible and latent heat actually *requires* that  $\bar{w} \neq 0$ , and as such mean scalar transport  $\bar{w}\bar{\chi} \neq 0$ . In practice,  $\bar{w}$  is too small to quantify given the combined

effects of instrument resolution / levelling and terrain effects, but the implications for measurement of trace gas fluxes are significant.

With respect to CO<sub>2</sub>, infra-red gas analysers measure molar density rather than mixing ratio, and open path IRGAs measure fluctuations along a measurement path in which air density fluctuates at high frequency due to the different densities of updrafts and downdrafts of eddies. This results in an erroneous apparent transfer of CO<sub>2</sub> to the surface, because the compensating contribution of  $\overline{wCO_2}$  is missed by the measurement system. This can be largely compensated for if the air is brought to constant temperature before measurement, as may be approximately the case in closed-path systems. However, in open path systems this is not the case, and correction is thus required. The correction – proposed by Webb *et al.* and subsequently referred to as Webb Pearman Leuning (WPL) is detailed in Webb *et al.* (1980) and is not discussed further here.

#### 2.5.3.4 IRGA Heating correction

The particular IRGA model used in this study – the Licor LI7500 – can cause trace gas flux biases to arise (particularly at low temperatures) due to heat generated by the IRGA both through radiation loading and effects of the instrument electronics (Burba *et al.*, 2008). The latter is more problematic because the LI-7500 is designed to maintain the temperature of certain components at nearly 30°C, such that at low temperatures the difference between surface and air temperatures can approach 10°C, inducing significant sensible heat flux (i.e. additional to the ambient flux) in the IRGA optical path. The initial WPL correction is made using the ambient sensible heat flux (i.e. as measured by the sonic anemometer), and thus under certain conditions (e.g. cold, clear, calm conditions when significant instrument surface – atmosphere temperature gradients may develop), sensible heat flux in the IRGA optical path may be substantially (up to 14%) higher. This in turn causes underestimation of the WPL correction magnitude and a corresponding bias towards surface CO<sub>2</sub> uptake, which may manifest as an unrealistically strong CO<sub>2</sub> sink when unexpected (for example over snow). This effect can be corrected either by direct measurement of heating in the IRGA path or by applying a semi-empirical correction in which path heating is estimated using a semi-empirical equations with standard weather variables (see Burba *et al.*, 2008 for details). The latter approach was used here.

#### 2.5.4 Uncertainties

Uncertainties inevitably arise in final (i.e. corrected) CO<sub>2</sub> fluxes, both for reasons related to the instrumentation and to the extent to which the previously discussed underlying assumptions are violated under certain conditions. These take two main forms: random and systematic uncertainties (Figure 2.15).

Random uncertainties arise due to unpredictable errors in measurement associated with: i) the flux measurement system; ii) the stochastic and intermittent nature of turbulent transport processes, and; iii) the varying locations and activities of the flux exchange sites (Hollinger and Richardson, 2005). Their effect on cumulative flux estimates – for example time-integrated estimates of ecosystem-scale NEE drawn from continuous measurements of CO<sub>2</sub> fluxes – are generally relatively mild because the summing of random errors over increasing time causes the error to diminish according to  $1/\sqrt{n}$ , where  $n$  = number of data points (Moncrieff *et al.*, 1996). In the case of annual NEE measurements, errors are generally within the range of  $\pm 10\text{--}30\text{gC m}^{-2}\text{ a}^{-1}$  (Richardson and Hollinger, 2007).

Systematic uncertainty arises due to (theoretically) predictable, persistent errors in measurement which result in measurement bias that does not – in contrast to random error – diminish with increasing time scale. These errors are difficult to detect for the fundamental reason that there is not an independent measure of the same quantity that can be used as a ‘standard’ for comparison (which would render the measurement program redundant) (Moncrieff *et al.*, 1996). These errors may be associated with the accuracy of the measurements themselves – for example, persistent signal offset or gain errors in either the sonic anemometer or IRGA measurements. Data vigilance and careful ongoing maintenance can thus minimise this problem. On the other hand, they may be due to persistent violation of the previously outlined underlying assumptions of eddy covariance measurements. When systematic errors arise for this reason, another serious problem arises in tandem: the extent to which assumptions are violated depends on measurement conditions, and these conditions vary systematically in time. As a result, errors may be *selectively* systematic, meaning that they are more likely to apply during some periods than others (Moncrieff *et al.*, 1996).

Two systematic errors in particular are considered to be among the most serious affecting eddy covariance-based flux measurements (Finnigan, 2008): i) the general failure to close the surface energy balance, and; ii) the apparent underestimation of nocturnal surface / atmosphere

exchanges. In the context of long-term measurements of NEE they represent a particular problem. In the case of energy balance closure, to the extent that this is caused by turbulent flux underestimation (as opposed to measurement errors in the other components of the surface energy balance), systematic errors in measurement of turbulent energy exchanges may translate equally to measurements of CO<sub>2</sub> exchanges. With respect to nocturnal underestimation, this is problematic because of the different behaviour of the ecosystem itself between day (when photosynthetic activity generally results in net carbon uptake during the growing season) and night (when ecosystem respiration is occurring and thus there is continual release of carbon from the surface). Thus when integrating over time, if periods of CO<sub>2</sub> release are underestimated, then net CO<sub>2</sub> uptake is systematically overestimated.

A brief discussion of both of these errors is provided below. Prior to this discussion, a third source of uncertainty associated with the estimation of long-term (e.g. annual) sums of NEE requires mention: that due to imputation or gap filling. Gaps arise both due to data loss and – as detailed in section 2.5.4.2 – data rejection where violation of fundamental assumptions is suspected. Average data losses across flux sites due to both sources has been estimated at around 35%, but ranges from 20-60% (Falge *et al.*, 2001; Moffat *et al.*, 2007). A number of different imputation methods may be used, including mean diurnal variation (MDV), lookup tables, artificial neural networks, nonlinear regressions and process models (see Papale, 2012 for a review).

All are premised on the use of meteorological and often ecophysiological data as predictors for the behaviour of CO<sub>2</sub> fluxes. All are also imperfect descriptors of reality, due to: i) errors in the observational data (i.e. either in the modelled quantity or in the variables used to predict it); ii) the failure of the model to adequately reflect the underlying processes or empirical relationships between the modelled quantity and the variables used to predict it, or; iii) exclusion of observational data crucial to the accurate capture of system response. Nonetheless, comprehensive comparisons of the above methods indicate that the additional uncertainty added by imputation is relatively small (particularly in comparison to the potential effects of systematic error), with broadly similar performance across different methods, the more sophisticated of which approach the noise limits of the data (Moffat *et al.*, 2007).

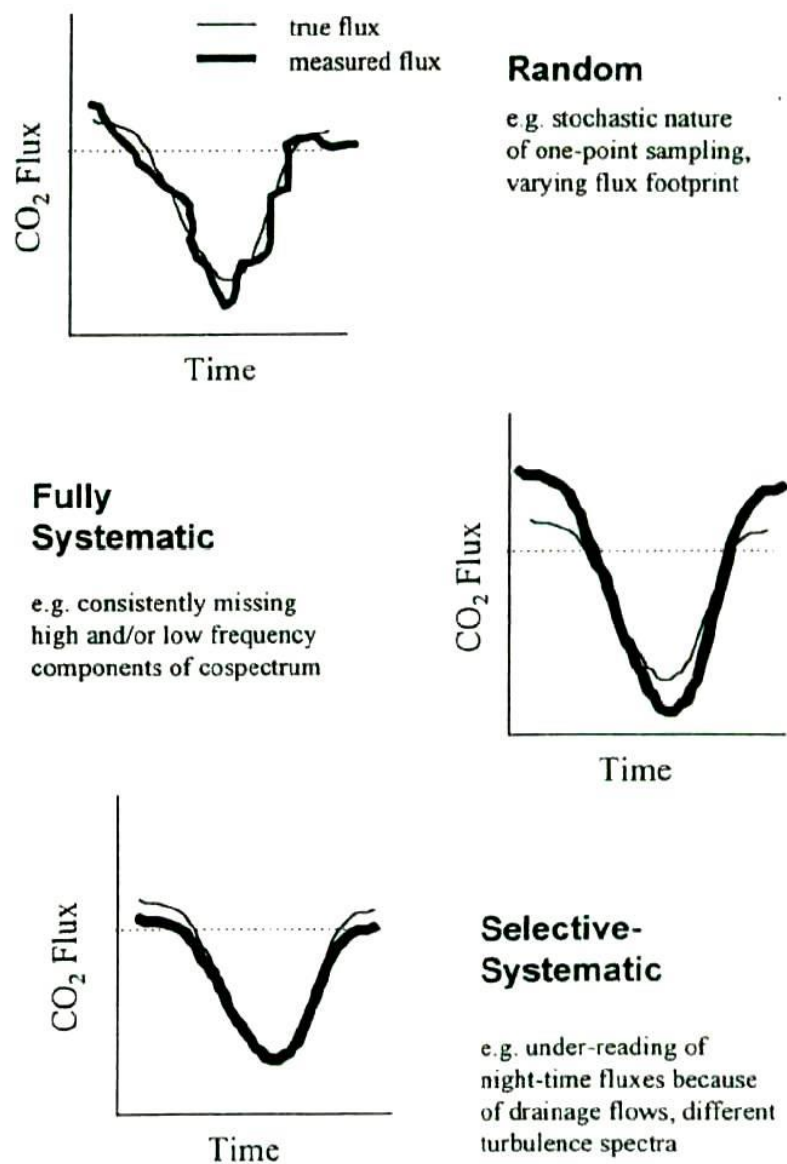


Figure 2.15: schematic representation of error categories (random and fully / selectively systematic) (from Moncrieff *et al.*, 1996, p234).

#### 2.5.4.1 Energy balance non-closure

The first law of thermodynamics requires that the net radiant energy surplus or deficit at the surface must be balanced by the sum of the convective (sensible and latent) energy fluxes and changes in energy storage (Baldocchi, 2003), as follows (Oke, 1987):

$$R_n = H + LE + G + S$$
Equation 2-9

Where  $R_n$  is the net radiation,  $H$  and  $LE$  are the turbulent sensible and latent heat fluxes, respectively,  $G$  represents subsurface energy storage and  $S$  represents additional energy storage terms (e.g. air enthalpy and moisture changes between the surface and the measurement height, biomass heat storage, biochemical energy storage). However, it is a consistent observation across eddy covariance sites that these quantities do not balance; almost universally, radiant fluxes exceed non-radiant fluxes by between 10-30% (Wilson *et al.*, 2002).

A number of hypotheses have been proposed to explain systematic shortfalls in energy balance closure. These include: sampling errors, instrument biases, low and high pass filtering, neglected energy sinks and advection (Wilson *et al.*, 2002). However, it has generally been considered most likely that the underestimation is due to deficiencies in measurement of the turbulent energy fluxes (Foken *et al.*, 2006). This is because most potential error sources associated with turbulent flux measurements are expected to result in underestimation of true fluxes (Leuning *et al.*, 2012).

Foken (2008) argues that most of the traditionally cited causes of energy balance non-closure have been adequately addressed, and that the principal cause is likely to be neglect of important low frequency contributions to surface fluxes due to the selection of short averaging periods. There is some observational support for this, with Finnigan *et al.* (2003) reporting that in complex terrain and over tall canopies low frequency contributions to fluxes are larger than classical surface-layer spectral forms predict. This is because, topographic structures may induce regular landscape circulations and eddy size scales with height above the surface. Large scale circulations (i.e. very low frequency eddies) may also arise due to heterogeneities in land surface aerodynamic, thermal and optical properties (Foken *et al.*, 2010). This effective high pass filtering of the turbulence spectrum means that all turbulent fluxes –  $\text{CO}_2$  included - are affected.

For this reason, some researchers have increased all turbulent fluxes (including CO<sub>2</sub>) by the proportion required to close the energy balance (eg. Twine *et al.*, 2000; Barr *et al.*, 2006). Baldocchi (2008) has criticised this approach on the basis that other potential causes specific to the energy fluxes have not been comprehensively ruled out. Moreover, this approach is particularly problematic in the case of open-path IRGAs, because even if either or both of the turbulent energy fluxes are underestimated, this does not necessarily imply corresponding underestimation of CO<sub>2</sub> fluxes (Baldocchi, 2008). Because errors in H and LE propagate through the WPL correction in open-path IRGA-based EC measurements, Liu *et al.* (2006) report that ‘... *either an overestimation or underestimation of CO<sub>2</sub> fluxes is possible depending on local atmospheric conditions and measurement errors in the sensible heat, latent heat, and CO<sub>2</sub> fluxes*’.

While the use of long averaging intervals may appear to be a prudent approach, this also increases the likelihood of time series nonstationarity (Mahrt, 2010) and reduces the resolution of the flux measurements. The inclusion of low-frequency flux content also complicates interpretation – for example, it is unclear whether these contributions are related to the local surface or features of the wider landscape (Malhi *et al.*, 2004).

In ecosystems with short vegetation such as grasslands, typically low measurement heights mean that peak eddy frequencies are shifted towards the higher end of the spectrum (Foken *et al.*, 2012b). In these ecosystems it is generally observed that energy balance closure is better (Meyers and Hollinger, 2004; Jacobs *et al.*, 2008), and short (e.g. half-hourly) averaging periods are sufficient to adequately capture the flux (Sun *et al.*, 2006). Nonetheless, the effects of complex surrounding terrain and surface heterogeneity may still result in significant contributions of low-frequency eddies to fluxes. This may be important in alpine ecosystems, where such characteristics are generally typical of the landscape. Eddy covariance studies in alpine areas generally report deficits in energy balance closure similar to those for taller forested sites (e.g. 20-25%) (Hammerle *et al.*, 2007; Hiller *et al.*, 2008).

More recently, however, Leuning *et al.* (2012) have argued that poor energy balance closure may instead relate primarily to the underestimation of energy storage terms, noting that the mean energy balance closure deficits of Fluxnet sites of 25% for half-hourly data (eg. Franssen *et al.*, 2010) was reduced to 10% when evaluated over a 24-hour period (in which net energy storage changes are expected to be negligible). Correspondingly, a number of other authors have also argued that careful evaluation of storage terms greatly improves energy balance closure (Meyers and Hollinger, 2004; Haverd *et al.*, 2007; Lindroth *et al.*, 2010). It has also been argued that the general methods for evaluating soil heat fluxes may be inadequate, and that in ecosystems with minimal vegetation this

may contribute significantly to energy balance non-closure (Heusinkveld *et al.*, 2004; Jacobs *et al.*, 2008). Jacobs (2008) demonstrated that the use of harmonic analysis increased soil heat flux twofold relative to the traditional combination method and improved energy balance closure in a temperate grassland from 87% to 96%.

From observational evidence it appears likely that both of these sources of error may contribute to flux underestimation, with their relative levels of importance likely to depend on local landscape and meteorological conditions. In alpine ecosystems, the same site selection rules apply as for others: flat, level terrain and large expanse of homogeneous vegetation are favourable. Such ideal sites are clearly rare in alpine locations (see Chapter 3 for discussion of site characteristics).

#### 2.5.4.2 *Nocturnal underestimation*

Two lines of evidence suggest that nocturnal CO<sub>2</sub> fluxes are generally underestimated by eddy covariance systems. First, estimates of nocturnal respiration derived from eddy covariance systems tend to be lower than those from other measurement methods (e.g. extrapolation from chambers) (Goulden *et al.*, 1997; Law *et al.*, 1999). However, differences between methods also tend to be less pronounced under more vigorous turbulent mixing, which raises the second line of evidence: nocturnal eddy covariance measurements of CO<sub>2</sub> exchange are sensitive to the magnitude of friction velocity (a measure of average turbulent activity), an observation with no plausible biological basis (Goulden *et al.*, 1996b). Nonetheless, this observation has been noted at numerous sites in a range of different ecosystem types including forests, savannas and grasslands (Aubinet *et al.*, 1999), leading to the conclusion that it is an artefact of the measurements.

It is thought to arise primarily as a result of three main mechanisms, all of which are more pronounced under stable conditions: turbulent intermittency, land breezes and gravity flows (Finnigan, 2008). Turbulent intermittency – extended calm periods punctuated by occasional bursts of turbulent activity - has a range of causes (e.g. downward transfer of shear turbulence associated with the nocturnal jet), but its key effect is to cause strongly instationary conditions over the averaging period (Aubinet, 2008), thus violating Reynolds averaging rules as previously discussed. More seriously, both land breezes (generated by contrasts in radiative / thermal properties and differential heating/cooling between adjacent surfaces) and drainage flows (gravity-driven downslope drainage of air cooled by the underlying surface) cause the horizontal and vertical advection terms (terms III and IV in Equation 2-7) to become significant or even dominant terms in



the nocturnal mass balance (Aubinet, 2008). As a result, the fundamental assumption that unmeasured terms in the mass balance are negligible is violated.

As such, estimates of surface-atmosphere CO<sub>2</sub> exchanges that only take into account turbulent transfer and changes in storage are in error of a magnitude equal to the sum of the advection terms. Because the strongly stable conditions under which these problems occur tend to be largely confined to the nocturnal situation, over time scales of a day or longer, estimates of NEE may overestimate ecosystem uptake of carbon i.e. a selectively systematic error is induced. However, while it is thus important not to ignore the effects of advection, its measurement is extremely difficult in practice, and even with sophisticated instrument installations has generally produced ambiguous results (Feigenwinter *et al.*, 2008; Leuning *et al.*, 2008, and references therein; Aubinet *et al.*, 2010). Thus while this remains an active area of research, the preferred solution remains the identification and exclusion of data that are recorded during conditions in which the advection terms are likely to be non-negligible.

The common historical approach to this issue has been to apply a filter to nocturnal data on the basis of the relationship between friction velocity ( $u^*$ ) and the apparent value of the nocturnal ecosystem CO<sub>2</sub> flux (Goulden *et al.*, 1996b). It has been observed that under calm conditions CO<sub>2</sub> flux shows some dependence on  $u^*$ ; at increasing values this dependency is reduced until at some site-dependent threshold the CO<sub>2</sub> flux becomes insensitive to the degree of turbulence (Goulden *et al.*, 1996b). This is thought to reflect the decreasing importance of the above issues – advection in particular - with more effective mixing and weakening of stable stratification in the surface layer. The so-called ' $u^*$  threshold' can therefore be used as a diagnostic criterion in which CO<sub>2</sub> flux data concomitant with  $u^*$  values below the derived threshold may be rejected and replaced with modelled estimates of the true biological flux.

One of the shortcomings of the approach is that  $u^*$  may exhibit diurnal and seasonal patterns that may be correlated with temperature, to which respiratory fluxes are highly sensitive, as outlined in section 2.4.3.1 (Gu *et al.*, 2005b). This thus obscures the response of CO<sub>2</sub> to  $u^*$  and must be removed before determination of the threshold. Moreover, the threshold may be difficult to discern in some cases (in part due to the lower signal:noise ratio of nocturnal measurements, as well as the effects of the previously-discussed issue of intermittent turbulence) and is in practice often visually (and therefore somewhat subjectively) determined (Gu *et al.*, 2005b). As such, objective techniques that account for  $u^*$ /temperature correlations are required for rigorous determination of  $u^*$  thresholds (see for example Gu *et al.*, 2005b; Reichstein *et al.*, 2005). For details of the approach used here, see Chapter 3 (section 3.4).

## 2.6 **Summary**

There is a wealth of international literature addressing carbon storage and exchange in subalpine grasslands, but very little in Australian alpine grasslands. The literature summarised here emphasises the complexity of interacting factors that contribute to the carbon dynamics of these ecosystems, but as ecosystems in which growing season length and corresponding productivity are temperature-dependent, it follows that temperature is an important determinant of these dynamics. The following chapter describes the methodological approach employed to quantify these dynamics for two subalpine Australian grasslands using the eddy covariance technique.

# 3. Site Selection and Methodology

---

## 3.1 Introduction

Meeting the research objectives set out in Chapter 1 required: i) sites of the appropriate ecosystem type; ii) a high-resolution, high-quality record of exchanges of carbon between those ecosystems and the atmosphere; iii) simultaneous climate measurements, and; iv) relevant supporting measurements of vegetation and soil characteristics. This chapter discusses the methodological approach employed to meet these requirements, and is divided into the following sections:

- General description of sites (3.2);
- Site instrumentation and measurement (03.3);
- Post processing of 10Hz eddy covariance data (3.4);
- Imputation of missing data (3.5);
- Flux uncertainty analysis (3.6);
- Flux partitioning (3.7)
- Vegetation and soil sampling (03.8);

## 3.2 Site Descriptions

As discussed in Chapter 1.3.3, two sites were established for the current study. The criteria for their selection were first that they both be ecosystems that fall into the same broad ecosystem category (i.e. subalpine grassland), second that they be characterised by different climatic regimes – specifically, a relatively cool, moist higher altitude reference site and a warmer, drier lower altitude site - and third, that they be geographically appropriate for the application of the research methodology (i.e. the eddy covariance technique).

These criteria were broadly met, with some qualifications. First, due to difficulties in securing agreement to establish visible research infrastructure on public land, both sites are located on private land, and were subject to very low-intensity seasonal cattle grazing during the research period. However, given that large tracts of the Alpine National Park were until recently also subject to low-intensity grazing, there is no reason to expect adjacent areas of public land necessarily to be any more ‘representative’ than those chosen here. And second, in both cases, the local topographic features were non-ideal for eddy covariance in respect of the criteria discussed in Chapter 2 - namely, a flat, extensive and homogeneous surface (Kaimal and Finnigan, 1994). This is to be expected, since flat terrain is difficult to find when studying mountain ecosystems; yet with cautious data analysis, the eddy covariance technique can be applied with reasonable success in terrain far more challenging than that presented by the sites in the current study (see for example Hammerle *et al.*, 2007; Hiller *et al.*, 2008).

The sites were on the Dargo High Plains (herein referred to as ‘Dargo’), approximately 19km south of Mt. Hotham in Victoria (Figure 3.1), and Nimmo Plain (herein referred to as ‘Nimmo’) approximately 35km northeast of Mt Kosciuszko in southern New South Wales. The sites were separated by approximately 160km with an elevation difference of approximately 200m. General features of the sites are listed in Table 3.1, and a brief description of the sites given below. A more detailed comparison of climatic conditions can be found in Chapter 5.

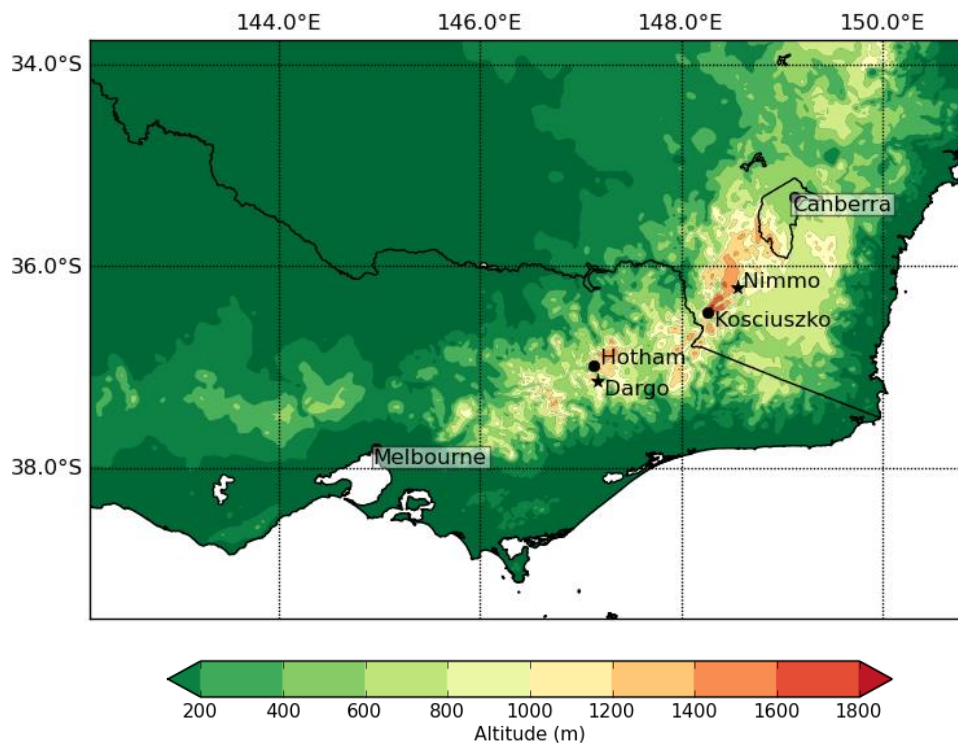


Figure 3.1: locations of Dargo and Nimmo study sites.

Table 3.1: general attributes of field sites (note: meteorological data [ $\pm$ SE] is from present study, with the exception of the precipitation totals presented in parentheses, which are calculated from SILO<sup>19</sup> 1961-90 estimates).

Attribute	Dargo	Nimmo
Latitude / Longitude	S37° 08.003' E147° 10.258'	S36° 12.933' E148° 33.190'
Date established	November 2006	November 2006
Elevation (m)	1518	1326
Topography	Plateau plain (slope <2°, southeasterly aspect)	Valley plain (slope 1-1.5°, variable aspect)
Parent material	Basalt	Granodiorite
Dominant spp.	<i>P. hiemata</i>	<i>P. sieberiana</i>
Annual Temperature (°C)	6.8 $\pm$ 0.2	7.7 $\pm$ 0.2
Annual precipitation (mm)	948 $\pm$ 136 (1545 $\pm$ 62)	933 $\pm$ 63 (1208 $\pm$ 52)

<sup>19</sup> SILO is a database of approximately 120 years of continuous daily weather records for Australia that was developed by the Australian Bureau of Meteorology. The data drill facility offers spatially interpolated synthetic estimates of daily weather variables at 5x5km resolution across the continent (for more information, see <http://www.longpaddock.qld.gov.au/silo/index.html>). Details of the methodology is available in Jeffrey *et al.* (2001).

### 3.2.1 Dargo

Dargo is located at the boundary of the Alpine National Park at 1518m elevation on the southern flanks of the Alps. It lies on a broad plain with a small gradient (approximately 2°) of generally south-easterly aspect (Table 3.1; Figure 3.2a). The site's location along the southern flanks of the Alps means that it is dominated by winter rainfall and experiences snow cover for several of the winter months. Precipitation was close to 1000mm in both years, though this is less than long-term averages derived from spatial interpolation of nearby historical Bureau of Meteorology weather station data (Table 3.1; and see Chapter 5). During the two years of the current study (2007/08), the mean annual temperature at Dargo was approximately 6.8°C, with mean warmest month (January) temperature of 14.4°C.

While a formal analysis of species composition was not undertaken, tussock-forming snow grasses – the dominant species of which is *P. hiemata* (with minor representation of *P. fawcettiae* and *R. nudiflorum*) – represented approximately 90% of surface cover, with a smaller complement of various forbs as well as associations of *Sphagnum* sp. and *Empodisma minus* occurring in wetter parts of the landscape (e.g. small drainage depressions and bogs). The presence of these species' underscores the relatively moist nature of the Dargo site. The grass tussocks at Dargo consisted predominantly of standing dead matter, a typical characteristic of alpine grasses, and the vegetation canopy was dense and closed.

In most directions the vegetation remained contiguous and highly homogeneous over larger distances (for example, to the northwest for at least 500m, as seen in Figure 3.2b); however, snow gum woodland lay within the expected EC measurement footprint in the southeast quadrant, and a narrow band of trees oriented NW-SE was located approximately 150m to the north of the tower. However, easterly winds were exceedingly rare, and the tower was intentionally sited to maximise fetch in the prevailing westerly wind direction. Thus data recorded when winds were arriving from the sector containing the bulk of the woodland (i.e. east / southeast) were explicitly rejected with only minor impact on data retention.

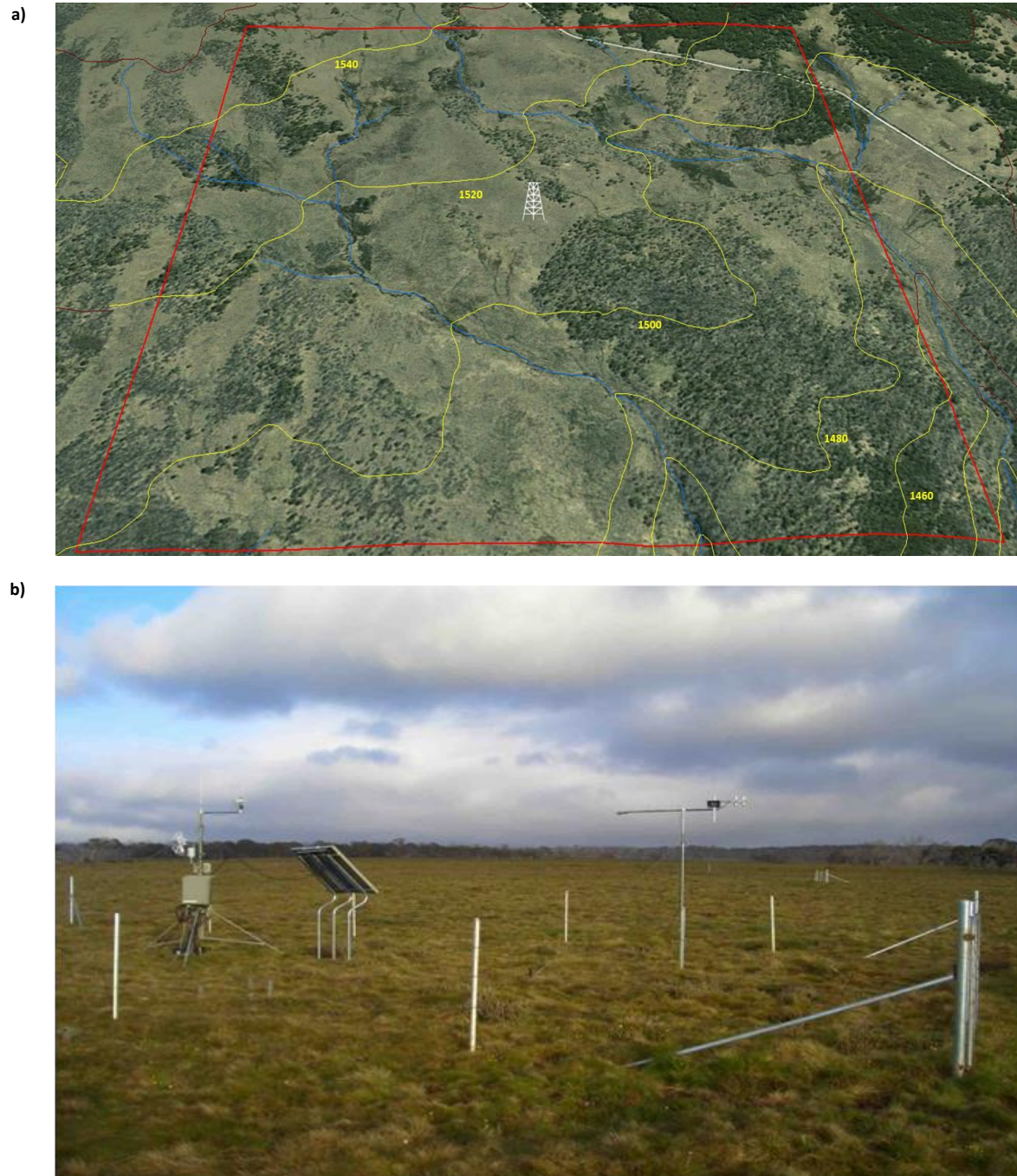


Figure 3.2: topographic representation of Dargo High Plains site (a; tilt angle:  $65^{\circ}$  [from zenith], view azimuth:  $0^{\circ}$ ) with 20m contours (yellow), watercourses (blue) and boundary of 2km x 2km tile (red) centred on the EC tower (Source: Google Earth. 'Dargo High Plains'.  $37^{\circ}8'0.18''S$  /  $147^{\circ}10'15.48''$ . Image date: 14/08/2009, access date: 15/01/2013); view towards northwest (b).

### 3.2.2 Nimmo

In New South Wales the Alps are more meridionally oriented than in much of Victoria, and Nimmo is located at 1326m elevation on the lower eastern slopes of the range, adjacent to Kosciuszko National Park. Nimmo Plain forms the broad floor of the Gungahlin River valley. While the topography in the immediate vicinity of the tower (*i.e.* within 100m radius) is almost flat, the terrain closer to the river slopes down gently, such that the slope aspect is radially variable rather than constant (though generally less than 2°), while to the northwest of the tower (~150m) the topography slopes more steeply upward (Figure 3.3a).

The region east of the Alps at this latitude generally experiences a significant rain shadow effect as it is in the lee of the ranges relative to the predominantly westerly flow. But while available historic precipitation data suggests that Nimmo is on average drier than Dargo (Table 3.1), in the study years of 2007 and 2008, measured precipitation at the sites was relatively similar. Nimmo was however generally warmer than Dargo, largely due to its lower altitude (see Chapter 5). The 2007/08 mean annual temperature at Nimmo was approximately 7.7°C, with a mean warmest month (January) temperature of 15.7°C.

The nocturnal cold air drainage phenomenon noted in Chapter 2 is chiefly responsible for the presence of the grassland at this relatively low altitude, a classic example of the inverted treeline phenomenon (as can be seen in Figure 3.3a, the surrounding hillsides are predominantly covered by *Eucalypt* woodland). The vegetation community at Nimmo is also broadly characterised as sod tussock grassland (Benson, 1994). Grasses were the dominant vegetation structural type (90-95%), with shrubs essentially absent. *P. sieberiana* was the dominant species in the locality of the tower; *R. nivicola* was also common, with more limited representation of *D. crassiuscula*. As with Dargo, a number of native forbs were also present. There was less standing biomass than at Dargo, and the site was drier, as indicated by both the absence of the bog species' seen at Dargo, and the fact that the tussock-forming *P. labillardieri* typical of well-watered grasslands in this region was found only in low lying areas along the edge of the river (Lamp *et al.*, 2001). While the site was also grazed, there was little direct evidence of damage from cattle at Nimmo, and surface canopy cover of approximately 100%. The vegetation within the expected tower footprint was more homogeneous at Nimmo, as clearly seen in Figure 3.3b.



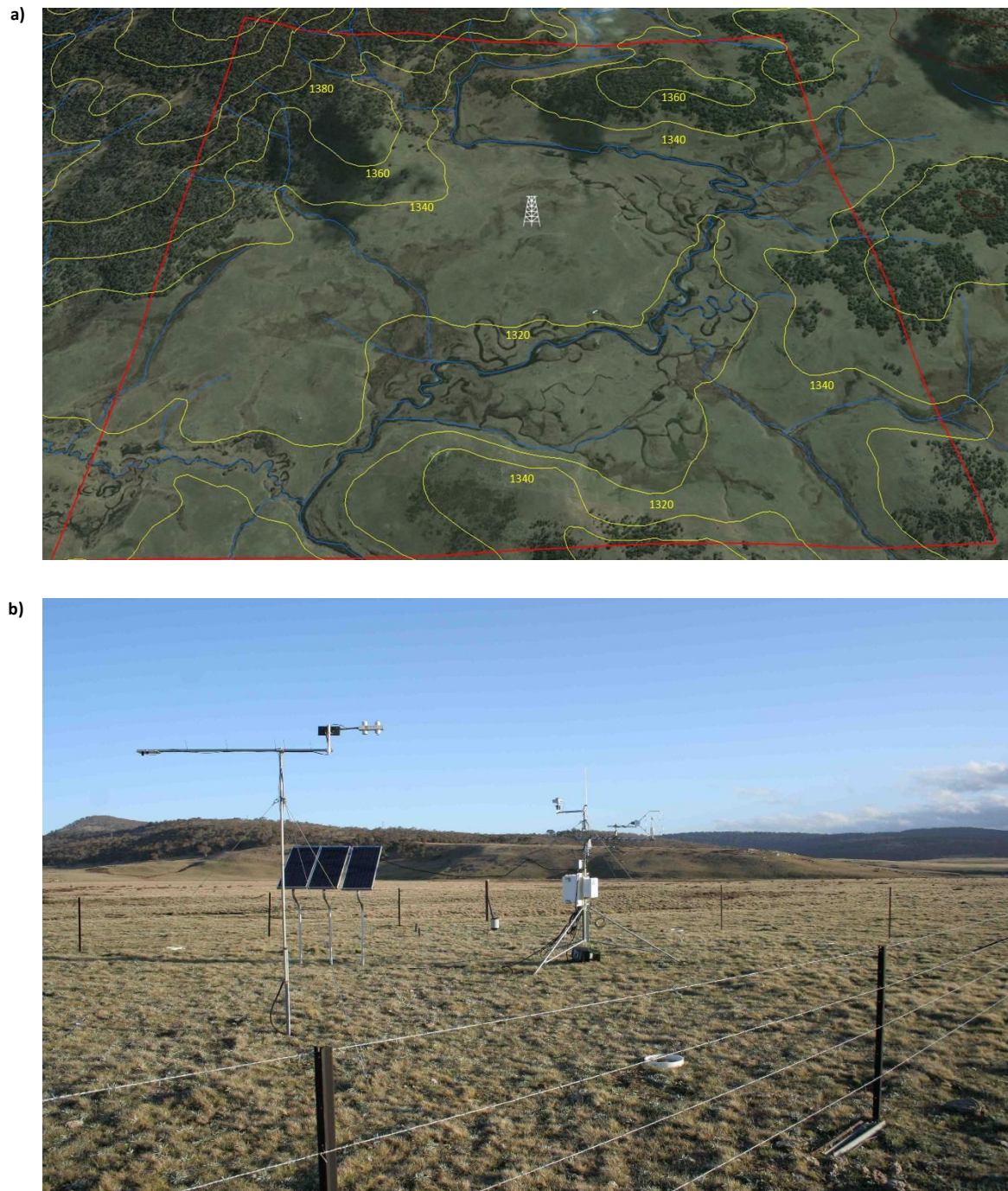


Figure 3.3: topographic representation of Nimmo Plain site (a; tilt angle:  $45^\circ$  [from zenith], view azimuth:  $0^\circ$  with 20m contours (yellow), watercourses (blue), and boundary of 2km x 2km tile (red) centred on the EC tower (Source: Google Earth. 'Nimmo Plain'.  $36^\circ 12' 56.03''\text{S}$  /  $148^\circ 33' 11.42''$ . Image date: 13/09/2010, access date: 15/01/2013); b) view towards south.

### 3.3 Site instrumentation

#### 3.3.1 Micrometeorological installation

Instrumentation at the sites was located with a view to optimising fetch while minimising topographic variation or large scale vegetation heterogeneities within the tower footprint area. In neither case was 'ideal' site placement possible, but the short-statured vegetation (<0.3m) allowed low measurement heights for the eddy covariance equipment and thus relatively small measurement footprints. Each site was powered by a 180W photovoltaic panel array charging a 12V 200Ah deep cycle battery bank. An open path eddy covariance system was used to measure CO<sub>2</sub>, H<sub>2</sub>O and energy fluxes, with an additional suite of instrumentation to measure the surface radiation balance, subsurface heat flux, temperature and moisture, and standard meteorological variables.

Figure 3.4 presents the instrument configuration at the Nimmo site (essentially duplicated at Dargo), and the full suite of measurement instrumentation deployed is listed in Table 3.2.

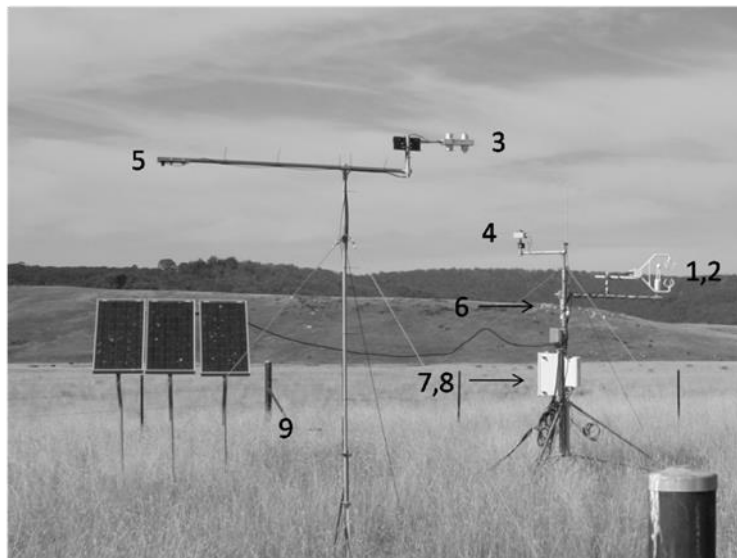


Figure 3.4: general instrument deployment (numbers correspond to instrumentation listed in Table 3.2).

**Table 3.2: site instrumentation.**

Measurement	Instrument	Model & Manufacturer	No.
Wind vectors / sonic temperature	3D Ultrasonic anemometer	CSAT3, Campbell Scientific Instruments, Logan USA	1
CO <sub>2</sub> and H <sub>2</sub> O vapour concentration	Infra-red gas analyser (IRGA)	LI7500, Licor Inc., Lincoln USA	2
Short / long wave radiation	Integrated pyranometer / pyrgeometer	CNR1, Kipp & Zonen, Delft Netherlands	3
Photosynthetically active radiation (↓)	Photodiode sensor	BF-3, Delta-T Devices, Cambridge UK	4
Photosynthetically active radiation (↑)	Silicon photovoltaic detector	QSO, Apogee Instruments, Logan USA	5
Temperature / relative humidity	Platinum resistance thermometer (PRT) / capacitive humidity sensor	HMP45C, Vaisala, Helsinki Finland	6
Barometric pressure	Silicon capacitive pressure sensor	PTB101B, Vaisala	7
Soil heat flux	Thermopile in ceramic-plastic composite	HFP-01, Hukseflux, Delft Netherlands	NA
Soil moisture	Time domain reflectometer (TDR)	CS616, Campbell Scientific Instruments	NA
Soil temperature	Averaging thermocouple thermometer	TCAV, Campbell Scientific Instruments	NA
Data logging	20+ channel, 16 bit analogue-digital measurement & processing unit	CR5000, Campbell Scientific Instruments	8
Rainfall	Tipping bucket rain gauge	TB3, Hydrological Services, Sydney, Aus	9

A 3D sonic anemometer mounted at a height of 2.3m measured wind vectors and sonic temperature while an infra-red gas analyser (IRGA) measured fluctuations in CO<sub>2</sub> and H<sub>2</sub>O vapour (both at frequency 10Hz). The IRGA was tilted approximately 30° (towards the south) to minimise accumulation of dust, water or snow on the windows, and was cleaned and calibrated approximately monthly. Level five purity molecular nitrogen (99.999% N<sub>2</sub>) was used to calibrate the IRGA zero point (offset). CO<sub>2</sub> span (gain) was calibrated with a 402.83ppm (±0.03) CO<sub>2</sub> (in dry air) standard, provided by the CMDL Carbon Cycle Greenhouse Gas group (NOAA, Boulder USA). Water vapour span was calibrated with a dew point generator (LI610, LICOR Inc., Lincoln USA). Flux data (i.e. sonic anemometer and IRGA output, including diagnostics) were locally written to flash memory cards that were collected during maintenance trips. Half-hourly estimates of fluxes as well as averages of other measured quantities (with the exception of rainfall, which was totalised, and pressure which was only sampled once per half hour) were also transferred via telemetry to Monash University.

Radiation sensors (measuring incoming and outgoing short-wave, photosynthetically active and long-wave radiation, as well as incoming photosynthetically active diffuse radiation) were mounted separately from the main instrument tripod, at a height of 3.5m. Temperature and humidity sensors were mounted at 2m above the soil surface on the main tripod, while a tipping bucket rain gauge was mounted separately at ground level, at a distance from obstacles appropriate to minimise interference with the wind field (see Sevruk and Zahlavova, 1994). These instruments are inappropriate for the measurement of snowfall, however, and during periods in which albedo measurements indicated snow on the ground, rainfall data (including the 24-hour periods immediately preceding and succeeding the indicated snowfall) was excluded from the record. Further details about the methods used to gap-fill missing data can be found in section 3.5. Wind speed and direction data were derived from the sonic anemometer.

Belowground, soil instrumentation was deployed to determine soil moisture and temperature fluctuations and subsurface energy fluxes. Two separate, randomly selected soil microsites were established at each site, with the soil heat flux plate installed at a depth of 8cm, and heat storage in the 0-8cm layer measured using soil averaging thermocouple thermometers deployed at 2 and 6cm depth (Figure 3.5). Soil moisture was measured using frequency domain reflectometry probes, inserted at 0.04m.

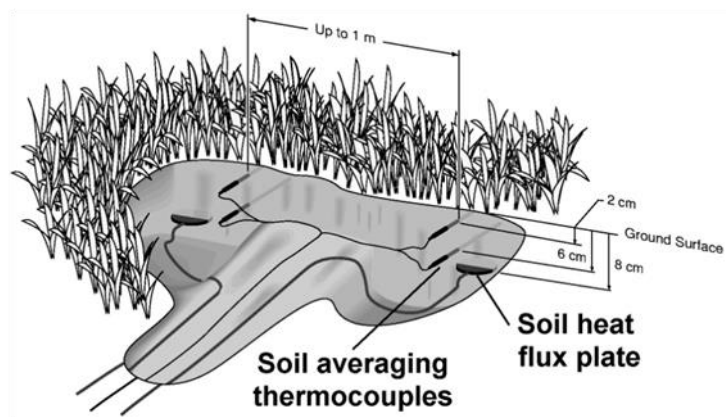


Figure 3.5: deployment of sensors to measure soil heat flux (from CSI, 2003, p2).

Soil heat fluxes were measured using the well-established combination method (Fuchs and Tanner, 1968) - which involves the direct measurement of subsurface fluxes at a given depth and the calorimetric determination of energy storage changes in the overlying soil layer, as follows:

$$G = G_s + G_z$$

Equation 3-1

Where  $G$  ( $\text{W m}^{-2}$ ) is the corrected subsurface heat flux,  $G_z$  is the measured flux at depth  $z$  and  $G_s$  is the calorimetrically derived energy storage correction. The combination method has been shown to compare favourably with more direct soil heat flux measurement methods (Cobos and Baker, 2003). To estimate energy storage from changes in temperature of the soil layer overlying the heat flux plates, an accurate estimate of aggregate soil thermal properties – and thus of the relative abundances of the significant soil components (organic and mineral soils, and water) - was needed. The method used to ascertain these quantities is described subsequently in section 3.8.2.

The volumetric heat capacity ( $C_v$ ) of the soil layer was then calculated as the weighted average of the soil constituents according to their relative abundances, as follows (Oke, 1987):

$$C_v = \rho_m c_m + \rho_o c_o + \rho_w c_w$$

Equation 3-2

Where  $\rho$  represents the density of the relevant constituent ( $\text{kg m}^{-3}$ ) and  $c$  the specific heat capacity ( $\text{kJ kg}^{-1} \text{K}^{-1}$ ), while the subscripts denote the mineral ( $m$ ), organic ( $o$ ) and water ( $w$ ) components (the contribution of air is negligible). The specific densities for the organic and mineral components were calculated from the relative mass fractions and soil bulk density (for example, for the mineral component at Dargo:  $\rho_m = 0.66 \times 521 = 344 \text{kg m}^{-3}$ ), whereas soil water was measured as a volumetric quantity (i.e. volumetric water content of 0.33 implies bulk water density of  $330 \text{kg m}^{-3}$ ). Specific heat capacity values ( $0.9$ ,  $1.92$  and  $4.18 \text{kJ kg}^{-1} \text{K}^{-1}$  for mineral, organic and water components, respectively) were taken from Monteith and Unsworth (2008). The storage term was calculated as follows (Oke, 1987):

$$G_s = C_v \frac{\Delta T}{\Delta t} z$$

Equation 3-3

Where  $\Delta T$  represents the change in temperature ( $^{\circ}\text{C}$ ) for time interval  $\Delta t$  (s) and  $z$  the depth of the lower boundary of the layer (m).



### 3.3.2 Chamber system

A chamber system was used as a secondary measurement of ecosystem respiration ( $R_e$ ), and thus as a quality check of both nocturnal measurements from the eddy-covariance system and the performance of temperature response functions used to estimate  $R_e$ . Given the small stature of grassland vegetation, it was possible to use a small portable chamber system to measure whole-ecosystem carbon exchanges. Following the classification of Livingston and Hutchinson (1995), the chamber system used here (Figure 3.6) was a non-steady state system, in which the chamber volume is isolated from the outside air over a fixed surface area and time-dependent changes in headspace concentration measured.

The clear acrylic cylindrical chamber had an internal volume of 31.8L and a surface area of approximately  $0.071\text{m}^2$ . An open path IRGA (GMP343; Vaisala, Helsinki, Finland) was mounted inside the chamber rather than the more common method of pumping air through tubing to an external closed-path IRGA, ensuring a light, efficient, portable and integrated system. The IRGA dust filter was removed to reduce response time to  $<2\text{s}$ , and the IRGA placed so that the transmission window and mirror were oriented vertically and would thus not readily accumulate dust. Two small computer fans continually mixed air in the chamber during measurement (wind speed at chamber base level =  $0.6\text{m s}^{-1}$ ), and internal pressure (PTB101B; Vaisala, Helsinki, Finland), temperature and moisture (HMP50; Vaisala, Helsinki, Finland) were simultaneously monitored so that the corrected  $\text{CO}_2$  mixing ratio could be continuously calculated on board the logger from the raw IRGA output using a set of externally applied compensation algorithms. The temperature sensor was constantly aspirated by being placed directly behind the chamber fan, and housed in a white shield to prevent radiation loading. The system was also vented using a length of  $\frac{1}{4}$ " OD Bev-a-line tubing attached to a small port in the top of the chamber to ensure pressure equilibration.

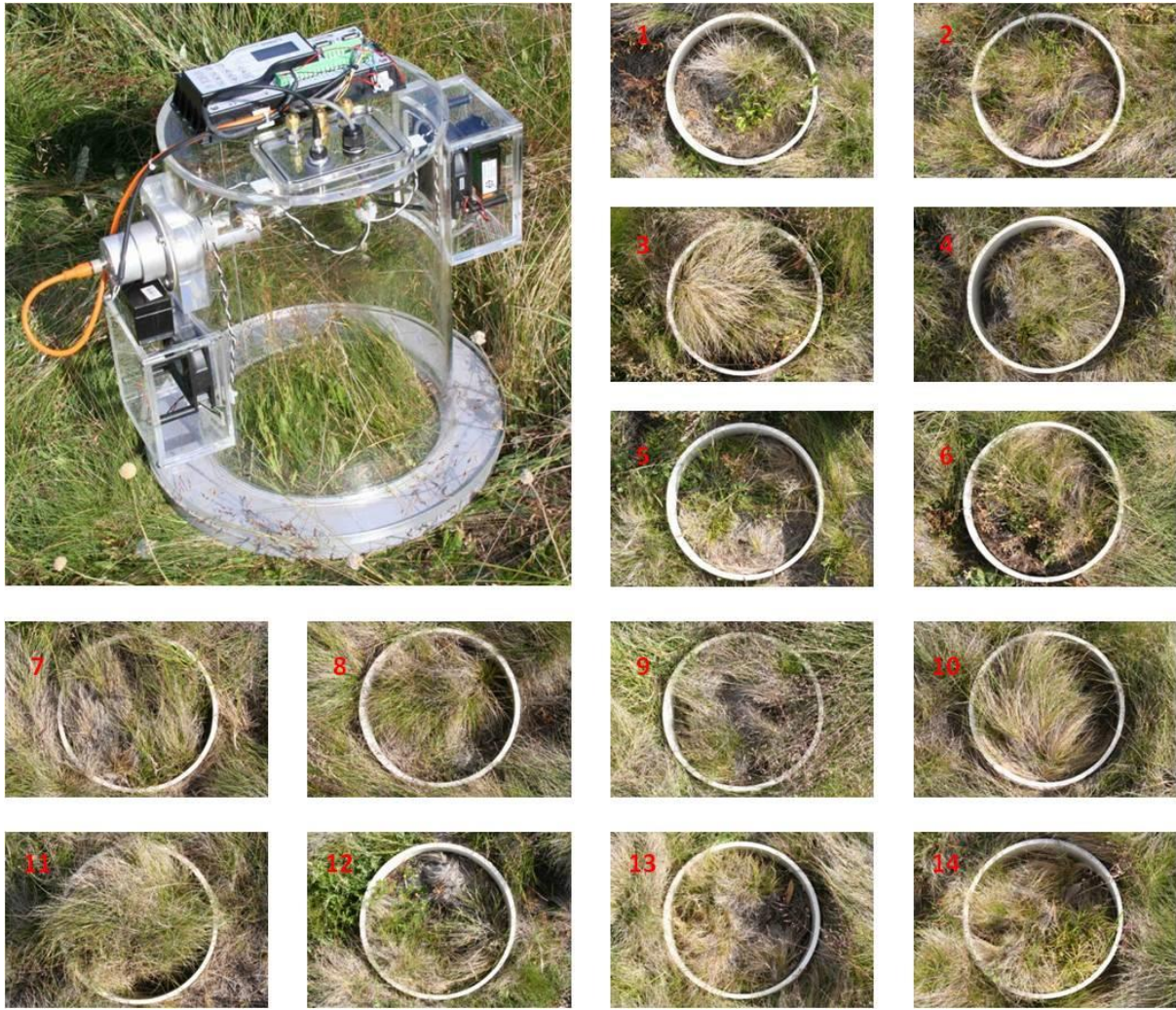


Figure 3.6: manual portable chamber system and permanent collars 1-14 at Dargo.

The system was deployed at Dargo during a five-day (21/01/08 – 25/01/08) intensive field campaign in which measurements were made four-hourly. Daytime  $R_e$  measurements were accomplished by covering the clear chamber with a heavy-duty opaque hood. During measurement, the chamber was fitted to 300mm ID PVC collars ( $n = 14$  - see Figure 3.6) permanently installed in the ground. Chamber fans were automatically switched on by the logger 10 seconds prior to the beginning of the measurement period of 120s (sampling interval = 2s) to ensure sufficient mixing.

Chamber  $CO_2$  flux rates ( $F_c$ ) were estimated from the time rate of change in  $CO_2$  mole fraction estimated by the slope of the linear regression line fitted to the data (Figure 3.7). Each two minute sample was visually inspected for evidence of asymptotic behaviour associated with  $CO_2$  saturation (which was not evident) or other measurement artefacts, and samples where  $r^2$  of the regression line was less than 0.95 were rejected. The rate of change of the mixing ratio was

converted to mass quantities and scaled according to the chamber volume and surface area, as follows:

$$F_c = \frac{\Delta[CO_2]}{\Delta t} \cdot \frac{PV}{R_c T} \cdot \frac{1}{a} \quad \text{Equation 3-4}$$

Where  $F_c$  is the  $CO_2$  flux ( $mgCO_2 m^{-2} s^{-1}$ ),  $\Delta[CO_2]/\Delta t$  the time (in s) rate of change in  $CO_2$  mole fraction in the enclosed volume,  $P$  ambient air pressure (Pa),  $V$  the combined volume of the space enclosed by the chamber and the collar ( $0.0381m^3$ ),  $R_c$  the specific gas constant for  $CO_2$  ( $188.96J g^{-1} K^{-1}$ ),  $T$  the chamber air temperature (K) and  $a$  the unit surface area ( $0.071m^2$ ) of the chamber system. The individual estimates for each of the 14 collars were then averaged to produce a site average flux estimate.

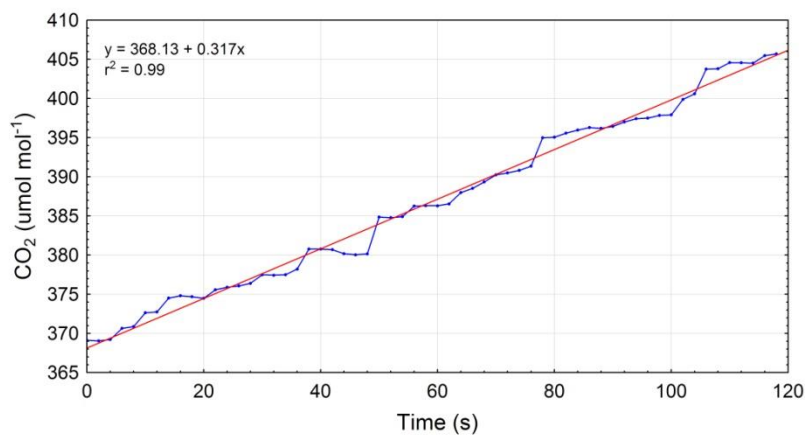


Figure 3.7: sample chamber incubation from collar #14 at 15:43 on 23/01/08; slope corresponds to ecosystem respiration of approximately  $0.27mgCO_2 m^{-2} s^{-1}$ .

While Pumpanen *et al.* (2004) undertook a comprehensive chamber inter-comparison, the system used here is not directly comparable to any of them. The study of Pumpanen *et al.* (2004) does however highlight the significant variations that occur between designs when compared to a standard. Every effort was made to minimise through design, calibration and data analysis potential sources of error. However, as outlined by Davidson *et al.* (2002), there is always some unavoidable disturbance by the measurement system of the object of measurement, which may therefore introduce some unquantified uncertainty.



### 3.4 Post-processing of eddy covariance data

As detailed in Chapter 2, while the theoretical basis of eddy covariance measurements is relatively simple, the practical application is more complex (Lee *et al.*, 2004b; Aubinet *et al.*, 2012b). The most complex and resource-intensive process of data preparation in this investigation was therefore associated with the eddy covariance data. This process is described below. A generalised description of the procedure used to produce finalised high quality flux datasets is presented in Figure 3.8. The process involved five steps: i) data acquisition and archiving; ii) raw data processing to produce meaningful flux estimates; iii) data quality assessment; iv) gap-filling of missing data; v) estimation of uncertainty in final data.

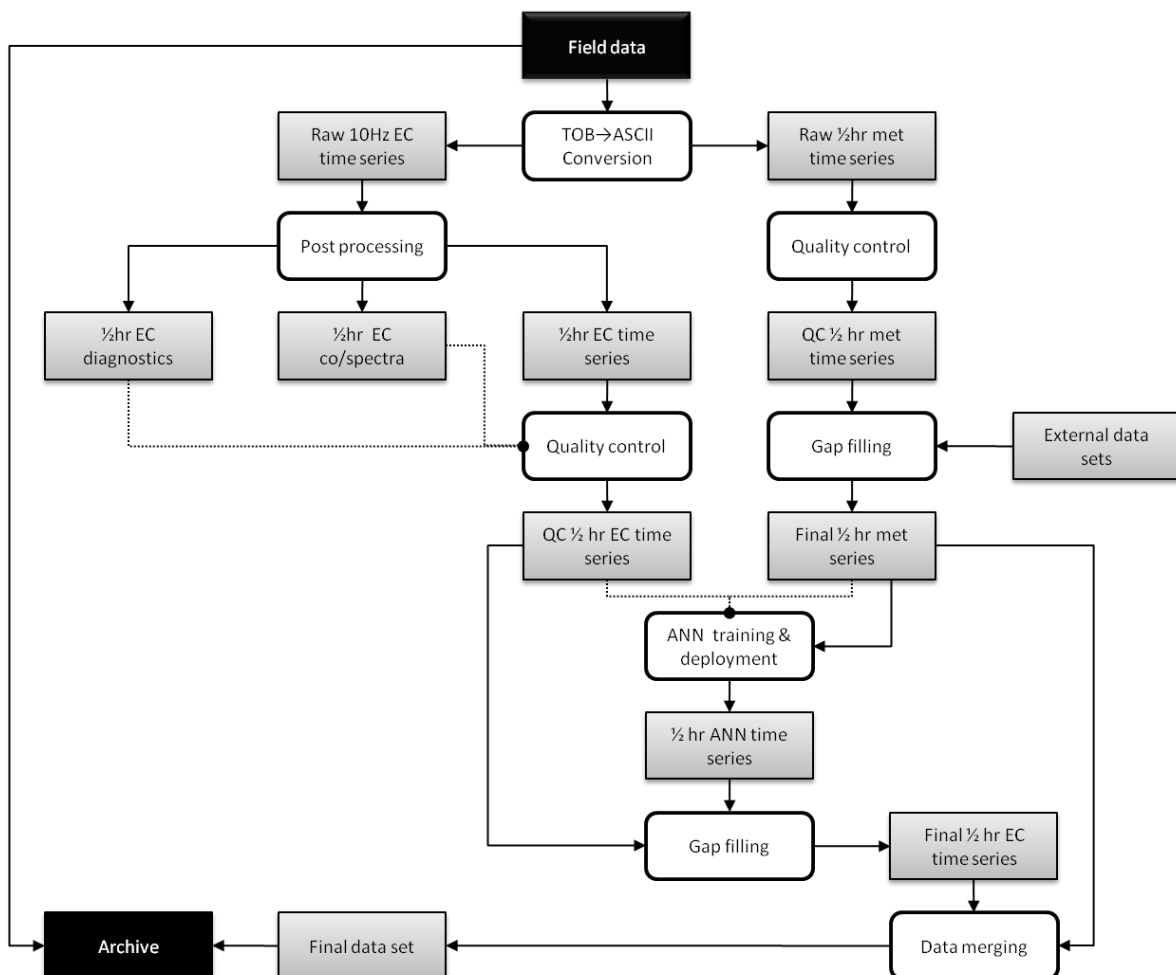


Figure 3.8: flux data processing and quality assurance procedure (grey boxes represent discreet data products; round boxes represent procedures applied to the incoming data set; dashed lines connect diagnostic data sets to the procedures in which they were used as reference data, or in the case of artificial neural network [ANN] training as input / target pairs for the training procedure, as detailed in section 3.5.1).

### 3.4.1 Raw data processing

Data processing techniques for eddy covariance data are in continual development and refinement, and a comprehensive evaluation of the more complex associated issues will not be attempted here (for an overview, see Lee *et al.*, 2004c; Mahrt, 2010). The raw 10Hz eddy covariance data was processed using the University of Edinburgh's EdiRE software, which has been shown to perform reliably in software intercomparison studies (Mauder *et al.*, 2008). The key elements of the processing procedure are detailed in Figure 3.9 below. The processing steps reflects a broad consensus about the most theoretically appropriate approach, as detailed in Burba and Anderson (2010). Some key aspects of the processing procedure that require further elaboration are discussed subsequently.

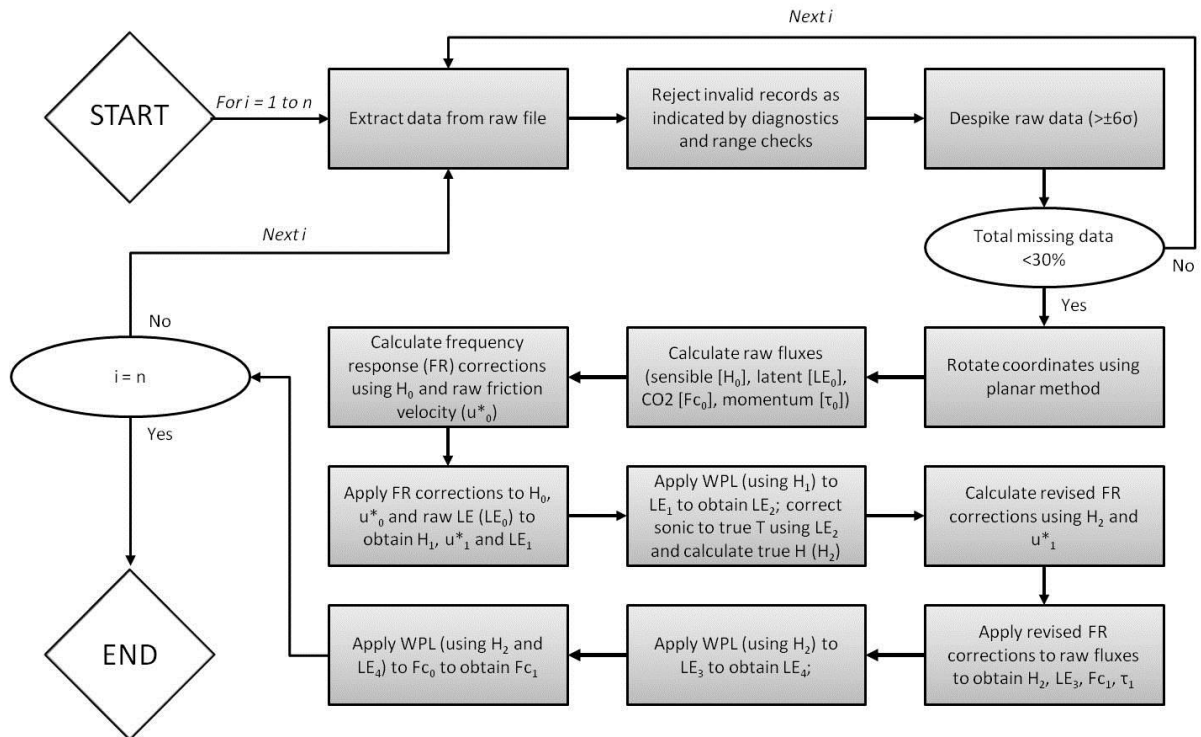


Figure 3.9: flow chart of EdiRE processing procedure to generate raw half-hourly flux estimates for each  $i$  of  $n$  half-hourly 10Hz eddy covariance data files (adapted from Burba and Anderson, 2010, p112). Note that subscripts refer to the number of iterative corrections applied, as indicated in the text.

## 1. Data rejection

Records were excluded if they coincided with IRGA / anemometer diagnostic errors or if they fell outside broad range limits. This was almost always caused by obscuring of the IRGA windows / anemometer transducers, generally by water. A count of the number of records removed (to which those with identified spikes – see below – was added) was retained as a diagnostic variable for each half-hourly file.

## 2. Despiking

While the above process removed the majority of non-physical data from the time series, an additional spike detection algorithm was employed to remove any short duration, large amplitude fluctuations (here defined as points  $>6\sigma$  from the time series mean), which may also be induced by random noise in the electronics (Foken *et al.*, 2004).

## 3. Rotation of wind vectors

As discussed in Chapter 2, the planar rotation method has come to be recommended as the most theoretically appropriate and reliable method of rotation (Finnigan *et al.*, 2003) – particularly in complex terrain - and was used accordingly in this study. The coordinate frame was recalculated for each month of data using a six-week window (i.e. with one week either side of the month for which rotations were applied). This minimised the introduction of potential step changes in fluxes that might otherwise be induced by an instantaneous change in the orientation of the coordinate frame.

## 4. Raw covariances / flux calculation

A standard block averaging procedure was used to calculate fluxes at half-hourly intervals, in which the flux was calculated from the interval mean of the covariances of the rotated vertical velocities and the relevant scalar quantity (Moncrieff *et al.*, 2004). While a half-hourly averaging interval is often insufficient to contain the full frequency spectrum of atmospheric motion that contributes to the flux, this is more commonly observed at sites with tall vegetation and / or particularly complex terrain (Finnigan *et al.*, 2003). The appropriateness of a half-hourly time interval was tested by plotting ogives (see Figure 4.6, Chapter 4), and found to be sufficient, with over 95% of the flux contribution occurring at frequencies above 0.0011Hz ( $\approx 15$  minutes).

## 5. Frequency response corrections

As discussed in Chapter 2, frequency response corrections account for losses in the observed flux measurements associated with frequency response attenuation by the measurement system and the flux calculations. Here the theoretical or 'transfer function' approach (described briefly in section 2.5.3.2) was used. There is a small circularity problem in that a cospectral model is required to calculate flux corrections, but the fluxes themselves (sensible heat flux [H]) – or quantities directly related to them (friction velocity [ $u^*$ ]) - are required to calculate the corrections (Burba and Anderson, 2010). A related problem is that H must be used to calculate the WPL correction for the water vapour flux before the sonic temperature (similar to virtual temperature) can be converted to 'true' temperature fluctuations. An iterative procedure was used to minimise the error introduced by these issues (as outlined in Figure 3.9).

## 6. Webb, Pearman and Leuning (WPL) density correction

Density corrections are required to account for differences in the density between ascending and descending air when the surface is a significant heat or mass source or sink (see Chapter 2). WPL corrections were applied after all other corrections, as suggested in Massman (2004). Water vapour fluxes were first corrected for the density effects of sensible heat flux, and CO<sub>2</sub> fluxes were then corrected for the effects of both sensible heat and water vapour.

## 7. IRGA heating correction

This correction is important for sites which periodically experience low daytime temperatures, during which differences in sensible heat flux arise between ambient measurements derived from the sonic anemometer and its actual value within the optical path of the IRGA (Burba *et al.*, 2008). However, since optical path sensible heat flux was not measured during this investigation, a semi-empirical approach – based on experimentally-derived correction factors expressed as a linear function of meteorological conditions (see Burba *et al.*, 2008 for details) - was used instead. It was applied only below a temperature threshold of 5°C. While this approach is

inevitably less accurate than direct measurements, Burba *et al.* (2008) report that it nonetheless provides more accurate flux estimates than applying no correction.

## 8. Storage within the control volume

This accounts for changes in storage of relevant quantities in the air layer between the surface and the measurement height (i.e. air enthalpy, biochemical energy storage<sup>20</sup>, moisture and CO<sub>2</sub>), and is thus added to the eddy covariance-calculated fluxes. Given the short measurement heights used in this study, storage within the control volume is a less critical issue than is the case for taller (e.g. forest) canopies, and measurements of changes in the above quantities below the measurement height were therefore not undertaken. Instead it was assumed that measurements at the instrument height provided a reasonable estimate of the true vertically-integrated quantities. While this is clearly not strictly accurate, during periods in which this assumption is substantially violated (e.g. stable conditions), data are far more likely to have been rejected on the basis of quality control criteria anyway (see below).

### 3.4.2 Quality assurance

Half-hourly flux data resulting from the previous process were filtered in several stages. The first involved the application of simple diagnostic criteria indicating whether measurements occurred during conditions under which the measurement system was expected to return invalid data. Where this was the case, fluxes were automatically rejected (referred to below as *automatic* rejection). The second involved assessment of whether the statistical properties of each half-hourly block of 10Hz data conformed to the assumptions underpinning the calculation of half-hourly fluxes. Objective quality ratings for three separate criteria were applied, and a final data quality flag derived from these. Data were rejected if they lay outside an acceptable range for the final quality flag (referred to below as *conditional* rejection). The third stage was the application of a statistical filter to the remaining data in the time series following the first two procedures (referred to below as

---

<sup>20</sup> Biochemical energy storage represents a daytime energy sink that may be a significant component of the energy balance (Meyers and Hollinger, 2004). Here it was calculated from the magnitude of gross canopy assimilation and the estimated energy required to break the bonds of the photosynthetic reactants (CO<sub>2</sub> and H<sub>2</sub>O) to form CH<sub>2</sub>O and O<sub>2</sub> (the Gibbs free energy). The value used was 454 kJ mol<sup>-1</sup> CO<sub>2</sub> fixed by photosynthesis (Nobel, 1983), corresponding to an energy storage rate of approximately 10.3 W mg<sup>-1</sup> CO<sub>2</sub> m<sup>-2</sup>.

*statistical* rejection). The fourth stage imposed a low-turbulence threshold on acceptability of nocturnal data (referred to below as *nocturnal* rejection). The fifth stage applied two passive evaluation methods<sup>21</sup> to gauge the extent to which the finalised flux data were affected by systematic measurement error. These steps are detailed below.

## 1. Automatic rejection

Half-hourly flux estimates were rejected when they coincided with *any* of the following conditions:

- Periods of instrument removal, maintenance, recorded or probable damage, or calibration;
- Measured rainfall;
- Mean wind direction 'behind' the tower (i.e. within a 20° sector centred 180° from the orientation of the sonic anemometer (Figure 3.10 below));
- Momentum flux directed away from the surface;
- H<sub>2</sub>O and CO<sub>2</sub> fluxes where sensible heat flux was invalid; CO<sub>2</sub> flux where H<sub>2</sub>O heat flux was invalid.

Range limits are also often employed to remove fluxes that exhibit clearly non-physical behaviour. This was avoided here, because it can create serious biases in the data set (Mahrt, 2010). For example, while nocturnal net surface CO<sub>2</sub> absorption is not plausible in this environment, it most likely occurs as a result of the noise (i.e. random error) superimposed on the flux signal. However, random errors of equal magnitude but opposite sign will not be removed by this process, and thus one tail of the error frequency distribution is trimmed while the other is not (Mahrt, 2010). The use of a statistical filter (see below) was thus considered a more objective approach to the removal of the remaining bad data.

---

<sup>21</sup> These were indicative rather than diagnostic measures of global data quality, and are passive in the sense that no further rejection / correction of data was undertaken on the basis of their results.

## 2. Conditional rejection

The second step involved the assessment of the remaining data on the basis of the data quality criteria proposed by Foken *et al.* (2004), which forms the basis of the EUROFLUX methodology (Aubinet *et al.*, 1999), and in which a total quality classification is constructed based on the extent to which data diverge from the idealised conditions that underpin the assumptions inherent in EC. These criteria are as follows:

Stationarity test. Time series instationarity violates the rules of the Reynolds averaging procedure required to derive flux estimates, which should thus theoretically be rejected under instationary conditions. In practice, a finite time series is necessarily instationary to some degree, and errors are small when mild instationarity is observed (Kaimal and Finnigan, 1994). The stationarity test used here - from Foken and Wichura (1996) – compares the statistical characteristics of the covariance time series (e.g.  $s_{wC}$ ) of the averaging interval (0.5hr) with that of a series of shorter intervals (5min) within it, as follows:

$$s_{wC} = 100 \left| \frac{\overline{w'C'}_{run} - \overline{w'C'}_{seg}}{\overline{w'C'}_{run}} \right| \quad \text{Equation 3-5}$$

Where  $\overline{w'C'}_{run}$  is the complete time-interval covariance, and  $\overline{w'C'}_{seg}$  is the mean of  $n=6$  short interval covariances:

$$\overline{w'C'}_{seg} = \left( \frac{1}{n} \right) \sum_{i=1}^n |\overline{w'C'}|_i \quad \text{Equation 3-6}$$

As described below, the degree of instationarity was rated on a numerical scale (1-9) and combined with the subsequently described tests to form a total quality rating.



Integral turbulence test. The integral turbulence test characterises the extent to which turbulence is well-developed according to the similarity theory of turbulent fluctuations (Aubinet *et al.*, 1999). Where windward obstructions are present (e.g. in the landscape or the instrumentation and support structure itself), measured values of integral turbulence are significantly higher than estimates from theory. These estimates are derived as follows (Aubinet *et al.*, 1999):

$$\frac{\sigma_w}{u^*} = a[\varphi_m(\zeta)]^b \quad \text{Equation 3-7}$$

Where  $\sigma_w$  is the standard deviation of the vertical wind velocity,  $u^*$  is friction velocity,  $a$  and  $b$  are predefined empirical coefficients,  $\varphi_m$  is the surface layer similarity function and  $\zeta$  is the Monin Obhukov stability parameter.

Wind direction test. The design of the sonic anemometer favours the measurement of winds that blow into the sampling space between the transducers without first encountering the instrument's support structure, such that the most favourable wind directions are those within a 180° field aligned opposite this structure (i.e. such that the x-vector in the anemometers coordinate system is > 0) (Figure 3.10). As winds move increasingly parallel with the instrument's major axis 'behind' the transducers (i.e.  $x < 0$ ,  $y \rightarrow 0$ ), the tower, its associated hardware and the instrument's support structure may induce additional mechanically-generated turbulence upwind of the sampling space. The problem is minimised by aligning the anemometer such that the expected prevailing wind (here westerly) is encountered as indicated in Figure 3.10.

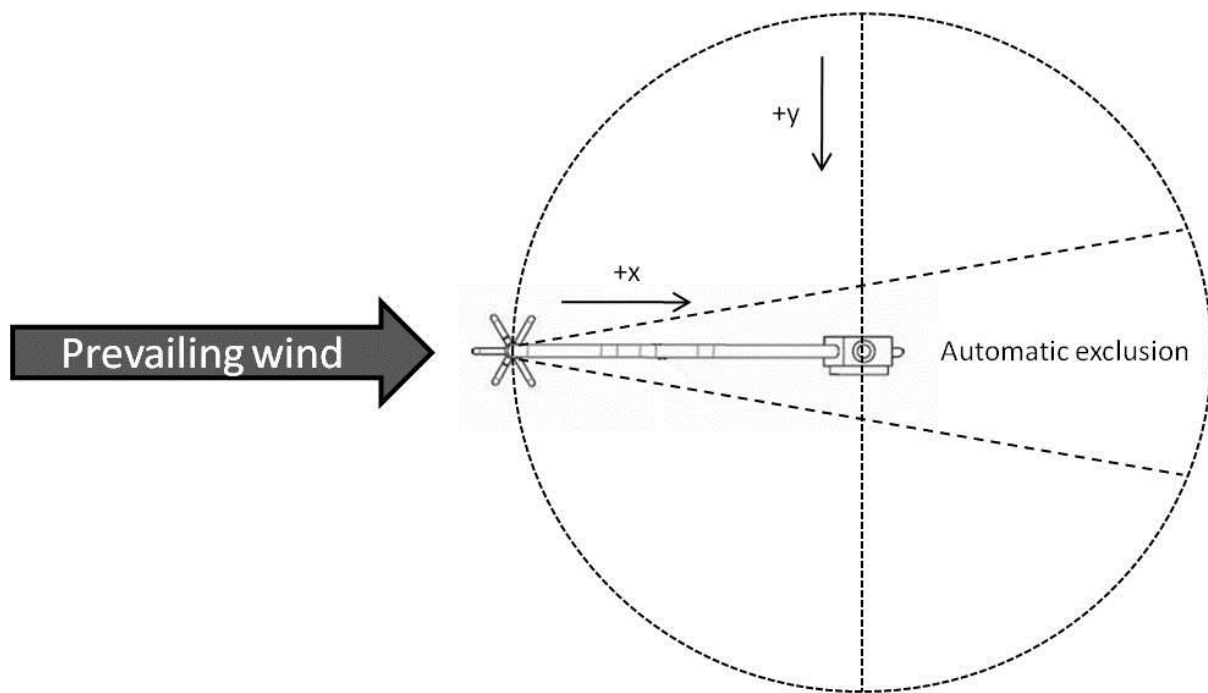


Figure 3.10: ideal orientation of sonic anemometer relative to prevailing wind ; winds originating within a  $20^\circ$  sector centred  $180^\circ$  from the orientation of the sonic anemometer were excluded, as described in the text (diagram adapted from CSI, 2007).

Quality classes for each of the above criteria are shown in Table 3.3. A general data quality classification (based on the scheme of Foken *et al.*, 2004) was then calculated according to the description in Table 3.4.

**Table 3.3: flux data quality classification scheme of Foken *et al.* (2004); note that the anemometer orientation is the angle of the prevailing wind direction for the time period relative to the +x-axis of the anemometer coordinate system.**

Stationarity (a)		Integral turbulence (b)		Anemometer orientation (c)	
Range (%)	Class	Range (%)	Class	Range ( $\pm^\circ$ )	Class
0-15	1	0-15	1	0-30	1
16-30	2	16-30	2	31-60	2
31-50	3	31-50	3	61-100	3
51-75	4	51-75	4	101-150	4
76-100	5	76-100	5	101-150	5
101-250	6	101-250	6	151-170	6
251-500	7	251-500	7	151-170	7
501-1000	8	501-1000	8	151-170	8
>1000	9	>1000	9	> 171	9

**Table 3.4: suggested combined data quality classes of Foken *et al.* (2004).**

Class	A	b	c
1	1	1-2	1-5
2	2	1-2	1-5
3	1-2	3-4	1-5
4	3-4	1-2	1-5
5	1-4	3-5	1-5
6	5	$\leq 5$	1-5
7	$\leq 6$	$\leq 6$	$\leq 8$
8	$\leq 8$	$\leq 8$	$\leq 8$
9	-	-	-

Classes 1-3 are considered to be of sufficiently high quality to be used for fundamental research such as model parameterisation; class 9 data is removed; classes 4-6 are considered to be sufficiently robust to remain as part of the relevant time series; class 6-8 data are more equivocal - Foken *et al.* (2004) recommend that data in this class may be used so long as they do not deviate significantly from neighbouring observations. The statistical procedure described below is used to detect such deviations and remove data accordingly.

### 3. Statistical rejection

The third stage involved the use of a statistical filter to detect and remove remaining outliers. Outliers were detected on the basis of a double-differencing technique, in which an observation is accepted or rejected depending on the extent to which the difference between it and neighbouring data exceeds the median of the absolute deviation from the median of differences of a larger block of data, as described in Papale *et al.* (2006). This is a more robust identifier of outliers than methods based on the standard deviation, since it provides a measure of spread much more resistant to large outliers. Here the method was applied to 10-day blocks of data with separate treatment for daytime and nocturnal data (nocturnal = global short-wave radiation  $<10\text{Wm}^{-2}$ ). For each of  $i$  half-hourly NEE values ( $NEE_i$ ), a 'difference' value ( $d_i$ ) was calculated as follows:

$$d_i = (NEE_i - NEE_{i-1}) - (NEE_{i+1} - NEE_i) \quad \text{Equation 3-8}$$

The median of the absolute deviation (MAD) of each  $d_i$  in the block from its median ( $M_d$ ) was then calculated as follows:

$$MAD = \text{median}(|d_i - M_d|) \quad \text{Equation 3-9}$$

A datum was rejected as a spike if:

$$d_i < M_d - \left(\frac{z \cdot MAD}{0.6745}\right) \quad \text{Or} \quad d_i > M_d + \left(\frac{z \cdot MAD}{0.6745}\right) \quad \text{Equation 3-10}$$

Where  $z$  is a threshold value, here set to four as per convention (Papale *et al.*, 2006).

#### 4. Low turbulence rejection

To correct for the effects of flux divergence under stable nocturnal conditions, the method of using a friction velocity threshold below which carbon fluxes were rejected was used (see Chapter 2, section 2.5.4.2). The objective threshold determination approach of Reichstein *et al.* (2005) was used here. It involves the separation of nocturnal CO<sub>2</sub> flux measurements into six temperature classes (by quantile), each of which was then divided into 20 u\* classes (also by quantile). In each of the temperature classes, the threshold was defined by comparing mean fluxes within each u\* class (in ascending order) to mean fluxes of all classes of higher u\*. When the class mean flux reaches 95% of the aggregate mean, the threshold value is taken as the mean u\* for that class. This value is accepted only if there is low or no correlation (i.e.  $r^2 < 0.4$ ) between u\* and temperature for that temperature class. The final u\* threshold is determined as the median of the  $n = 6$  temperature classes. Though this was done separately for each season, seasonal differences were minimal (data not shown).

#### 3.4.3 Passive evaluation

Two methods were used to gauge the extent to which measurements were affected by the two key systematic errors that remain as serious sources of uncertainty in eddy covariance measurements: energy balance closure and nocturnal underestimation of turbulent fluxes (Finnigan, 2008). Where both radiant and convective energy fluxes as well as energy storage terms are adequately characterised by the measurement system (as is assumed to be the case here), the degree of energy balance closure is generally considered a useful diagnostic indicator of system performance that also applies to the measurement of other mass fluxes measured by the same system (Baldocchi, 2003). The chamber system described in section 3.3.2 was also used to provide an independent measure of ecosystem respiration as a gauge of the accuracy of both nocturnal ecosystem / atmosphere exchanges of CO<sub>2</sub> and the response functions used to estimate them. Results are reported in Chapter 4.

### 3.5 Imputation of flux and meteorological data

Gaps in the final data sets occur as a result of both data losses due to rejection of low quality data (as detailed above) and system malfunction. Given that one of the aims of the current study is to calculate annual net ecosystem exchange of carbon, these data losses necessitate accurate methods for imputation (gap-filling) of missing flux data. A number of methods have been employed in the literature, including look up tables, mean diurnal variation techniques, empirical (generally non-linear regression) and process-based models, and artificial neural networks (Falge *et al.*, 2001; Moffat *et al.*, 2007). With the exception of process-based models, all of these methods involve the development of empirical relationships between the target variable (in this study, ecosystem / atmosphere exchanges of CO<sub>2</sub>) and a set of (primarily abiotic) environmental controls (for example, meteorological variables). As such, a complete time series of each of these controls or ‘drivers’ is a necessary prerequisite of imputation of CO<sub>2</sub> fluxes. Below, the processes for the imputation of: 1) CO<sub>2</sub> fluxes and; 2) meteorological drivers is described.

#### 3.5.1 CO<sub>2</sub> fluxes

This study used artificial neural networks (ANNs) to gap-fill missing CO<sub>2</sub> flux data. ANNs are highly specialised empirical non-linear regression models, and offer generally superior performance to other methods (Richardson *et al.*, 2006a; Moffat *et al.*, 2007). In contrast to traditional parametric approaches, however, relationships between dependent and independent variables are not prescribed in closed mathematical form. The fact that these relationships aren’t required to be defined *a priori* constitutes the great advantage of ANNs; their utility thus ranges from benchmarking the performance of land surface models (Abramowitz, 2005) to gap-filling of ecological datasets (Leuning *et al.*, 2005), and as a tool for the investigation of hierarchies of multivariate ecological dependencies of, for example, net ecosystem exchange (Moffat *et al.*, 2010). The corresponding disadvantage of ANNs is what has been described as the ‘black box’ problem (Ooba *et al.*, 2006) – the system generally cannot be more than superficially interrogated to elucidate the form of those relationships. In the current study their use is largely limited to gap-filling, and traditional parametric methods are used for analysis of ecosystem responses to environmental variables.

The architecture of ANNs consists of a network of interconnected nodes, with input, hidden and output layers (Figure 3.11). This is the basic topology of multi-layer perceptrons (MLPs) (Henseler, 1995), the type of network used here, which work as follows. Input (independent) and target (dependent) variables are presented to the network. At each node, the incoming signal is transformed by an (typically sigmoidal) activation function defined for the layer and passed forward to the next node via weighted connections. These weights alter the strength of the signal passed forward from the previous node, and training of the model involves the use of a back-propagation algorithm (here Broyden Fletcher Goldfarb Shanno, or BFGS) to iteratively adjust these weights to minimise differences between model output and target variable pairs. The weights thus effectively represent the model regression parameters (Bishop, 1995). The MLP is a feed-forward back propagation network, the properties of which are: i) each node connects to all of those in the subsequent layer; ii) no lateral connections between nodes occur within a layer; iii) computational flow is unidirectional – forward from input through hidden layer to output - with no feedback connections; iv) information about the estimation error between target and network output is propagated back through the network, and the connection weightings adjusted to minimise the error (Bishop, 1995; Rao and Srinivas, 2003).

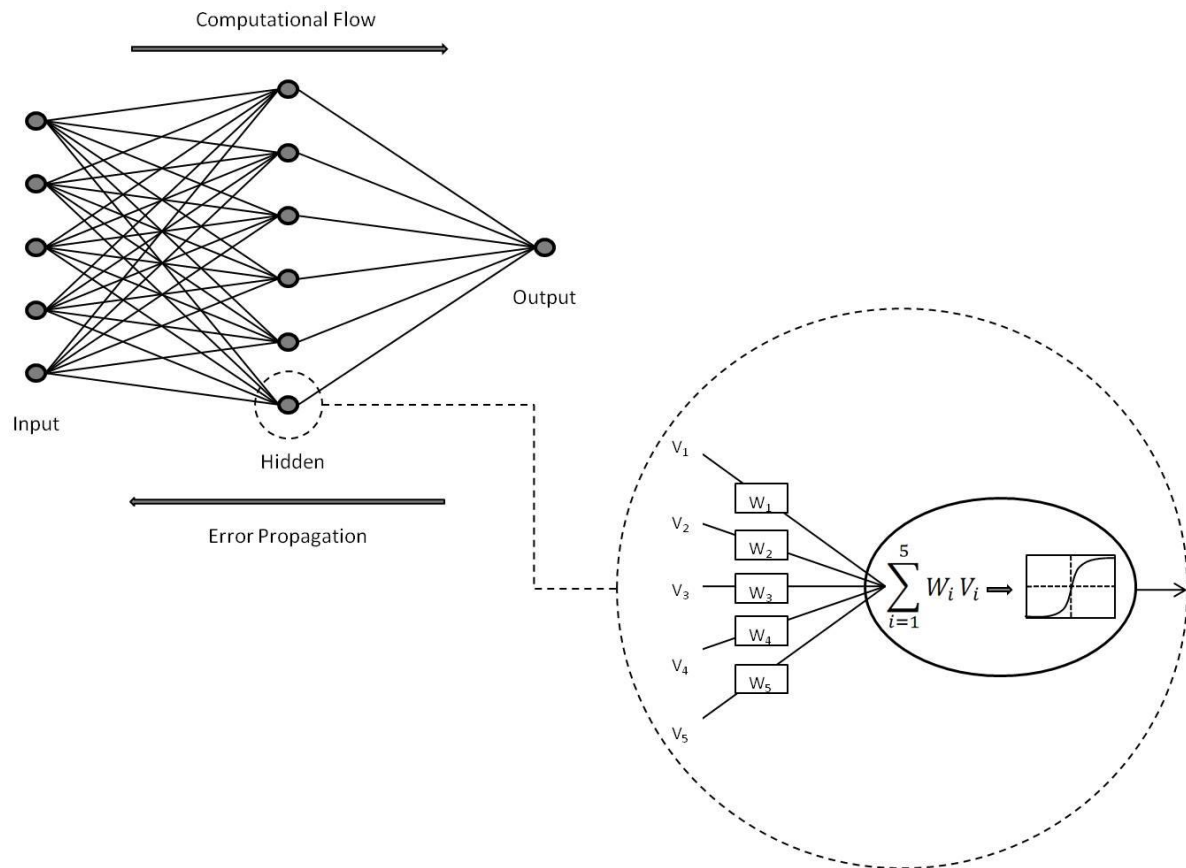


Figure 3.11: generic 5-6-1 multi-layer perceptron (MLP) neural network architecture and representation of single hidden layer node;  $V_i$  is the  $i$ th variable and  $W_i$  its weight.

The architecture of the neural network is a critical determinant of its performance. With sufficient degrees of freedom (more nodes and connection weights), the network may be trained so that it approaches zero prediction error. However, this occurs at the expense of the network's ability to predict unseen data (i.e. data that was not presented during training) or 'generalise'. In other words, the output of the network becomes less constrained by the information about the target behaviour actually contained in the input variables and instead increasingly reflects the complex structure of the network. This 'overfitting' is avoided by the use of an appropriate stopping criterion. The approach used here - early stopping - randomly allocates fixed proportions of the data between two separate data sets: a set with which the network is trained, and a set never presented to the network that is instead used to assess its generalisation performance following successive iterations. Training is terminated when the network's ability to predict the unseen data ceases to improve, irrespective of whether the fit to the training data continues to improve.

The artificial neural network module of the Statistica 10 software package (StatSoft, Tulsa) was used for construction of the ANNs used to predict missing data in this study. The variables used



as network input are listed in Table 3.5. The inclusion of outgoing photosynthetically active radiation provides a very broad canopy-integrated measure of vegetation phenological response to ambient changing meteorological conditions, and was found to greatly improve the performance of the networks.

The choice of the particular variables was informed by a basic understanding of their importance to ecosystem function; in this sense, the process of using ANNs to characterise ecosystem function in terms of a set of climatic drivers is not entirely free of *a priori* assumptions. While there is no question of the relevance of the included variables, the exclusion of other relevant variables (i.e. those which elicit a unique response from the ecosystem in addition to those included) inevitably degrades performance. As such, the proportion of variability in the target variable that is explained by the input variables (i.e.  $r^2$ ) is an important metric for the evaluation of model performance and is also presented in this study (see Chapter 4).

**Table 3.5: control variables used as inputs for artificial neural networks.**

Target Variable	Input Variable
NEE	1. Incoming photosynthetically active radiation (PAR)
	2. Reflected PAR
	3. Air temperature (2m)
	4. Vapour pressure deficit (2m)
	5. Soil temperature (0.04m)
	6. Volumetric soil moisture content (0-10cm)

The cost function used to assess network performance was sum-of-squares error. The activation functions of the input and output nodes were set to the identity (i.e. the neuronal signal is passed forward unchanged), and a sigmoidal function used for the hidden layer nodes. The approach used was to train 1000 networks for each of day and night and retain the best ten on the basis of the above performance criterion. The ensemble output mean of the retained networks was used to fill all missing data for the study period.

### 3.5.2 Meteorological drivers

The quality of radiation and meteorological data was generally high, with very little removal required (bad data were detected by visual inspection and basic range checks). Virtually all of the losses of this data occurred due to total system malfunction. Gap filling of missing data was accomplished using several methods. For smaller gaps, the following generic gap-filling approaches were used for all meteorological variables:

- gaps of two hours or less ( $n \leq 4$ ): simple linear interpolation of the time series data points neighbouring the gap;
- longer sub-day gaps ( $4 < n \leq 48$ ): mean diurnal variation method (MDV; Falge *et al.*, 2001), in which each gap is filled with the mean of the given time period for  $n$  neighbouring days (in this study,  $n = 10$  was used, which was short enough to avoid seasonal trend changes in the time series but long enough to account for synoptically-generated variability).

These methods were judged to be appropriate over shorter time periods because they provided superior continuity with the existing data. Longer gaps ( $> 1$  day) were primarily filled using data sets supplied by external agencies, as detailed in Table 3.6.

**Table 3.6: data sources for imputation of meteorological drivers.**

Variable	Data Source
Incoming PAR	BAWAP <sup>1</sup> interpolated insolation surfaces estimated from hourly visible-band geostationary satellite data (currently MTSAT-1R) using a physical atmospheric radiative transfer model and water vapour amount estimated from a numerical weather prediction model (Grant <i>et al.</i> , 2008). A downscaling algorithm incorporating orbital parameters to estimate the sun's position and an optimisation routine to estimate the extinction coefficient was used to estimate half-hourly values from daily data. A scaling coefficient of 0.45 (derived from available data) was used to estimate PAR from insolation.
Outgoing visible-wavelength radiation	MODIS <sup>2</sup> Collection 5 land surface visible wavelength albedo product MCD43A3 (ORNL DAAC, 2009) was linearly interpolated to daily frequency and used in conjunction with incoming PAR (assuming fixed albedo across daylight hours) to downscale to half-hourly frequency.
Air temperature	Bureau of Meteorology station data. Dargo: Mount Hotham Airport (station ID 083055 - approximately 17.2km northeast of and 223m lower than field site); Nimmo: Cabramurra AWS (ID 072161 - approximately 31.7 km northwest and 136m higher than field site). Linear transforms were applied to data using regression parameters.
Humidity	Bureau of Meteorology station data as described above.
Precipitation	SILO <sup>3</sup> interpolated precipitation surfaces, which uses a three stage procedure to interpolate measured precipitation from BOM stations to create a gridded dataset for the Australian continent for the period 1899-present (Jeffrey <i>et al.</i> , 2001). SILO data was used for precipitation rather than AWAP data because it was found generally to be subject to slightly lower error close to the east coast in a comparison study (Beesley <i>et al.</i> , 2009), and with respect to the data in the current study.
Soil moisture	Australian Water Availability Project soil moisture estimates derived using the WaterDyn model. The model adopts a mass balance approach in which soil moisture within the control volume (i.e. within the specified layer) is determined by the balance between inflows (precipitation) and outflows (evapotranspiration, runoff and infiltration through to deeper layers). These quantities are derived using a combination of gridded observational reanalysis surfaces, remotely sensed data and modelled estimates (see Raupach <i>et al.</i> , 2008).
Soil temperature	Adopted methodology similar to Zheng <i>et al.</i> (1993), where a running average of local daily air temperature was used to estimate soil temperature. The optimum interval for the running average was found by calculating the coefficient of determination ( $r^2$ ) for successively increasing running average windows and selecting the window that maximised $r^2$ . Downscaling to half-hourly frequency was accomplished by finding for each day the six days with the closest daily average soil temperatures, and averaging their half-hourly values.

<sup>1</sup> Bureau of Meteorology and Australian Water Availability Project.

<sup>2</sup> MODerate-resolution Imaging Spectroradiometer.

<sup>3</sup> SILO is a database of approximately 120 years of continuous daily weather records for Australia that was developed by the Australian Bureau of Meteorology. The data drill facility offers spatially interpolated synthetic estimates of daily weather variables at 5x5km resolution across the continent (for more information, see <http://www.longpaddock.qld.gov.au/silo/index.html>). Details of the methodology is available in Jeffrey *et al.* (2001).

### 3.6 Flux uncertainty analysis

As discussed in Chapter 2, there are numerous sources of error inherent in the measurement of turbulent fluxes using eddy covariance. These errors create uncertainty in flux estimates, and include systematic (i.e. bias-inducing), model (gap-filling) and random errors. Systematic errors were discussed in Chapter 2, and relate to the interactive effects of the measurement limitations of the observation system with surface conditions and meteorology. Gap-filling error arises as the result of the inability of the gap-filling method to make perfect predictions, due to systematic and random error in the observational data, shortcomings in the model used to make predictions, and missing input data to the model. Random errors in eddy covariance measurements arise as a result of: i) the flux measurement system itself; ii) the stochastic and intermittent nature of turbulent transport, and; iii) footprint heterogeneity (Hollinger and Richardson, 2005). The approach used to explore these uncertainty sources is outlined below.

#### 3.6.1 Systematic error

This error is difficult to account for in the absence of an independent and accurate standard estimate. If this was available, the eddy covariance system would be redundant. Since the major sources of potential systematic error remain a topic of ongoing fundamental research (Mahrt, 2010), here the approach has simply been to adopt data treatment methods that minimise the influence of known sources of systematic error while acknowledging that additional unknown and unquantifiable systematic errors cannot be comprehensively ruled out. By definition, such errors cannot be accounted for, but all studies based on real world (and thus error-prone) measurements are similarly subject to the same qualifications. The two key indicators of potential systematic data error in eddy covariance measurements – poor energy balance closure and nocturnal flux underestimation (see discussion in Chapter 22.5.4) – are used as passive indicators of data quality (i.e. no corrections are applied) in this study.

### 3.6.2 Model error

Errors in the model used to gap-fill the time series are generally the primary source of uncertainty in time-integrated sums of net ecosystem exchange (Dragoni *et al.*, 2007). Model error ( $\hat{\varepsilon}_M$ ) was simply calculated as:

$$\hat{\varepsilon}_M = F_c - F_M \quad \text{Equation 3-11}$$

Where  $F_c$  and  $F_M$  represent observed and model-generated data. Here it was assumed that  $\hat{\varepsilon}_M$  for periods with missing observational data could be estimated from the  $\hat{\varepsilon}_M$  population for adjacent periods (estimates were drawn appropriately from separate day and night error populations). For each day in the time series, random draws (with replacement) were made from an error population in a 10-day moving window (centred on the day) for each point with missing observational data. Where the error population was less than 10% of the total number of potential records, (due to occasional long gaps in the data set), an alternative method of error estimation was used. The standard deviation of  $\hat{\varepsilon}_M$  [ $\sigma(\hat{\varepsilon}_M)$ ] was calculated for all 20-day windows with sufficient data in the time series, and missing periods interpolated using a fitted sinusoidal function based on time of year (model error was greatest during summer and least during winter). Random estimates were then drawn from a normal distribution scaled according to the value of  $\sigma(\hat{\varepsilon}_M)$ .

Errors were summed (together with those for random error where observational data was present – see below) for each day and across all days in the time series. Monte-Carlo simulation was then used to assess the accumulated uncertainty through time, by repeating the above process  $10^4$  times, and calculating the uncertainty as the  $2\sigma$  confidence interval of the (normally distributed) trial outcomes. This inevitably slightly overestimates model error because as calculated  $\hat{\varepsilon}_M$  contains *both* random measurement (see below) *and* gap-filling errors, whereas by definition model estimates do not contain the latter. If it is assumed that random and model errors are independent, their variances can theoretically be separated as (Dragoni *et al.*, 2007):

$$\sigma^2(\varepsilon_M) = \sigma^2(F_c - F_M) - \sigma^2(\delta) \quad \text{Equation 3-12}$$

Where  $\varepsilon_M$ ,  $F_C$ ,  $F_M$  and  $\delta$  represent ‘true’ model error, measured CO<sub>2</sub> flux, model-estimated CO<sub>2</sub> flux and random error (see section 3.6.3 below), respectively. However, it was found in this study that model error was actually slightly lower in magnitude than random error, indicating that estimates of random error are too high and/or that model performance is approaching the noise limits of the data. Moffat *et al.* (2007) also report the latter to be the case for model estimates using artificial neural networks across multiple Fluxnet sites. As a result, it was not possible to reliably separate these error sources here, and reported uncertainty bounds are therefore likely overestimated.

### 3.6.3 Random error

While generally not the primary source of uncertainty in time-integrated sums of net ecosystem exchange, random error is nonetheless an important error source (Richardson *et al.*, 2006b; Dragoni *et al.*, 2007). While random error is best quantified using paired measurement systems, this was not an option here. Instead, the ‘successive days’ approach was used, in which the magnitude of random error was estimated from the difference ( $\delta$ ) between flux observations at the same time of day separated by 24 hours under similar environmental conditions (Hollinger and Richardson, 2005). Following Hollinger *et al.* (2005), the following environmental difference thresholds were used: i) photosynthetic photon flux density:  $\leq 20 \text{ Wm}^{-2}$ ; air temperature:  $\leq 3^\circ\text{C}$ , and; wind speed:  $\leq 1 \text{ ms}^{-1}$ . For both sites the imposition of these conditions restricted the number of estimates of  $\delta$  to <10% of total retained flux measurements.

Since the imposition of *identical* conditions would exclude all data, the relaxation of environmental difference thresholds inevitably also includes a component of ‘true’ flux difference (i.e. derived from differences in environmental drivers, and thus *signal* rather than *noise*) in addition to the random error, and thus  $\delta$  is most likely overestimated. Hollinger and Richardson (2005) report overestimation of 20-25% for CO<sub>2</sub> fluxes relative to the paired measurement system approach, though Dragoni *et al.* (2007) report that it may in some cases be up to a factor of two.

Given the characteristic heteroschedasticity of eddy covariance data, statistical measures of random error (here the standard deviation,  $\sigma(\delta)$ ) must be expressed as a function of flux magnitude (Richardson and Hollinger, 2005). This was done by binning the data (into  $j$  bins) as follows (Dragoni *et al.*, 2007):

$$\sigma(\delta)_j = \sqrt{2} \frac{1}{n} \sum_{i=1}^n |\delta_{i,j} - \bar{\delta}_{i,j}| \quad \text{Equation 3-13}$$

Where  $\bar{\delta}_{i,j}$  is the mean bin random error for each  $i$  of  $n$  data in bin  $j$ . This was linearly regressed against the corresponding bin average flux to approximate continuous distributions for  $\sigma(\delta)$  under nocturnal and daytime conditions.

Following the procedure of Dragoni *et al.* (2007), these regression relationships were then used to generate random error estimates for each measured flux observation remaining in the time series ( $\sigma[\delta]$  was retrieved as a function of the model rather than the observed flux estimate, since the latter contains random error). Because random error in eddy covariance data is highly leptokurtic (approximately Laplacian) (Hollinger and Richardson, 2005),  $\delta$  was estimated by random draw from a Laplace distribution with a scaling parameter ( $\beta$ ) related to  $\sigma(\delta)$  as  $\beta = \sigma(\delta)/\sqrt{2}$ . Thus a random cumulative probability value ( $p$ ) between 0-1 was generated and the corresponding  $\delta$  derived by inversion of the cumulative density function of the Laplace distribution, as follows:

$$f^{-1}(p) = \begin{cases} \ln(2p)\beta - \mu, & p < 0.5 \\ -\ln(2[1-p])\beta - \mu, & p \geq 0.5 \end{cases} \quad \text{Equation 3-14}$$

Where  $\mu$  is a location parameter (here = 0). The derived estimate of  $\delta$  was summed for all periods with observational data across all days in the time series as part of the Monte-Carlo procedure used to estimate cumulative total random error-derived uncertainty as described above. The uncertainties for random and model error sum in quadrature as:

$$\sigma_{tot} = \sqrt{\sigma(\delta)^2 + \sigma(\varepsilon_M)^2} \quad \text{Equation 3-15}$$

A continuous estimated time series for ecosystem respiration was also generated from empirical response functions derived from the relationship between nocturnal CO<sub>2</sub> fluxes and environmental variables (soil temperature and moisture; further detail is found in 3.7.1). Uncertainties in this series were assessed by: i) generating a noiseless synthetic time series from the best-fit parameterised response functions (see section 3.7.1 for details) and the observational time

series' of soil temperature and moisture; ii) imposing on the time series random error scaled according to the flux magnitude (as described above); iii) deriving new parameter estimates by fitting the response functions to the new time series containing signal and noise, and; iv) calculating time-integrated ecosystem respiration sums. This process was repeated  $10^4$  times, and the uncertainty in respiratory sums expressed as the  $2\sigma$  confidence interval of the (normally distributed) trial outcomes over that period. This process allowed quantification of the effect of multiple simultaneous parameter uncertainties on ecosystem respiration, as well as of the individual parameter uncertainties. Since gross primary production is equal to the difference between net ecosystem exchange and ecosystem respiration, the uncertainties in partitioning of GPP propagate directly to GPP.

### 3.7 Flux partitioning and data analysis

The assembly of carefully quality controlled time series' is a necessary step in producing datasets that can be used for accurate statistical characterisation of climatic and ecosystem properties with minimal bias and artefacts. Most analytical procedures discussed in the thesis are relatively simple and self-explanatory and thus are not described here. However, a detailed description of the empirical models used to describe, quantify and compare assimilatory and respiratory fluxes is given below. All data analysis in this study was undertaken using the Statistica 10 non-linear estimation module. Parameter optimisation employed the Levenberg-Marquardt algorithm.

#### 3.7.1 Ecosystem respiration model

Since net ecosystem exchange (NEE) represents the sum of gross primary production (GPP) and ecosystem respiration ( $R_e$ ) (see Chapter 2), an estimate of either of these components can be used to derive the other. The most common approach is to estimate  $R_e$  by fitting environmental response functions to the available nocturnal data (when  $NEE = R_e$ ). As previously discussed,  $R_e$  responds strongly (and non-linearly) to temperature, and thus response functions based on temperature are generally used. However, since soil moisture is often also an important driver of  $R_e$ , a second function accounting for soil moisture was used to modulate the temperature-derived estimate of  $R_e$ .



An Arrhenius-type temperature response function as described by Lloyd and Taylor (1994) was used to estimate ecosystem respiration. This function allows temperature sensitivity to vary inversely with temperature, a property of respiration that has long been understood and that is borne out in the more recent literature on soil respiration (Lloyd and Taylor, 1994; Kirschbaum, 1995). It effectively prescribes a sigmoidal temperature response, which is more theoretically appropriate than conventional exponential and Arrhenius functions, which generally underestimate respiration at low temperatures and overestimate at high temperatures. It has been found to offer superior performance to Arrhenius models with non-varying sensitivity and simple exponential models (Richardson *et al.*, 2006a), and is thus widely used to estimate  $R_e$  (Lasslop *et al.*, 2010). Its form is as follows (Lloyd and Taylor, 1994):

$$R_e = R_{ref} e^{E_0 \left( \frac{1}{T_{ref} - T_0} - \frac{1}{T_s - T_0} \right)} \quad \text{Equation 3-16}$$

$R_{ref}$  represents a base respiration rate at a reference level (effectively a fixed scaling coefficient, in  $\text{mgCO}_2 \text{ m}^{-2} \text{ s}^{-1}$ ).  $E_0$  is a temperature sensitivity parameter equivalent to the activation energy (the minimum energy required to generate a chemical reaction in  $\text{J mol}^{-1}$ ) divided by the universal gas constant ( $\text{J K}^{-1} \text{ mol}^{-1}$ ).  $T_s$  is the observed 0-0.1m layer soil temperature,  $T_{ref}$  an arbitrary reference temperature and  $T_0$  the temperature at which respiration reaches zero. Here  $T_{ref}$  was set to 283.15K as in the original equation. Although air temperature can be used instead of soil temperature (which may be appropriate where a large quantity of aboveground biomass e.g. forests leads to expectation of a dominant role for  $R_a$ ), here correlation coefficients were higher when soil temperature was used (data not shown). This is expected given the small quantity of live biomass in grasslands; Gilmanov *et al.* (2007) and Hunt *et al.* (2004) report that the contribution of heterotrophic respiration to  $R_e$  was approximately 75% in a temperate managed grassland and 85% in a temperate tussock grassland, respectively.

While Richardson *et al.* (2006a) report that this form of the Lloyd and Taylor equation performs well in comparison to other models, they also report very high correlation between these parameters and suggest that at least one is redundant (as also found by Reichstein *et al.*, 2005). Richardson *et al.* (2007) thus recommend fixing one of the remaining parameters to constrain the values of the free parameters. Here  $T_0$  was set to 227.13K as in the original equation with  $R_{ref}$  and  $E_0$  remaining as free parameters. Reichstein *et al.* (2005) also report that short- (hour to hour) and long-term (seasonal) temperature sensitivities vary within ecosystems due to factors other than

temperature that may either constrain or enhance long-term temperature sensitivity, thus potentially causing biases when extrapolating  $R_e$  from nocturnal to daytime conditions (as was done here). The authors thus alter the Lloyd / Taylor equation to allow  $R_{ref}$  to vary over time. In this study, however, soil moisture was also included as a driver of  $R_e$  (see below), and when  $R_{ref}$  was allowed to vary temporally, no seasonal variation was apparent. Therefore  $R_{ref}$  was fixed annually also.

In this study, it was necessary to account for the effects of soil moisture on  $R_e$  in addition to those of temperature. Following the general approach of Richardson *et al.* (2007), the temperature response function was conceptualised as describing a ‘potential’ rate of respiration ( $\dot{R}_e$ ) that may be inhibited by low soil moisture. A sigmoidal scalar function was thus used to describe the effects of low soil moisture on observed ecosystem respiration ( $R_e$ ), as follows:

$$R_e = \dot{R}_e \frac{1}{1 + e^{\theta_1 - \theta_2 VWC}} \quad \text{Equation 3-17}$$

Where  $\theta_1$  and  $\theta_2$  are parameters that describe the shape of the response sigmoid. However, the simultaneous fitting of both temperature and soil moisture response functions led to poorly constrained parameter estimates. Therefore the equation was first fitted using all data available for 2007-08. Because ecosystem respiration is insensitive to soil moisture availability above a relatively low soil moisture threshold (reflected in the sigmoid shape of the soil moisture response) (Suh *et al.*, 2009), in relatively well-watered ecosystems (such as those of the Australian High Country), the effect of low soil moisture on  $R_e$  is expected to be confined to short periods of the year during summer. Given these limitations,  $\theta_1$  and  $\theta_2$  were derived for the bi-annual period and held fixed for the remainder of the analysis.

### 3.7.2 Gross primary production model

Though not directly measured, GPP can be estimated by subtracting from measured NEE estimates of  $R_e$  extrapolated to the daytime using the empirical models outlined above with the observational time series’ of temperature and soil moisture as inputs. Any bias inherent in these models (or in the original observational data) thus translates to bias in estimates of GPP. However, biases in a range of different GPP /  $R_e$  decomposition techniques were analysed by Desai *et al.*

(2008) and found to be relatively low in temperate ecosystems. The previously described chamber system provides an independent measure of daytime  $R_e$  to test the consistency of extrapolated estimates derived from nocturnal data.

Characterisation and comparison of ecosystem assimilatory responses to the light environment is undertaken using a Michaelis Menten-type rectangular hyperbolic light response function (Ruimy *et al.*, 1995). It has been slightly modified as per Falge *et al.* (2001), in which a parameter describing saturation-point GPP (as photosynthetic photon flux density [Q] approaches  $\infty$ ), commonly  $A_{max}$ , is replaced with estimated GPP at  $Q = 2000 \mu\text{mol quantum m}^{-2} \text{s}^{-1}$ , or  $A_{opt}$  ( $\mu\text{mol CO}_2 \text{m}^{-2} \text{s}^{-1}$ ). Its form is as follows:

$$GPP = \frac{\alpha Q}{\left(1 - (Q/2000) + (\alpha Q/A_{opt})\right)} \quad \text{Equation 3-18}$$

Where  $\alpha$  is initial quantum yield ( $\mu\text{molCO}_2 \text{m}^{-2} \text{s}^{-1} / \mu\text{mol quantum m}^{-2} \text{s}^{-1}$ ). A ten-day moving window was used to fit the light response curves for periods with PPFD  $> 0 \text{Wm}^{-2}$ , with estimates excluded if less than 50 data points were available or the model fit was non-significant at the 95% level. Snow-covered periods were also excluded and replaced with a simple average.

While it has been reported that a *non*-rectangular hyperbolic function is more flexible and often provides a better fit to the data (Gilmanov *et al.*, 2007), here the more parsimonious model described above was favoured because it has one less free parameter (describing curvature), and the remaining parameters are thus better constrained given the relatively limited data sets available for this study. Moreover, it has also been reported that a modifying term for  $A_{opt}$  is required to account for the effects of high vapour pressure deficits on photosynthesis via stomatal closure (which reduces the diffusion of  $\text{CO}_2$  into the leaf) (Lasslop *et al.*, 2010). The modifying term takes the form:

$$A_{opt} = \begin{cases} A_{opt_0} e^{(-k[VPD-VPD_0])}, & VPD > VPD_0 \\ A_{opt_0} = A_{opt}, & VPD < VPD_0 \end{cases} \quad \text{Equation 3-19}$$

Where  $k$  is an exponential decay coefficient and  $VPD_0$  is the vapour pressure deficit threshold above which a stomatal response occurs (generally set to 1kPa in accordance with previously published leaf-level findings, with only  $k$  allowed to vary). However, in contrast with the

findings of Lasslop *et al.* (Lasslop *et al.*, 2010), it was generally found that the parameter estimates were poorly constrained with the addition of this term. This may be because in comparison to forests, the aerodynamically smooth canopy of grasslands results in poor coupling with the atmosphere such that vapour pressure deficit at screen level is not representative of vapour pressure deficit at leaf level. This term was thus not included in this study.

A secondary function of the model was to provide estimates of  $R_e$  for further assessment of nocturnal eddy covariance  $\text{CO}_2$  flux data quality. For this purpose, a modified version of Equation 3-18 was fitted to NEE, in which  $R_e$  was simply evaluated as a residual term in the model as follows:

$$NEE = \frac{\alpha Q}{\left(1 - (Q/2000) + (\alpha Q/A_{opt})\right)} + R_e \quad \text{Equation 3-20}$$

### 3.7.3 Growing season index model

In this study, a simple growing season index (GSI) model was used to analyse the effects of different climate variables on seasonal variations in light response. The rationalisation for this approach is that variations in leaf area are a key determinant of seasonal variations in canopy light response, and as such a simple foliar phenology model such as GSI should capture a large proportion of the variance in light response parameters. In the original model of Jolly *et al.* (2005), the variables used to predict foliar phenology are daily minimum temperature, photoperiod and VPD. Ramp functions define indices expressing the response over a range of values of foliar phenology to each variable, with minimum and maximum values of 0 and 1, respectively. The ramp function for minimum temperature is as follows:

$$T_{ind} = \begin{cases} 0, & T \leq T_{min} \\ (T - T_{min})/(T_{max} - T_{min}), & T_{max} > T > T_{min} \\ 1, & T \geq T_{max} \end{cases} \quad \text{Equation 3-21}$$

Where  $T_{ind}$  is the temperature index,  $T_{min}$  is the temperature below which activity is completely constrained, and  $T_{max}$  is the temperature above which activity is completely unconstrained. An analogous index is defined for photoperiod and VPD (although in the case of the latter, low values are unconstraining and high values are constraining). Jolly *et al.* (2005) use literature values to set minima and maxima for temperature (-2 to 5°C, respectively), photoperiod (10 to 11 hours) and VPD (1 to 4.1kPa). In this study, vapour pressure deficit was excluded for the reasons noted above; moreover, since the canopy responds on short (e.g. hourly) time scales to VPD, if a response is not evident at these time scales (using the light response functions defined above), a response is unlikely to be manifest in light response parameters derived from 10-day windows (see Chapter 0, section 7.4.2.2 for further discussion). Instead, a function was included to model the effects of volumetric water content of the soil, which was shown to strongly influence the accuracy of the model. Moreover, use of the fixed parameters cited by Jolly *et al.* (2005) resulted in a very poor fit of the model to the data, so a similar approach was taken to that of Migliavacca *et al.* (2011), in which parameters were adjusted to optimise the model fit to the data.

A snow index was also used to express the effects of snow cover. However, this index was not defined by a ramp function; it was simply set to one when snow cover was absent (defined using an albedo threshold of 0.4), and zero when snow cover was present.

### 3.8 Vegetation and soil sampling

#### 3.8.1 Vegetation

Aboveground phytomass was harvested at the sites periodically. Given the distance to the sites, intervals between sampling were irregular, depending on timing of site maintenance visits (12 harvests were undertaken during the two-year campaign). At each visit, ten 0.25m<sup>2</sup> randomly placed quadrats of biomass were harvested. To minimise air drying following harvesting, samples were sealed in Ziploc bags and kept refrigerated, and were generally analysed within 72 hours of harvesting. Samples were oven dried (for 96 hours at 70°C) and weighed to derive total phytomass. Since the primary aim of this task was to ascertain the carbon content of vegetation, carbon was assumed to represent approximately 45% of the dry weight of the harvested phytomass (Chapin *et al.*, 2002).

#### 3.8.2 Soils

At each site, samples were collected to characterise bulk density, soil pH, total and organic carbon, and total nitrogen and phosphorus in early March 2007. Ten separate pits were dug at each site. At Dargo, pits had to be relocated on several occasions when the basalt bedrock was encountered above 0.3m. At Nimmo, a gravel layer was also encountered at approximately 0.25-0.3m in several of the pits. In each pit samples were taken from three depths (0-0.1, 0.1-0.2 and 0.2-0.3m). Four cores were taken (for each depth in each pit), bulked and then dried at 110°C for 72 hours. Each sample was then sieved to 100µm and a 10g subsample taken and sent for chemical analysis of the above elements at a professional laboratory.

The pH of the upper (0-0.1m) layer was also measured using a HI9025 (Hanna Instruments, Woonsocket USA) pH meter. Ten 10g samples of dried, sieved soil were each diluted with 50ml of deionised water, and mixed in an end-over-end shaker for one hour before analysis. Mass quantities of soil mineral and organic components were also ascertained for the surface (0-10cm) layer, by combusting dried 10g samples of sieved soil at 550°C for two hours; this fires off the organic matter, such that the resulting mass loss represents the total organic content and the residual the mineral content. These measurements were required to appropriately characterise the thermal properties of the soil for calculation of the soil heat storage term (section 3.3.1).

Given that soil pits were only dug to 0.3m, simple depth functions were also fitted to the data in order to extrapolate estimates to greater depth. For each layer, carbon density ( $\rho_c$ ) was estimated from the soil mass fraction of carbon ( $C_f$ ) and the bulk density of the layer ( $\rho_s$ ) for each depth:

$$\rho_c = C_f \rho_s z \quad \text{Equation 3-22}$$

Carbon density was then estimated as a function of depth using a simple depth-dependent exponential decay model of the form:

$$\rho_c = a \cdot e^{-(bz)} \quad \text{Equation 3-23}$$

Where  $a$  and  $b$  are fitted parameters, and  $z$  is depth. It should be noted that large uncertainties apply to the extrapolated estimates using these equations due to sampling variability, the simplicity of the model and the unknown depth of the soil profile. The effects of sampling variability was accounted for by using Monte-Carlo simulation in which estimates of the two free parameters in Equation 3-23 were drawn randomly from normal distributions (scaled according to the error estimates derived from the parameter optimisation process). For each trial, cumulative carbon density with depth was calculated using 0.01m increments down to a depth of 1m (since this has been cited as a typical depth limit for alpine soils, e.g. Costin *et al.*, 1952). This was repeated  $10^4$  times, with the uncertainty in the extrapolated estimate represented by the 95% confidence interval of the  $10^4$  trials.

This does not however account for points (ii) and (iii) above, which necessarily remain unknown. However, with respect to the representativeness of the empirical functions, since the observed data document a steep decline in carbon density with depth (Chapter 6, section 6.2), absolute errors in carbon density estimation are likely to be small even if relative errors are large. With respect to depth, the estimates derived from extrapolation to 1m are considered an upper limit on profile-integrated soil carbon density, while those derived from the analysis of the soil layers between 0-0.3m constitute a lower limit.

# 4. Data Quality Analysis

---

## 4.1 Introduction

This chapter focuses on data quality, with an emphasis on CO<sub>2</sub> flux data – or other data that have implications for CO<sub>2</sub> flux data quality - in particular. Potential sources of error in eddy covariance data were discussed in Chapter 2, and in Chapter 3 the methodological approach to minimising the effects of these errors was outlined. Here the results of a number of critical quality assurance procedures and analyses are presented. To avoid duplication, the discussion largely focuses on Dargo, with the relevant parallel statistics for Nimmo reported where appropriate, and discussed in detail only where there was significant divergence in the results between sites. The discussion begins by addressing the actual quantities of data that were retained at each site, before moving on to three key sources of error in gap-filled eddy covariance data: i) systematic measurement error; ii) random measurement error, and; iii) model error.



## 4.1 Data retention

Differences in raw data acquisition between sites in 2007/08 were large – 92.2% of all possible records were logged at Dargo compared to just 67.5% at Nimmo (Figure 4.1). Total data losses occurred due to periodic equipment malfunction, and were relatively uniformly distributed seasonally.

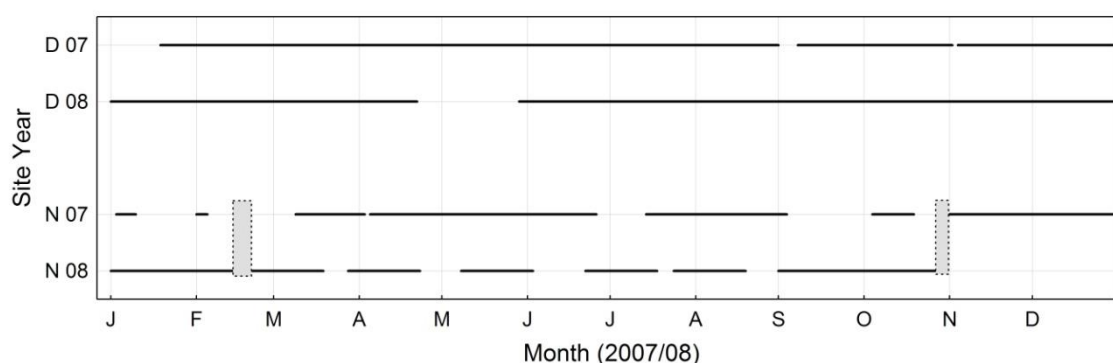


Figure 4.1: seasonal distribution of data coverage (D = Dargo, N = Nimmo) for 2007/08 (breaks in solid line represent periods of missing data; grey vertical bars represent intervals during which there is no coverage for either year).

Relative contributions (by half-hourly time step) of quality control classes (see Chapter 3, section 3.4.2) to CO<sub>2</sub> flux data rejection for the sites are presented in Figure 4.2. At both sites there was a clear diurnal pattern in data rejection, with much larger rates of loss occurring nocturnally. At Dargo, application of (automatic and conditional) exclusion criteria removed approximately 22% of available data diurnally, whereas at Nimmo more than 30% was removed. Cross-site differences were minor during the day and more pronounced nocturnally. In combination with the previously discussed missing records, total retention for the study period at Dargo was approximately 72%; at Nimmo it was less than 50%. This is, respectively, slightly better and substantially worse than the 65% average rate of retention of eddy covariance data reported by Falge *et al.* (2001).

Diurnally averaged, the quantity of available data removed by the conditional rejection criteria was in all classes larger at Nimmo than Dargo, with retention in the 'highest quality' classes (1-3) around 55% (of available data) at Dargo (marked by the dashed line in Figure 4.2) and 42% at Nimmo. The difference was particularly pronounced nocturnally – only 34% of available nocturnal data was in the highest quality class at Nimmo, whereas at Dargo the figure was 51%. This contrast is also related to the conditions discussed above – very stable surface conditions at Nimmo resulted in

intermittent turbulence and correspondingly highly instationary time series. At Dargo maximum data losses in classes 1-3 occurred across the hours encompassing sunrise and sunset, associated primarily with the strong instationarity due to rapidly changing scalar source/sink activity that tends to occur at these times.

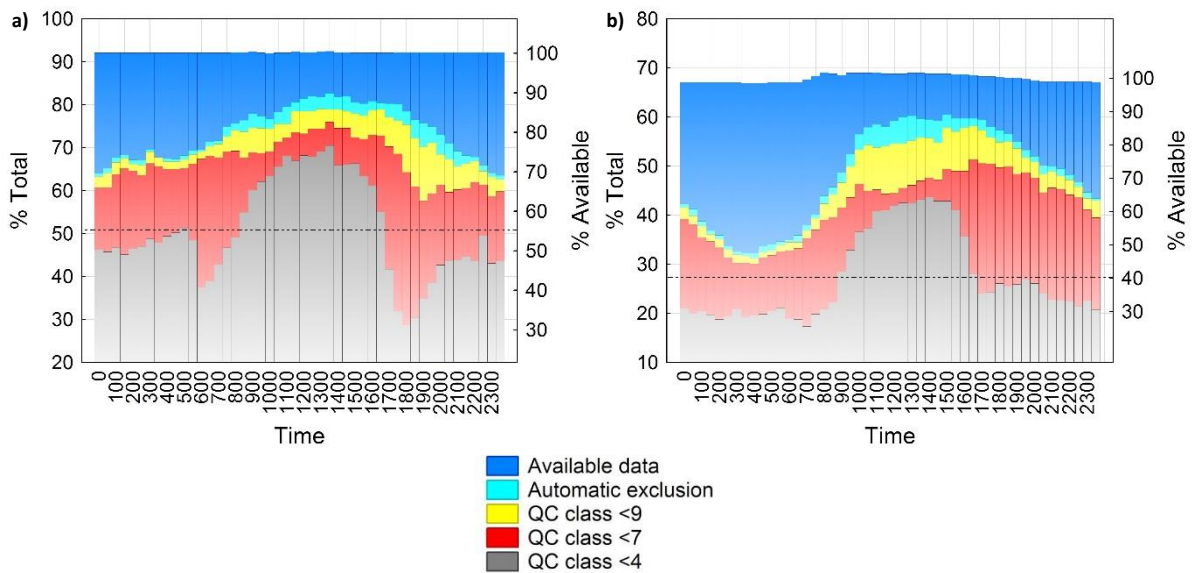


Figure 4.2: Percentage of available and acceptable raw C flux data remaining after application of QC criteria for: a) Dargo, and; b) Nimmo. Dashed line represent diurnal mean percentage retention of QC classes 1-3. Left hand axis represents the percentage of all possible data records that were retained; right hand axis represents the percentage of the recorded data that were retained. Note that according to Foken (2004), classes 1-3 are of sufficient quality to be used for fundamental research such as model parameterisation; classes 4-6 are sufficiently robust to unequivocally remain as part of the relevant time series, and class 6-8 data may be used so long as they do not deviate significantly from neighbouring observations.

The reduced availability of high quality data at Nimmo nocturnally is likely to be related to the stable nocturnal conditions that more commonly prevailed there, which arises due to two characteristics of the site, both related to topography (albeit at different scales). The first is the location of the site in a valley, which reduces wind speeds at the surface and inhibits shear-induced mixing. While this triggers instability and thus buoyant mixing during the day (due to surface warming), nocturnally the opposite occurs as the surface cools radiatively. This cooling is made more effective by the relatively clear conditions promoted by the location of the site in a rain shadow region on the western edge of the Alps. Moreover, the location of the site in a valley also means that cold air drains downlope and accumulates there nocturnally (indeed, it is this phenomenon that is

thought to be responsible for the presence of the grassland on the valley floor at Nimmo), a phenomenon described in Chapter 2, section 2.5.4.2. It is for this reason that data retention at Nimmo reaches a minimum at the time when conditions are expected to be coldest (and thereby generally most stable) – prior to sunrise.

## 4.2 Systematic Measurement Error

In this section, the resulting quality of the final datasets is assessed. Since: i) there is no continuous, independent standard against which to compare measured turbulent fluxes, and; ii) some potentially important transport mechanisms cannot be measured by a single set of eddy covariance instrumentation, systematic errors are difficult to reliably quantify. Thus system accuracy must be inferred on the basis of either theoretical expectations or alternatively derived estimates of similar quantities. Given the significant uncertainties that this entails, the results of this analysis are treated as indicative rather than conclusive determinations of accuracy, and are not used to make further corrections. Nonetheless, this process provides a reliable indication of the confidence that can be placed in the results reported in subsequent chapters.

It is also clear from the discussion in Chapter 2 that systematic errors are expected to be most pronounced nocturnally. As noted there, this is of crucial importance because nocturnal CO<sub>2</sub> fluxes are often relatively large and generally of opposite sign to fluxes during the day. Consistent nocturnal measurement error thus inevitably translates to systematic error (i.e. bias) in time-integrated ecosystem carbon balances. An emphasis is thus placed on nocturnal data quality in the analyses below. Nevertheless, the first of these analyses addresses the degree of surface energy balance closure - considered a highly robust indicator of *general* data quality – across the diurnal cycle. This is followed by a more targeted analysis of nocturnal CO<sub>2</sub> fluxes in particular. The effects of low turbulence on nocturnal CO<sub>2</sub> fluxes – and the thresholds below which they are considered suspect - is assessed, followed by comparison of nocturnal eddy covariance-derived data with quasi-independent (derived from light response function analysis) and independent (derived from chamber measurements) ecosystem respiration estimates.

#### 4.2.1 Surface energy balance closure

As discussed in Chapter 2, the first law of thermodynamics requires that the surface net radiant energy surplus or deficit is balanced by the sum of surface convective and conductive energy fluxes. Any sustained imbalances are thus indicative of systematic measurement error. To the extent that this reflects errors in the convective energy fluxes driven by mischaracterisation or neglect of atmospheric transport mechanisms, these errors necessarily translate to CO<sub>2</sub> fluxes also.

In the context of flux sites generally, energy balance closure in this investigation was excellent at both sites. Diurnally, relative energy balance (EB) deficits calculated on a half-hourly basis were 8% and 11% for Dargo and Nimmo, respectively (Table 4.1). At both sites, relative EB deficit was reduced by a further 1-2% if calculated by forcing the origin through zero. However, the regression intercept may in itself indicate a systematic source of measurement offset in the data (Franssen *et al.*, 2010). In comparison, Wilson *et al.* (2002) report an average relative EB deficit of approximately 21% across 22 Fluxnet sites, while a more recent and comprehensive review (Franssen *et al.*, 2010) found an average value of 25.8% across 50 European Fluxnet sites.

However, the majority of ecosystems surveyed in the above studies were forests, whereas smaller relative EB deficits are to be expected at sites with low measurement heights, homogeneous surface properties and relatively flat terrain because conditions in which the underlying assumptions of the eddy covariance technique are violated arise less commonly (Finnigan *et al.*, 2003). Despite the more complex terrain of the surrounding landscapes, the sites in this study broadly satisfy these ideal conditions. Thus the diurnal closure reported here is similar to that reported in the literature for similar vegetation types; for example, Jacobs *et al.* (2008) report diurnal closure of 96% for a mid-latitude grassland, while Runyuan and Qiang (2011) report a value of around 88% for a subalpine meadow, though energy balance closure in functionally similar ecosystems in complex mountain terrain is moderately lower (e.g. 82%, Hiller *et al.*, 2008).

**Table 4.1: linear best fit regression parameters of turbulent energy fluxes on available energy** (turbulent energy fluxes:  $H + LE$  [sensible and latent heat fluxes, respectively]; available energy:  $R_n - G - S$  [net radiation, subsurface heat storage, and combined air enthalpy, moisture and biochemical energy storage, respectively]) calculated for all valid half-hourly observational data points in the time series.

	Intercept		Slope		r <sup>2</sup>
	Best fit	SE	Best fit	SE	
Dargo					
Rn > 0	-4.45	1.15	0.96	0.003	0.94
Rn < 0	6.84	0.44	0.68	0.007	0.69
All data	11.33	0.5	0.92	0.002	0.96
Nimmo					
Rn > 0	-10.55	1.82	0.93	0.004	0.93
Rn < 0	1.22	1.23	0.65	0.02	0.62
All data	6.1	0.98	0.89	0.003	0.96

Despite the good energy balance closure reported here, there was a marked difference between day and night (Figure 4.3a). The excellent daytime closure (0.96 and 0.93 for Dargo and Nimmo, respectively) and strong correlation ( $r^2$  of 0.94 and 0.93, respectively) between the radiative and non-radiative energy balance components reported for both sites suggests that daytime measurements are of high integrity and lend confidence to the accuracy of the eddy covariance system as a whole in the absence of an independent benchmark.

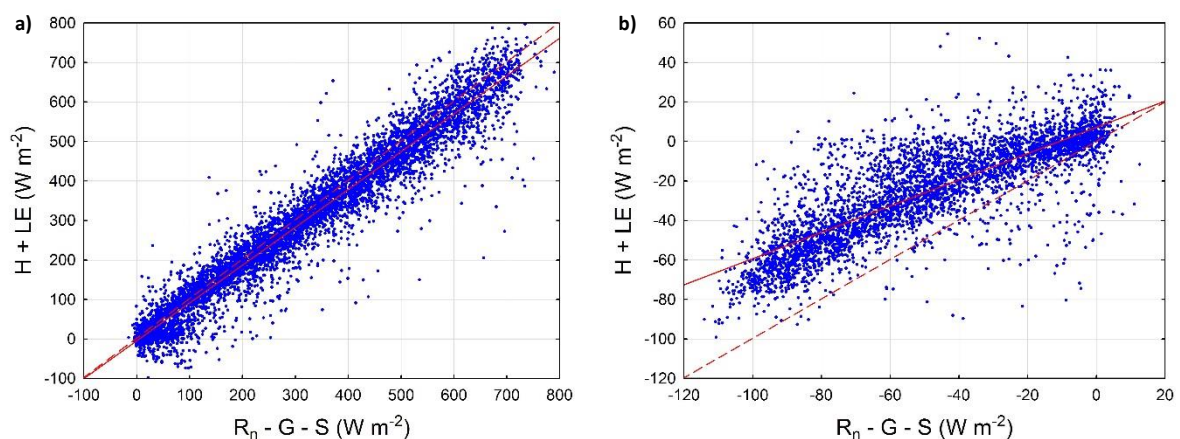


**Figure 4.3: energy balance closure at Dargo** for: a)  $R_n > 0$ , and; b)  $R_n < 0$  ( $R_n$  is net radiation,  $H$  and  $LE$  are sensible and latent heat fluxes, respectively,  $G$  is subsurface heat storage and  $S$  is air enthalpy, moisture and biochemical energy storage). Solid lines show line of best fit and dashed lines the 1:1 line.

Nocturnally, relative EB deficits were far larger, exceeding 30% at both sites. Like the general non-closure of the diurnal energy balance, much larger nocturnal relative EB deficits (in comparison to the daytime) are a commonly-noted characteristic of eddy covariance systems (Wilson *et al.*, 2002; Zhengquan *et al.*, 2005; Franssen *et al.*, 2010), with average nocturnal relative EB deficits of close to 40% across Fluxnet sites (Franssen *et al.*, 2010). However, larger nocturnal relative EB deficits also coincided with smaller absolute EB deficits. The effect of this can be seen in Figure 4.4 – larger absolute deficits occurred during the day, but were relatively smaller because available energy was much larger. The opposite occurred nocturnally. During both night and day, with the exception of transition periods, relative EB deficits were both relatively stable and clearly different.

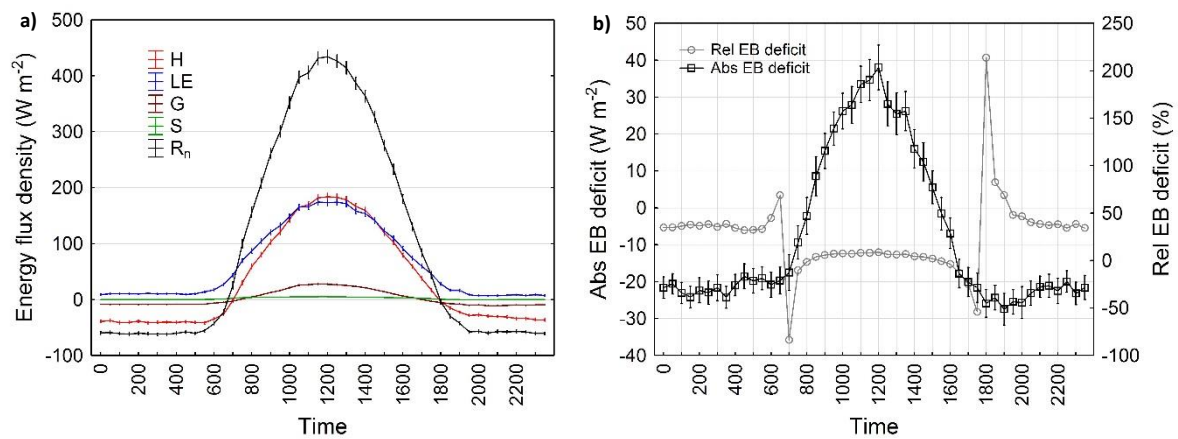


**Figure 4.4:** mean diurnal energy balance ( $\pm$ SE) for Dargo site (a;  $R_n$  is net all-wave radiation,  $H$  and  $LE$  sensible and latent heat fluxes,  $G$  subsurface heat flux and  $S$  the sum of biochemical, thermal and evaporative energy storage, excluding biomass heat); composite relative and absolute ( $\pm$ SE) energy balance deficit for the diurnal energy balance (b).

There are a range of possible reasons for energy balance non-closure generally, and for the larger effect often seen nocturnally. An exhaustive survey of potential contributing error sources is not attempted here (see Wilson *et al.*, 2002; Foken, 2008; Leuning *et al.*, 2012 for a more comprehensive review), but some plausible explanations are considered below. As discussed in Chapter 2, EB deficits may arise due to errors in any of the measurement systems (i.e. radiation, conduction or convection) that contribute to the energy balance. Given the emphasis of this study on surface/atmosphere  $\text{CO}_2$  exchange, errors arising in the turbulent flux measurements are most problematic. There are two key sources of potential error. The first is neglect of unmeasured and non-negligible non-turbulent terms in the mass balance (i.e. horizontal and/or vertical advection), and the second is filtering of the turbulent spectrum due to system limitations and time averaging.

These error sources are discussed first, followed by those in the non-convective measurement systems. While the latter have no direct bearing on the quality of CO<sub>2</sub> flux measurements, if errors in the non-turbulent components of the energy balance can plausibly explain the observed EB deficits, this lends further confidence to the robustness of the turbulent flux measurement.

#### 4.2.1.1 *Advection*

As previously noted, underestimation of convective fluxes can occur as a result of significant horizontal and vertical advection, arising when local- to meso-scale circulations develop due to the interaction between specific meteorological conditions and landscape surface or terrain heterogeneities (Wilson *et al.*, 2002; Katul *et al.*, 2006; Aubinet, 2008). For example, nocturnally (most relevant here since daytime relative EB deficits were small), gravity-driven downslope drainage of cold air (as described previously) is thought to be a key driver of advection in non-level terrain (Aubinet, 2008). Despite the modest slopes in the immediate vicinity of the towers in this study, such flows can be initiated on slopes of less than 1° (Whiteman and Zhong, 2008). Moreover, the development of such flows may be governed by larger-scale (i.e. outside the expected flux source area of the eddy covariance system) topographic features, which in this study – given that the locations were in the Australian Alps - were highly complex.

Thus it is highly likely that such flows occur at the sites, but the potential magnitude of the advective terms cannot be directly measured for the reasons discussed in Chapter 2. However, it is possible to indirectly infer – at least qualitatively - the potential effects of such factors from available data. For example, it is clear that such flows must be initiated under generally stable surface conditions (Aubinet *et al.*, 2003), which develop when shear-induced turbulence is weak (and skies generally clear). It is therefore expected that nocturnal periods of weak mixing should correspond with larger relative EB deficits. In the current study, an increase was observed in EB deficits at low friction velocity ( $u^*$ ). At Dargo, there was an apparent threshold in the sensitivity of the EB to  $u^*$  at approximately  $u^* = 0.1 \text{ m s}^{-1}$  (Figure 4.5<sup>22</sup>). As  $u^*$  continued to decrease below this threshold, both relative and absolute EB deficit rapidly increased. With increasing  $u^*$  above  $0.1 \text{ m s}^{-1}$ , there was a weak continuing decrease in relative EB deficit, and effectively no response of absolute EB deficit, with increasing  $u^*$ . At Nimmo, a threshold was more difficult to discern, which is thought to relate to

---

<sup>22</sup> The apparently higher relative EB deficits (compared to those in Table 4.1) in Figure 4.5 are due to the fact that data were averaged across  $0.1 \text{ m s}^{-1} u^*$  bins and expressed as a proportion of  $R_n$  averaged across the same bins. Reporting of the regression slope alone accurately characterises the *response* of the measured convective energy fluxes to available energy but provides an artificially low estimate of relative EB deficit when  $R_n$  is small and the regression intercept is positive (as was the case here).

the fact that a larger proportion of nocturnal data was removed by the quality control filters at that site. Similar  $u^*$  dependent thresholds in energy balance closure have been reported in the literature (Wilson *et al.*, 2002; Zhengquan *et al.*, 2005; Franssen *et al.*, 2010)

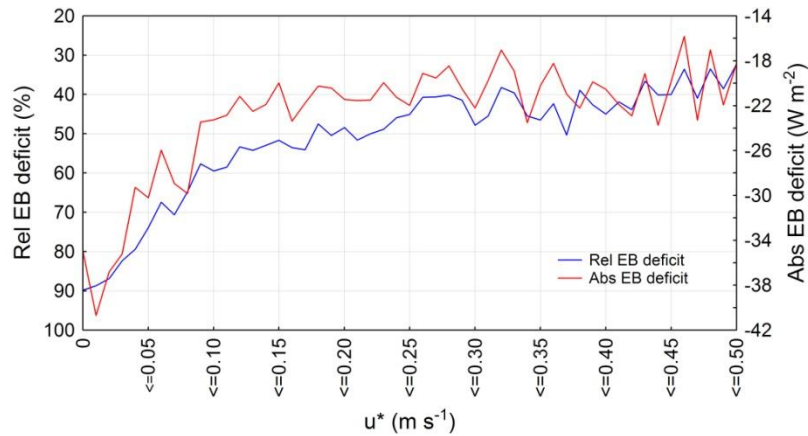


Figure 4.5: relative and absolute energy balance closure as a function of friction velocity ( $u^*$ ) at Dargo.

Nonetheless, Figure 4.5 also indicates that even at high friction velocity, the turbulent energy fluxes accounted for little more than 60% of available energy at Dargo. Thus while it is clear that energy balance closure was degraded under very calm conditions, relative EB deficits remained large even with the most vigorous mixing. While it cannot be discounted that advection of sensible and latent heat may still play some role in this deficit (Aubinet *et al.*, 2010), the mechanisms that might potentially be involved are unclear. Thus while it can be concluded that the behaviour of nocturnal energy balance closure is potentially *consistent* with the effects of advection at low  $u^*$ , it appears unlikely that this is the reason for relatively poor nocturnal closure *in general*. It is for this reason that other methods of independently validating  $\text{CO}_2$  fluxes are important, as addressed in section 4.2.2. Prior to that discussion, other potential causes of energy balance non-closure are discussed below.



#### 4.2.1.2 Low and high pass filtering

Loss of either high- or low-frequency covariance (due to either instrument sampling issues at high frequencies or the effects of imposing finite flux calculation periods at low frequencies) is also a serious potential problem because, like advection, it applies to the behaviour of turbulent fluxes in general rather than to the flux of any particular scalar. However, for this to be a plausible explanation of the results reported here (very small and very large daytime and nocturnal relative EB deficits, respectively), it is necessary to establish why their effects would be systematically different between day and night. As discussed in Chapter 2, Foken (2008) argues that the failure of the turbulent fluxes to close the energy balance is primarily a result of implicit high pass filtering of the turbulent spectrum resulting from selection of averaging intervals too short to capture all of the vertical motions contributing to the flux.

However, low frequency motions are expected to be more prevalent under unstable conditions during the day, when surface heating of complex terrain and / or heterogeneous surfaces may drive the development of organised convection and local- to mesoscale circulations (Finnigan *et al.*, 2003). Yet it was during the day that relative EB deficits were lowest in this study. Nonetheless, ogive plots were used to test whether the averaging period chosen (30 minutes) was sufficient to capture all relevant frequencies of vertical motion, as described in Moncrieff *et al.* (2004). Ogives plot the integral under the cospectral density curve, and thus show the cumulative contribution of eddies of increasing period to vertical transport.

Figure 4.6 presents an ogive plot for a warm day at Dargo in January 2008 with relatively unstable daytime conditions, under which landscape-induced low-frequency eddies are more likely to be present. It nonetheless confirms that virtually all cospectral power was contained within atmospheric motions with periods under 15 minutes, suggesting that the averaging interval used was conservative. A virtually identical result was obtained for Nimmo. These results are similar to those reported for a short crop in China, in which virtually all of the flux was captured in a 15-minute period (Sun *et al.*, 2006). This is perhaps not a surprising result, given that higher-altitude temperate climate sites are – by virtue of generally moist conditions, relatively high winds and, as is the case here, low summertime Bowen ratios - generally not strongly conducive to the development of vigorous convective planetary boundary layer motions. Even at Nimmo, where the topography tends to simultaneously reduce wind speeds at the surface and promote local-scale terrain-induced flows, evidence for low-frequency flux contributions remains minimal.

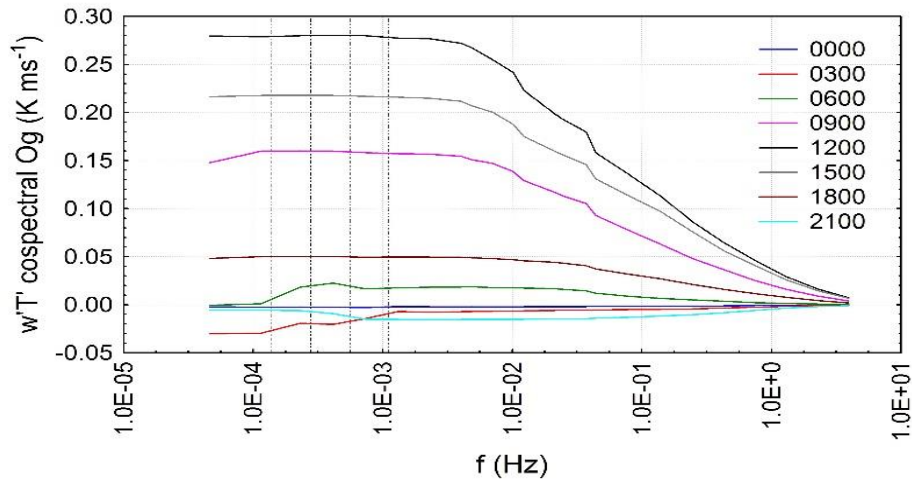


Figure 4.6: Ogive plots of kinematic heat flux ( $\overline{w'T_s'}$ ) at Dargo on 28/1/08; calculated from cospectra of 3 hour period centred on each time period (vertical dashed lines from left to right represent 120, 60, 30 and 15 minute periods, respectively).

Nocturnally, on the other hand, stable conditions suppress vertical motion and the turbulence field is more likely to be characterised by intermittent, high-frequency bursts of activity (Aubinet, 2008). Moreover, it was established previously that large nocturnal EB deficits were – with the exception of very stable conditions – largely independent of turbulent activity. As such, inadvertent high-pass filtering of the data would appear, a priori, to be unlikely to explain poor relative EB deficits in this study.

#### 4.2.1.3 Other energy sources / sinks

Another possible source of error may be inadequate quantification of energy stores and sinks. In this study, the storage term (S) included air enthalpy and moisture changes as well as biochemical storage due to photosynthesis. The latter was the primary energy storage (excluding the subsurface) component during the day, improving energy balance closure by approximately 2% (data not shown). Given the low measurement height employed in this study, the other components were negligible. The improvements in daytime relative EB deficit reported here (i.e. less than 5%) are similar to those for other grassland sites (Jacobs *et al.*, 2008; Runyuan and Qiang, 2011). Nocturnal energy balance closure, however, was largely unaffected, since the storage terms were all negligible nocturnally, as seen in Figure 4.4a. However, biomass enthalpy change was excluded, since reliable long-term measurements of biomass amount and water content were unavailable. In ecosystems

such as forests where large amounts of biomass are present, this may be a significant term in the energy balance (e.g. Lindroth *et al.*, 2010), but in grasslands this is not expected to be the case.

During the day it is expected that the effects of energy storage by the vegetation would be approximately balanced over the course of the day i.e. neglect of warming before and cooling after solar noon would result in under- and overestimation of  $S$ , respectively. This may induce minor daytime hysteresis in the relative EB deficit, but is expected to have little effect on linear regression parameters for the daytime as a whole. Here hysteresis in the daytime energy balance was evident (Figure 4.7a). The residuals from the regression in Figure 4.7a approximate the absolute departure from the average diurnal behaviour of the energy balance and thus can be compared to first order approximations<sup>23</sup> of the absolute contribution of biomass enthalpy change to the energy balance. As presented in Figure 4.7b, the daytime amplitudes were approximately similar at Dargo, suggesting that the observed hysteresis may be induced by neglect of the biomass enthalpy term. This hysteresis is nonetheless unlikely to cause systematic daytime relative EB deficits for the reasons outlined previously.

On the other hand, biomass enthalpy change may have implications for nocturnal energy balance closure, because in contrast to the daytime situation, the surface continually cools throughout the evening. However, it is also clear from Figure 4.7b that it was negligible nocturnally. As such, it is concluded that neglecting energy storage explains neither daytime nor nocturnal relative EB deficits. This points to the possibility of systematic error in the measurement of other terms in the energy balance. This may involve errors in sensible and / or latent heat unrelated to atmospheric effects (e.g. IRGA calibration errors), or in the remaining terms that determine available energy (net radiation and soil heat flux).

---

<sup>23</sup> Assuming dry phytomass of approximately  $0.5 \text{ kg m}^{-2}$  (at Dargo) with a moisture content of 70%, and specific heat capacities of  $1.92$  and  $4.18 \text{ kJ kg}^{-1} \text{ K}^{-1}$  for organic matter and water respectively (Monteith and Unsworth, 2008).

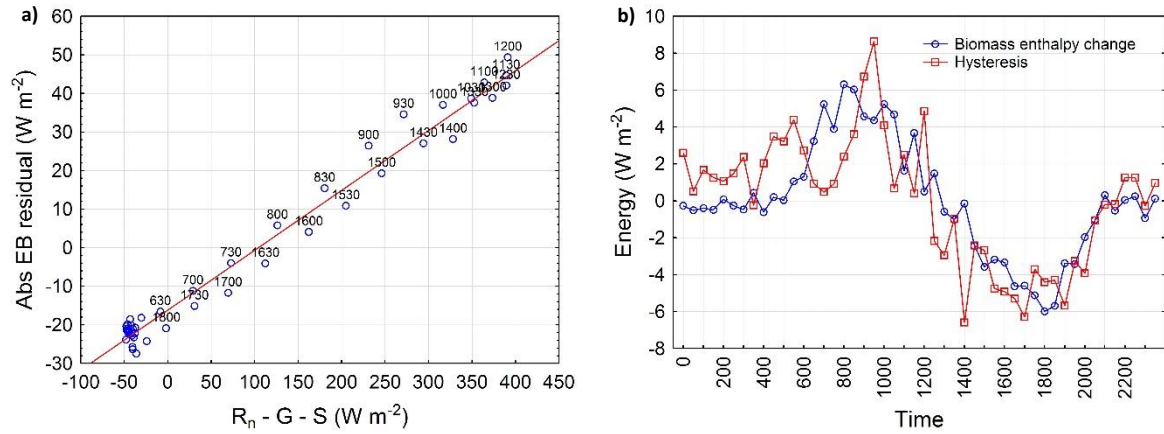


Figure 4.7: a) half-hourly composite absolute energy balance residual as a function of available energy; b) comparison of hysteresis and approximated magnitude of biomass enthalpy change (hysteresis is the regression residuals from Figure [a]; biomass enthalpy change is calculated using half-hourly surface radiative temperature change and assumed values for biomass and water content, as outlined in the text).

#### 4.2.1.4 Sampling errors

Sampling errors may arise due to mismatches in flux source area between different measurement instrumentation (Schmid, 1997). While the footprints of the radiant and convective flux measurement systems are expected to be different<sup>24</sup>, they both lie at scales between the two principal scales of surface heterogeneity: the microscale (e.g. tussock / intertussock spaces) and the local- to mesoscale (the subalpine mosaic of vegetation communities). As such, this is not expected to be a likely source of significant sampling error. However, large errors in energy balance closure may arise as a result of undersampling of soil heat flux, which has a very small flux footprint (on the scale of metres), and is expected to be highly spatially heterogeneous.

As previously discussed, it has recently been argued that neglect of storage terms (including soil heat flux) explains much of the surface energy imbalance observed across Fluxnet (Leuning *et al.*, 2012). Since the storage components are on average negligible over 24 hours, energy balance aggregated over a day effectively excludes their effects. The results of this study are consistent with the findings of Leuning *et al.* (2012). In the case of Dargo, the energy balance was approximately closed over 24 hours, with a slope of 1:1 between the turbulent energy fluxes and available energy (Figure 4.8a). This represents an improvement of approximately 8% over the half-hourly regressions

<sup>24</sup> The traditional micrometeorological approximation of the measurement height: fetch radius ratio of 1:100 for neutral conditions yields a footprint of more than  $1.5 \times 10^4 \text{ m}^2$  for a turbulent flux measurement height of 2.3m (Moncrieff *et al.*, 1996). The source area of the radiant flux measurement instrumentation is proportional to measurement height, with 99% of measured radiation arising within radius 10h (where h = measurement height) of the sensor (Kipp and Zonen, 2002). Here this equates to an area of approximately  $3.8 \times 10^3 \text{ m}^2$ , approximately 2.5% of the turbulent footprint.

listed in Table 4.1 **Error! Reference source not found.** The reason for the non-zero intercept is not clear (when the regression was forced through the origin, the slope was 1.06), but the general result is approximate closure of the energy balance, compared to a diurnal regression slope of 0.92 using half-hourly values (from Table 4.1). At Nimmo, the regression slope was 0.96, an improvement of approximately 7% (data not shown); however, only 8 days with complete measurements for all energy balance components and all periods were available, and thus the result was not statistically robust.

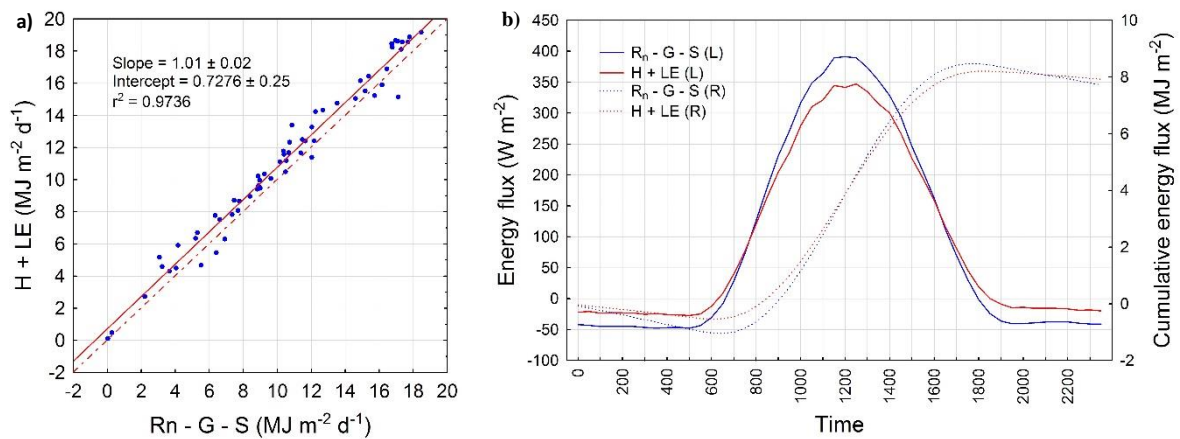


Figure 4.8: a) Dargo site regression of cumulative daily sensible and latent heat fluxes on available energy; b) mean diurnal half hourly average and cumulative energy fluxes ( $H$  – sensible heat flux;  $LE$  – latent heat flux;  $R_n$  – net radiation;  $G$  – soil heat flux;  $S$  – summed additional storage terms)

The approximate balancing (on average) of daytime and nocturnal shortfalls in energy balance closure is also evident in Figure 4.8b. This also implies that the source of the error in energy balance closure applies over the entire diurnal cycle, since errors that generally occurred only nocturnally would cause imbalances at the daily time scale. However, given the asymmetry in relative EB deficit between day and night, this further implies that the error is likely to be in an energy balance component that represents a larger proportion of  $R_n$  nocturnally than during the day. This therefore suggests that  $H$  and  $LE$  (which exhibit the opposite pattern) are not the primary source of the error, and since it has already been demonstrated that biomass energy storage was negligible, this suggests that the observed EB deficit patterns is consistent with errors in soil heat flux ( $G$ ). If  $G$  is consistently underestimated (for example, by a fixed proportion), half-hourly relative EB deficits will be larger nocturnally (when turbulent energy fluxes are weak and  $G$  accounts for 25–50% of net radiation) than during the day (when turbulent energy fluxes are well-developed and  $G$  accounts for <10% of net radiation). This is consistent with what was reported previously.

Quantitatively, however, it would be necessary to invoke two- to threefold underestimation of  $G$  at Dargo (Figure 4.9a). Nonetheless, there are several inherent limitations of the soil heat flux sampling protocol that may result in large underestimation of  $G$ . It is unlikely that this is related to undersampling of (horizontal) spatial heterogeneities in soil thermal properties, despite the fact that there were only two microsites. At the sites in the current study, the soil heat storage correction was approximately five-fold larger than the heat flux across the plate at depth (Figure 4.9b), and thus the total soil heat flux estimate is strongly dependent on the accuracy of measured soil thermal properties. At Dargo, the mean volumetric heat capacity ( $C_v$ ) of the soil was  $1.69 \text{ MJ m}^{-3} \text{ K}^{-1}$  on 09/03/07 (the number of samples was 10; see Table 4.2), with a 95%CI for the sample standard deviation of  $0.35 \text{ MJ m}^{-3} \text{ K}^{-1}$  (Table 4.2). To explain the observed absolute EB deficit, either the estimate of  $C_v$  or the time rate of change of soil temperature would need to effectively double. Neither is considered plausible.

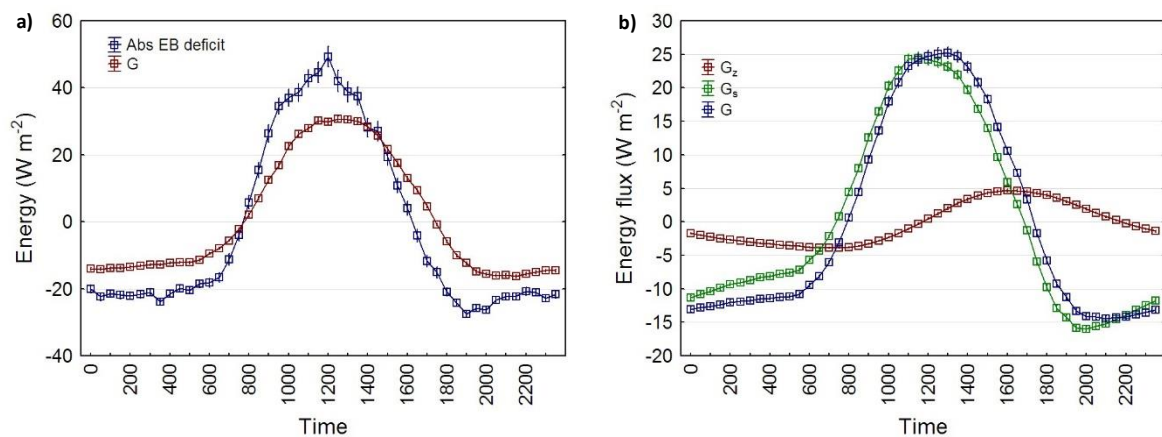


Figure 4.9: diurnal average ( $\pm\text{SE}$ ) for Dargo of: a) soil heat flux ( $G$ ) and absolute EB deficit; b) soil heat flux components ( $G_z$  = flux measured at 8cm;  $G_s$  = estimated storage in soil layer overlying heat flux plate;  $G$  = reconstructed surface soil heat flux i.e.  $G_z + G_s$ ).

Table 4.2: measured mass quantities ( $\pm 95\%$ CI of sample mean) and thermal properties of soil constituents (collection date 09/03/07,  $n = 10$ ;  $C_v$  - volumetric heat capacity estimated from gravimetrically weighted average of soil constituents - see Chapter 3, section 3.3.1;  $\kappa_s$  - thermal diffusivity calculated from harmonic analysis for period 06/03/07 to 14/03/07 using soil temperature and soil heat flux measurements;  $k$  - thermal conductivity calculated from  $k = \kappa C_v$ ). Note that soil moisture was determined from in situ TDR probe measurements – sample size was insufficient to determine statistically robust variances.

	Organic ( $\text{kg m}^{-3}$ )	Mineral ( $\text{kg m}^{-3}$ )	$\text{H}_2\text{O}$ ( $\text{kg m}^{-3}$ )	$C_v$ ( $\text{MJ m}^{-3} \text{ K}^{-1}$ )	$\kappa$ ( $\text{m}^2 \text{ s}^{-1} \times 10^6$ )	$k$ ( $\text{W m}^{-1} \text{ K}^{-1}$ )
Dargo	$178.4 \pm 9.0$	$342.3 \pm 14.1$	250.7	$2.20 \pm 0.03$	0.10	0.21
Nimmo	$123.6 \pm 12.5$	$595.4 \pm 59.7$	175.9	$1.69 \pm 0.05$	0.26	0.44

Instead, it is more likely that the error is related to inadequate vertical sampling of temperature and soil thermal properties. The limitations of the combination method for measurement of  $G$  have been widely documented (eg. Massman, 1992; Sauer, 2005). In particular, the method implicitly assumes that: i) soil properties are vertically homogeneous, and; ii) the true vertical temperature profile can be approximated from finite (typically 1-2 depths) vertical temperature sampling. In alpine soils both assumptions may be questionable given: i) often steep vertical gradients in soil properties due to the large quantities of organic matter close to the surface, and; ii) the characteristically low thermal conductivities of organic-rich soils (Bonan, 2002). The effect of both of these factors would be to promote strong energy convergence in the soil layers adjacent to the surface and correspondingly rapid, non-linear attenuation of temperature with depth. In such cases, Gentine *et al.* (2012) conclude that '*... measurements even at a few centimetres deep in the soil profile miss a large part of the surface soil heat flux signal*'.

The fact that the soil heat flux at 0.08m was only approximately 20% of the calculated surface value confirms the rapid diminution of energy transfer with depth in these soils. Nonetheless, the contribution of  $G_z$  to  $G$  may still be underestimated if the true temperature profile is significantly non-linear, as would be expected in soils with poor thermal conductivity, since the layer above the soil temperature probes may heat up much more than deeper layers. In this study, soil temperatures were averaged from measurements at 0.02 and 0.06m, which implicitly assumes linearity in the 0-0.08m soil layer. Harmonic analysis, an alternative approach to the combination method that does not require the assumption of linearity in the depth-dependence of temperature, has been found to increase estimates of  $G$  (and correspondingly improve energy balance closure) in ecosystems such as grasslands in which soil heat flux contributes substantially to the energy balance (Heusinkveld *et al.*, 2004; Jacobs *et al.*, 2008). Jacobs *et al.* (2008) report approximate twofold increases in  $G$  in a mid-latitude grassland using harmonic analysis in comparison to the combination method. Such an increase in the current study would effectively close the energy balance (to within instrument uncertainties; see section 4.2.1.5 below).

#### 4.2.1.5 Instrument errors

Measurement error – and consequent contributions to energy balance shortfalls - may occur in any of the instrument systems (i.e. radiation, convection or storage). With respect to turbulent fluxes, assuming appropriate calibration and data processing, sensible and latent heat fluxes with ‘Class A’ sonic anemometers such as the CSAT-3 have estimated uncertainties of up to 10 and  $20\text{Wm}^{-2}$ , respectively, in the highest data quality classes (1-3, as calculated on the basis of the quality assessment schema outlined in Chapter 3) (Mauder *et al.*, 2006). In lower (but still acceptable) quality classes (i.e. 3-6), these uncertainties rise to 20 and  $30\text{Wm}^{-2}$ , respectively. Additionally, differences in  $\text{CO}_2$  flux estimates on the order of 5-10% are observed between data processing software packages, occurring primarily as a result of different conceptual approaches to the application of corrections (Mauder *et al.*, 2008).

With respect to radiation sensors, Kohsiek *et al.* (2007) cite errors in net radiation measurements of up to 25 and  $10\text{Wm}^{-2}$  during day and night, respectively, although Blonquist Jr *et al.* (2009) report that the Kipp and Zonen CNR1 used in this study is among the most accurate instruments available. Similarly, Hukseflux (2009) rates the error for the HFP01 heat flux plates used in this study at  $\pm 20\%$ , and Sauer *et al.* (2007) have estimated thermal contact resistance errors in heat flux plate measurements at less than 10% in moist, medium-textured soils.

These uncertainties are in many cases of similar magnitude to absolute EB deficits reported in this study, and thus may plausibly contribute to the observed energy imbalances. However, it is not clear that these errors would necessarily translate to systematic closure shortfalls of turbulent relative to non-turbulent flux measurements, as observed in this and almost all other eddy-covariance studies. As such, the most likely explanation for energy balance deficits in this study remains the systematic underestimation of the storage component of the soil heat flux. In turn, this suggests that – with the exception of periods of weak turbulent mixing – large relative energy balance deficits nocturnally do not indicate systematic underestimation of nocturnal turbulent fluxes. The effects of these periods on  $\text{CO}_2$  fluxes in particular are addressed below.



#### 4.2.2 Nocturnal CO<sub>2</sub> flux underestimation

In section 4.2.1.4 it was concluded that the consistent non-closure of the nocturnal energy balance at higher  $u^*$  was most likely due to errors in estimates of  $G$  than in eddy flux measurements. However, it was also clear that there was further degradation of energy balance closure below a given  $u^*$  threshold, and it was concluded that this was most likely due to the effects of advection under calm nocturnal conditions. If this is the case, CO<sub>2</sub> fluxes should also be underestimated under such conditions, and affected data should thus be excluded from subsequent analysis. This question is addressed in section 4.2.2.1 below.

Following the filtering of affected data, the accuracy of the remaining data is evaluated via comparison with two alternative methods of estimating nocturnal ecosystem respiration ( $R_e$ ). The first approach used light response function analysis to derive estimates of  $R_e$  from daytime flux measurements (section 4.2.2.2). This is a quasi-independent estimate in that the same measurement system was used, but the data from which the  $R_e$  estimates were drawn is not affected by the issues which occur nocturnally. The second approach involved the use of a chamber system to independently measure  $R_e$  (section 4.2.2.3). The rationale for using two approaches is that while neither represents an independent ‘standard’ for comparison, good agreement between approaches can – with appropriate caution - be taken to indicate that the nocturnal CO<sub>2</sub> flux data remaining in the time series is of reasonable quality and not systematically and substantially in error.

##### 4.2.2.1 *Friction velocity ( $u^*$ ) threshold*

As discussed in Chapter 2, the phenomenon of nocturnal CO<sub>2</sub> flux underestimation is thought to be related to turbulence intermittency and significant or even dominant advective terms in the mass balance of the system control volume, both of which occur under stable conditions (Aubinet, 2008). This phenomenon manifests as a progressive decline in CO<sub>2</sub> fluxes at low  $u^*$ , which has no explainable basis in ecosystem function. As discussed in Chapter 3, a stationarity criterion was used during data quality control to reduce the potential effects of intermittency, while an objective determination technique was used to ascertain the  $u^*$  threshold below which turbulent flux measurements become unreliable.

In section 4.2.1.1, it was shown that energy balance closure was substantially and progressively degraded at  $u^* < 0.1 \text{ m s}^{-1}$ , and concluded that this was most likely driven by non-

turbulent transport of sensible and latent heat. Assuming that this explanation is valid, fluxes of other scalars – such as CO<sub>2</sub> – should be similarly underestimated. Thus the technique used to estimate  $u^*$  thresholds for CO<sub>2</sub> fluxes should in principle yield results consistent with those observed with respect to energy fluxes. Correspondingly, the analysis of CO<sub>2</sub> fluxes yielded a  $u^*$  threshold of approximately 0.094 m s<sup>-1</sup> for Dargo (Table 4.3), consistent with the threshold at approximately 0.1 m s<sup>-1</sup> apparent in the nocturnal energy balance analysis. The threshold was also seasonally consistent. The analysis of six separate temperature classes (drawn from the entire dataset) is also presented in Figure 4.10<sup>25</sup>. In almost all cases, nocturnal CO<sub>2</sub> flux (i.e.  $R_e$ ) increased with  $u^*$  at low values, while above the  $u^*$  threshold, it was largely insensitive to further increases. The increase observed in some cases at very high  $u^*$  may be associated with the pumping effect of sporadically high surface shear stress forcing air of high CO<sub>2</sub> partial pressure out of the soil (Gu *et al.*, 2005a).

The consistent responses of both CO<sub>2</sub> and energy balance closure to low  $u^*$  suggests that other mechanisms – as discussed previously, most likely advective transfer – become significant terms in the mass balance equation, such that the measurement system no longer accurately characterises the true surface flux. As such, this data must be removed to prevent systematic errors in aggregate estimates (e.g. at daily time scales and beyond) of CO<sub>2</sub> fluxes. At both sites, nocturnal flux data that were below the seasonal thresholds were thus excluded from the time series, resulting in loss of approximately 20 and 30% of remaining nocturnal data at Dargo and Nimmo, respectively.

**Table 4.3: seasonal and annual friction velocity ( $u^*$ ) thresholds for Dargo and Nimmo.**

	Summer	Autumn	Winter	Spring	Annual
<i>Dargo</i>	0.11	0.091	0.095	0.104	0.094
<i>Nimmo</i>	0.045	0.068	0.081	0.067	0.062

<sup>25</sup> Separation of data into temperature classes prevents potential seasonal associations between temperature and  $u^*$  from causing spurious correlation.

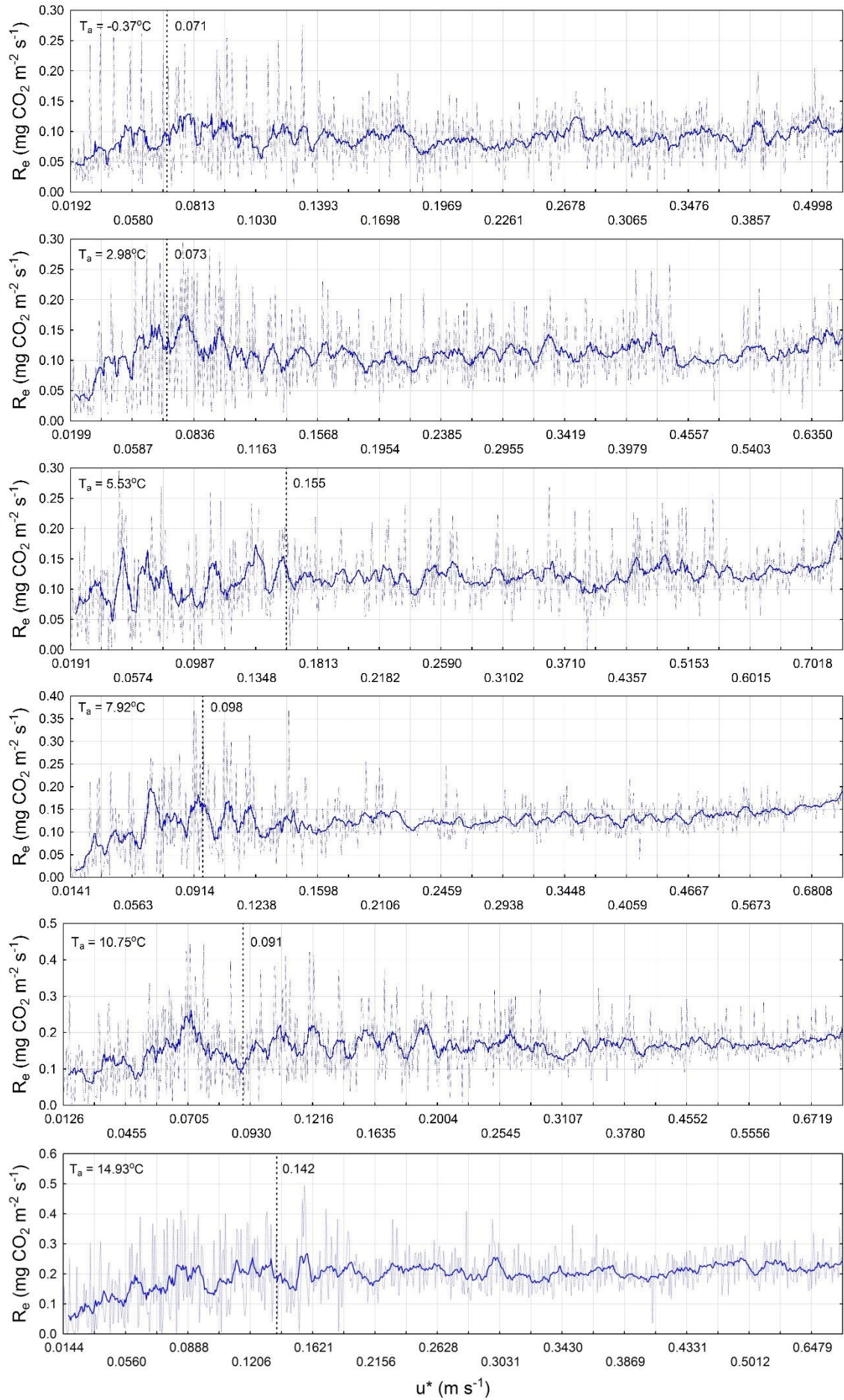


Figure 4.10: friction velocity ( $u^*$ ) and applicable thresholds for six temperature classes (using all data; solid line represents 10-point running mean of raw data [dotted line]; median threshold = 0.094).

#### 4.2.2.2 Light response function analysis

At Dargo, direct nocturnal  $R_e$  estimates were on average approximately 9.8% larger than light response function (LRF)-derived  $R_e$  (herein LRF- $R_e$ ) estimates, with high correlation between the two series ( $r^2 = 0.84$ ) (Figure 4.11a and b; Table 4.4). At Nimmo, the corresponding numbers were 7% and  $r^2 = 0.8$ . However, the  $R_e$  measurements themselves are not directly comparable, since the time intervals they represent do not overlap, and thus the environmental drivers of  $R_e$  (primarily temperature) differ between them. Therefore, as described in Chapter 3 (section 3.7.1), the Lloyd and Taylor (1994) temperature response function used in this study was fitted to the LRF- $R_e$  estimates using simultaneous soil temperature data, such that differences between sites could be analysed in terms of differences in temperature response.

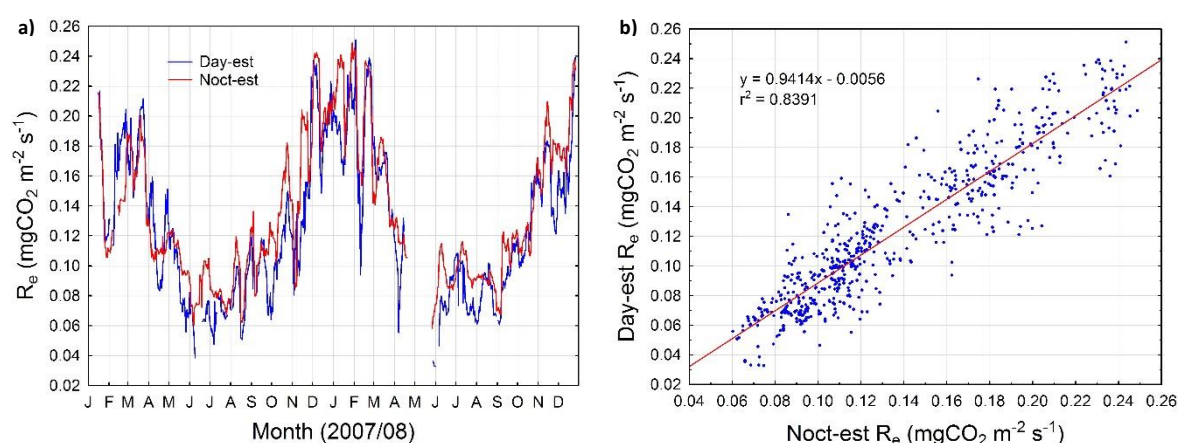


Figure 4.11: a) 2007/08 time series of nocturnally- and daytime-derived ecosystem respiration ( $R_e$ ) for Dargo site; b) least squares regression of LRF- on nocturnal- $R_e$ .

Table 4.4: Lloyd and Taylor temperature response function parameter estimates ( $\pm$ SE) fitted to Dargo site nocturnally- and daytime-derived  $R_e$  (daytime and nocturnal parameter estimates were significantly different at  $p > 0.05$ ).

	Noct $R_e$ / LRF- $R_e$	$r^2$	$R_{ref}$		$E_o$	
			Nocturnal	Daytime	Nocturnal	Daytime
Dargo	1.10	0.83	0.159 $\pm$ 0.001	0.145 $\pm$ 0.001	206.8 $\pm$ 4.07	225.2 $\pm$ 5.46
Nimmo	1.07	0.81	0.163 $\pm$ 0.001	0.142 $\pm$ 0.001	219.9 $\pm$ 4.59	319.7 $\pm$ 6.1

At Dargo, this yielded higher (approximately 10%) reference respiration ( $R_{ref}$ ) and lower (approximately 10%) temperature sensitivity ( $E_o$ ) parameter estimates for nocturnal  $R_e$  relative to the daytime-derived estimates (Table 4.4). However,  $R_e$  is much more sensitive to changes in  $R_{ref}$  than  $E_o$ . Since  $E_o$  is the exponent of the L&T function, it determines the curvature of the temperature response (i.e. temperature sensitivity), whereas  $R_{ref}$  is a simple linear scaling parameter that represents the expected respiration at the reference temperature ( $10^{\circ}\text{C}$ ). Thus it is clear from the relatively constant offset between the curves for nocturnal and LRF- $R_e$  (Figure 4.12) that  $R_e$  was much more sensitive to changes in  $R_{ref}$  than  $E_o$  over the range of environmental temperatures at Dargo. As such, the difference between  $R_{ref}$  for nocturnal- and LRF- $R_e$  explains almost all of the difference in the magnitude of  $R_e$ .

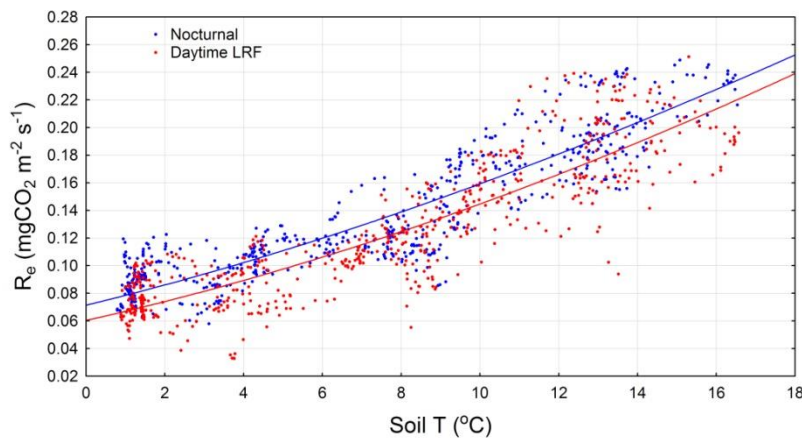


Figure 4.12: comparison of Lloyd and Taylor temperature response functions fitted to nocturnal- and LRF- $R_e$  for Dargo site.

The temperature-independent differences in  $R_e$  due to nocturnal and daytime parameter differences can be estimated by calculating and summing respiration estimates for the whole time series calculated from the L&T function and soil temperatures. At Dargo, this resulted in nocturnal  $R_e$  estimates approximately 10.4% larger than those from LRF- $R_e$  (Figure 4.13). At Nimmo, it was 7.2%. Lower LRF-estimated  $R_e$  in comparison to nocturnal measurements (by up to 20%) has similarly been reported for grassland ecosystems in numerous studies (Suyker and Verma, 2001; Falge *et al.*, 2002; Gilmanov *et al.*, 2003; Xu and Baldocchi, 2004). However, this is in marked contrast to a multi-site comparative analysis of different  $R_e$  estimation approaches by van Gorsel *et al.* (2009), who conclude that nocturnal eddy covariance data yielded systematically *lower* estimates of  $R_e$  than those drawn from LRF analysis. This may be partly associated with the fact that all selected sites for that study

were forested; the severity of the problem of nocturnal underestimation is likely to be far greater in forest ecosystems with large control volumes and significant potential for decoupling of above- and below-canopy flow (Finnigan *et al.*, 2003).

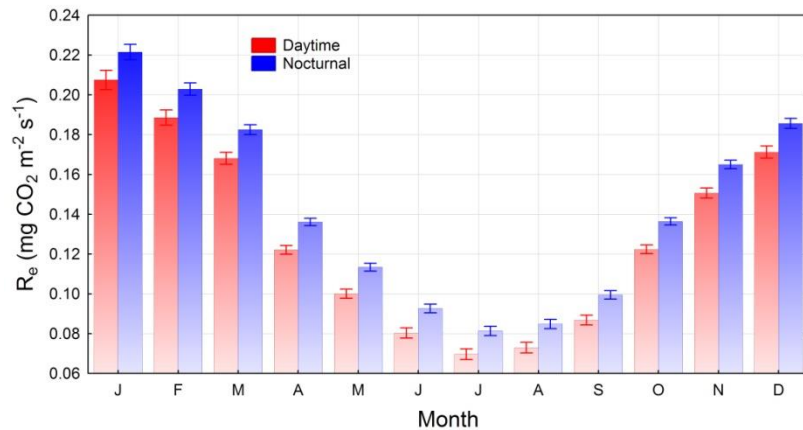


Figure 4.13: monthly mean diurnal respiration calculated from L&T function and soil temperatures using daytime and nocturnal best-fit parameters (error bars represent 95%CI for parameter uncertainty).

The difference between  $R_e$  estimates reported here may be associated with light-induced inhibition of leaf respiration (Hurry *et al.*, 2005). Wohlfahrt *et al.* (2005b) modelled the potential effects of this phenomenon in a mountain meadow and concluded that  $R_e$  may be reduced by 5-20%, though the authors conclude that the upper bound of this estimate is most likely lower. In a direct observational study, Cai *et al.* (2010) correspondingly report slightly lower reduction of 5-9% in a boreal peatland. These estimates are consistent with those reported for the current study. However, it is unclear whether this phenomenon is driven by real light-induced reductions in  $R_a$  (Atkin *et al.*, 1998) or whether it is an apparent phenomenon arising from the fact that the photosynthetic refixation of respired CO<sub>2</sub> is not accounted for by the measurement system (Pinelli and Loreto, 2003). If the latter is the case, then estimation of  $R_e$  using light response function analysis is correspondingly underestimated, since some proportion of the contribution of  $R_a$  to  $R_e$  is missed by the measurement system. This issue remains the subject of debate within the literature (Hoefnagel *et al.*, 1998), and is not pursued further here.

Thus differences between nocturnally-derived and light response function-derived  $R_e$  were relatively small, and may potentially be explained by a known inhibitory mechanism. This provides further evidence that with appropriate corrections to the data, nocturnal turbulent fluxes – and CO<sub>2</sub> fluxes in particular – are not systematically underestimated by the eddy covariance system.



However, while this analysis establishes confidence in the consistency of the performance of the eddy covariance system between day and night, it doesn't demonstrate that the system accurately captures the true magnitude of exchange of CO<sub>2</sub> between ecosystem and atmosphere (and in particular, R<sub>e</sub>), since both daytime and nocturnal data are drawn from the same system. This question can be further investigated through a measurement system that provides a completely independent set of observations of comparable quantities to those produced by the eddy covariance system.

#### 4.2.2.3 Chamber analysis

In contrast to light response function analysis, the use of a chamber system provides a truly independent measure of R<sub>e</sub>. However, uncertainties arise due to the fact that potential error sources are independent, and potentially relatively large (Davidson *et al.*, 2002). Moreover, the chamber system samples a much smaller area than the eddy covariance system. This is only a problem if spatial sampling of the chamber system does not adequately capture the area-weighted heterogeneity of the eddy covariance system's flux source area. In the current study the relative homogeneity of the vegetation canopies suggests that this is not likely to be a major problem.

Direct real-time comparison of chamber- and eddy covariance-based estimates of R<sub>e</sub> was not possible due to the fact that during the limited periods in which nocturnal chamber measurements were made, most nocturnal eddy covariance data were rejected due to low quality. Moreover, since random error during nocturnal periods is large relative to flux magnitude (see section 4.3), such real-time comparisons may not be particularly meaningful. However, chamber measurements were also made during the day, and thus for both nocturnal and daytime periods, chamber-measured R<sub>e</sub> can be compared with R<sub>e</sub> estimates derived from temperature response functions in combination with observed soil temperatures. Since these functions were parameterised using observational data, this comparison tests both the validity of that data and of the temperature-based model of R<sub>e</sub>.

The comparison reveals very strong agreement between the two methods (Figure 4.14). Both the magnitude of R<sub>e</sub> and the amplitude of its diurnal variation showed a high degree of consistency between chamber measurements and empirical estimates. On average, the chamber estimates were approximately 4% larger than the model estimates (measurement period averages of 0.23 and 0.22 mgCO<sub>2</sub> m<sup>-2</sup> s<sup>-1</sup>, respectively), but owing to the large uncertainties in the chamber measurements in particular, the difference between them is not significant. Moreover, the volume

estimate for the chamber collars embedded in the ground ( $\sim 7.07\text{L}$ ) were relatively uncertain, due both to the unevenness of the surface within the collar and the volume occupied by the vegetation itself. This inevitably contributes additional uncertainty that is not quantified here.

The amplitude of the chamber measurements also appears slightly larger than for empirically-estimated  $R_e$ . Given the small number of points, this apparent effect may simply be a minor measurement artefact. However, it may partly reflect the fact that the use of soil temperature does not capture the temporal dynamic of the system perfectly, since for example respiration from aboveground plant tissue may respond more closely to air than soil temperature. Since the diurnal temperature amplitude is higher for near-surface air than for the 0-10cm soil layer (as is clear from Figure 4.14), this may result in slightly higher amplitude of  $R_e$  than predicted from soil temperatures alone. Nonetheless, on balance the choice of soil temperature as the key driver of  $R_e$  appears to be well-justified, given that the chamber measurements followed soil temperatures (and soil temperature-derived  $R_e$ ) much more closely than air temperature (as is clear from Figure 4.14). The lower amplitude may also reflect slight underestimation of short-term respiration. This occurs due to a mismatch between long-term (e.g. seasonal) and short-term (e.g. hour to hour) temperature sensitivity of respiration (see discussion in Reichstein *et al.*, 2005); since the temperature response function is fitted to all data, periodic biases may thus arise in the temperature sensitivity (and thus diurnal amplitude) of  $R_e$ .

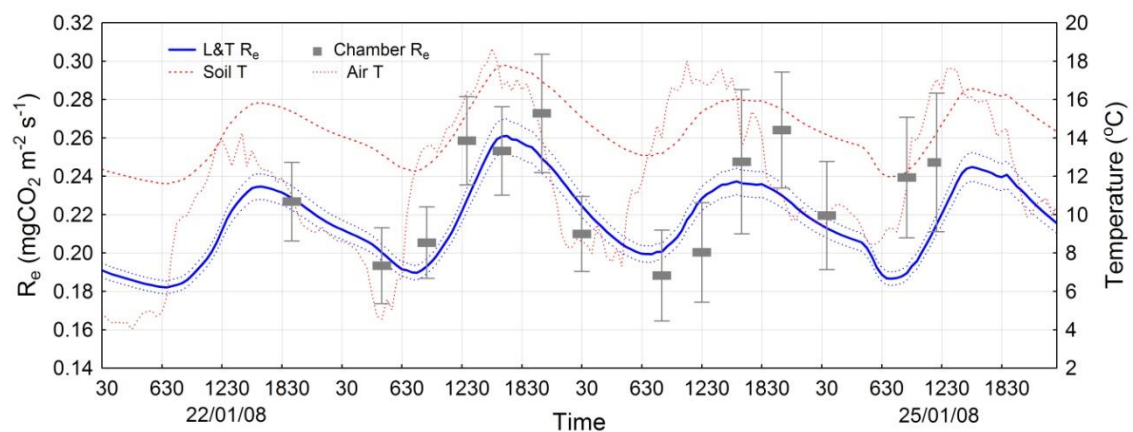


Figure 4.14: comparison of  $R_e$  from chamber measurements with  $R_e$  estimated from Lloyd and Taylor (L&T) function parameterised using 2008 nocturnal eddy covariance data from Dargo site (whiskers represent 95%CI for the mean; dashed blue lines represent 95%CI for compound model parameter uncertainty).

The degree of consistency between chambers and empirical estimates reported here is relatively uncommon. With few exceptions (eg. Liang *et al.*, 2004), it has generally been observed



that eddy-covariance estimates of fluxes are substantially lower than those from chamber systems (Goulden *et al.*, 1996a; Janssens *et al.*, 2000; Kabwe *et al.*, 2005; Wohlfahrt *et al.*, 2005a; Fox *et al.*, 2008; Myklebust *et al.*, 2008; Schrier-Uijl *et al.*, 2010). This may simply reflect the relatively 'ideal' conditions in which measurements were made: short vegetation and relatively flat terrain make accurate measurement of turbulent fluxes more likely, while the fact that the entire ecosystem atmosphere CO<sub>2</sub> exchange can also be measured using a single chamber system also reduces potential errors in chamber measurements.

These results thus provide further evidence that there is no systematic nocturnal error in the capacity of the eddy covariance system at Dargo to measure turbulent fluxes. Nonetheless, uncertainty inevitably remains as to whether this approach would produce equally consistent results at Nimmo. Given its known topographic complexities and the resulting strongly stable conditions that often attain there nocturnally (see Chapter 5, section 5.3.1), the possibility of systematic nocturnal biases in CO<sub>2</sub> flux measurements cannot be ruled out. On the other hand, higher rates of nocturnal data rejection occur at Nimmo precisely because such conditions occur more frequently. Thus to the extent that the rejection criteria are able to identify systematically erroneous flux measurements, nocturnal CO<sub>2</sub> flux measurements at Nimmo are considered unlikely to be systematically underestimated. In fact, given the topographic characteristics of Nimmo, slight overestimation of nocturnal R<sub>e</sub> is also possible given that R<sub>e</sub> is likely to be higher on the warmer valley slopes than on the valley floor, such that downslope transport may result in relative CO<sub>2</sub>-enrichment of air at the valley floor.

Despite the similarity of results between eddy-covariance- and chamber-based systems reported here, the latter are themselves also subject to various sources of potential error and thus measurement uncertainty. These include: i) alteration of diffusion gradients (in non-steady state systems); ii) system-induced pressure differentials between ambient and internal volume air; iii) environmental disturbance due to installation or operation of system or system components, and; iv) sampling uncertainties in heterogeneous ecosystems (Davidson *et al.*, 2002).

With respect to i), it has been documented that non-steady state chamber systems such as used here often underestimate fluxes due to gradual weakening of the diffusion gradient between soil and headspace, as well as the fact that the volume calculation accounts only for aboveground airspace (Pumpanen *et al.*, 2004). The use of short incubation times has been recommended to minimise the effects of these issues (Davidson *et al.*, 2002), and in this study, a two-minute measurement interval was used. As documented in Chapter 3.3.2), there was no evidence of asymptotic behaviour that would be expected in a system moving towards saturation. As such it is

concluded that the effect of this issue – estimated (by Pumpanen *et al.*, 2004) to cause underestimation of 4-14% in non-steady state systems - is likely small, though it is not further quantified here. With respect to the remaining issues, as discussed in Chapter 3, system venting and early installation of collars were measures aimed at addressing ii) and iii) above, respectively. With respect to iv), the number of collars and their spacing was considered sufficient given the relative homogeneity of surface cover at Dargo.

The results reported here are thus taken as a measure of further confidence that the nocturnal data as measured by the eddy covariance system adequately capture ecosystem processes. This in turn supports the general validity of the approach taken to collection, processing and quality assurance of eddy covariance data, and thereby the results presented subsequently.

### 4.3 Random error

As discussed in Chapter 3, random measurement error is characteristic of all eddy covariance data, and contributes to uncertainty in both time-integrated sums of relevant scalar quantities (here CO<sub>2</sub>) and estimation of model parameters used for gap-filling and partitioning of NEE into GPP and R<sub>e</sub>. This random error is also characterised by its heteroschedasticity and non-normal frequency distribution. In this investigation, differences between fluxes on successive days under similar environmental conditions were used as a measure of random error ( $\delta$ ; see Chapter 3). This method is known to overestimate random error due to the fact that it inevitably counts some environmentally-induced variation (i.e. signal) in fluxes as random error (i.e. noise) (Hollinger and Richardson, 2005; Dragoni *et al.*, 2007). As such, the effects of random error on flux uncertainty are likely to be overestimated here.

In this study, the observational data clearly showed the characteristic Laplacian random error frequency distribution reported elsewhere; for illustration, the frequency distribution of  $\delta$  is presented for Dargo in Figure 4.15a, in which the fitted Gaussian function is clearly inappropriate. The data also show increasing variance in random error [ $\sigma(\delta)$ ] as a function of flux magnitude (i.e. heteroschedasticity; Figure 4.15b). At both sites, there was an underlying, base level of uncertainty - for both positive and negative values of CO<sub>2</sub> flux (effectively day and night, respectively), the regression intercept of  $\sigma(\delta)$  at flux magnitudes approaching zero was close to 0.05mgCO<sub>2</sub> m<sup>-2</sup> s<sup>-1</sup> (see Table 4.5). Moreover, the slope of the line was much greater nocturnally at both sites, though the effect was less pronounced at Dargo than Nimmo (0.32 and 0.59, respectively). In other words, the nocturnal rate of change in random error represented nearly 60% of the increase in flux magnitude at Nimmo, approximately double that of Dargo.

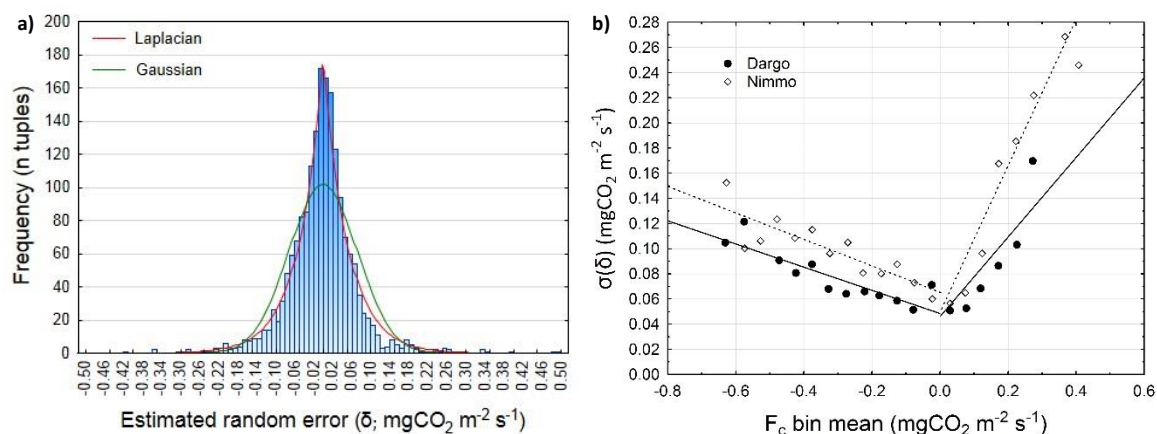


Figure 4.15: a) frequency distribution of random error ( $\delta$ ) at Dargo; b) random error variance as a function of CO<sub>2</sub> flux magnitude for both sites.

Table 4.5: linear regression coefficients for random error variance as a function of CO<sub>2</sub> flux magnitude.

	$F_c < 0$			$F_c > 0$		
	Slope	Intercept	$r^2$	Slope	Intercept	$r^2$
Dargo	-0.092	0.049	0.73	0.315	0.047	0.66
Nimmo	-0.105	0.065	0.77	0.586	0.049	0.91

The generally larger  $\sigma(\delta)$  observed nocturnally is most likely associated with the increased intermittency of turbulence relative to the daytime (Richardson *et al.*, 2006b). The reasons for the larger uncertainty at Nimmo are not clear, though the much larger nocturnal differences may be related to a greater degree of turbulent intermittency associated with the tendency towards more strongly stable conditions at nimmo nocturnally. There are two other major factors thought to contribute to random error: the operation of the system itself and heterogeneities in flux source area (Hollinger and Richardson, 2005). It is conceivable that nocturnal environmental conditions may affect the operation of the system – for example, condensation may affect IRGA or sonic anemometer performance. However, data were generally rejected when such conditions were indicated by instrument diagnostic flags. This is considered a more unequivocal measure of poor measurement conditions than the combined stationarity / integral turbulence / wind direction quality rating. The latter is more likely to result in acceptance of occasional poor quality data, such as may occur due to flux intermittence. With respect to flux source area, heterogeneity also seems

unlikely to be a major cause of random error at these sites given the strong surface homogeneity over a relatively large area.

As demonstrated in Figure 4.16, despite the fact that the frequency distribution of random error in the original eddy covariance measurements is Laplacian, the frequency distribution of the Monte-Carlo trials ( $n = 10^4$ ) of cumulative random error is Gaussian, and the 95% confidence intervals (approximately  $2\sigma$  for the  $t$ -distribution where  $n = 10^4$ ) are reported in Table 4.6. At Dargo, the contribution of random error to uncertainty in net ecosystem exchange (NEE) was less than  $20\text{gCO}_2 \text{ m}^{-2}$  in either year, whereas at Nimmo it was generally much (up to 70%) higher (greater than  $27\text{gCO}_2 \text{ m}^{-2}$ ). This was due to the fact that while there were less data available at Nimmo, the remaining data were subject to larger random errors than at Dargo, as illustrated in Figure 4.15b.

It is worth reiterating that, for reasons previously discussed, these uncertainties are most likely overestimates. Nonetheless, they are significantly smaller than estimates of cumulative random error reported by Dragoni *et al.* (2007) of  $36\text{--}45\text{gCO}_2 \text{ m}^{-2}$ , and Richardson and Hollinger (2005) of around  $60\text{g}$ . However, cumulative uncertainties due to random error are likely to vary widely due to differences between studies in terms of data retention and mean flux magnitudes, increases in either of which would tend to cause concomitant increases in uncertainty. Dragoni *et al.* (2007) also report that the majority of uncertainty in annual NEE is due to model rather than random error, a topic which is discussed in further detail below.

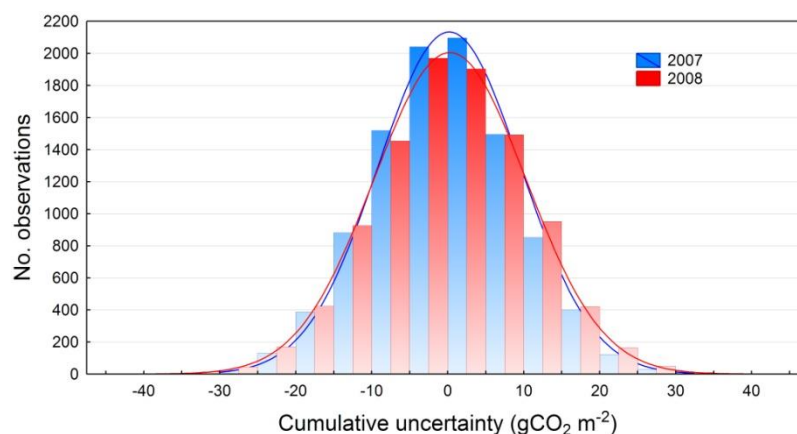


Figure 4.16: Monte Carlo-simulated cumulative random uncertainty estimates for Dargo 2007/08 ( $n = 8270$  and  $8823$  for 2007 and 2008, respectively).

**Table 4.6: Monte Carlo-simulated cumulative random uncertainty estimates for Dargo 2007/08.**

	Number of observations		Cumulative uncertainty (gCO <sub>2</sub> m <sup>-2</sup> )	
	2007	2008	2007	2008
<i>Dargo</i>	8270	8823	17.2	19.2
<i>Nimmo</i>	6999	7003	29.5	27.6

#### 4.4 Model error

Since a model is required to fill gaps in the data resulting from data rejection or system failure, model performance has a critical influence on the reliability of the final data. Failure of models to accurately describe the temporal dynamics of a system may be due to: i) errors in the observational data (i.e. either in the modelled quantity or in the variables used to predict it); ii) the failure of the model to adequately reflect the underlying processes or empirical relationships between the modelled quantity and the variables used to predict it, or; iii) exclusion of observational data crucial to the accurate capture of system response.

With respect to errors in the observational data ([i] above), the previous analysis suggests that the effect of systematic error on the flux data is relatively limited; moreover, the effects of random error is less problematic since the early stopping criterion of the ANN training algorithm (see section 3.5.1 of Chapter 3) effectively prevents the network from fitting to noise superimposed on the signal. It is also assumed here that measurement error – either systematic or random - in the environmental driving variables (following basic quality control procedures) is minimal<sup>26</sup>. With respect to structural failures ([ii] above), artificial neural networks make no *a priori* assumptions about relationships or processes, and thus are less prone to significant errors arising from this source. Thus the most likely source of model error in this study is the exclusion of important driving variables ([ii] above). A brief discussion of model performance and uncertainties arising from inherent errors is provided below.

<sup>26</sup> There are likely to be some additional error associated with the fact that periodic total system failures necessitated gap-filling of these data; however, this aspect of uncertainty is not pursued in further detail here.

The ANNs generally explained approximately 90% of the variance in daytime measured CO<sub>2</sub> fluxes, a similar proportion during the day alone, and less than 40% nocturnally (Figure 4.17). This much lower nocturnal correlation appears to be common to flux sites generally (see for example Moffat *et al.*, 2007), and most likely primarily reflects the effects of random error, since the signal:noise ratio (i.e. flux magnitude as a proportion of random error) is much lower nocturnally, as clearly shown in Figure 4.15c.

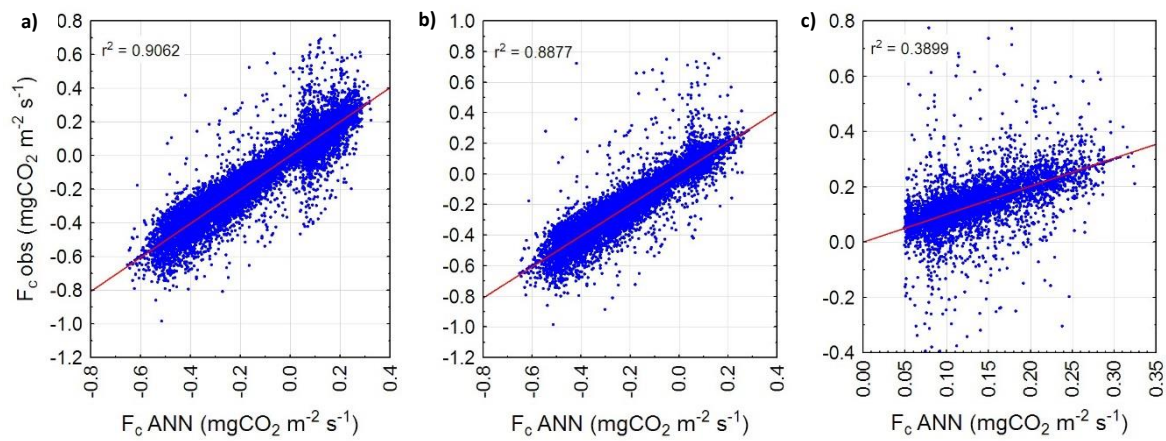


**Figure 4.17: comparison of observed CO<sub>2</sub> fluxes with artificial neural network output ( $F_{c, \text{obs}}$  and  $F_{c, \text{ANN}}$ , respectively) for: a) all data; b) day (insolation >  $0 \text{ W m}^{-2}$ ), and; c) night (insolation =  $0 \text{ W m}^{-2}$ ).**

Some indication of the contribution of random error to signal variance can be gained by comparing the correlation of the initially noise (i.e. random error)-free ANN output to both the original observational CO<sub>2</sub> flux time series and the ANN output with noise artificially imposed on it. The results of this analysis are presented in Figure 4.18. Imposing random error of the magnitude originally derived in section 4.3 actually resulted in a coefficient of determination ( $r^2$ ) below that found between the observational CO<sub>2</sub> flux time series and the ANN output, both during the day and nocturnally. This is an impossible result, implying a ‘more than perfect’ model, thus demonstrating conclusively that the daily difference method overestimates  $\sigma(\delta)$  (see section 4.3). When the complete time series is considered,  $r^2$  was approximately equal when random error was reduced to 80% of its original estimated value. This still implies that all of the unexplained variance in the observational time series is due to random error.

A similar result is observed for the daytime data. Nocturnally, however,  $r^2$  for the artificial noise-imposed time series was less than the observational data even when the imposed random

error was only 80% of its estimated value. Only when reduced to approximately 66% of the original random error estimate did the  $r^2$  of the artificial noise-imposed time series rise above that of the original data. This suggests that the nocturnal estimate of  $\sigma(\delta)$  was overestimated by a larger amount than its daytime value. In any case, it can be seen that for the complete observational time series, even if  $\sigma(\delta)$  is overestimated by a factor of 2, the difference between  $r^2$  values (which represents the proportion of unexplained variance contributed by model error) was still only approximately 7%. In other words, even under assumptions of minimised random error, model error contribution to the unexplained variance between ANN and CO<sub>2</sub> flux signals was very small. This is consistent with the findings of Moffat *et al.* (2007), who report that several of the more sophisticated gap-filling methods – including ANNs – in an analysis of different gap filling methods approached the noise level in the data (i.e. the models – and corresponding driving variables – effectively accounted for almost all of the non-random variation in the CO<sub>2</sub> flux signal).

The broader significance of this result is that a small number of environmental variables used by the ANN to predict CO<sub>2</sub> fluxes (six: incoming and reflected photosynthetically active radiation, air and soil temperature, soil moisture and vapour pressure deficit) contained almost all of the information required to statistically reproduce the target signal in this ecosystem. The remaining model error – which cannot meaningfully be quantified here – may possibly relate either to missing information important in modelling of NEE (e.g. phenologically-driven threshold responses to, for example, smoothly-varying seasonal changes in light or temperature), or to small remaining systematic errors in the measurements. However, further consideration of this issue is beyond the scope of this investigation.

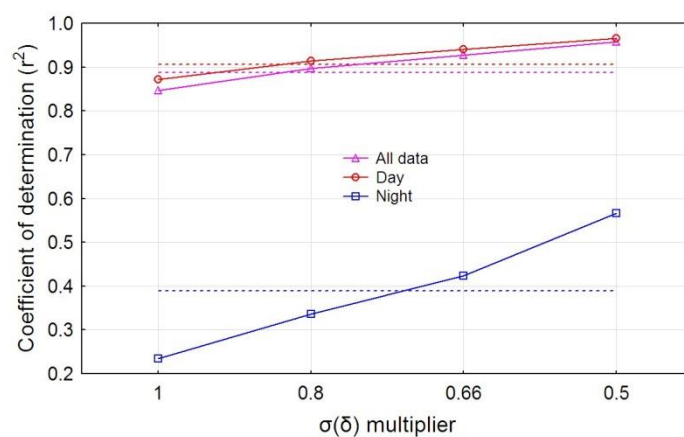


Figure 4.18: effects of decreasing random error on correlation between noiseless artificial neural network CO<sub>2</sub> flux time series and the same series with artificial noise imposed (dashed lines represent  $r^2$  between observed CO<sub>2</sub> flux time series and ANN output).



## 4.5 Uncertainty analysis

Uncertainty estimates are complicated by the fact that random and model error cannot be easily separated for the reasons discussed above. As noted in Chapter 3 (section 3.6.2), the randomised statistical method used to estimate model error inevitably includes random error because the observational data from which model estimates are subtracted to calculate model error already contain random error. Without a reliable estimate of random error (as previously discussed), this cannot be excluded. As such, the sum of model and random error as calculated here (Equation 3-15) overestimates the total error.

The cumulative increase in uncertainty is presented in Figure 4.19. The effects of total data losses are clear, with large increases in uncertainty occurring during those periods. The apparently anomalous jump in uncertainty in February 2007 is due to the fact that an anomalously large proportion of data was removed by the quality control filters due to a confluence of circumstances (including south-easterly winds, resulting in automatic data rejection), such that there was almost no flux data for this period. Thus the eventual uncertainties in annual sums are largely driven by total data losses. Nonetheless, it is clear from the significant increases in uncertainty in early 2008 (where only routine data losses associated with filtering occurred) compared with the much smaller rates of change during winter that the increases in uncertainty occur during periods with larger fluxes. Thus, as has been reported by other authors (for example, Richardson and Hollinger, 2007), the timing of data losses is important. Though there were no total system failures during winter at Dargo, rates of data rejection were high, yet little additional uncertainty was contributed during this period. Since model error is proportional to flux magnitude, reduced wintertime CO<sub>2</sub> fluxes translate to reduced uncertainties. This also applies to nocturnal data: whereas much larger proportions of nocturnal data were removed by the QC procedures, its effect on uncertainty is limited by the fact that flux magnitudes were generally smaller. This is despite the fact that more data was missing nocturnally. On the other hand, the magnitude – and thus model error – of the daytime data was larger. But the actual contribution to uncertainty of daytime data is also constrained by the fact that far less of it was removed by filtering procedures.

**Table 4.7: annual total uncertainty (sum of random and model error-derived uncertainties) in  $\text{gCO}_2 \text{ a}^{-1}$  for Dargo and Nimmo 2007/08** (note: as documented in Chapter 3.6.33 [section 3.5.3], total error ( $\sigma_{\text{tot}}$ ) was calculated as the sum in quadrature of random  $\sigma(\delta)$  and model  $\sigma(\epsilon_M)$  error, as per Equation 3-15:  $\sigma_{\text{tot}} = \sqrt{\sigma(\delta)^2 + \sigma(\epsilon_M)^2}$ ).

	Uncertainty component	2007	2008
Dargo	$\sigma(\delta)$	25.8	27.3
	$\sigma(\epsilon_M)$	48.0	33.9
	$\sigma_{\text{TOT}}$	54.8	43.5
Nimmo	$\sigma(\delta)$	27.5	28.4
	$\sigma(\epsilon_M)$	82.9	99.3
	$\sigma_{\text{TOT}}$	87.4	103.3

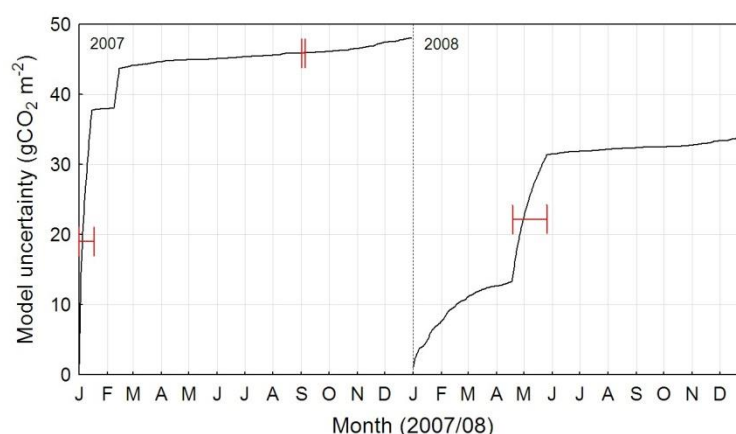


**Figure 4.19: cumulative model uncertainty for Dargo 2007/08** (periods of complete system failure – and thus data loss – are shown in red).

The annual uncertainties reported for Dargo here (54.8 and 43.5  $\text{gCO}_2 \text{ a}^{-1}$  for 2007 and 2008, respectively) are relatively small in comparison to those reported elsewhere (-110 to +290  $\text{gCO}_2 \text{ m}^{-2} \text{ a}^{-1}$ , Goulden *et al.*, 1996b;  $\pm 183 \text{ gCO}_2 \text{ m}^{-2} \text{ a}^{-1}$ , Lee *et al.*, 1999;  $\pm 73 - 440 \text{ gCO}_2 \text{ m}^{-2} \text{ a}^{-1}$ , Griffis *et al.*, 2003;  $\pm 147 \text{ gCO}_2 \text{ m}^{-2} \text{ a}^{-1}$ , Morgenstern *et al.*, 2004;  $\pm 91 \text{ gCO}_2 \text{ m}^{-2} \text{ a}^{-1}$ , Richardson and Hollinger, 2005). Those for Nimmo (87.4 and 103.3  $\text{gCO}_2 \text{ a}^{-1}$  for 2007 and 2008, respectively) are more comparable to the above uncertainty. The larger uncertainty at Nimmo results from higher random error (which may relate to the reduced quality and availability of nocturnal data in particular) and lower data coverage, such that the model error component increases simply as a result of its increased frequency. However, as highlighted by Richardson and Hollinger (2005), the methods used to assess uncertainty (and the sources of uncertainty quantified) vary between studies such that direct comparisons are not always meaningful. Moreover, uncertainties tend to scale with flux

magnitude (Loescher *et al.*, 2006), such that sites with larger fluxes will also have larger uncertainties.

#### 4.6 Summary

In conclusion, there is limited evidence to support systematic error in the measurement of net ecosystem exchange at either site, though data quality at Nimmo was generally slightly lower. Nonetheless, the possibility that the time series' for both sites are affected by largely unquantified (or even unknown) sources of potential systematic error cannot be entirely discounted. As with effectively all eddy covariance-based analyses, the two most significant sources of such error are the effects of advection and of inadvertent filtering of turbulence at either high or low frequency. However, the evidence presented here suggests that such errors are likely to be relatively minor, and that the methods used to account for them were effective. Energy balance closure was excellent at both sites, and the small shortfall in the sum of turbulent fluxes relative to available energy is most likely due to underestimation of soil heat fluxes. It is because the soil heat flux is a proportionally more important component of the energy balance nocturnally that a larger relative energy balance deficit was observed nocturnally.

Nonetheless, there was clear evidence to suggest that the vertical turbulent flux was not a representative measure of surface flux during periods of low nocturnal turbulence, as evident in progressive declines in both energy balance closure and ecosystem respiration below a given friction velocity ( $u^*$ ) threshold. Optimisation of ecosystem respiration ( $R_e$ ) model parameters using  $u^*$ -filtered nocturnal eddy covariance data produced reliable estimates of  $R_e$  as compared to quasi-independent (light response function analysis) and independent (chamber measurements) estimates of  $R_e$ . Thus it is concluded here that the measurements from the eddy covariance are – from the indications provided in this analysis – robust and accurate. Uncertainties associated with random and model error at both sites were also moderate in comparison to values cited in the literature. Uncertainty was nonetheless higher at Nimmo due to the combination of larger data losses and higher random error at that site.

Before discussing both stocks and flows of carbon within the grassland ecosystems at Dargo and Nimmo, a brief description of climatic conditions at the sites is provided in Chapter 5. This provides important context for the chapters discussing both ecosystem carbon storage (Chapter 6)

and ecosystem / atmosphere carbon exchanges (Chapter 7), since climatic factors are key drivers of net ecosystem exchange.

# 5. Site Meteorological Characteristics

---

## 5.1 Introduction

As discussed in Chapter 2, differences in carbon balance between ecosystems arise due to contrasts in both abiotic conditions – primarily climate – and the biotic response to these conditions. The two sites in this study represent climatologically contrasting instances of the same categorical ecosystem type (subalpine grasslands). It is well established that such climatological contrasts give rise to corresponding differences in ecosystem carbon dynamics, in terms of both short-term exchanges and long-term storage. Since quantifying and understanding such differences is a central aim of this study, this chapter provides a brief description of key climatic controls on ecosystem carbon dynamics. These controls are: insolation, the energy source for photosynthesis, air and soil temperatures, which influence photosynthetic and respiratory reaction rates via effects on enzyme kinetics, and moisture availability, since water is a fundamental ecological requirement.

## 5.2 Solar radiation

Incident photosynthetically active radiation (herein PAR) was comparable at the sites (Table 5.1; Figure 5.1a). Though on average slightly higher at Nimmo (both annually and in all seasons but summer 2008) – differences were not statistically significant (at  $p < 0.05$ ) either annually or – with the exception of winter (JAS) – seasonally. However, this is because the within-site variance in PAR was large (due to the inherent variability - over multiple time scales - of insolation) relative to the small between-site difference in PAR. While this means that conclusions about possible systematic cross-site PAR differences cannot be reliably drawn, given that PAR is the energy source that drives photosynthesis it must be emphasised that the observed difference in PAR is in ecological terms very real, amounting to cumulative annual differences in radiation receipt of 146 and 109.5 MJ  $m^{-2} a^{-1}$  in 2007 and 2008, respectively.

The seasonal cross-site PAR differences that were statistically significant (i.e. during winter) are most likely related to the previously discussed geographic characteristics of the sites (Chapter 3): Dargo is at slightly higher altitude and generally directly exposed to the influence of disturbances embedded in the prevailing westerlies, whereas Nimmo is on the edge of the Monaro Plain in the lee of the Australian Alps (i.e. on the eastern side of the more meridionally oriented New South Wales extent of the range). Thus during winter, when the westerly storm track is located over southern Australia, the effects of these contrasting geographical characteristics are likely to be accentuated, resulting in greater cloud formation at Dargo. During summer, on the other hand, differences are expected to be least, as generally observed (in both relative and absolute terms).

**Table 5.1: seasonal and annual average daily total incident photosynthetically active radiation (PAR, units MJ m<sup>-2</sup> d<sup>-1</sup>) (note: \* and \*\* denote statistically significant differences at  $p<0.05$  and  $p<0.01$ , respectively).**

	2007		2008	
	Dargo	Nimmo	Dargo	Nimmo
JFM	10.7	10.9	11.2	11.1
AMJ	6.4	6.8	6.7	7.2
JAS	4.3 *	4.8	4.2 **	4.9
OND	9.0	9.5	9.8	10.1
Annual	7.6	8.0	8.0	8.3

More important from the perspective of photosynthesis is the amount of photosynthetically active radiation (PAR) absorbed by the plant canopy. The fraction of incident PAR absorbed (fPAR) was typically larger at Dargo i.e. the albedo of the surface in the photosynthetically active portion of the spectrum (approximately 0.4-0.7 $\mu$ m) was lower than at Nimmo (Figure 5.1a). This may be partly related to the darker soils at Dargo, but given the very dense vegetation cover it may also relate to the more architecturally complex canopy (associated with the more pronounced tussock form of the vegetation) relative to Nimmo. As a result of the slightly higher fPAR at Dargo, the absolute absorption of PAR (aPAR) was effectively indistinguishable at both sites in all seasons except winter - when persistent snow cover at Dargo caused strong reflectance of incoming radiation in the visible band- and early spring (Figure 5.1c).

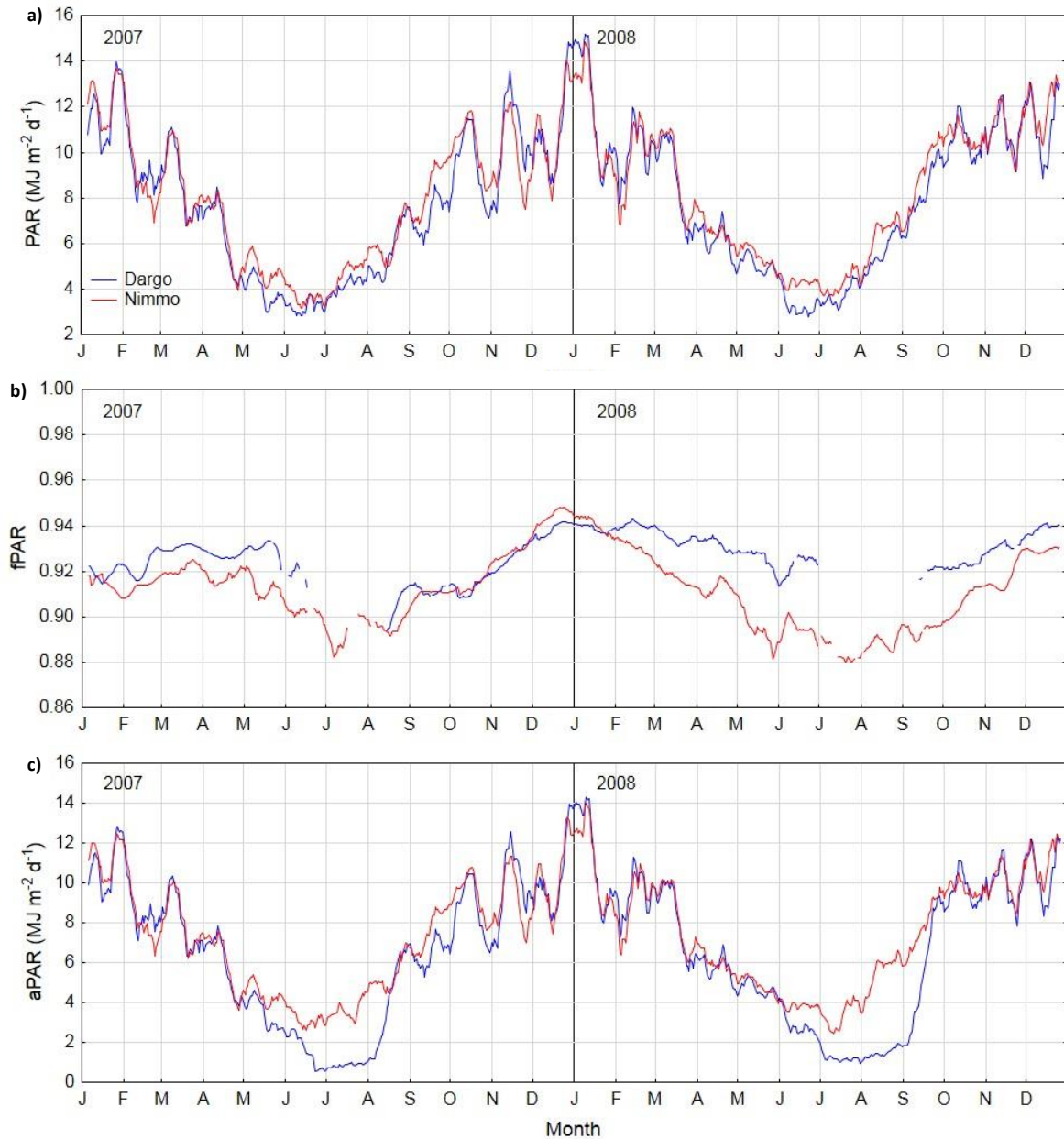


Figure 5.1: cross-site comparison of 2007/08 daily photosynthetically active radiation components : a) incident photosynthetically active radiation (PAR); b) absorbed fraction of incident photosynthetically active radiation (aPAR), and; c) absolute absorbed photosynthetically active radiation (aPAR) (note: data was smoothed using a 10-day moving average; data from snow covered periods removed).



## 5.3 Temperature

### 5.3.1 Air temperature

Daily screen level air temperatures in 2007/08 were significantly cooler at the higher-altitude Dargo (6.8°C) than at Nimmo (7.7°C), and at both sites almost 1°C higher in 2007 than in 2008 (Table 5.2; Figure 5.2a). While temperatures were lower during all seasons in 2008, it was primarily the early months of the year (summer [JFM] and autumn [MAM]) that contributed to this difference between years at the sites. The timing of winter minimum temperatures was also shifted between years: the two coldest months were June and July in 2007 and July and August in 2008, resulting in the later snowpack establishment and subsequent melt.

The diurnal amplitude of temperature was also lower at Dargo than at Nimmo. Daytime temperatures were approximately 2°C colder at Dargo, whereas nocturnal temperatures were slightly warmer (Figure 5.2b). These differences are related to the effects of differences in altitude and topography, as discussed below.

**Table 5.2: 2007/08 seasonal and annual average daily, daytime and nocturnal site air temperatures (note: \* and \*\* denote statistical significance at  $p<0.05$  and  $p<0.01$ , respectively).**

	Daily (°C)			Daytime (°C)			Nocturnal (°C)		
	Dargo		Nimmo	Dargo		Nimmo	Dargo		Nimmo
2007									
JFM	13.3	**	14.8	15.3	**	17.6	10.2		10.6
AMJ	8.2		8.5	10.1	**	11.8	6.3	*	5.3
JAS	0.8	*	1.6	1.8	**	3.8	-0.1		-0.2
OND	7.0	*	8.1	8.7	**	10.7	4.9		4.8
Annual	7.3	**	8.2	8.9	**	10.9	5.3		5.1
2008									
JFM	11.4	**	12.7	13.2	**	15.2	8.7		8.9
AMJ	6.9		6.6	9.4	*	10.4	4.7	**	3.1
JAS	0.7	**	1.5	1.8	**	4.1	-0.1		-0.4
OND	6.6	*	7.8	8.3	**	10.4	4.4		4.5
Annual	6.4	**	7.2	8.2	**	10.0	4.4		4.0
Biannual	6.8	**	7.7	8.5	**	10.5	4.9		4.6

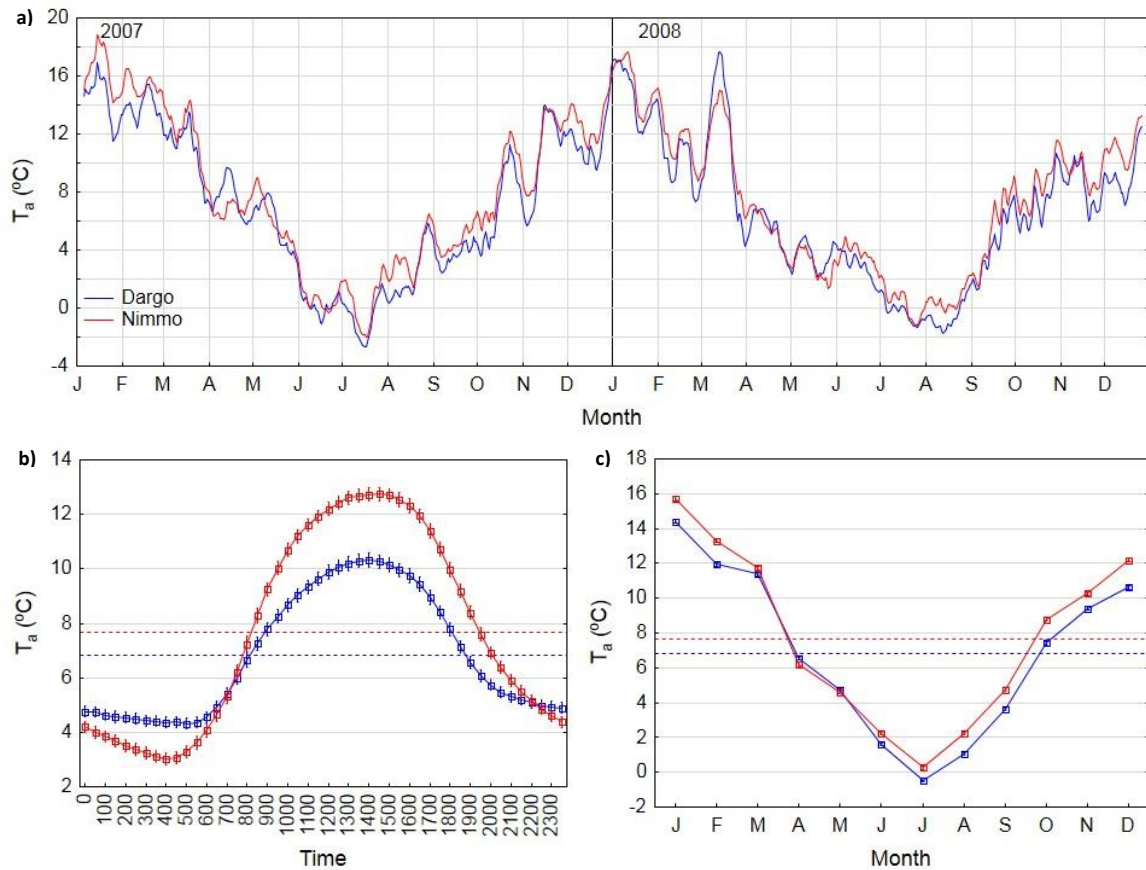


Figure 5.2: cross-site comparison of 2007/08 air temperatures : a) moving average (n=10) of daily air temperature time series; b) diurnal average air temperature ( $\pm$ SE; dashed line represents biannual average); c) monthly average air temperature.

With respect to altitude, the difference in daytime temperature is an expected consequence of the daytime temperature lapse rate. Slatyer (1978) reports that the average altitudinal gradient in the Australian alps for daytime maximum temperatures conforms closely to the dry adiabatic lapse rate ( $9.8^{\circ}\text{C km}^{-1}$ ), implying an expected daytime temperature difference between sites of  $9.8^{\circ}\text{C km}^{-1} \times 189\text{m} = 1.85^{\circ}\text{C}$ , comparable to that noted above. Nocturnally, however, Dargo was on average  $0.3^{\circ}\text{C}$  warmer (though in most seasons this difference was statistically non-significant). This is thought to relate to the contrasting topographic characteristics of the sites: the more exposed plateau location of Dargo versus the sheltered valley floor location of Nimmo.

The valley location acts to partially shelter the site at Nimmo from synoptically-driven surface winds. During clear, calm days, radiatively-driven heating may be enhanced in valleys by reduced shear-induced turbulent mixing, but the resulting instability triggers convection that in turn couples the surface with synoptic conditions (including momentum mixed downward from aloft),

thus moderating heating (Whiteman, 2000). Nocturnally, however, such convective activity quickly collapses as radiative cooling drives the development of a stable inversion. Air cooled by the surface becomes increasingly dense and eventually overcomes surface friction, flowing downhill under the influence of gravity and pooling in low-lying parts of the landscape. This process in turn promotes an intensifying situation of stable stratification and decoupling between the cold air in the valley and the overlying atmosphere.

Thus differences in nocturnal temperatures were most pronounced during calm, clear days that generally coincide with the passage of large high pressure cells over southern Australia. This can be seen in Figure 5.3, which presents time series of potential temperature ( $T_\theta$ ) and wind speed for May 11<sup>th</sup> to 24<sup>th</sup> in 2007. The first week of this period was characterised by a dominant high pressure centre over the southeast of the continent (Figure 5.3b), with clear skies and light winds. During the day,  $T_\theta$  was broadly comparable between sites, demonstrating that daytime cross-site temperature differences were, as noted above, largely a function of altitude difference. Nocturnally, however,  $T_\theta$  was up to 15K lower at Nimmo. In contrast, the second week was characterised by low pressure, cloudiness, strong winds and the passage of several fronts (Figure 5.3c). During this period,  $T_\theta$  was very similar at the sites both day and night.

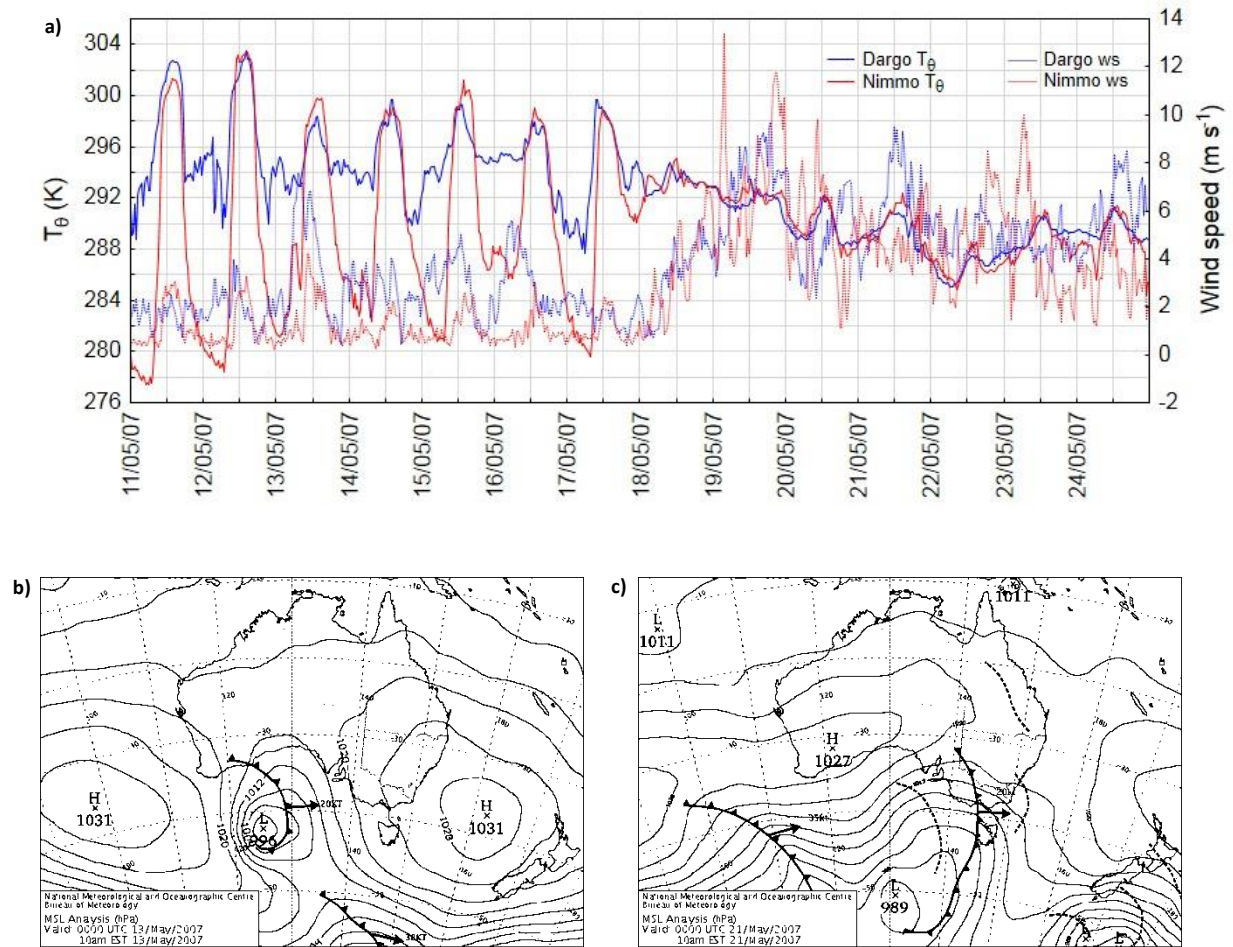


Figure 5.3: a) potential temperature ( $T_\theta$ ) and wind speeds for Dargo and Nimmo for period 11/05/07 – 24/05/07; b) Bureau of Meteorology mean seal level pressure (MSLP) analysis for 13/05; c) MSLP analysis for 21/05.

### 5.3.2 Soil temperature

Annual average temperature in the 0-0.08m soil layer ( $T_s$ ) was higher at Nimmo ( $10^\circ\text{C}$ ) than Dargo ( $7.8^\circ\text{C}$ ), and higher at both sites in 2007 than in 2008 (Table 5.3). While this is qualitatively similar to the case with air temperature, the difference in annual average soil temperature between sites was larger. As previously discussed, while daytime air temperature contrasts reflected the adiabatic effects of altitude, nocturnal contrasts were enhanced by topographic effects at Nimmo. The associated convective dynamics are an atmospheric phenomenon which reduced cross-site mean daily temperature differences by lowering nocturnal temperatures at Nimmo. While this may be expected to have some thermal effects on the soil, the effect would be strongly reduced by the

soil's higher heat capacity. As such, larger differences between sites than was observed with respect to air temperature.

**Table 5.3: 2007/08 seasonal and annual average daily soil temperatures (note that \* and \*\* denote statistical significance at  $p<0.05$  and  $p<0.01$ , respectively).**

	2007			2008		
	Dargo		Nimmo	Dargo		Nimmo
JFM	14.0	**	17.8	13.6	**	16.7
AMJ	9.0	**	10.7	7.9	**	9.9
JAS	1.9	**	2.5	2.1	**	3.3
OND	7.7	**	9.8	6.8	**	9.8
Annual	8.1	**	10.2	7.6	**	9.9
Biannual	7.8	**	10.0	7.8	**	10.0

The daily and seasonal cycles were also different between sites, with reduced amplitude apparent at Dargo relative to Nimmo (Figure 5.4), as was the case with respect to air temperature. However, in contrast to air temperature, nocturnal soil temperatures on average remained higher – though only slightly – at Nimmo than Dargo. In both the diurnal and seasonal cases, this is thought to be related to the difference in surface conditions at the sites. Specifically, at Dargo, the soil was both richer in organic matter (see section 6.2 of Chapter 6) and wetter (see section 5.4.4 below), and the quantity of standing phytomass was greater (see section 6.3 of Chapter 6) than at Nimmo.

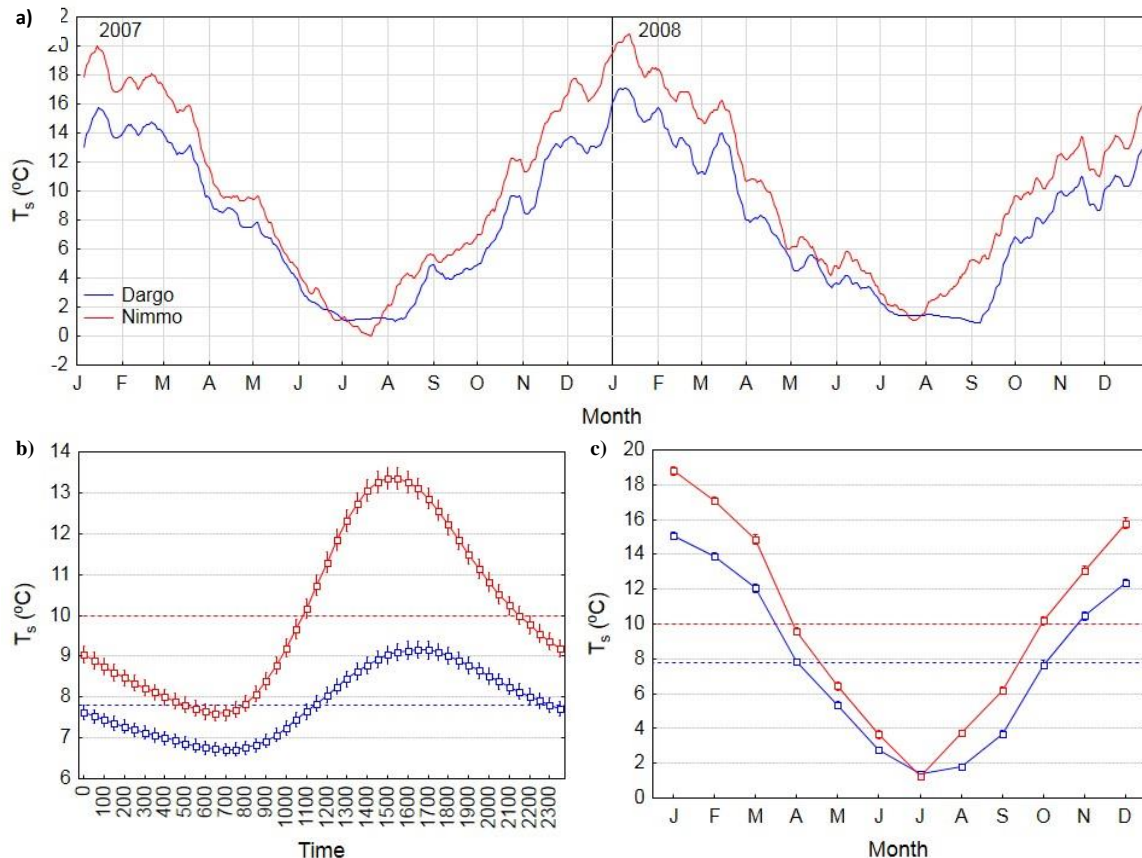


Figure 5.4: cross-site comparison of 2007/08 soil temperatures: a) moving average (n=10) of daily soil temperature time series; b) diurnal average soil temperature ( $\pm$ SE; dashed line represents biannual average); c) monthly average soil temperature.

The combination of greater soil organic content and moisture at Dargo both increases the soil heat capacity and reduces its thermal diffusivity (see Table 4.2). This in turn has the effect of reducing the rate of propagation of energy through the soil (as can be seen from the later diurnal peak in temperature at Dargo in Figure 5.4b), as well as its temperature response (i.e. diurnal and seasonal amplitude). The soil thermal diffusivity at Dargo ( $\kappa_s$ ) was  $0.095 \times 10^6 \text{ m}^2 \text{ s}^{-1}$ , less than half that at Nimmo (0.26) (see Table 4.2). As such the rate of decrease of the amplitude of the daily temperature wave is greater at Dargo: for example, an amplitude decrease (relative to the surface) of 50% corresponds to a depth of 3.5cm at Dargo but 5.9cm at Nimmo. The  $\kappa_s$  at Dargo was comparable to that of peat soils, whereas that of Nimmo was transitional between peat soils and more mineral-dominated soils with low / medium moisture levels (Monteith and Unsworth, 2008).

With respect to the canopy, the greater phytomass quantity may have the secondary effects of reducing the propagation of energy into the soil surface relative to Nimmo. This effect is likely to

be small, however; storage accounted for less than  $10\text{Wm}^{-2}$  of the surface energy balance even around midday (Chapter 4, section 4.2.1.4), and surface albedo was broadly comparable (section 5.2). The only exception to this was during winter, when soil temperatures were periodically lower at Nimmo. At Dargo, however, snow cover provided additional surface insulation and prevented subsurface temperatures from freezing in 2007/08. It also greatly reduced the daily soil temperature amplitude to almost zero. At Nimmo, however (where snow cover was ephemeral – section 5.3.1), surface layer soils froze during two periods in 2007: during all but the early afternoon hours on 24<sup>th</sup> and 25<sup>th</sup> June, and again almost continuously during 16<sup>th</sup> – 23<sup>rd</sup> July. Nonetheless, as has been noted elsewhere (e.g. Warren and Taranto, 2011), the effect of snow on soil temperature in Australia is relatively limited because of the comparatively mild winter mountain climate.

## 5.4 **Moisture availability**

### 5.4.1 Precipitation

At close to 1000mm, precipitation was broadly similar at the sites (Table 5.4). At both sites there was a moderate decline in rainfall from 2007 to 2008 for both. This decline was larger at Dargo. As a result, while Dargo had higher rainfall than Nimmo in 2007, the pattern was reversed in 2008. Placing these short-term precipitation totals into historical context is difficult in topographically complex locations because spatial precipitation variability is extremely high and historical data from nearby locations is therefore not necessarily locally representative. However, gridded products such as the SILO dataset (described in Chapter 3) provide the best available means of estimating climatologies where historical site measurements are not available.

Accordingly, SILO estimates (also presented in Table 5.4) indicate that in both years of this study, precipitation was below the 1961-90 average at both sites, particularly at Dargo (where it was at least 30% lower). Thus it appears that the years during which this study was conducted were relatively dry. This is clear from the precipitation percentile maps presented in Figure 5.5, which also illustrates the far more severe drought conditions experienced across south-eastern Australia in 2006, particularly in the High Country where well below 20% of the long-term average precipitation fell (Figure 5.5).



**Table 5.4: annual precipitation totals for Dargo and Nimmo, and 1961-90 mean estimated for sites from SILO data (see Chapter 3 for details).**

Year	Dargo	Nimmo
2007	1084	996
2008	812	870
1961-90 mean ( $\pm$ SD)	1545 $\pm$ 340	1208 $\pm$ 285

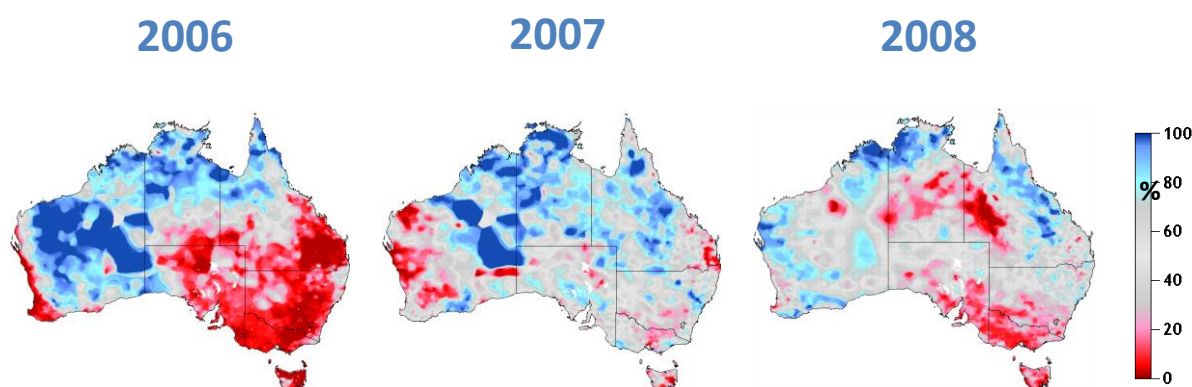


**Figure 5.5: Australian Water Availability Project annual precipitation percentile maps (% of 1961-90 mean baseline).**

With respect to temporal patterns, the higher precipitation observed in 2007 (relative to 2006 and – to a lesser extent - 2008) at both sites is evident in Figure 5.6. As discussed in Chapter 3, the expectation from respective geographical characteristics was that Dargo would have higher precipitation totals and a more winter-dominated seasonal precipitation pattern than Nimmo. However, such patterns are unlikely to be reliably manifested over the shorter periods of this study. As noted above, precipitation was very low at both sites in 2006. In 2007/08, coherent seasonal precipitation patterns were not strongly apparent. While at Dargo there was a winter peak in precipitation in 2007, very high precipitation in summer 2007/08 was also observed. At Nimmo, relatively consistent precipitation occurred across seasons in 2007, peaking in summer 2007/08. At both sites precipitation was extremely low during autumn 2008, increased during the middle of the year and declined to very low levels in summer 2008-09, during which rainfall was far lower than the same time in preceding years.

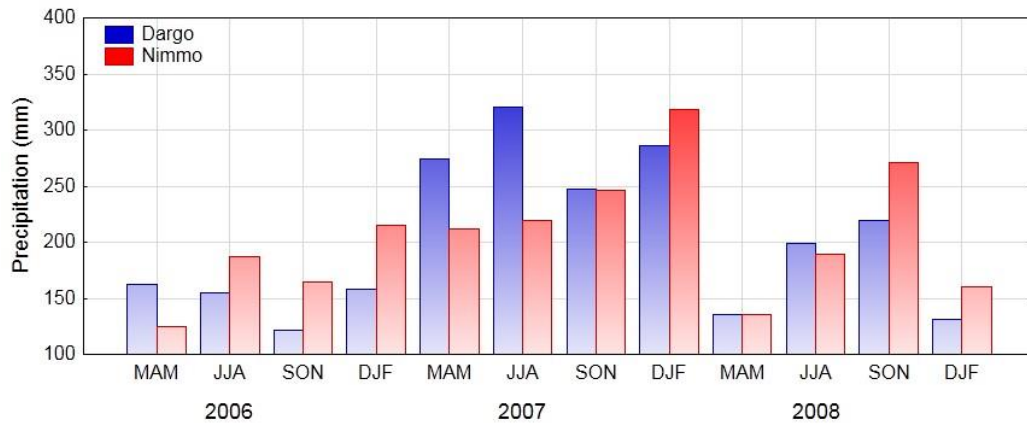


Figure 5.6: seasonal precipitation totals (estimates extended beyond study period – i.e. back to 2006 and forward through summer 2008-09 - using linear regression relationship between bi-weekly aggregate site and SILO data).

As also discussed in Chapter 3, at Dargo there was persistent winter snow cover in both years, while at the warmer Nimmo site, snow cover was generally brief. As is clear from site albedo observations in Figure 5.7, snow cover was continuous at Dargo for several months in each year: from 12<sup>th</sup> June to 16<sup>th</sup> August in 2007 (66 days continuous) and 30<sup>th</sup> June to 13<sup>th</sup> September in 2008 (76 days continuous). It is also clear from Figure 5.7 that winter snow cover at Nimmo generally persisted for no more than a few days: the longest periods of continuous snow cover (using an albedo threshold of 0.4 to indicate snow cover; Oke, 1987) were three days in each year, 18<sup>th</sup>-20<sup>th</sup> July in 2007 and 11<sup>th</sup>-13<sup>th</sup> July in 2008. It is unknown whether the patterns observed during the study period are historically representative, but anecdotal indications from the respective landowners suggest persistent winter snow cover at Dargo and a general absence at Nimmo.

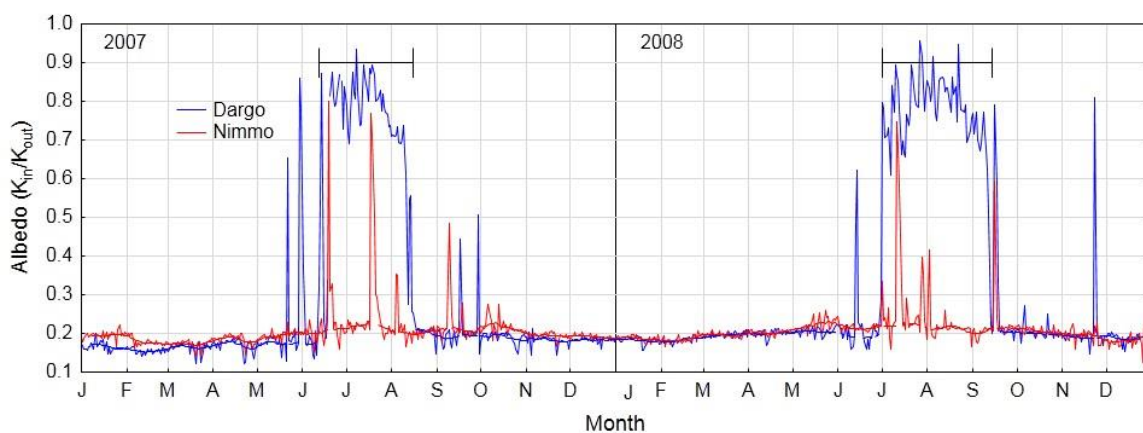


Figure 5.7: 2007/08 daily mean site albedo.

#### 5.4.2 Humidity

Vapour pressure was approximately equivalent at the sites (Figure 5.8a). This is not surprising given the close proximity of the sites such that they are generally subject to similar synoptic air mass properties. However, the lower daytime temperatures at Dargo resulted in lower daytime (i.e. average over all hours during which insolation was non-zero) vapour pressure deficit (VPD) than at Nimmo (0.48 and 0.62kPa, respectively) (Figure 5.8b). This difference remained consistent in all seasons throughout the measurement period. The effects of interannual differences in temperature on VPD are also apparent. As detailed in section 5.3, the beginning of 2007 was marked by high temperatures (relative to the same time in 2008), whereas the end of 2008 was marked by low temperatures (relative to the same time in 2007). Whereas vapour pressure was relatively consistent between years, the effect of these temperature variations was to cause high VPD in early 2007 and low VPD in late 2008.

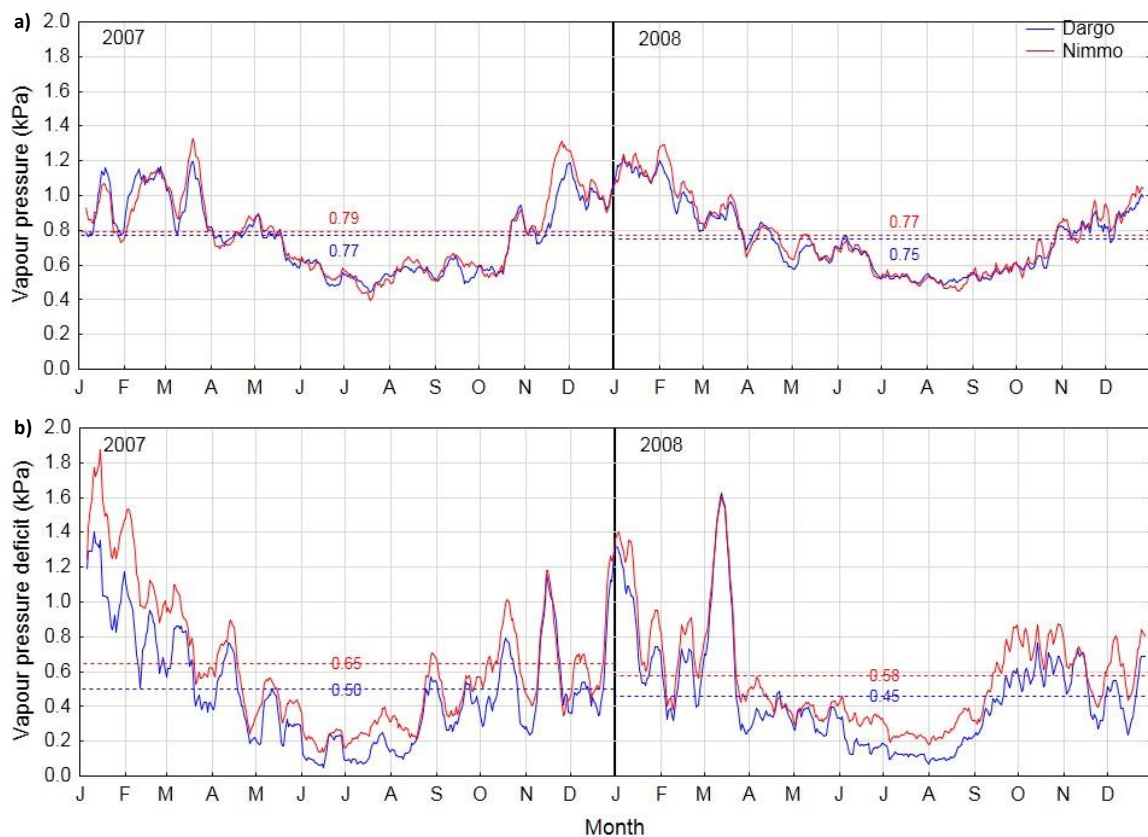


Figure 5.8: cross-site comparison of 2007/08 humidity : a) daily vapour pressure; b) daytime ( $K_{\downarrow} > 0 \text{ W m}^{-2}$ ) vapour pressure deficit (note: solid line represents ten-day moving average, horizontal dashed lines represent annual average).

### 5.4.3 Evapotranspiration

The lower vapour pressure deficit at Dargo in turn translated to lower evapotranspiration relative to Nimmo (Figure 5.9). Lower evapotranspiration may however also arise as a result of differences in radiant energy supply or in aerodynamic or stomatal resistance. However, in this study differences in radiant energy supply were small (see section 5.2), and aerodynamic and bulk surface resistances (which in the presence of closed canopies is controlled by stomatal resistance; Raupach, 1995) were generally comparable during most of the day (Figure 5.10a and b, respectively). Thus differences in temperature are most likely the primary driver of differences in evapotranspiration at the sites.

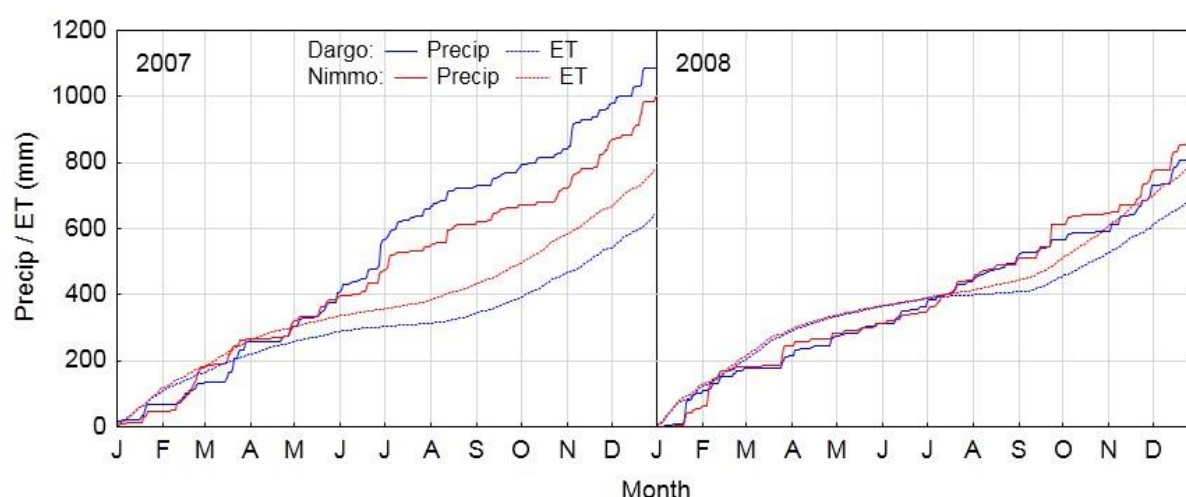


Figure 5.9: cumulative precipitation (P) and evapotranspiration (ET) for sites in 2007/08.

Figure 5.10: a) average bulk surface resistance ( $\pm 95\%$  confidence interval for mean) during daylight hours for all available data during study period, and; b) average aerodynamic resistance during daylight hours.

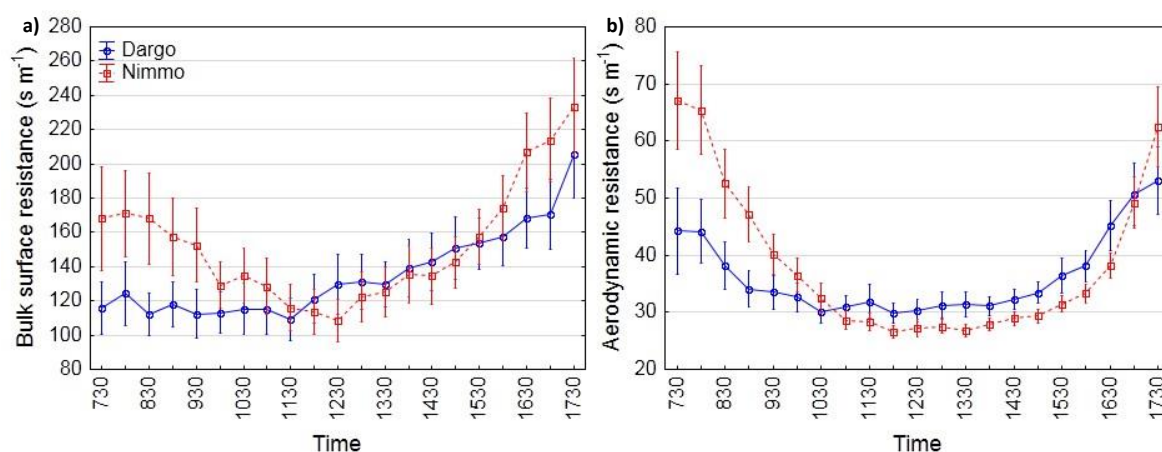


Figure 5.11: a) average bulk surface resistance during daylight hours for all available data during study period, and; b) average aerodynamic resistance during daylight hours (whiskers denote  $\pm 95\%$  confidence interval for mean).

#### 5.4.4 Soil moisture

While precipitation generally exceeded evapotranspiration in both years at the sites (albeit by a substantially larger amount in 2007), the amount of moisture stored in the upper layers of the soil was consistently higher at Dargo than Nimmo (Figure 5.12). On average, volumetric soil moisture during the study period (2007/08) was 40% and 25% at Dargo and Nimmo respectively, and was almost the same in both years.

In the first months of 2007, soils reached their driest point for the analysis period, dropping well below 20% and 10% at Dargo and Nimmo, respectively. This followed the extremely low rainfall year of 2006, as outlined in section 5.3.1. In the summer of 2007/08, while soil moisture rapidly declined throughout January as in the previous year, it was continually replenished by higher summer rainfall, and soil moisture generally remained much higher than during the previous year. At Nimmo, there was also a clear difference between years in autumn, with generally higher soil moisture in 2008. Thus while on average soil moisture was approximately similar between years, the timing of rainfall resulted in different seasonal dynamics, most notably in the first four months of the year. Such differences in timing can be critical in determining ecological and corresponding carbon cycle dynamics (Chou *et al.*, 2008).

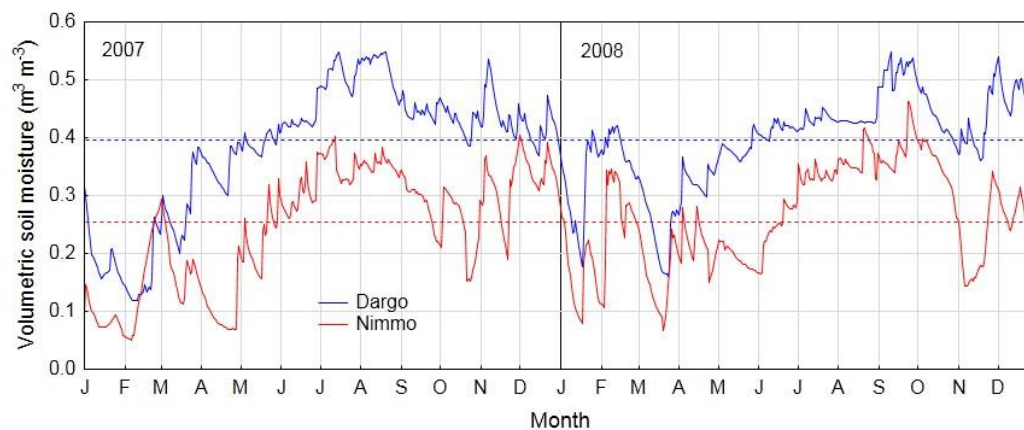


Figure 5.12: 2007/08 volumetric soil moisture (dashed lines represent averages).

Given that not all components of the water balance were measured at the sites, the reason for the consistent contrast in soil moisture between them cannot be reliably ascertained. Soil moisture depends on exchanges across the boundaries of a given volume via precipitation, evapotranspiration, percolation to deeper levels and surface runoff (Bonan, 2002). As noted above, at both sites precipitation exceeded evapotranspiration. This suggests that contrasts in soil moisture between sites were instead primarily regulated by the non-atmospheric components of the water balance – runoff and downward percolation through the soil profile, which depend on the characteristics of the surface (including the vegetation canopy) as well as those of the soil profile.

With respect to vegetation, the more pronounced tussock form of the grasses at Dargo may aid in reducing runoff. With respect to soils, topographic and geologic features of the landscape as well as the mineralogy of parent material affect soil characteristics such as depth, chemical composition, physical structure and drainage, all of which may affect soil moisture (Torn *et al.*, 2009). Differences in the thickness of soil strata and in the nature and drainage characteristics of the underlying parent rock may contribute to differences in drainage – and correspondingly the volumetric water content – of the soil profiles in this study. Alpine humus soils are generally less than 1m deep (Chapter 2, section 2.2.5), and in this study bedrock was occasionally encountered at 0.2-0.3m when digging soil pits at Dargo. In contrast to the plateau location of Dargo, the valley floor location of Nimmo suggests that it is likely to be a depositional environment, with potentially deeper soils. Such contrasts may lead to differences in drainage and therefore soil moisture retention in the upper soil profile.

At Dargo, the soil was also much richer in organic matter (see Chapter 6, section 6.2), which enhances soil moisture retention (Brady and Weil, 2002). However, high soil moisture is also a causal

factor in the retention of soil organic matter (Torn *et al.*, 2009). Thus it is possible that soil moisture may to some extent be progressively augmented during the development of the soil profile by a feedback process, in which low soil temperatures retard the decomposition of soil organic matter (Torn *et al.*, 2009), which promotes the retention of soil moisture, which in turn also slows the decomposition of soil organic matter. Moreover, if rainfall is on average higher at Dargo than Nimmo, this may also have aided in the development of substantially organic rich surface soils. However, clay content also influences soil moisture (Schimel *et al.*, 1994), and while at Nimmo the mineral component of the soil was volumetrically higher than at Dargo (see Chapter 6), the particle size distribution of the soil was not analysed. However, it is likely that soil texture differs substantially between sites, given their different topographic and geological settings.

While further analysis of this question is beyond the scope of this study, it is thus concluded here that the differences in soil moisture between sites most likely arise due to a combination of climatic differences (which have short and long-term effects) as well as geologic and topographic factors that influence the properties of the soil and underlying parent material.

## 5.5 Summary

In summary, the most ecologically relevant differences in meteorological conditions at the sites were temperature, soil moisture availability and winter snow cover. Warmer temperatures at Nimmo (and the consequent lack of sustained snow cover) were primarily associated with the difference in altitude between the sites. However, the topography at Nimmo also resulted in colder nocturnal conditions. As detailed previously, this is in fact the reason why grassland ecosystems are found at Nimmo: nocturnal cold air drainage prevents the establishment of tree seedlings on the valley floor. With respect to soil temperatures, the surface and soil properties at Nimmo also resulted in greater diurnal and seasonal soil temperature variation.

With respect to moisture availability, while the sites both received relatively similar precipitation during the study period, it is considered likely that Nimmo is generally subject to lower precipitation. Despite similar air mass characteristics across the sites, the higher temperatures at Nimmo resulted in higher atmospheric water vapour demand and thus higher evapotranspiration. On an annual basis, however, both sites received more precipitation than evapotranspiration, suggesting that the large and consistent difference observed in soil moisture may be partially related to differences in infiltration and subsurface transport of moisture.

There were also substantial differences between years, with warmer average temperatures in 2007, and a period of very low soil moisture at the sites during early 2007 (this was particularly pronounced at Nimmo, where soil moisture was on average substantially lower than at Dargo), despite the fact that soil moisture on average was similar in both years. It should also be noted that the minimum soil moisture observed at both sites in early 2007 followed on from severe drought conditions across the region in 2006. In contrast, soil moisture in early 2008 was substantially higher than in 2007 due to higher summer rainfall. The cooler temperatures in 2008 also resulted in a longer snow season (by 10 days), which also occurred later in the year (snowmelt date was approximately one month later in 2008).

The following chapters discuss differences in carbon storage and balance in the context of the climatic differences established here.



# 6. Ecosystem carbon storage

---

## 6.1 Introduction

As discussed in Chapter 1, the amount of carbon stored in ecosystems at present is relevant to ecosystem carbon cycle responses to future changes in climate for two main reasons. First, the amount of carbon stored in an ecosystem fundamentally constrains the amount of carbon that can be lost from the ecosystem. Second, spatial variations in carbon storage provide information about how carbon storage is related to spatial variability in climate, which in turn can be used as a possible analogue for the effects of temporal changes in climate. This chapter therefore addresses the aim of quantifying the carbon storage at the sites (objective 1 from Chapter 1, section 1.3). Carbon storage is quantified for soils and vegetation at both sites, and relevant differences between sites discussed.

## 6.2 Soils

As discussed in Chapter 2, alpine humus soils are generally low in nutrients, acidic and rich in organic matter (Costin *et al.*, 2000). The characteristics of the soils of the current study were broadly consistent with these observations (see Table 6.1) and comparable in absolute terms to values cited in the literature (Costin *et al.*, 1952; Spain *et al.*, 1983; Jenkins and Adams, 2010). It should be noted that while measures of total nitrogen (N) and phosphorus (P) are provided, they are not indicative of probable nutrient supply, since neither their form (i.e. organic/inorganic) nor rates of mineralisation were analysed. However, Jenkins and Adams (2010) report that grasslands are among the most nutrient poor of subalpine vegetation communities. Given the cold, moist and acidic conditions, it is probable that much of both the measured N and P is sequestered in undecomposed organic compounds, and that nutrients in more mobile forms are either absorbed or leached downward through the profile, resulting in low levels of plant available forms of these nutrients in the soil matrix (Körner, 2003).

**Table 6.1: average ( $\pm$ SE) soil physical and chemical properties (note: \* and \*\* denote statistically significant difference between sites at  $p<0.05$  and  $p<0.01$ , respectively).**

Sampling depth	0-0.1m			0.1-0.2m			0.2-0.3m			0-0.3m sum / <u>average</u>		
Site	Dargo		Nimmo	Dargo		Nimmo	Dargo		Nimmo	Dargo		Nimmo
Bulk density	520.7 $\pm$ 11.4	**	719 $\pm$ 36.1	587.7 $\pm$ 16.7	**	1038.6 $\pm$ 24.6	654.8 $\pm$ 13.0	**	1128.6 $\pm$ 20.3	<u>587.7<math>\pm</math>7.6</u>	**	<u>962.1<math>\pm</math>21.6</u>
Porosity (% volume) <sup>†</sup>	55	N/A	46	-		-	-		-	-		-
Organic carbon (kg m <sup>-2</sup> )	8.02 $\pm$ 0.17	**	4.93 $\pm$ 0.26	6.55 $\pm$ 0.35	**	4.69 $\pm$ 0.20	4.87 $\pm$ 0.20	**	3.79 $\pm$ 0.19	19.43 $\pm$ 0.61	**	13.40 $\pm$ 0.57
Total nitrogen (g m <sup>-2</sup> )	3.8 $\pm$ 0.1		3.8 $\pm$ 0.2	3.9 $\pm$ 0.1	*	3.4 $\pm$ 0.2	3.0 $\pm$ 0.1	*	2.6 $\pm$ 0.1	10.7 $\pm$ 0.2		9.8 $\pm$ 0.4
Total phosphorus (g m <sup>-2</sup> )	1.2 $\pm$ 0.1	**	0.7 $\pm$ 0.1	1.2 $\pm$ 0.1	**	0.8 $\pm$ 0.1	1.1 $\pm$ 0.1	**	0.8 $\pm$ 0.1	3.5 $\pm$ 0.2	**	2.3 $\pm$ 0.2
pH (in H <sub>2</sub> O)	5.02 $\pm$ 0.05		5.03 $\pm$ 0.03	-		-	-		-	-		-
Root phytomass (g m <sup>-2</sup> )	464.3 $\pm$ 62.5		352.4 $\pm$ 43.8	165.4 $\pm$ 21.5	**	76.6 $\pm$ 9.9	75.6 $\pm$ 18.7	*	32.6 $\pm$ 6.6	705.2 $\pm$ 77.9	*	461.7 $\pm$ 43.6
Soil organic matter (% dry mass)	34.6 $\pm$ 1.1	**	17.2 $\pm$ 0.8									

<sup>†</sup> Estimated by packing a 30L cylinder with the mass of soil required to be equivalent to field-measured bulk density, and then filling the cylinder to capacity with water. The volume displaced by the water provides an estimate of soil porosity. A single bulked sample was used for each site, hence the lack of statistics for this measure.

<sup>††</sup> Excludes roots and large (i.e. larger than sieve pore size [= 250 $\mu$ m]) particulate organic matter.

With respect to soil organic carbon (SOC), at all depths the amount at Dargo exceeded that at Nimmo, and in all cases with statistical significance at 99% level, although the absolute and relative contrast in soil carbon between sites nonetheless declined with depth (Table 6.1; Figure 6.1). The cumulative total for the 0-0.3m soil layer at Dargo was  $19.43\text{kgC m}^{-2}$ , 45% greater than at Nimmo ( $13.40\text{kgC m}^{-2}$ ). The values for both sites fall within the ranges detailed in Chapter 2 (section 2.3.2). SOC at Dargo is similar to the literature values reported for comparable montane tussock grasslands in New Zealand (Tate *et al.*, 2000,  $19.9\text{kgC m}^{-2}$ ) and Scotland (Grieve, 2000,  $20\text{kgC m}^{-2}$ ). It is also consistent with earlier SOC estimates of mean values for alpine ecosystems ( $21.6\text{kgC m}^{-2}$ ) provided by Schlesinger (1977), and those for wet tundra ( $22.2\text{kgC m}^{-2}$ ) reported by Post *et al.* (1982). The lower values reported for Nimmo are more consistent with the value of  $13\text{kgC m}^{-2}$  reported by Adams *et al.* (1990) for temperate and montane grasslands, and some individual site estimates for European (e.g. Djukic *et al.*, 2010,  $13\text{kgC m}^{-2}$  for an alpine meadow at 1700m) and Asian mountain grasslands (e.g. Wu *et al.*, 2003, 9.5 and  $16.6\text{kgC m}^{-2}$  for alpine and subalpine meadows, respectively) cited in Chapter 2 (section 2.3.2).

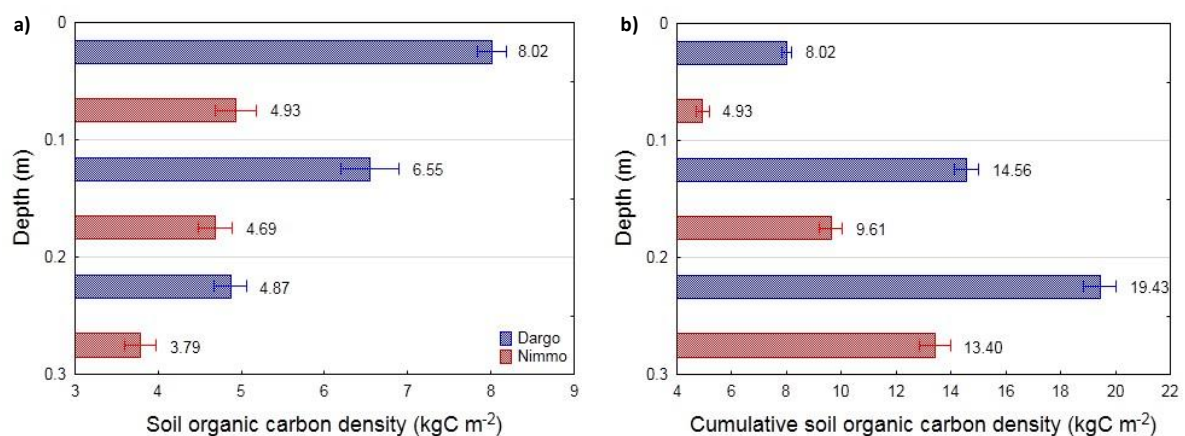


Figure 6.1: layer average (a) and cumulative (b) depth profiles of soil organic carbon density ( $\pm\text{SE}$ ;  $n = 10$ ).

However, while the estimates reported here are for the upper 0.3m of the soil profile only, at both sites they are higher than any of the literature values cited for the 0-0.3m layer in Chapter 2. This suggests that over the complete depth of the soil profile, both sites (Dargo in particular) are likely to be of very high SOC density relative to comparable sites in the literature. Some indication of potential total soil profile carbon can be gained by extrapolating SOC density as a function of depth in the soil profile. Jobbagy and Jackson (2000) report that on average, the upper 0.2m soil layer in

grasslands contain approximately 42% of the cumulative SOC to 1m. This yields estimates of 33.8 and 22.45kgC m<sup>-2</sup> for Dargo and Nimmo, respectively. On the other hand, Yang *et al.* (2010a) report that the 0-0.2m soil layer contains approximately 55% of the total in the upper 1m of a Tibetan alpine grassland soil profile. This yields lower estimates of 25.8 and 17.1kgC m<sup>-2</sup> for both sites, respectively.

Depth-dependent declines in SOC density can also be approximated by extrapolating fitted depth functions to the existing data (Figure 6.2; see Chapter 3, section 3.8.2 for details of depth functions). At Dargo, the estimated SOC density in the first 1m of soil (since alpine humus soil profiles are generally less than 1m deep) was 30.4±4.6kgC m<sup>-2</sup>, with storage in the upper 0.2m representing approximately 46% of the total. At Nimmo, the integrated 0-1m SOC density estimate was 21.5±3.2kgC m<sup>-2</sup>, with storage in the upper 0.2m representing approximately 31% of the profile. Total profile estimated carbon at Dargo remained approximately 40% greater than at Nimmo.

The extrapolated estimate for Nimmo is consistent with those for alpine and temperate grasslands and tundra, as discussed above in relation to Dargo. At Dargo, however, the extrapolated estimate was significantly higher, and is more comparable to the estimates of Post *et al.* (1982) for 'rain' tundra (36.6kgC m<sup>-2</sup>) than wet tundra. While such extrapolation is subject to a large degree of uncertainty<sup>27</sup> (and is intended as indicative of potential quantities rather than as rigorous prediction), it is virtually certain that some quantity of additional carbon is stored below 0.3m in these soils, and thus the true value is likely to lie between the measured and extrapolated estimates. Again, this suggests that the subalpine grasslands are large stores of soil carbon in comparison to similar ecosystems worldwide.

---

<sup>27</sup> The wide uncertainty bounds of the extrapolated curves reflect the large parameter uncertainties for soil bulk density and proportional carbon mass, resulting from both sampling variability and the limited number of depths sampled. Additional uncertainty arises from the fact that the true depth of the profiles is unknown and the implicit assumption that relationships observed between 0-0.3m also hold at greater depth.

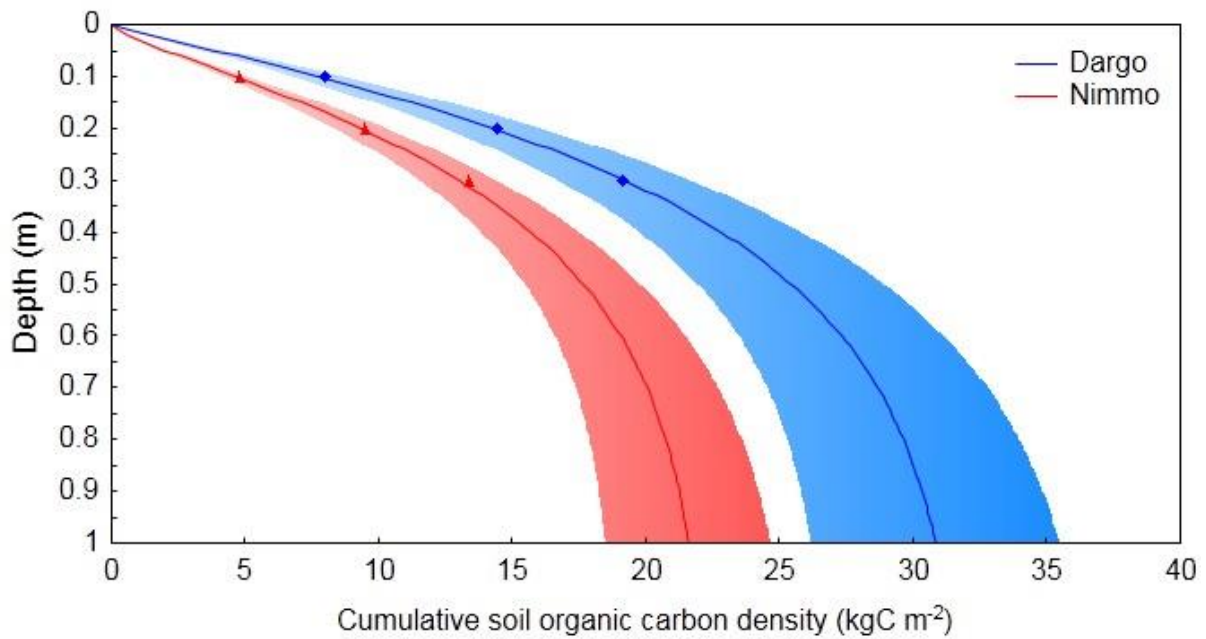


Figure 6.2: extrapolated cumulative soil organic carbon (SOC) density curve for Dargo and Nimmo sites (symbols represent observed cumulative SOC density; solid lines represent estimate using maximum likelihood parameters; bands represent  $\pm 2\sigma$  parameter estimate uncertainties from Monte-Carlo simulation).

With respect to the difference in carbon storage between sites, the patterns reported here are broadly consistent with the widely noted relationships between soil carbon and climate (as discussed in Chapter 2). Low temperatures and high soil moisture (which correspondingly reduces oxygen availability within the soil matrix) constrains decomposer activity (Jobbágy and Jackson, 2000; Bird *et al.*, 2001), such that soil carbon is inversely correlated with temperature and directly correlated with precipitation (Post *et al.*, 1982). Accordingly, the cooler and wetter of the sites in this study (Dargo) stored significantly more carbon in its soils than the warmer and drier site (Nimmo). Moreover, the vertical distributions of carbon through the soil profile also suggest that the differences between sites are shaped by the difference in soil climate conditions. Steeper depth-dependent declines are typical of sites in which decomposition is more restricted by climatic conditions, since climate has more effect on SOC near the surface than on older, recalcitrant or stabilised carbon at depth (Jobbágy and Jackson, 2000). Correspondingly, at Dargo a more pronounced decline in carbon content occurred with depth than at Nimmo: the difference in C density relative to Nimmo declined from approximately 62 to 40 to 28% (for the 0-0.1, 0.1-0.2 and 0.2-0.3m layers, respectively). Patterns of soil organic carbon storage are thus qualitatively consistent with the common climate-soil carbon relationships described above and in Chapter 2. Namely, the site with warmer and drier conditions has lower soil carbon than the cooler, wetter site.

### 6.3 Vegetation

Storage of carbon in above- and belowground vegetation was both much lower and more uncertain than storage of carbon in soils. At Dargo, total above-and belowground phytomass carbon density during the peak of the growing season (January 2008) was  $704.0 \pm 61.3 \text{ gC m}^{-2}$  (Table 6.2), over twice the amount at Nimmo ( $346.9 \pm 20.7 \text{ gC m}^{-2}$ ). More carbon was found in both above- and belowground pools at Dargo than at Nimmo, with the difference particularly pronounced aboveground (primarily due to the very large quantity of necromass at Dargo – as represented in Figure 6.3).

Comparison of vegetation carbon storage quantities with similar ecosystems globally is complicated by the fact that the range of variation is large (see Chapter 2, section 2.3.1). In general, most available estimates are at the higher end of those reported here. For example, Adams *et al.* (1990) estimate vegetation carbon storage in temperate and montane grasslands at  $1 \text{ kgC m}^{-2}$ , and in tundra ecosystems  $700 \text{ gC m}^{-2}$ . Likewise, Tappeiner (2008) report  $870 - 1120 \text{ kgC m}^{-2}$  for alpine meadows. These values are consistent with (though generally slightly larger than) those reported for Dargo. However, other estimates encompass those of this study; Fang *et al.* (2010) report values ranging from  $220 - 1290 \text{ kgC m}^{-2}$  for alpine and temperate grasslands, while Ma *et al.* (2010a) report values of  $300$  and  $600 \text{ kgC m}^{-2}$  for alpine and mountain meadows, respectively.

Table 6.2: average ( $\pm$ SE) above- and belowground phytomass (separated into biomass and necromass components for aboveground vegetation only) carbon (note: \* and \*\* denote statistically significant difference between sites at  $p<0.05$  and  $p<0.01$ , respectively).

	Dargo		Nimmo
Aboveground: 09/01/08			
Total phytomass ( $\text{gC m}^{-2}$ ):	386.7 $\pm$ 53.8	**	139.1 $\pm$ 7.1
○ Biomass	108.6 $\pm$ 15.1		107.4 $\pm$ 5.5
○ Necromass	278.1 $\pm$ 38.7	**	31.7 $\pm$ 1.6
Aboveground: 01/06/08			
Total phytomass ( $\text{gC m}^{-2}$ ):	114.1 $\pm$ 23.6	*	45.3 $\pm$ 6.5
○ Biomass	53.8 $\pm$ 11.1	*	28.3 $\pm$ 4.1
○ Necromass	60.3 $\pm$ 12.5	**	17.0 $\pm$ 2.5
Belowground: 09/03/07			
Total phytomass ( $\text{gC m}^{-2}$ ):	317.3 $\pm$ 35.1	*	207.7 $\pm$ 19.6
○ 0-0.1m	208.9 $\pm$ 28.1		158.6 $\pm$ 19.7
○ 0.1-0.2m	74.4 $\pm$ 9.7	**	34.5 $\pm$ 4.5
○ 0.2-0.3m	34.0 $\pm$ 8.4	*	14.7 $\pm$ 3.0
Above-/belowground phytomass ( $\text{gC m}^{-2}$ ):	704.0 $\pm$ 61.3	**	346.9 $\pm$ 20.7

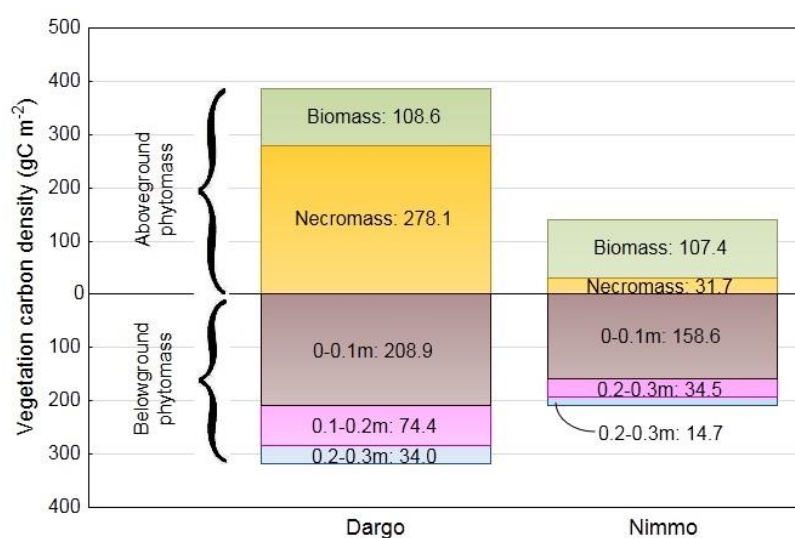


Figure 6.3: allocation of carbon to above- and belowground phytomass carbon pools.

Few reports of vegetation carbon storage in Australian subalpine grasslands were found. However, Warren and Taranto (2011) report peak (summer) aboveground plant dry mass estimates of  $605\text{g m}^{-2}$  in Australian subalpine grasslands. Assuming a ratio of carbon to plant dry mass of 0.45 (Chapin *et al.*, 2002), this yields approximately  $272\text{gC m}^{-2}$ , intermediate between the total phytomass quantities found for the sites in this study. Bear and Pickering (2006) also report



aboveground plant dry mass of approximately  $1000\text{gC m}^{-2}$ , yielding slightly higher estimates of vegetation carbon density of approximately  $450\text{gC m}^{-2}$ . Assuming a typical ratio of necromass:biomass of 2.86:1 (similar to the ratio of 2.56:1 at Dargo in this study) (Hofstede *et al.*, 1995; Ni, 2004), this yields estimates of necromass and biomass carbon content of approximately  $370$  and  $130\text{gC m}^{-2}$ , respectively. With respect to biomass, given the relatively large uncertainty (as evidenced by the large standard errors reported in Table 6.2) in the estimates in this study (a function of the large degree of spatial variability in phytomass quantity), the above estimates are broadly consistent with those reported for the sites here.

With respect to aboveground phytomass, while the amount of aboveground biomass carbon at the sites was almost identical ( $108.6$  versus  $107.4\text{gC m}^{-2}$  for Dargo and Nimmo, respectively), the large difference in aboveground phytomass carbon density was due to the much greater proportion of aboveground necromass at Dargo ( $278.1\text{gC m}^{-2}$ , almost an order of magnitude larger than Nimmo's  $31.7\text{gC m}^{-2}$ ). At Dargo, this necromass contributed almost three times more carbon to the total aboveground vegetation pool than biomass, whereas the ratio was effectively reversed at Nimmo. As discussed in Chapter 2, the retention of necromass is thought to be an adaptation to low temperatures that provides some insulation to the vulnerable growing parts of the plant (Körner, 2003). Interestingly, however, as discussed in Chapter 5, the lowest recorded temperatures occurred at Nimmo, where nocturnal temperatures could be up to  $15^{\circ}\text{C}$  lower than at Dargo. This suggests that the retention of standing dead material may be an adaptation to average ambient air temperatures rather than to periodic low temperature extremes.

With respect to belowground phytomass, no separation of live from dead root matter was undertaken. Rather, the entire root content was quantified for the 0-0.1, 0.1-0.2 and 0.2-0.3m layers. At  $317.3\pm 35.1\text{gC m}^{-2}$ , belowground phytomass carbon density was slightly over 50% larger at Dargo than Nimmo ( $207.7\pm 19.6\text{gC m}^{-2}$ ). The largest relative differences between sites were observed below 0.1m. In fact, in the 0-0.1m layer, while root phytomass carbon was larger at Dargo, the difference was not statistically significant (at  $p < 0.05$ ). In the deeper layers, differences were much larger (root phytomass was more than twofold larger at Dargo) and statistically significant in both layers. At Nimmo bulk density increased rapidly below 0.1m (Table 6.1); thus the steeper decline in root mass may be associated with the fact that root penetration into this denser layer is more difficult than in the more organic-rich soil at Dargo.

The observed pattern of difference in vegetation carbon storage between sites contrasts with general expectations on the basis of climate alone i.e. all else being equal, a warmer, snow-free site might be expected to support larger quantities of plant matter (Jonas *et al.*, 2008; and see

discussion in Chapter 2), and thus carbon. Instead, the warmer of the sites in this study supported lower amounts of phytomass and thus a smaller vegetation carbon pool. However, as discussed above, essentially all of the difference at least in aboveground phytomass can be ascribed to the difference in necromass. Moreover, as established in Chapter 5, conditions at Nimmo were not only warmer but also drier (in terms of plant available water, despite comparable precipitation) than at Dargo. Such conditions may cause growth constraints or favour growth forms of relatively limited biomass (it is not only cold but dry conditions that may promote prostrate growth forms, since the consequent aerodynamic decoupling reduces the influence of ambient conditions, be they low temperatures or high vapour pressure deficits, at the surface).

#### 6.4 Total ecosystem carbon storage

At Dargo, ecosystem carbon storage ( $20.13 \pm 0.59 \text{ kgC m}^{-2}$ ; Table 6.3) was approximately 46% greater than at Nimmo ( $13.75 \pm 0.57 \text{ kgC m}^{-2}$ ), subject to the uncertainties previously discussed (Figure 6.4). Estimated total ecosystem carbon storage at Dargo was similar to that reported for tundra ( $22.7 \text{ kgC m}^{-2}$ ) by Adams *et al.* (1990), whereas at Nimmo it was comparable to that reported for temperate / montane grasslands ( $14 \text{ kgC m}^{-2}$ ). It is clear from the previous discussion – and Figure 6.4 – that by far the greatest contribution to ecosystem carbon storage was soil organic carbon. At both sites, phytomass carbon represented approximately 3% of total ecosystem carbon storage. These estimates are not unusual: Körner (2003) reports that >92% of the total ecosystem carbon pool in alpine ecosystems is contained in soil organic matter.

**Table 6.3: average ecosystem carbon storage ( $\pm \text{SE}$ ) in soil and phytomass for Dargo and Nimmo (\*\* denotes statistically significant difference between sites at  $p < 0.01$ ).**

	Dargo		Nimmo
Soil ( $\text{kgC m}^{-2}$ )	$19.43 \pm 0.61$	**	$13.40 \pm 0.57$
Vegetation ( $\text{kgC m}^{-2}$ )	$0.704 \pm 0.0613$	**	$0.3469 \pm 0.0207$
Total ( $\text{kgC m}^{-2}$ )	$20.13 \pm 0.59$	**	$13.75 \pm 0.57$

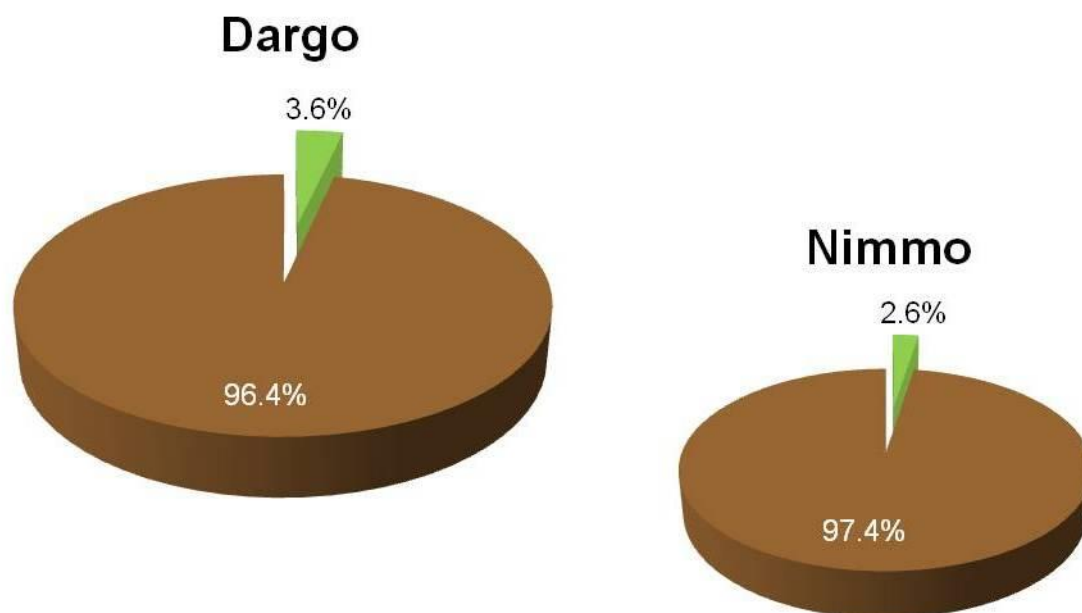


Figure 6.4: relative magnitudes of ecosystem (soil + phytomass) carbon storage for Dargo and Nimmo.

Even without accounting for the likely underestimation of soil organic carbon, total ecosystem carbon storage at Dargo is comparable to some forest and woodland ecosystem types (Adams *et al.*, 1990). If extrapolated estimates of additional soil carbon are included, it is comparable to values reported for temperate broadleaved forest (e.g. 29 and 33kgC m<sup>-2</sup> for deciduous and evergreen, respectively). At Nimmo, the values reported here are similar to carbon storage in woodland ecosystems (e.g. tropical and Mediterranean woodlands); similarly, extrapolated estimates of additional soil carbon at Nimmo shift it towards the existing estimate for Dargo (i.e. similar to tundra).

## 6.5 Summary

Australian subalpine grasslands represent substantial stores of organic carbon at present. Almost all of this carbon is stored in their soils, thought to be primarily associated with cool, relatively moist soil conditions that constrain decomposition of organic matter. The observed differences in soil carbon between sites in this study are broadly consistent with this explanation,

with the warmer, drier site at Nimmo storing less carbon than Dargo (although effects of other local factors cannot be comprehensively ruled out). On the other hand, it is generally observed that at warmer temperatures (in the absence of water limitation), the amount of carbon stored in vegetation increases. This was not observed in this study, with Nimmo storing less carbon in vegetation than Dargo. This is related to the nocturnal thermal conditions at the sites – as established in Chapter 5 (section 5.3.1), nocturnal temperatures are frequently more than 10°C cooler at Nimmo, due to drainage of cold air from the surrounding hillslopes. This temperature regime is thought to preclude the establishment of trees, despite warmer daytime temperatures (the difference in daytime temperatures is largely related to adiabatic effects of altitude).

With respect to climate change, it can reasonably be expected that on average, a likely outcome of expected warming and drying of the climate of the Australian High Country (see Chapter 1, 1.2.4) will be a net reduction in soil carbon storage in these ecosystems. This is likely to be particularly pronounced in the case of Dargo, where the cooler, wetter conditions result in higher carbon storage at present. There is a positive association between total quantity of soil carbon and quantity of labile carbon for Australian alpine and subalpine ecosystems (Jenkins and Adams, 2010), suggesting that the carbon stored in the soil at Dargo may be (initially) more readily respired to the atmosphere.

Any potential changes in vegetation carbon storage will depend crucially on the specific nature of climatic change. Warmer conditions may be expected to enhance vegetation carbon storage by enhancing growth and offsetting the low temperature penalty incurred by taller growth habit, but will be limited by the genotypic and phenotypic adaptive capacities of the extant species or by the rate of colonisation of potentially more productive species. Since the treeline tree species (*E. pauciflora*) has relatively poor seed dispersal, mass colonisation of the alpine and subalpine tract by trees is unlikely to occur quickly, and while additional warming may to some extent increase the biomass of extant grasses (Rammig *et al.*, 2010), there are clear structural limitations to the additional increment possible. Moreover, expected future increases in drought recurrence may also to an increasing extent limit additional growth and related biomass increment. The combination of remaining long-term ecological constraints on increases in vegetation carbon storage with the potential easing of climatic constraints on soil organic matter decomposition in the High Country imply that net losses of carbon from these ecosystems are more likely than gains in the near future.

The long term dynamics of ecosystem carbon storage are fundamentally dependent on the balance between ecosystem processes of carbon import and export. As discussed in Chapter 2 and alluded to above, these processes are highly sensitive to climatic factors. In the next section, the

investigation focuses on analysis of annual carbon balances in 2007/08, and the factors that explain variability between sites.

# 7. Ecosystem Carbon Exchange

---

## 7.1 Introduction

As discussed previously, carbon storage at an ecosystem depends on the long-term processes of carbon import and export, which are in turn dependent on climate. Long-term changes in climate are expected to drive changes in the carbon balance. While only two years of data are available for this study, it provides a preliminary assessment of these carbon cycle / climate linkages in Australian subalpine grasslands. In this Chapter, annual and seasonal net carbon exchange are quantified (objective 2 from Chapter 1, section 1.30), as are corresponding photosynthetic and respiratory fluxes (objective 3), which are linked to environmental (primary climatic) factors (objective 4). Relevant cross-site differences are explored.

## 7.2 Annual carbon balance

### 7.2.1 NEE

In both years, both sites were carbon sinks (Table 7.1). At Dargo, the magnitude of the sink was  $-93.0\text{gC m}^{-2}$  and  $-111.4\text{gC m}^{-2}$  in 2007 and 2008, respectively. At Nimmo, the magnitude of the sink was approximately two- and threefold larger than at Dargo for 2007 ( $-203.8\text{gC m}^{-2}$ ) and 2008 ( $-322.0\text{gC m}^{-2}$ ) respectively. For both sites, NEE was within the range reported in the available literature for mountain grasslands (approximately  $+250$  to  $-290\text{gC m}^{-2} \text{a}^{-1}$  - see Chapter 2, section 2.4.4). However, carbon uptake at Nimmo in 2007 was towards the high end of annual uptake estimates, and in 2008 it was among the highest values reported. Annual NEE for Dargo was also consistent with the global relationship between NEE and mean annual temperature for ecosystems classified as primarily temperature-limited (see Yi *et al.*, 2010) in the Fluxnet global database (Figure 7.1). This was also true for Nimmo in 2007, though in 2008 uptake at this site was substantially higher than expected for a site with its mean annual temperature ( $7.2^{\circ}\text{C}$ ).

**Table 7.1: annual sums ( $\text{gC m}^{-2}$ ) of ecosystem respiration ( $R_e$ ), gross primary production (GPP) and net ecosystem exchange (NEE)  $\pm 95\%$  confidence intervals (\* and \*\* denote statistically significant difference between sites at  $p < 0.05$  and  $p < 0.01$ , respectively). Note that confidence intervals for partitioned fluxes represent partitioning uncertainty (since GPP is calculated as the residual of  $\text{NEE} - R_e$ , the uncertainty for  $R_e$  necessarily propagates to GPP, such that the values are the same for both quantities), whereas those for NEE represent the combined uncertainties contributed by random and model error.**

	2007		2008	
	Dargo	Nimmo	Dargo	Nimmo
$R_e$	$1039.5 \pm 29.6$	$1022.4 \pm 31.0$	$1144.3 \pm 27.5$	$1185.0 \pm 32.6$
GPP	$-1132.5 \pm 29.6$	$-1226.2 \pm 31.0$	$-1255.7 \pm 27.5$	$-1507.0 \pm 32.6$
NEE	$-93.0 \pm 14.9$	$-203.8 \pm 22.4$	$-111.4 \pm 13.5$	$-322.0 \pm 25.1$

In the context of NEE of eddy covariance sites globally, annual carbon uptake at Dargo in both years was lower than the global Fluxnet database average of approximately  $-181\text{gC m}^{-2} \text{a}^{-1}$  reported by Baldocchi (2008). This is expected, given that while the terrestrial biosphere is currently a net carbon sink overall, the sink strength is related to the primary productivity of ecosystems. Specifically, as discussed in Chapter 2, available flux measurements across different biomes confirm

that assimilation on average currently exceeds respiration (by a ratio of 1.2:1 according to Law *et al.*, 2002, and; 1.3:1 according to more recent and comprehensive estimates by Baldocchi, 2008). Since the length of the growing season is in turn a strong predictor of primary production (Körner, 2003; Baldocchi, 2008), warmer sites are on average expected to be stronger carbon sinks than cooler sites (such as mountain grasslands). In the context of sites in which primary production is limited by low temperatures, this is confirmed by the general relationship depicted in Figure 7.1. The between-sites results of this study are consistent with this: the warmer Nimmo site absorbed more carbon in both years than the cooler Dargo site.

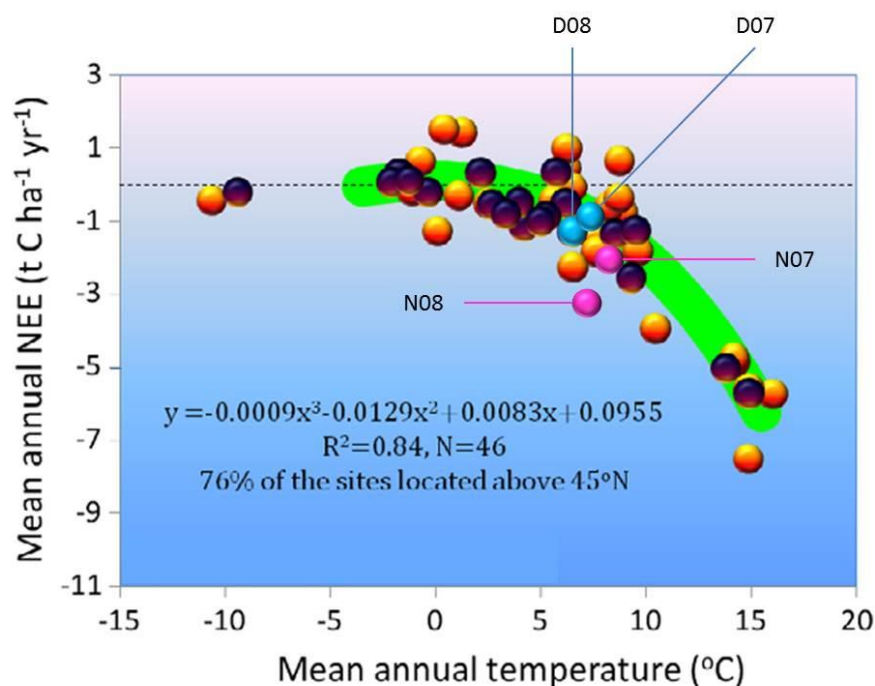


Figure 7.1: comparison of annual NEE (this study) with primarily temperature-limited ecosystems in the Fluxnet global database (D07 = Dargo 2007, D08 = Dargo 2008, N07 = Nimmo 2007, N08 = Nimmo 2008; figure modified from Yi *et al.*, 2010, p7).

But while NEE at Nimmo was comparable to the global Fluxnet NEE average in 2007, in 2008 carbon uptake was almost twofold higher. Thus the difference between years at Nimmo was the opposite of expectation on the basis of temperature alone: carbon uptake was higher in the cooler year (2008) than in the warmer year (2007) (although this was also qualitatively true of Dargo, the difference between years was small at that site). But while temperature is the primary limitation on length of growing season in these ecosystems, the High Country is, as discussed in Chapter 2



(section 2.4.5), also subject to (primarily) ENSO<sup>28</sup>-driven climatic variability and associated periodic drought occurrence. Drought has substantial effects on the carbon balance (van der Molen *et al.*, 2011), and as previously noted, extreme drought conditions prevailed in much of south-eastern Australia during 2006 and the lowest soil moisture at the sites was recorded in early 2007 (Chapter 5, section 5.4). Such influences are likely to be superimposed on underlying temperature relationships in time, particularly given that the quasi-decadal ENSO cycle is generally longer than the time horizons of the current project. Possible effects of drought are examined further in section 7.3.

## 7.2.2 Ecosystem respiration ( $R_e$ ) and gross primary production (GPP)

Examination of  $R_e$  and GPP indicates that annual differences in NEE between the sites – as well as the increase in cross-site NEE difference from 2007 to 2008 – was primarily due to GPP rather than  $R_e$  (Table 7.1). Annual  $R_e$  was broadly comparable, and increased from 2007 to 2008 at both sites. At Dargo, annual  $R_e$  increased 10.1% from  $1039.5\text{gC m}^{-2}\text{ a}^{-1}$  in 2007 to  $1144.2\text{gC m}^{-2}\text{ a}^{-1}$  in 2008.  $R_e$  at Nimmo in 2007 was  $1022.5\text{gC m}^{-2}\text{ a}^{-1}$ , slightly less (1.6%) than at Dargo, and increased 15.9% to  $1185.0\text{gC m}^{-2}\text{ a}^{-1}$  in 2008, slightly greater (3.6%) than Dargo. However, differences were not statistically significant in either year. The values reported here are similar to chamber-based estimates obtained by Warren and Taranto (2011) in a subalpine grassland in the same region as Nimmo. The authors report  $R_e$  of  $1210\text{gC m}^{-2}\text{ a}^{-1}$  in 2007/08 (May to May), respectively.  $R_e$  at Nimmo for the equivalent annual period in this study was  $1153.8\text{gC m}^{-2}\text{ a}^{-1}$ .

In the context of comparable ecosystems internationally,  $R_e$  in this study was in the mid-range (see Chapter 2). For grasslands of the Tibetan Plateau subject to lower average temperatures (and in many cases very dry conditions), annual  $R_e$  values between  $200\text{--}600\text{gC m}^{-2}\text{ a}^{-1}$  are typically reported (Kato *et al.*, 2006; Fu *et al.*, 2009). Warmer, more productive ecosystems are generally subject to higher  $R_e$ , and as such it is not surprising that the relatively mild subalpine conditions of the Australian High Country should be subject to higher  $R_e$ . Much higher values are nonetheless reported for some European mountain grasslands (Bahn *et al.*, 2008:  $1743$  and  $1792\text{gC m}^{-2}\text{ a}^{-1}$ ; Rogiers *et al.*, 2008:  $1300\text{--}1600\text{gC m}^{-2}\text{ a}^{-1}$ ). However, these sites were pastures managed to

---

<sup>28</sup> El-Niño southern oscillation – a dynamically coupled ocean / atmosphere phenomenon that affects regional and global climate variability. During el Nino phase, the equatorial trade winds weaken or reverse, resulting in warmer waters in the central and eastern Pacific; for south-eastern Australia, el Niño events generally bring warmer and drier conditions to the region. During la Niña phase, the trade winds strengthen, bringing warmer water to the western Pacific and cold upwelling to the equatorial ocean east of the Americas; for south-eastern Australia, la Niña events generally bring cooler and drier conditions to the region (Sturman and Tapper, 2005).

maximise productivity (e.g. via fertiliser input), and since  $R_e$  is strongly linked to primary production (Janssens *et al.*, 2001; Bahn *et al.*, 2008), higher  $R_e$  may be expected. In comparison to European sites with similar mean annual temperatures,  $R_e$  in this study was comparable, or slightly higher than the expected value on the basis of relationships between  $R_e$  and mean annual temperature reported internationally (Figure 7.2) (Bahn *et al.*, 2008).

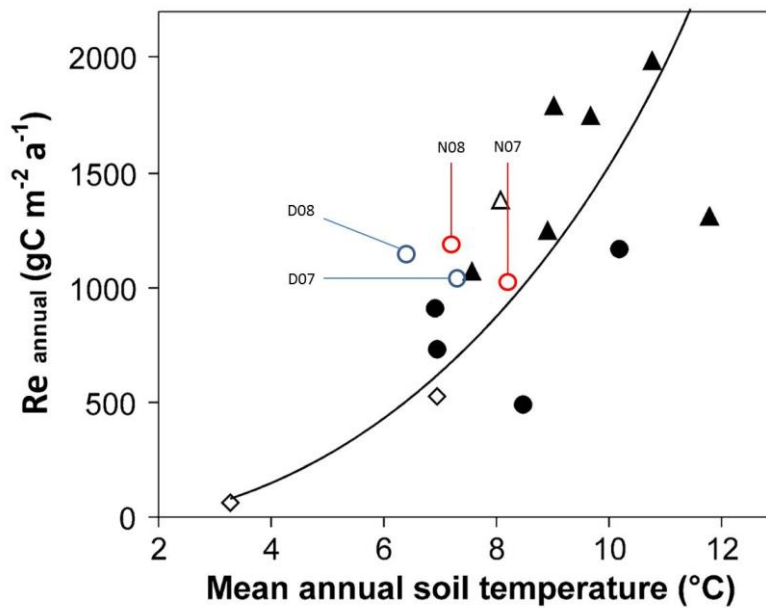


Figure 7.2: relationship between annual ecosystem respiration and mean annual temperature for European grasslands (where triangles = meadows, solid circles = pastures and diamonds = unmanaged northern grasslands) with results from current study superimposed (adapted from Bahn *et al.*, 2008, p1361).

As was the case with  $R_e$ , GPP increased from 2007 to 2008 at both sites. However, in both years, GPP was higher at Nimmo than Dargo, with the difference increasing from 2007 to 2008. At Dargo, there was an increase of 10.9% between years, from  $1132.5 \text{ gC m}^{-2} \text{ a}^{-1}$  in 2007 to  $1255.7 \text{ gC m}^{-2} \text{ a}^{-1}$  in 2008 (similar to that for  $R_e$ , thus largely neutralising cross-year NEE differences). At Nimmo, annual GPP was  $1226.2 \text{ gC m}^{-2} \text{ a}^{-1}$  in 2007, rising 22.9% to  $1507.0 \text{ gC m}^{-2} \text{ a}^{-1}$  in 2008. GPP was also significantly different (at  $p < 0.05$ ) between sites in both years. There are no local estimates available for comparison to these results, which are the first estimates of annual GPP for Australian subalpine grasslands.

Relative to literature estimates of GPP, a similar finding is evident to that reported for  $R_e$  above. GPP in this study was within the range of values reported in the literature, but towards the higher end. Again, the lowest values are typically reported for the Tibetan Plateau (200-700gC m<sup>-2</sup> a<sup>-1</sup>; Kato *et al.*, 2006; Fu *et al.*, 2009). It is also the case that the highest values are reported for the intensively managed grassland discussed above (Bahn *et al.*, 2008: 1358 and 1697gC m<sup>-2</sup> a<sup>-1</sup>; Rogiers *et al.*, 2008: 1321-1614gC m<sup>-2</sup> a<sup>-1</sup>), similar to the values reported at Nimmo in 2008.

Thus in both years, the difference between sites in annual NEE was primarily associated with differences in GPP rather than  $R_e$ . In 2007, the difference in annual NEE between sites (110.7gC m<sup>-2</sup> less carbon uptake at Dargo) resulted jointly from lower  $R_e$  (17.0gC m<sup>-2</sup>, 15%) and higher GPP (93.7gC m<sup>-2</sup>, 85%) at Nimmo. In contrast, in 2008, given that  $R_e$  was actually higher at Nimmo than Dargo (by 40.8gC m<sup>-2</sup>), the higher carbon uptake at Nimmo (by 210.6gC m<sup>-2</sup> a<sup>-1</sup> relative to Dargo) was entirely attributable to the difference in GPP (251.3gC m<sup>-2</sup>). As previously noted, a recent study estimated GPP: $R_e$  across Fluxnet sites internationally at approximately 1.3 (Baldocchi, 2008); as illustrated in Figure 7.3, the estimates for the sites in this study fall close to those for undisturbed ecosystems. GPP: $R_e$  estimates for 2007 and 2008 for Dargo were very similar, at 1.09 and 1.10, reflecting the fact that GPP and  $R_e$  changed by similar amounts between years. At Nimmo, however, GPP: $R_e$  was higher than at Dargo, and increased from 2007 (1.20) to 2008 (1.27), due to a large increase in GPP in 2008.

As was noted for NEE, the fact that GPP and  $R_e$  were higher at Nimmo than Dargo is qualitatively consistent with the effects of warmer conditions on the growing season and thus the magnitude of fluxes. All else being equal, higher GPP may be expected at Nimmo due to the direct (biochemical) and indirect (absence of winter snow) effects of higher temperatures on photosynthesis. Similarly, higher  $R_e$  may also be expected to result from the direct (stimulation of autotrophic and heterotrophic respiration) and indirect (increased production of photosynthetic assimilates) effects of higher temperature.

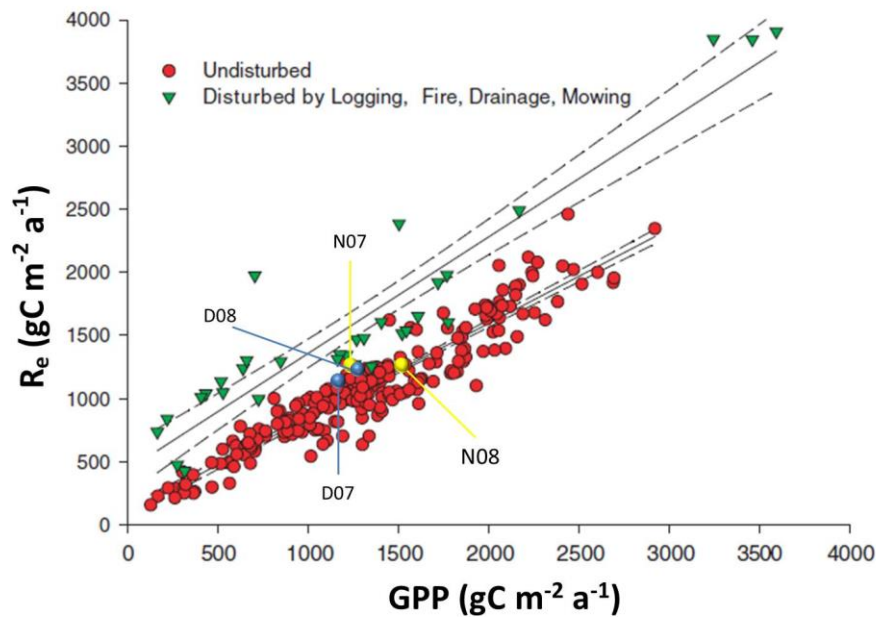


Figure 7.3: relationship between GPP and  $R_e$  for international Fluxnet sites (Baldocchi, 2008, p9)

However, also as noted in the case of NEE, in the absence of other factors, the increases in GPP and  $R_e$  from 2007 to 2008 are contrary to expectations in an ecosystems in which the length of the growth period is regulated primarily by (low) temperature, given the fact that 2008 was colder than 2007. Lower temperatures would be expected to reduce the length of the growing season (and thus plant growth and therefore GPP and the autotrophic component of  $R_e$ ) as well as reducing  $R_e$  (both due to the direct metabolic effects of temperature as well as indirect effects on heterotrophic respiration of reduced growth e.g. reduced supply of organic material in the form of assimilates and dead organic matter addition to the soil). As noted for NEE, this apparent discrepancy may be linked with the effects of other abiotic controls on the carbon balance – specifically, the preceding drought conditions that continued into early 2007 across the Australian High Country.

However, if drought conditions are implicated in between year NEE variations at the sites, it is clear that with respect to NEE, Nimmo was more clearly affected than Dargo. The substantial increase in net carbon uptake at Nimmo from 2007 to 2008 occurred due to both increased GPP in 2008, and to increased GPP: $R_e$ . At Dargo, the fact that increases in GPP and  $R_e$  were of similar magnitude – thereby resulting in minimal change in annual NEE and preservation of GPP: $R_e$  – suggests either that the site was unaffected by drought or that compensatory processes were involved. Examination of NEE dynamics at finer temporal scale provides further insight into these questions and is undertaken below.

## 7.3 Seasonal carbon balance dynamics

### 7.3.1 Summer (JFM<sup>29</sup>)

Cross-site NEE differences were generally small ( $<20\text{gC m}^{-2}$ ) during summer (JFM), but cross-year NEE differences were large at both sites (Table 7.2; Figure 7.4). Whereas in 2007 Dargo was a weak carbon sink ( $-16\text{gC m}^{-2}$ ) and Nimmo a weak source ( $4.7\text{gC m}^{-2}$ ; NEE was not statistically significantly different to zero at either site) in JFM, in 2008, both sites were carbon sinks in JFM in excess of  $100\text{gC m}^{-2}$  ( $112.4$  and  $131.6\text{gC m}^{-2}$  for Dargo and Nimmo, respectively). While both GPP and  $R_e$  increased at both sites from 2007 to 2008, the increase in GPP was larger, resulting in much stronger carbon uptake. GPP: $R_e$  increased from 1.05 to 1.28 at Dargo, and at Nimmo from 0.99 to 1.32. As discussed in Chapter 5 (section 5.4.4), during 2007 this period coincided with the lowest soil moistures observed during the two year study period, which also followed on from the extreme drought conditions of 2006.

---

<sup>29</sup> As detailed in Chapter 1 (section 1.7), summer, autumn, winter and spring refer to JFM, AMJ, JJA and OND, respectively.

Table 7.2: seasonal sums ( $\text{gC m}^{-2}$ ) of ecosystem respiration ( $R_e$ ), gross primary production (GPP) and net ecosystem exchange (NEE)  $\pm 95\%$  confidence intervals (\* and \*\* denote statistically significant difference between sites at  $p < 0.05$  and  $p < 0.01$ , respectively). Note that confidence intervals for partitioned fluxes represent partitioning uncertainty (since GPP is calculated as the residual of  $\text{NEE} - R_e$ , the uncertainty for  $R_e$  necessarily propagates to GPP, such that the values are the same for both quantities), whereas those for NEE represent the combined uncertainties contributed by random and model error.

	2007		2008	
	Dargo	Nimmo	Dargo	Nimmo
<i>R<sub>e</sub></i>				
JFM	329.2 $\pm$ 11.6	320.3 $\pm$ 16.7	402.8 $\pm$ 10.2	417.8 $\pm$ 17.7
AMJ	213.0 $\pm$ 5.6	** 188.3 $\pm$ 7.8	230.4 $\pm$ 5.0	231.5 $\pm$ 7.7
JAS	155.5 $\pm$ 4.9	** 181.8 $\pm$ 9.9	180.7 $\pm$ 5.3	187.1 $\pm$ 7.7
OND	341.8 $\pm$ 4.9	332.0 $\pm$ 8.5	330.3 $\pm$ 4.7	* 348.6 $\pm$ 8.0
Annual	1039.5 $\pm$ 19.7	1022.4 $\pm$ 31.0	1144.3 $\pm$ 18.7	1185.0 $\pm$ 32.6
<i>GPP</i>				
JFM	-345.2 $\pm$ 11.6	-315.6 $\pm$ 16.7	-515.2 $\pm$ 10.2	-549.8 $\pm$ 17.7
AMJ	-196.8 $\pm$ 5.6	-189.4 $\pm$ 7.8	-214.9 $\pm$ 5.0	* -246.8 $\pm$ 7.7
JAS	-93.9 $\pm$ 4.9	** -195.7 $\pm$ 9.9	-46.0 $\pm$ 5.3	** -166.5 $\pm$ 7.7
OND	-496.7 $\pm$ 4.9	* -525.6 $\pm$ 8.5	-479.6 $\pm$ 4.7	** -544.0 $\pm$ 8.0
Annual	-1132.5 $\pm$ 29.6	* -1226.2 $\pm$ 31.0	-1255.7 $\pm$ 27.5	** -1507.0 $\pm$ 32.6
<i>NEE</i>				
JFM	-16.0 $\pm$ 10.0	4.7 $\pm$ 10.1	-112.4 $\pm$ 5.6	-131.6 $\pm$ 15.1
AMJ	16.2 $\pm$ 7.3	-1.0 $\pm$ 14.2	15.5 $\pm$ 9.9	** -15.2 $\pm$ 11.4
JAS	61.6 $\pm$ 5.5	** -13.9 $\pm$ 8.2	134.8 $\pm$ 5.7	** 20.5 $\pm$ 7.3
OND	-154.9 $\pm$ 6.4	* -193.6 $\pm$ 11.8	-149.3 $\pm$ 5.3	** -195.3 $\pm$ 15.6
Annual	-93.0 $\pm$ 14.9	** -203.8 $\pm$ 22.4	-111.4 $\pm$ 13.5	** -322.0 $\pm$ 25.1

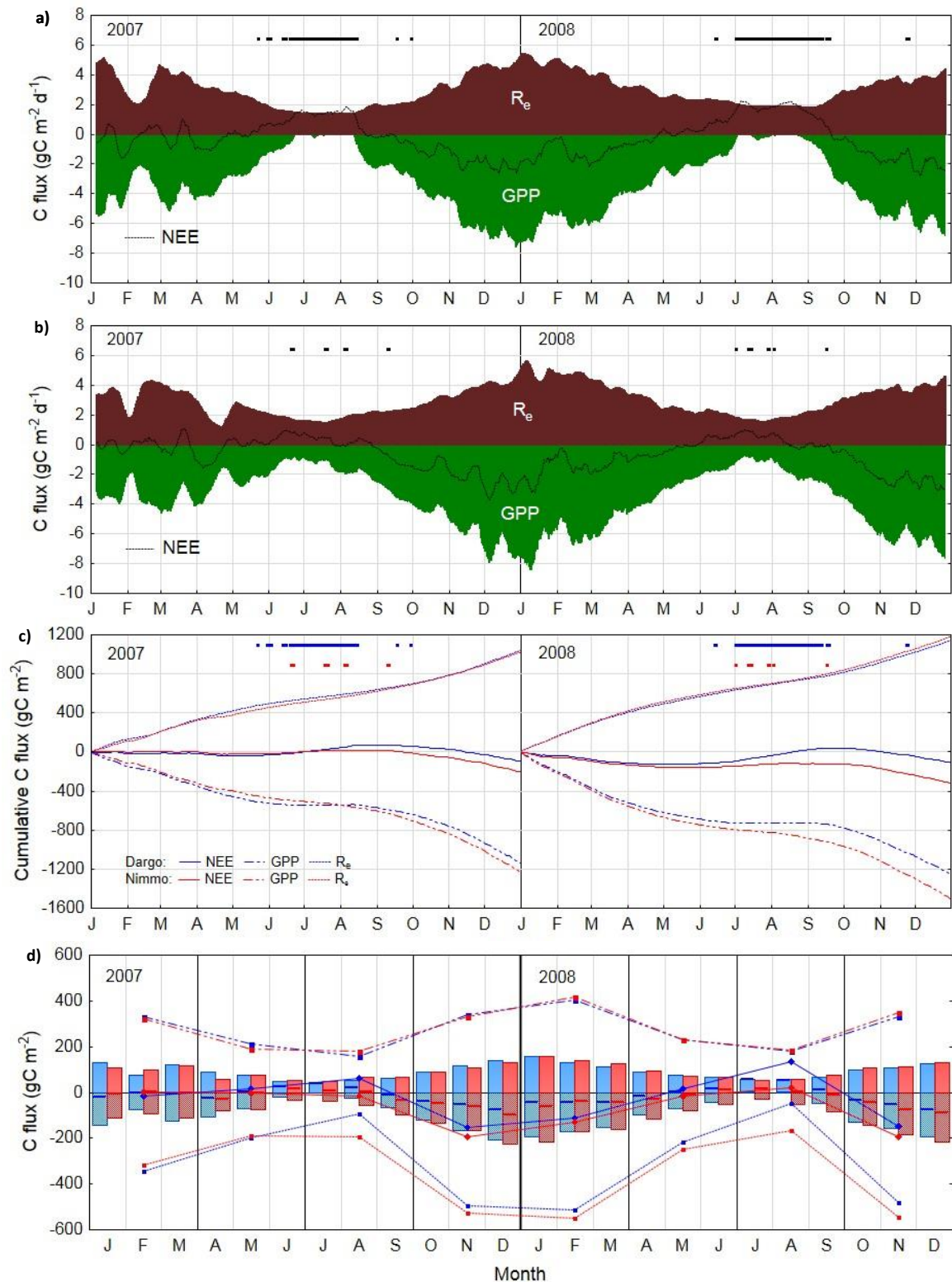


Figure 7.4: 2007/08 cross-site comparison of net ecosystem exchange (NEE), gross primary production (GPP) and ecosystem respiration ( $R_e$ ) : a) Dargo time series (smoothed with 14d running average; snow cover is represented by solid horizontal trace); b) Nimmo time series; c) cumulative comparative time series of GPP,  $R_e$  and NEE; d) monthly and seasonal sums of NEE, GPP and  $R_e$  (blue and red colours represent Dargo and Nimmo, respectively; bars > and < 0 represent monthly sums for  $R_e$  and GPP, respectively; solid lines overlaying bars represent monthly NEE; square, round and diamond symbols represent seasonal sums for  $R_e$ , GPP and NEE, respectively).

As outlined in Chapter 2, drought constrains both GPP (due to direct physiological effects of moisture limitation on the plant community) and  $R_e$  (due both to direct physiological effects of moisture limitation on autotrophic and heterotrophic organisms and also to the effects of reduced assimilate supply for metabolic activity). However, GPP is more sensitive to drought conditions than  $R_e$  (Schwalm *et al.*, 2010), such that drought reduces net uptake of carbon by ecosystems (Ciais *et al.*, 2005; Pereira *et al.*, 2007; Hussain *et al.*, 2011; Jongen *et al.*, 2011). In the Australian High Country, drought effects on plant mortality have previously been documented (Williams, 1990; Griffin and Hoffmann, 2011). Moreover, drought may also continue to affect the carbon balance following the breaking of drought conditions (van der Molen *et al.*, 2011), for example by inducing prior plant mortality which reduces the quantity of meristematic tissue per unit area and correspondingly the total live leaf area available for subsequent production, or by arresting leaf development or causing early senescence (Lauenroth and Sala, 1992; Yahdjian and Sala, 2006).

This is consistent with the results reported for JFM here. At both sites, both the magnitudes of GPP and  $R_e$  as well as their ratio (GPP: $R_e$ ) increased from the drought-affected conditions of JFM 2007 to the relatively moist summer conditions of 2008, with large corresponding increases in carbon uptake. The effect was also more pronounced at Nimmo. Only during summer and autumn of 2007 was GPP higher at Dargo, and the difference was most pronounced during summer. This may simply reflect the fact that plant growth (Gilgen and Buchmann, 2009) and the corresponding carbon balance of ecosystems (Wohlfahrt *et al.*, 2008) is more sensitive to the onset of drought conditions in persistently drier ecosystems. As a subset of the grassland biome, mountain grasslands are somewhat unique in that their distribution is primarily related to temperature rather than water limitation. Among water-limited lowland grasslands, both net primary production and the carbon balance as a whole are among the most interannually variable of all ecosystems because of the effects of stochastic interannual rainfall variability (Knapp and Smith, 2001; Sala, 2001; Yi *et al.*, 2012). Since Nimmo is a much drier site – in terms of soil water availability - drought conditions are therefore expected to have a more pronounced impact on growth and carbon uptake during summer than at Dargo.

The effect that dry conditions in early 2007 had on GPP at Nimmo is also reflected in satellite estimates of LAI, since photosynthetic activity is dependent on available live leaf area. Agreement between MODIS estimates of LAI and GPP were excellent (particularly given the granular nature of the MODIS data) at Nimmo (Figure 7.5), with MODIS LAI explaining approximately 85% of the variance in site GPP when using simple linear regression (data not shown). While the absolute accuracy of MODIS LAI estimates was not determined, GPP was estimated from the satellite data



using a logarithmic transform as shown in Figure 7.5. The extent of the effect of the 2006 drought on plant growth during the growing season of 2006/07 is clear, with maximum daily total GPP between October 2006 and April 2007 of  $<5\text{gC m}^{-2} \text{d}^{-1}$ , compared with up to  $8\text{gC m}^{-2} \text{d}^{-1}$  during the 2007/08 growing season. GPP during the early months of 2006 and final months of 2008 are also consistent with the 2007/08 growing season.

While a similar relationship is expected for Dargo, there was poor correspondence between LAI and site GPP. At Nimmo, the landscape patch containing the eddy covariance system is large and relatively homogeneous with respect to vegetation (see Chapter 3, Figure 3.2); accordingly, the IGBP<sup>30</sup> land cover class (used in the algorithm required to estimate LAI) was cropland (class 12). At Dargo, however, the site is much more locally heterogeneous, and thus the MODIS 1km pixel includes a range of vegetation types, with three land cover classes assigned: cropland (25%), evergreen broadleaf forest (class 2; 50%) and closed shrubland (class 6; 25%). As a result, there is far less confidence in MODIS-derived estimates of LAI at Dargo and they are not used here.

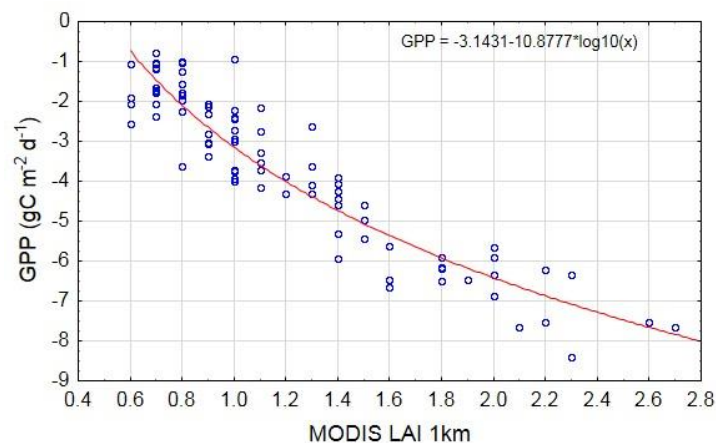


**Figure 7.5:** relationship between MODIS 1km LAI product (collection 5, TERRA product MOD15A2) and 10-day running mean of Nimmo site daily total GPP for 2007/08.

<sup>30</sup> International Geosphere-Biosphere Program.

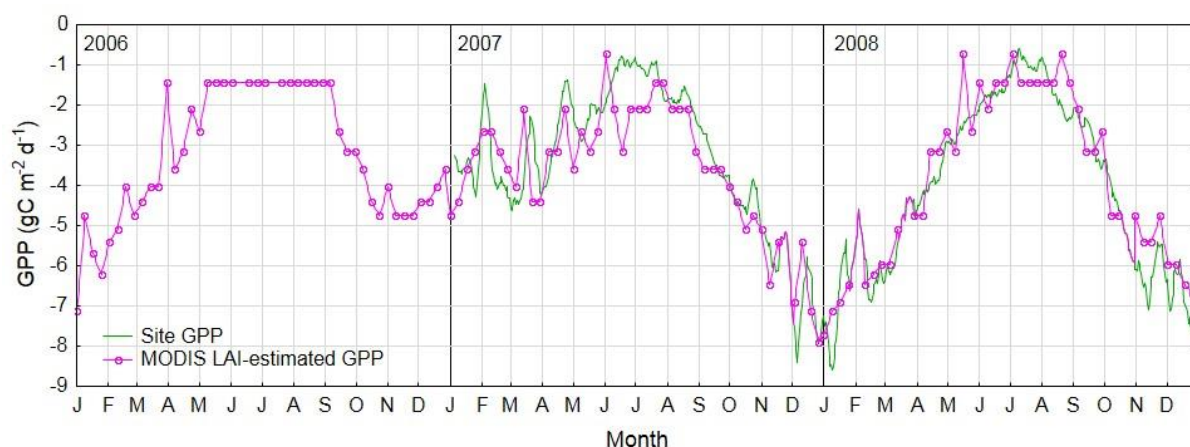


Figure 7.6: 2006-08 log-linear regression-estimated GPP (from MODIS LAI) and Nimmo site daily total GPP.

### 7.3.2 Autumn (AMJ)

Compared to JFM, NEE during AMJ was relatively consistent across sites and years. In both years at Dargo there was a small efflux of carbon during AMJ ( $16.2$  and  $15.5 \text{ gC m}^{-2}$  for 2007 and 2008, respectively). At Nimmo there was a small net influx of carbon (increasing from  $-1$  to  $-15.2 \text{ gC m}^{-2}$  from 2007 to 2008). At both sites both GPP and  $R_e$  increased from 2007 to 2008, possibly reflecting ongoing effects of the prior drought in 2007. The increase was particularly pronounced at Nimmo (with GPP and  $R_e$  increasing by over  $50 \text{ gC m}^{-2}$  and  $40 \text{ gC m}^{-2}$ , respectively, from 2007 to 2008), whereas at Dargo the change was less than  $20 \text{ gC m}^{-2}$  for both GPP and  $R_e$ . Thus whereas both GPP and  $R_e$  were lower at Nimmo than at Dargo in 2007, in 2008 they were both higher (although the difference in  $R_e$  was small and statistically non-significant). This also appears to reflect the previously noted tendency for drier ecosystems to respond more sensitively to changes in water status. As noted in Chapter 5 (5.4.4), following the dry conditions of summer 2007, there was a second interval of very low soil moisture at Nimmo in April. While there were reductions in soil moisture of comparable percentage magnitude during this period at Dargo, absolute soil moisture quantities remained more than twofold higher. Accordingly, whereas in May and June, GPP and  $R_e$  were higher at Nimmo, in April they were lower relative to Dargo.

Thus in common with the case during summer 2007, at Nimmo, there were large increases in autumn GPP and  $R_e$  from 2007 to 2008, but in contrast to summer this had relatively minimal effect on NEE. This is because whereas in summer GPP increased more rapidly than  $R_e$ , in autumn both components increased at a similar rate (such that GPP: $R_e$  increased only slightly; from 1 in 2007 to 1.06 in 2008). At Dargo, GPP: $R_e$  was the same in both years (0.93). As noted above, it is generally

expected that drought will affect GPP more than  $R_e$ ; however, since factors other than soil moisture affect both of these components, such results are not unexpected on seasonal time scales.

### 7.3.3 Winter (JAS)

The largest cross-site NEE differences were observed during JAS. Large carbon effluxes at Dargo in both years ( $61.6$  and  $134.8 \text{ gC m}^{-2}$  in 2007 and 2008, respectively) contrasted with moderate carbon uptake at Nimmo in 2007 ( $-13.9 \text{ gC m}^{-2}$ ) and moderate carbon efflux in 2008 ( $20.5 \text{ gC m}^{-2}$ ). The cross-site winter NEE difference represented 68 and 54% of annual NEE difference for 2007 and 2008 respectively. The larger magnitude of efflux at Dargo was because of the cessation of GPP in association with the establishment of snow cover. While limited photosynthesis may be possible under snow (Starr and Oberbauer, 2003), the snow pack at Dargo was clearly deep enough to reduce GPP to approximately zero. In contrast, at Nimmo, continued photosynthetic fixation of carbon through the winter reduced carbon effluxes greatly in comparison to Dargo.

The profound change in NEE caused by the establishment of the snowpack can be observed by comparing snow-free and snow-covered periods during winter (JAS). The difference in winter carbon balance between the sites was largely due to the effects of the snow pack at Dargo, where it persisted for approximately two months (despite different timing between years – see Chapter 5, section 5.4.1). Whereas winter NEE was similar at the sites in the absence of the snowpack at Dargo, following its establishment net carbon efflux increased greatly relative to Nimmo (Figure 7.7). This also had a profound effect on the diurnal dynamics of the carbon balance (Figure 7.8), with the establishment of the snowpack essentially removing the diurnal cycle in NEE because photosynthetic activity ceases and temperature-driven variation in  $R_e$  is reduced because of the lack of exposure of the soil surface to insolation and the insulating properties of the overlying snowpack.

Large effects of snow cover on the magnitude of  $R_e$  have also been reported in the literature for cold regions (e.g. Sommerfeld *et al.*, 1993; Monson *et al.*, 2006; Larsen *et al.*, 2007; Nobrega and Grogan, 2007). In contrast, however, despite the above-noted effect on the diurnal dynamics of  $R_e$  at Dargo, there was little apparent effect of snow cover on daily  $R_e$ . This is because the relatively mild winter climatic conditions of the Australian subalpine zone provide marginal support for snow because temperatures rarely drop far below  $0^\circ\text{C}$  for sustained periods, such that large air-soil temperature differentials are unlikely to develop even where snowpack is present (Warren and Taranto, 2011). While snow cover may alternatively reduce  $R_e$  by stopping the supply of

photosynthetic assimilates that support autotrophic and (to some extent) heterotrophic respiration, there is no clear evidence of sudden decline in  $R_e$  with the onset of the snowpack, suggesting the supply of labile carbon in the soil was adequate to support ongoing  $R_e$ . Thus while snow cover had little effect on  $R_e$ , it strongly reduced GPP. Thus the lower GPP: $R_e$  at Dargo (approximately 1.10) relative to Nimmo (1.20-1.27; see section 7.2.2) is largely due to the effects of winter snow at Dargo. For the snow free period, GPP: $R_e$  at Dargo was 1.20 (averaged across both years), in comparison to 1.29 for Nimmo.

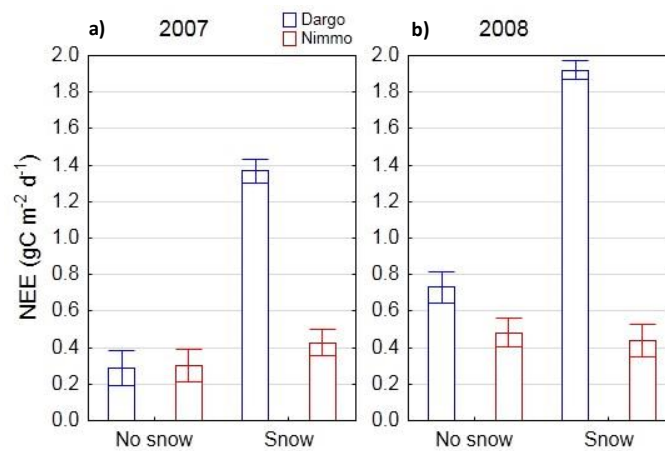


Figure 7.7: winter mean daily NEE ( $\pm$ SE) for snow-covered and snow-free conditions at Dargo in: a) 2007, and; b) 2008.

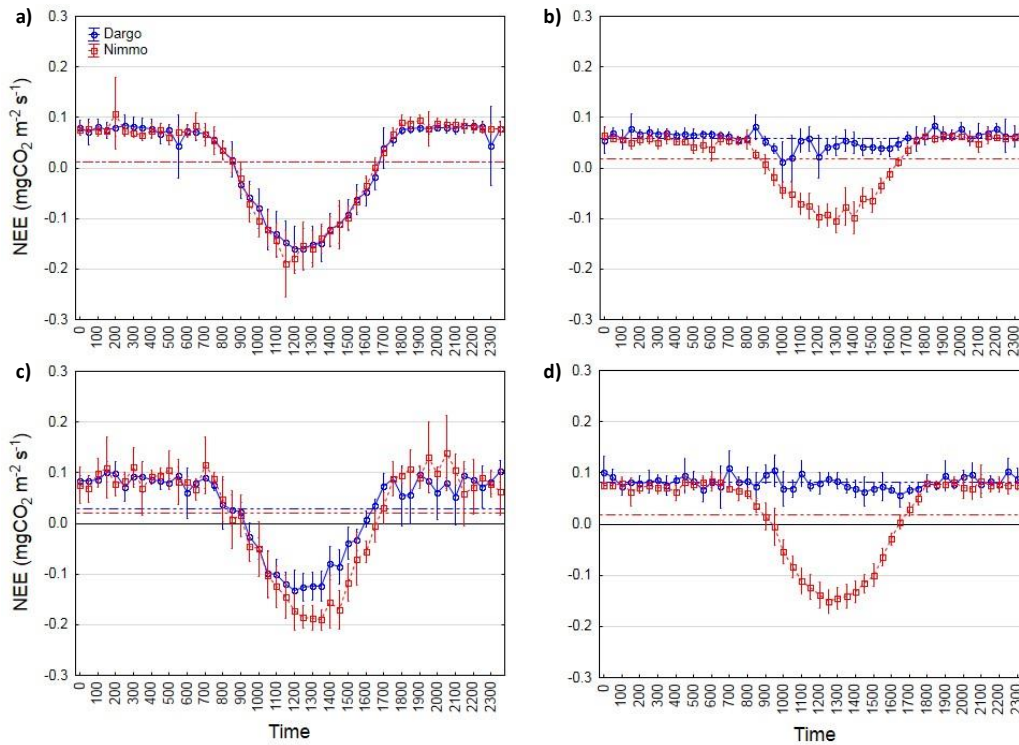


Figure 7.8: cross-site winter diurnal NEE ( $\pm$ SE) comparison for: a) no snowpack 2007; b) snowpack 2007; c) no snowpack 2008, and; d) snowpack 2008.

With respect to cross-year NEE contrasts during JAS, at Dargo there was a large increase in carbon efflux from 2007 to 2008 (from  $61.6$  to  $134.8 \text{ gC m}^{-2}$ , respectively). Reduction in GPP from 2007 to 2008 ( $47.9 \text{ gC m}^{-2}$ ) was responsible for approximately 65% of this increase in efflux. This was associated with the fact that the snow pack remained in place for ten days longer and until almost a month later in 2008 (melt-out on approximately 13<sup>th</sup> September) relative to 2007 (melt-out on approximately 16<sup>th</sup> August). Despite the later development of the snowpack in 2008 (30<sup>th</sup> June) relative to 2007 (12<sup>th</sup> June), both dates are close to the winter solstice, when insolation is already at a minimum, such that photosynthesis is correspondingly low. However, the melt-out date in 2008 was only a week before the equinox. As such, at Dargo the canopy remained under snow even as insolation increased rapidly during August and September. As a result, in contrast to 2007, GPP was effectively zero in August of 2008, and substantially reduced in September. Nonetheless, GPP was also reduced at Nimmo in JAS 2008 relative to 2007. Generally lower temperatures were observed at both sites, most notably in the latter part of 2008; whereas this had the effect of prolonging snow cover at Dargo, at Nimmo it may have constrained GPP.

It should also be noted that cross-year differences in  $R_e$  made a secondary contribution to the larger carbon efflux at Dargo during JAS 2008, with  $R_e$  increasing by approximately  $25.2 \text{ gC m}^{-2}$  from 2007 to 2008. Such differences might be explained by higher temperatures under snow in 2008, but the opposite was observed (JAS daily average soil temperatures at Dargo were  $2.6^\circ\text{C}$  and  $2.0^\circ\text{C}$  for 2007 and 2008, respectively). As noted in Chapter 2, respiration is relatively insensitive to soil moisture over a wide range, but is generally sensitive to very high or very low values. In 2008, volumetric soil moisture was lower at Dargo during JAS than in 2007, although the difference was small ( $0.52 \text{ m}^3 \text{ m}^{-3}$  in 2007 versus  $0.46 \text{ m}^3 \text{ m}^{-3}$  in 2008, compared with an estimated porosity of 0.55 for the 0-0.1m soil layer). However, differences may also be related to biotic rather than abiotic factors. This is discussed in further detail in section 7.4. This increase in winter carbon efflux at Dargo from 2007 to 2008 largely counterbalanced the increased carbon uptake during summer 2008, resulting in the increased difference in annual NEE observed between sites from 2007 to 2008.

#### 7.3.4 Spring (OND)

Whereas at both sites the largest carbon efflux occurred during winter, the largest carbon influx occurred during spring (OND). Of all seasons, NEE was also most consistent between years during OND. At Dargo, net carbon uptake was  $154.9$  and  $149.3 \text{ gC m}^{-2}$  (for 2007 and 2008, respectively) compared with  $193.6$  and  $195.3 \text{ gC m}^{-2}$  for Nimmo. Thus the consistency across years was also highest for OND, with respect to both NEE and the component fluxes (see Table 7.2).

The high rates of carbon uptake are expected, given that OND encompasses the months preceding and including the summer solstice (and – given the predominance of winter rainfall – therefore the insolation maximum), but is generally cooler (and correspondingly likely to have higher soil moisture) than the summer months succeeding the solstice. In particular, whereas temperature (the primary control of  $R_e$ ) reaches a maximum in January, maximum insolation (the primary control of GPP) occurred during December. This results in a phase shift between GPP and  $R_e$ . Thus while the highest GPP of any season was actually observed in JFM 2008 at both sites (a moist summer in terms of rainfall and soil moisture relative to 2007; see Chapter 5, section 5.4.1) rather than in OND of either year, GPP: $R_e$  was lower at the sites because of a larger increase in  $R_e$  from OND 2007 (GPP: $R_e$  of 1.45 and 1.58 for Dargo and Nimmo, respectively) to JFM (GPP: $R_e$  of 1.28 and 1.32 for Dargo and Nimmo, respectively).

Substantial (and statistically significant – see Table 7.2) cross-site differences in NEE were also evident during spring – with approximately  $40 \text{ gC m}^{-2}$  more carbon uptake at Nimmo in both years. This equated to 34 and 22% of the annual cross-site NEE difference, and was second only to JAS in terms of its effect on annual NEE. But while the absolute cross-site NEE difference was similar between years, the magnitudes of  $R_e$  and GPP varied. At Dargo, both GPP and  $R_e$  were reduced in 2008 relative to 2007, whereas at Nimmo the opposite occurred. At both sites GPP: $R_e$  was approximately preserved (for Dargo, 1.45 in both 2007 and 2008; the corresponding values for Nimmo were 1.58 and 1.56 for the respective years). GPP and  $R_e$  are expected to be linked by the fact that GPP provides the assimilates for respiration. The reasons for the different site responses are however unclear. The primary driver of GPP is insolation, but this was actually slightly higher in OND 2008 relative to 2007. This suggests it is more likely to be associated with light response of the canopy, which in turn may be affected by other meteorological variables (discussed further in section 7.4.2). Although it may also be related to the fact that snow at Dargo persisted until later in 2008 – the extension of dormancy for the plant canopy may have physiological consequences that affect subsequent productive capacity – reduction in GPP in 2008 relative to 2007 was least in

October, and then increased through November and December (data not shown). As noted above, cross-site differences in NEE were in most seasons primarily related to differences in GPP, and spring was no exception. Further discussion of the reasons for cross-site GPP differences is provided subsequently (see section 7.4.2).

In summarising the effects of seasonal carbon dynamics, cross-site annual NEE differences were primarily due to differences in winter and spring carbon dynamics at the sites, which arose for different reasons. In winter, differences were overwhelmingly related to the fact that the establishment of snow cover at Dargo causes a cessation of GPP. In spring, however, substantial differences in NEE also arose in association with higher GPP at Nimmo, suggesting that factors additional to snow cover affect the relative productivity of the two ecosystems. With respect to differences in annual NEE between years, the increase in carbon uptake at Nimmo occurred largely due to increases in summer carbon uptake in 2008 relative to 2007. While similar increases also occurred at Dargo, offsetting increases in winter carbon efflux also occurred. The discussion now turns to the environmental controls on the dynamics of GPP and  $R_e$ .



## 7.4 Controls on carbon balance dynamics

### 7.4.1 Ecosystem respiration ( $R_e$ )

#### 7.4.1.1 *Soil temperature*

Since temperature is a key control of respiration (see Chapter 2.4.3.12, section 2.5.3.1), the differing temperature regimes at the sites was important in determining the observed differences in  $R_e$ . As discussed in Chapter 5 (section 5.3.2), soil temperatures were on average approximately 2°C higher at Nimmo than Dargo, roughly in accordance with mean differences in ambient air temperature (in turn related to the adiabatic effects of altitude differences). Moreover, the amplitude of soil temperature variation at both diurnal and seasonal time scales was also higher at Nimmo. These differences between sites most likely relate to the contrasting properties of both the overlying surface (differences in vegetation cover and thus shading – see Chapter 6, section 6.3) and soil properties (differences in soil moisture and organic / mineral content – see Chapter 6, section 6.2).

During 2007, on seasonal time scales,  $R_e$  at Nimmo was slightly (though not statistically significantly) lower than at Dargo during the warmer months (i.e. JFM and OND), significantly lower during AMJ, and significantly higher during JAS (Table 7.2). While soil moisture was also an important periodic control on  $R_e$  (discussed below) at the sites, contrasting ecosystem responses to temperature were important in controlling  $R_e$ . These contrasting responses are expressed in differences in the parameters of the temperature response function (see Chapter 3, section 3.7.1 – and Equation 3-16 therein - for details) fitted to the observational data (Table 7.3). Specifically, basal respiration at 10°C ( $R_{ref}$ ) was statistically significantly higher at Dargo than Nimmo in both 2007 and 2008. The activation energy parameter ( $E_o$ ) that controls the rate of change of the temperature response of  $R_e$  (i.e. temperature sensitivity) was also significantly higher at Dargo in 2007, and slightly (though not statistically significantly) lower in 2008. The practical effect of these differences in terms of temperature-specific  $R_e$  is illustrated by comparison of response curves for the sites for each year (Figure 7.9).

In 2007,  $R_e$  at very low temperatures was similar at the sites (in fact, slightly lower at Dargo), but increased at a much greater rate with temperature at Dargo, such that at higher temperatures (e.g. during JFM and OND) there was a much larger difference in temperature-specific  $R_e$  between

sites. For example, at 20°C  $R_e$  at Dargo was approximately  $0.29 \text{ mgCO}_2 \text{ m}^{-2} \text{ s}^{-1}$ , almost 50% higher than the rate at Nimmo ( $0.20 \text{ mgCO}_2 \text{ m}^{-2} \text{ s}^{-1}$ ). However, as noted above, the amplitude of seasonal and diurnal soil temperature cycles was higher at Nimmo, with the largest cross-site differences (i.e. higher temperatures at Nimmo) occurring during summer. This partially compensated for the above-noted low temperature-specific  $R_e$  at the upper end of the observed temperature range, such that cross-site  $R_e$  differences during JFM and OND were small. The larger difference observed in AMJ (213gC at Dargo vs 188.3gC for Nimmo) was at least partially related to soil moisture effects (section 7.4.1.2, below). On the other hand, in winter, when soil moisture was plentiful,  $R_e$  was lower at Dargo, despite relatively similar soil temperatures. This was due to lower temperature-specific  $R_e$  at Dargo at lower temperatures (below approximately 5°C, which was routinely the case during winter and under snow).

**Table 7.3: 2007/08 comparison of fitted parameter values of Lloyd and Taylor (1994) temperature response function ( $R_{\text{ref}}$  - basal respiration at a reference temperature of 10°C;  $E_o$  - activation energy [see Chapter 3, section 3.7.1].**

	2007		2008	
	Dargo	Nimmo	Dargo	Nimmo
$R_{\text{ref}}$	0.145	**	0.125	**
$E_o$	261.1	**	210.7	215.6

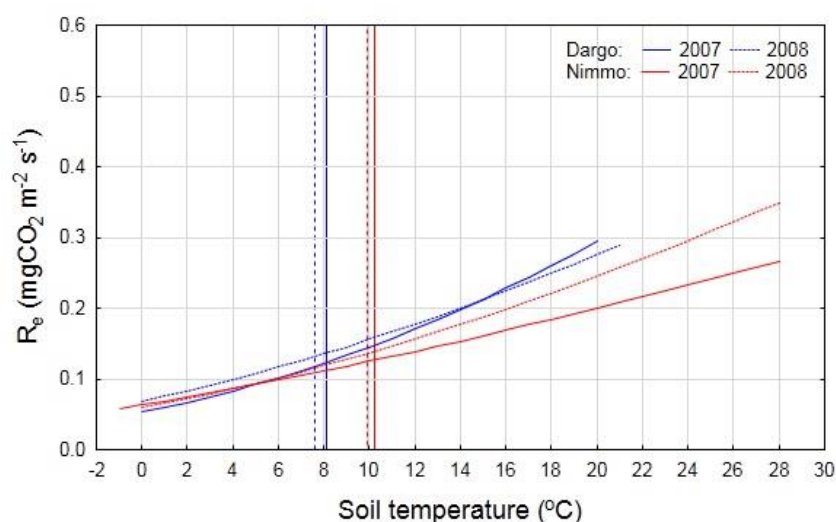


**Figure 7.9: ideal temperature response curves derived from temperature response function parameters in Table 7.3 (curves truncated at approximate maximum and minimum temperatures for each year); note vertical lines indicate mean temperatures for years with solid and dashed lines referencing 2007 and 2008, respectively.**

During 2008,  $R_e$  was instead higher at Nimmo, both annually and during all seasons (though not statistically significantly during AMJ or JAS). At both sites  $R_e$  increased relative to 2007 despite lower mean annual temperature due to an increase in temperature-specific  $R_e$ . This was partly driven by an increase in  $R_{ref}$ . However,  $R_{ref}$  increased by a similar amount at both sites (approximately 8 and 10% at Dargo and Nimmo, respectively), and thus does not explain the higher  $R_e$  at Nimmo in 2008 relative to Dargo. Instead, this is explained by the fact that  $E_o$  was comparable at the sites. This parameter controls the temperature sensitivity of respiration (i.e. the rate of change of  $R_e$  as a function of temperature). As a result, the large divergence in temperature-specific  $R_e$  between sites at high temperatures that was observed in 2007 was not evident in 2008. The lower basal respiration rate at Nimmo nonetheless resulted in consistently lower temperature-specific  $R_e$  than Dargo across the common temperature range of the sites. However, this was counterbalanced by consistently higher daytime temperatures at Nimmo; as noted previously, the largest cross-site soil temperature differences generally occurred during summer. Thus the higher Nimmo temperatures more than compensated for the lower temperature-specific  $R_e$ , resulting in higher observed  $R_e$  at Nimmo during JFM and OND in 2008. The reason for the lower winter  $R_e$  at Nimmo was that – as noted above - cross-site soil temperature differences were greatest during summer, and least during winter. As such, in winter the lower temperature-specific  $R_e$  at Nimmo also resulted in lower observed  $R_e$  relative to Dargo.

While differences in  $R_e$  between sites could plausibly also be associated with the effects of soil moisture (and at seasonal time scales in some cases were), since an explicit term was included to account for these effects when modelling  $R_e$  (Equation 3-17), they can be excluded from the analysis such that ‘potential’  $R_e$  ( $\dot{R}_e$ ) as determined exclusively by temperature can be expressed. This shows that in 2007, while  $\dot{R}_e$  was higher than  $R_e$  at both sites (i.e. soil moisture was constrained by  $R_e$  by approximately 8% and 2-3% at the sites in 2007 and 2008, respectively - see subsequent discussion), the relative and absolute differences between sites were approximately preserved, with  $\dot{R}_e$  still lower at Nimmo (Table 7.4). Similarly, in 2008, differences between sites in  $\dot{R}_e$  were approximately comparable to those of  $R_e$ , with  $R_e$  higher at Nimmo. Thus while soil moisture affected the magnitude of annual  $R_e$  at both sites, it had almost no effect on the observed cross site annual  $R_e$  difference. While soil moisture effects did contribute to seasonal cross-site  $R_e$  differences – specifically in summer and autumn 2007 – these effects were not large enough to change the sign of the difference between sites (data not shown).

Cross-site  $R_e$  differences were nonetheless – as previously noted – small relative to the NEE differences. If the temperature response of Nimmo was equivalent to that observed for Dargo, then

the higher temperatures at the site would drive much higher  $R_e$  than observed for the site. Conversely, if the temperature response of Dargo was equivalent to that observed for Nimmo, then the lower temperatures at the site would drive much lower  $R_e$  than observed for the site. However, the small observed difference in  $R_e$  between sites demonstrates that the effects of temperature difference between sites were largely counterbalanced by differences in ecosystem response to temperature. This apparent acclimation effect has been noted elsewhere, with basal respiration rates decreasing across European forest sites with increasing mean annual soil temperature (Janssens *et al.*, 2003; Rodeghiero and Cescatti, 2005), although Bahn *et al.* (2008) report that such relationships were not evident across European grasslands.

**Table 7.4: 2007/08 cross-site comparison of annual  $R_e$  and potential  $R_e$  ( $\dot{R}_e$ ).**

	2007				2008			
	Dargo	Nimmo	$\frac{\text{Dargo}}{\text{Nimmo}}$	Dargo - Nimmo	Dargo	Nimmo	$\frac{\text{Dargo}}{\text{Nimmo}}$	Dargo - Nimmo
$R_e$ (gC m <sup>-2</sup> a <sup>-1</sup> )	1039.5	1022.5	1.017	17.0	1144.2	1185.0	0.97	-40.8
$\dot{R}_e$	1131.2	1109.6	1.019	21.6	1167.9	1219.4	0.96	-51.5
$R_e/\dot{R}_e$	0.92	0.92			0.98	0.97		

Thus while soil temperature was the key control of  $R_e$  at the sites, cross-site  $R_e$  differences were less than expected on the basis of temperature differences alone because of counterbalancing differences in ecosystem response to temperature. This is expected given that, while  $R_e$  is often modelled as an exponential function of temperature, it is ultimately constrained by the labile carbon supply (which in the case of both autotrophic and heterotrophic respiration is tied to gross primary production in the short term, and in the case of heterotrophic respiration to the balance between GPP and  $R_e$  – and thus accumulation in soil pools of labile carbon – in the longer term). Thus at a warmer site like Nimmo,  $R_e$  can only increase to the extent that the supply of labile carbon can support it. However, as noted above, annual  $R_e$  was actually lower at the Nimmo site in 2007, underscoring the fact that the cross-site dynamics of  $R_e$  cannot be understood in the context of temperature alone. The discussion now turns to the effects of soil moisture.

#### 7.4.1.2 *Soil moisture availability*

While temperature is a key control on ecosystem respiration rates,  $R_e$  is also sensitive to soil moisture availability (Baldocchi and Valentini, 2004). As discussed in Chapter 5 (section 5.4.4), soil moisture was consistently higher at Dargo than Nimmo. At both sites, while mean soil moisture was similar between years, the lowest values were recorded in the first 3 months of 2007 (see Chapter 5, section 5.4.4). The drought conditions that had also been prevalent in 2006 subsequently eased; however, at Nimmo there was an additional period of low soil moisture in April 2007 that was not observed at Dargo.

As was the case with soil temperature, the contrasting responses of the sites to soil moisture variations may be expressed in terms of differences in the parameters of the soil moisture response function (see Chapter 3, section 3.7.1 – and Equation 3-17 therein - for details) fitted to the observational data (Table 7.5). While  $R_e$  at both sites was found to be sensitive to soil moisture, the sensitivity to a given soil moisture level was higher at Dargo than Nimmo (Figure 7.10a). At Dargo, the volumetric soil water content (VWC) level at which  $R_e$  reaches 95% of its potential value was approximately  $0.25\text{m}^3\text{m}^{-3}$ , whereas at Nimmo this sensitivity threshold was lower, at approximately  $0.14\text{m}^3\text{m}^{-3}$ . However, soil conditions were also drier at Nimmo. As a result, at both sites soil moisture constrained  $R_e$  during the study period, particularly during the early months of 2007, when  $R_e$  was reduced by more than 50% during some periods (Figure 7.10b). At Dargo, the sustained dry period during February strongly constrained  $R_e$ , whereas at Nimmo, the most prolonged period of pronounced soil moisture-driven  $R_e$  constraint was in April, when 0-0.1m soil moisture again occupied less than 10% of soil volume (this was the key reason for previously-noted lower AMJ  $R_e$  at Nimmo in 2007).

The much stronger constraint in 2007 at the sites reflects the drier conditions in the early part of the year relative to 2008. In 2008, the high rainfall during the preceding summer and into autumn continually replenished soil moisture such that the effect of soil moisture on  $R_e$  was much reduced relative to 2007. Nonetheless, the fact that there was still periodic soil moisture limitation of  $R_e$  during January-March 2008 despite relatively high rainfall in summer 2007/08 suggests that some degree of moisture limitation is a typical rather than exceptional feature of the summertime carbon balance in these ecosystems.

Table 7.5: 2007/08 comparison of fitted parameter values of sigmoid soil moisture response function.

	Dargo		Nimmo
$\Theta_1$	3.67		3.74
$\Theta_2$	26.70	**	48.34

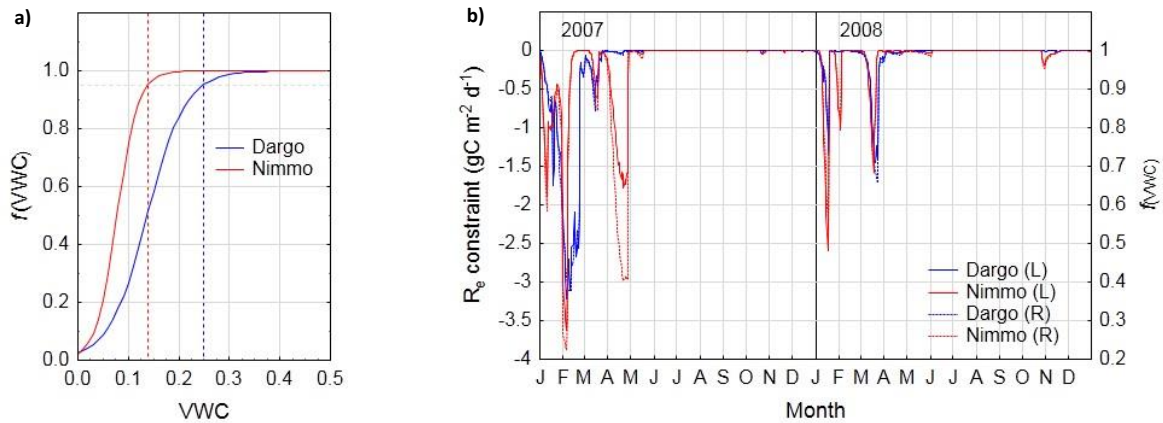


Figure 7.10: soil moisture response of  $R_e$  : a) idealised response  $f(vwc) = \frac{1}{(1+e^{\theta_1-\theta_2 vwc})}$ , where VWC = volumetric water content [ $m^3 m^{-3}$ ]; b) quantitative constraint on  $R_e$  (left hand axis) and value of response scalar (right hand axis) as a function of VWC with time in 2007/08 study period.

As discussed previously, despite differences in the temporal dynamics of VWC, the aggregate constraint on annual  $R_e$  was approximately equivalent at the sites. As presented in Table 7.4 above, in 2007 respiration was reduced by approximately 8% at both sites, equating to almost  $100gC m^{-2}$  annually. In 2008 the reduction was much less, approximately 2% and 3% at Dargo and Nimmo, respectively (equating to between 20 and  $40gC m^{-2}$ ). Thus while at both sites soil moisture played an important role in reducing  $R_e$  in 2007 relative to 2008, the observed cross-site  $R_e$  differences documented above were not directly associated with differences in soil moisture. A similar conclusion may therefore be drawn for the sites as that for temperature above: while both the soil moisture conditions and the ecosystem response to those conditions were different at the sites, those differences were largely counterbalancing, resulting in similar effects of soil moisture on  $R_e$ . Specifically, while the soil was drier at Nimmo, the threshold below which soil moisture began to progressively constrain  $R_e$  was also lower than at the wetter Dargo site.

In contrast to cross-site  $R_e$  differences, soil moisture had a much more important effect on cross-year  $R_e$  differences. At Dargo, the difference in  $\bar{R}_e$  between 2007 and 2008 was  $36.7gC m^{-2}$ . This represents the combined effects on  $R_e$  of cross-year variations in temperature and ecosystem

temperature response at Dargo in the absence of soil moisture limitation. However, the difference in  $R_e$  was  $104.7 \text{ gC m}^{-2}$ . Thus the difference in temperature / temperature response was responsible for only approximately one third of the interannual  $R_e$  difference at Dargo, with the remainder due to soil moisture differences. At Nimmo, the substantial change in temperature response between years resulted in a more important contribution of this factor to interannual  $R_e$  differences. At Nimmo, the interannual  $R_e$  difference was  $109.8 \text{ gC m}^{-2}$ , compared with an  $R_e$  difference of  $162.5 \text{ gC m}^{-2}$ . Thus two thirds of the interannual  $R_e$  difference at Nimmo was due to temperature / temperature response effects with the remainder associated with soil moisture differences.

The difference in response between years also underscores the important role of the timing of precipitation events. Average soil moisture content was approximately equivalent between years at both sites, but the timing of its delivery was very different. As a result in 2008 soil moisture was rarely low enough to reach the  $R_e$  sensitivity thresholds for the sites. In particular, since soil moisture generally reaches its lowest values during summer (due to lower precipitation and high evaporative demand), the dynamics of summer rainfall are clearly crucial in determining the extent to which  $R_e$  is constrained by low soil moisture in a given year, as has been noted elsewhere (Chou *et al.*, 2008).

With respect to the effects of high soil moisture on  $R_e$ , since soils at both sites approached saturation in winter, it is likely that this imposed some constraint on the heterotrophic component of respiration. For example, it has been reported for wet alpine sites that reductions in soil moisture from very high levels may result in increases in  $R_e$  (Koch *et al.*, 2008). Because the wettest conditions coincide with winter, when low temperatures also result in low  $R_e$ , it is likely that there is some confounding of the respiratory responses to these controls. However, potential inhibitory effects of high soil moisture on  $R_e$  during winter could not be identified in the data. This is not surprising given that the winter flux data is likely to be of lower quality due to potential effects of climate on the operation of equipment. This is manifested in relatively poor winter energy balance closure and the fact that the random error intercept at zero flux magnitude was non-zero (resulting in lower absolute error but higher signal to noise ratio; see Chapter 4, section 4.3).

#### 7.4.1.3 Discussion

In summary, differences in  $R_e$  between sites arose primarily in relation to temperature (and ecosystem temperature response) rather than soil moisture availability, despite the fact that the latter was instrumental in reducing  $R_e$  at both sites – by proportionately similar amounts - during 2007 relative to 2008. Cross-site  $R_e$  differences were small despite substantial differences in both temperature regime and ecosystem temperature response, because the combined effects of these contrasts were largely compensatory. Differences in  $R_e$  between years were thus much larger than those between sites: the average within-site cross-year annual  $R_e$  difference ( $133.6 \text{ gC m}^{-2} \text{ a}^{-1}$ ) exceeded the average within-year cross-site annual  $R_e$  difference ( $28.9 \text{ gC m}^{-2} \text{ a}^{-1}$ ) by a factor of 4.7.

As previously discussed, it is commonly observed that  $R_e$  on average increases with mean annual temperature (Janssens *et al.*, 2003; Bahn *et al.*, 2008). This relationship is clearly evident among alpine grasslands (Figure 7.2), and respiration at the current sites was comparable to results for western European alpine ecosystems. While the results from 2008 were consistent with this (i.e. respiration was higher at Nimmo, the warmer site), in 2007 the reverse occurred (i.e. respiration was higher at Dargo, the cooler site). While the low soil moisture in the first 3 months of 2007 does explain a large proportion of the cross-year  $R_e$  difference at each site, cross-site soil moisture differences do not explain why  $R_e$  was lower at Nimmo in 2007 and higher in 2008, since it was established that low soil moisture had approximately similar absolute and relative effects on  $R_e$  at both sites.

This may nonetheless be related to the effects of soil moisture in a cumulative sense. As previously noted, lower  $R_e$  at Nimmo in 2007 was due to lower respiration at high temperatures (e.g. summer) observed in 2007. The aggregate expression of ecosystem response to temperature via net fluxes of carbon at ecosystem scale as provided by eddy covariance do not allow deeper interrogation of the underlying mechanisms driving these responses; however, as detailed in Chapter 2 (section 2.4.3.3), ecosystem respiration is maintained by the supply of labile carbon ultimately sourced from assimilation (Baldocchi and Valentini, 2004). As such, while  $R_e$  in mountain grasslands is well-correlated with temperature (Bahn *et al.*, 2008; Wohlfahrt *et al.*, 2008), Bahn *et al.* (2008) argue that this is because assimilation – and thus the supply of assimilates for autotrophic and heterotrophic respiration - is controlled by temperature. This is supported by the fact that interruption of photosynthesis by grass clipping results in a reduction in respiration irrespective of temperature (Bahn *et al.*, 2006; Bahn *et al.*, 2008). As such, for sites in which temperature is an important control on plant production, a clear relationship between temperature and  $R_e$  may be



expected, but this may be mediated by plant growth responses to temperature rather than direct respiratory responses *per se*.

A number of authors (Koch *et al.*, 2008; Li *et al.*, 2008; Wohlfahrt *et al.*, 2008) also note that among drier alpine grassland sites, soil moisture may be an important control of  $R_e$ , as was established in this study. But as the above discussion makes clear, such effects may occur via indirect constraints on assimilate supply arising due to photosynthetic constraint. Thus the apparent response of ecosystem respiration to abiotic controls (for example, temperature) reflects not only the capacity of the biota to utilise the available labile carbon supply but also plant-mediated variation in that supply. In this study, both GPP and  $R_e$  were lower in summer and autumn of 2007 relative to 2008. And during summer and autumn of 2007, both GPP and  $R_e$  were lower at Nimmo than Dargo.

This is consistent with expectation given the strong documented linkage between assimilation and respiration. Lower assimilation of carbon at Nimmo in early 2007 reduced assimilate supply to support respiration, which was manifested in relatively low respiratory rates at high temperatures (the highest temperatures observed at either site occurred in early 2007). This coincided with a period of very low soil moisture. As previously noted, drought is known to periodically affect plant growth and induce mortality in the Australian High Country grasslands. Moreover, GPP is generally more sensitive to drought than  $R_e$  (Schwalm *et al.*, 2010), most likely contributing to the lower GPP:  $R_e$  observed in early 2007 at the sites. This is in contrast with winter and spring, when soil moisture was high at both sites, and both GPP and  $R_e$  were higher at Nimmo (although as previously discussed, winter differences in GPP were largely due to the presence of snow cover at Dargo – this would have the effect of reducing labile carbon supply for winter  $R_e$ ).

However, if the direct effects of soil moisture limitation on  $R_e$  were similar at the sites, why were indirect effects of the type discussed above apparently more pronounced at Nimmo? This may reflect the effects of lags in ecosystem response to antecedent drought conditions, and differences between sites in the nature of that response. It has been observed that plant growth (Gilgen and Buchmann, 2009) and the corresponding carbon balance of ecosystems (Wohlfahrt *et al.*, 2008) is more sensitive to the onset of drought conditions in persistently drier ecosystems. Since Nimmo is a much drier site, it is possible that the antecedent drought conditions had a more pronounced impact on subsequent plant productivity – and corresponding assimilate supply - than at Dargo during the growing season in 2006-07; some indication of the pronounced effects on GPP at Nimmo is provided by the MODIS data as illustrated in Figure 7.6.

The reason for the substantial increase in winter  $R_e$  at Dargo from 2007 to 2008 is not known, but may also be related to assimilate supply. Respiration under snow is derived primarily from both autotrophic and heterotrophic organisms metabolising recently fixed carbon (i.e. respiration from plant organs as well as mycorrhizal and rhizosphere-associated microbes), with a lesser contribution from microbial decomposition of bulk soil organic matter (Grogan *et al.*, 2001). While at Nimmo photosynthetic activity continued through the winter, thereby providing an ongoing – albeit limited – supply of labile carbon, at Dargo the virtual cessation of photosynthesis with the establishment of the snowpack means that the store of labile carbon present at the beginning of this period fundamentally constrained the respiratory budget available for its duration. Any factors that reduce carbon assimilation in the preceding growing season may thus result in reduced labile carbon supply during the snow-covered-period. For example, Grogan *et al.* (2001) report that clipping of vegetation in sub-Arctic tundra during the growing season substantially reduced  $R_e$  during the subsequent winter. Since photosynthesis is generally more sensitive to drought than respiration, the labile carbon reservoir within the ecosystem is eventually depleted by protracted drought conditions (van der Molen *et al.*, 2011). This may have been the effect of the drought conditions that were present in 2006 and continued into 2007, reducing GPP prior to winter (relative to 2008). Thus explanations of the behaviour of  $R_e$  broadly hinge on questions of assimilation, to which the discussion now turns.

## 7.4.2 Gross Primary Production (GPP)

### 7.4.2.1 Insolation

Since solar radiation is the energy source for photosynthesis, insolation is the key driver of gross primary production, and thus generally explains a large proportion of the variance in GPP (Baldocchi and Valentini, 2004). The approach used in this study was to fit light response curves (see Chapter 3, section 3.7.2) to the GPP data in order to extract the shape parameters of the curve for each site. As with the soil respiration parameters, these parameters are a measure of aggregate ecological response to an external abiotic control, in this case insolation.

In turn, relationships between these parameters and other biotic and abiotic controls can be further examined. The two parameters of the light response function used in this study are the initial quantum yield ( $\alpha$ ) – which represents the initial slope of the light response curve (Figure 7.11a) - and

the photosynthetic capacity at optimum light level ( $A_{opt}$ ; here optimum is set to 2000  $\mu\text{mol}$  photons of photosynthetically active radiation [PAR]). Time series of these quantities are provided in Figure 7.11b and Figure 7.11c, respectively. For both parameters, a maximum is generally observed in the summer months and a minimum in winter. This seasonal pattern may be related to variations in leaf area or to area-specific efficiency; however, it is generally recognised that photosynthetic capacity is relatively constant even across biomes when normalised for leaf area (Chapin *et al.*, 2002), as also observed across the seasonal cycle in this study (see discussion below).

With respect to cross-site comparisons, there was no clear difference in  $\alpha$ , which was also relatively noisy. This most likely relates to the fact that – as noted in Chapter 4 – signal:noise is lower at lower flux values, so there is expected to be more uncertainty in the  $\alpha$  parameter. Secondly, the higher proportion of standing dead material at Dargo (Chapter 6, section 6.3) may result in shading under direct sun conditions, whereas under lower light conditions – at high zenith angles or under cloud – the radiation field is more isotropic, such that canopy penetration by photons is increased and differences between sites in photosynthesis may correspondingly be reduced. Thirdly, differences in temperature between low light conditions after sunrise and before sunset may also result in uncertainty in both intercept and initial slope of light response curves (Aubinet *et al.*, 2012a). Regardless, to the extent that these parameters represent the physiological characteristics of the canopy, differences in GPP between sites were clearly not primarily related to  $\alpha$ , and thus the analysis herein explores variation in  $A_{opt}$  between sites.

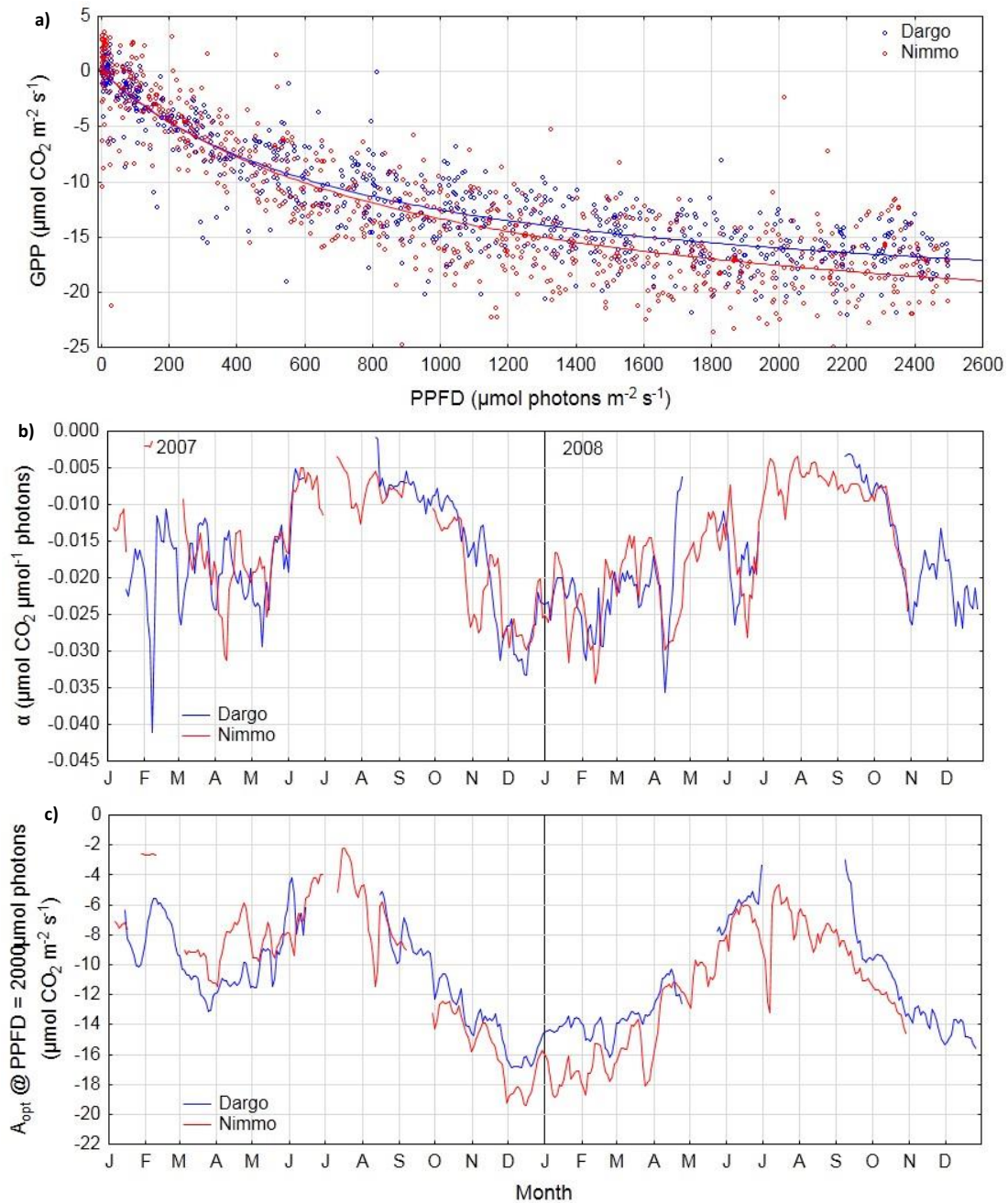


Figure 7.11: cross-site comparison of photosynthetic light response: a) light response of GPP to photosynthetic photon flux density (PPFD) for December 2007; b) 2007/08 time series of canopy quantum yield parameter ( $\alpha$ ) derived from light response function using a 10-day window with a 5-day step (see Chapter 3, section 3.7.2 for details); c) time series of canopy photosynthetic capacity at PPFD= $2000 \mu\text{mol photons m}^{-2} \text{ s}^{-1}$  ( $A_{\text{opt}}$ ) derived from light response function analysis.

$A_{\text{opt}}$  was consistently higher at Nimmo for most of the study period; only during the first 6 months of the year in 2007 was  $A_{\text{opt}}$  higher at Dargo. This is consistent with the previously reported differences in GPP between sites, with GPP larger at Dargo only during summer and autumn of 2007.

This was also the time when GPP was generally lower at both sites in association with low soil moisture. While differences in GPP could conceivably also be associated with differences in insolation between sites, the relative effects of light and the canopy light response can be gauged by crossing light conditions and response parameters between the sites. As discussed in section 5.2, insolation was very similar at the sites, with the largest differences between sites occurring during spring 2007. However, when the canopy light response parameters of Dargo were crossed with the light conditions of Nimmo for this period (Figure 7.12), the seasonal GPP was almost identical to that obtained using Dargo light conditions. On the other hand, crossing the canopy light response of Nimmo with the light conditions of Dargo essentially reproduced the seasonal GPP result of Nimmo, thereby confirming the relative unimportance of differences in light conditions to seasonal cross-site GPP differences.

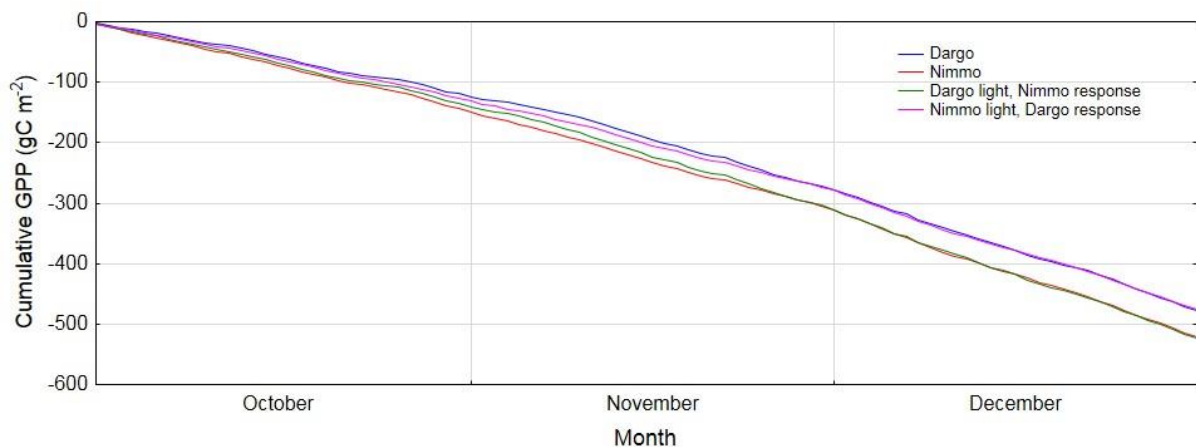


Figure 7.12: light response function estimates of GPP for sites using observed and crossed light conditions and response parameters (Dargo light, Nimmo response and Nimmo light, Dargo response).

One of the key drivers of variations in  $A_{opt}$  is expected to be leaf area index, since photosynthetic capacity is ultimately dependent on the available area of leaf surface. Since  $A_{opt}$  is a measure of light response, it is effectively normalised for light (whereas GPP varies with insolation on time scales – e.g. diurnal - that are independent of LAI variations), and would therefore theoretically be expected to have a stronger relationship with LAI than GPP. However, the method of deriving  $A_{opt}$  means that effects of inherent random error in measurements are likely to be accentuated in comparison to daily aggregates of GPP.

Nonetheless, the relationship was remarkably consistent (Figure 7.13;  $r^2$  for linear fit=0.73), showing a logarithmic pattern reflecting diminishing returns of increasing leaf area for plant

productivity, most likely due to increasing effects of mutual shading by leaf elements with increasing leaf area index. This is a similar pattern to that previously noted for GPP (section 7.3). As a function of LAI,  $A_{opt}$  showed no seasonal pattern (data not shown), suggesting that the primary response of the canopy to abiotic controls occurs via the modification of leaf area, while maintaining photosynthetic capacity per unit leaf area at an approximately consistent level: in this case, approximately  $9.0 \mu\text{molC s}^{-1} \text{ m}^{-2}$  leaf area at  $2000 \mu\text{mol photons PAR}$  (subject to the absolute accuracy of the MODIS-derived LAI estimates). This is expected given that the most economic strategy for plants is to maintain photosynthetic capacity per unit leaf area, thereby reducing unnecessary investment in additional leaf area (Lambers *et al.*, 2008). As such, rates of photosynthetic fixation of carbon across different biomes collapse to a relatively narrow range when normalised by leaf area ( $1\text{-}3 \text{gC m}^{-2} \text{ leaf area d}^{-1}$ ) (Chapin *et al.*, 2002), as was observed at Nimmo.

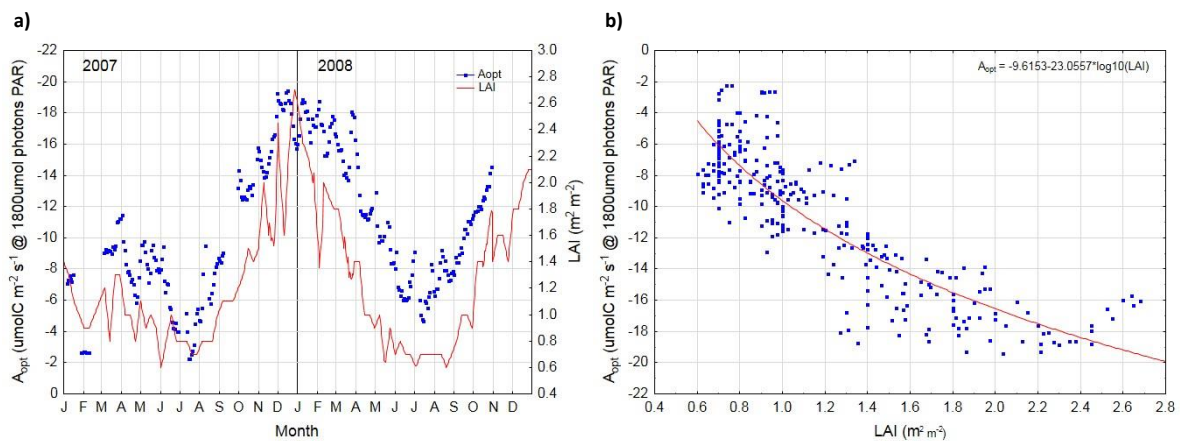


Figure 7.13: a) comparison of 2007/08 LAI and  $A_{opt}$  for Nimmo site; b) relationship between MODIS LAI and  $A_{opt}$  at Nimmo site.

This suggests that the proximate driver of variations in  $A_{opt}$  is LAI, whereas abiotic controls affect  $A_{opt}$  indirectly, via the canopy's control of leaf area. It is reasonable to expect this also to be the case at Dargo. However, linkages are drawn directly between  $A_{opt}$  and abiotic controls below, both because of the lack of ground-truthing of the MODIS data and the fact that there is no reliable MODIS data for Dargo due to the previously noted pixel classification problem (section 7.3.1). Nonetheless, since the above analysis indicates that most of the variation in  $A_{opt}$  is associated with changes in leaf area, the following discussion is couched in terms of phenological changes.

#### 7.4.2.2 Meteorological drivers of light response

The use of a light response function allows parameters to vary over time, and in turn relationships between those parameters and abiotic (e.g. meteorological) drivers can be analysed. Here the responses of  $A_{\text{opt}}$  to the following drivers are examined: temperature<sup>31</sup>, photoperiod, vapour pressure deficit (VPD)<sup>32</sup> and soil moisture availability. As detailed in Chapter 2 (section 2.4.2), these variables are well-documented drivers of variations in photosynthetic activity. Seasonal variation in  $A_{\text{opt}}$  is expected to reflect the effects of different controls exerting influence at different times of the year. While temperature and photoperiod are limiting during the cooler months (i.e. mid-autumn to mid-spring), the effects of VPD and soil moisture are more likely to be limiting during the warmest months (i.e. largely during summer, since these ecosystems are relatively cool and moist for most of the year), when photosynthetic sensitivities cross critical thresholds.

Thus optimum conditions for photosynthesis are expected to occur in periods when thermal / photoperiod and soil moisture / humidity limitations are at a minimum. Accordingly, at both sites, maximum photosynthesis appeared to be achieved at approximately 15°C, as indicated by GPP when plotted as a function of both temperature and insolation (Figure 7.14). This is a typical optimum temperature for photosynthesis for temperate C3-dominated ecosystems (Körner, 2003). The apparent decline in GPP at higher temperatures does not indicate effects of temperature *per se*, since alpine plants show thermal inhibition of photosynthesis only at very high temperatures (>38°C) (Körner, 2003). Instead, this is thought to reflect the effects of soil moisture availability and VPD, as noted above (and discussed in further detail below).

---

<sup>31</sup> With respect to temperature, here mean radiant daytime (insolation >10Wm<sup>-2</sup>) surface temperature (herein surface temperature) is used, since it represents the temperature actually experienced by the canopy. As also noted previously, there may be substantial divergence between screen level air temperature and short-statured vegetation, which are often more closely-coupled to the radiative rather than thermal environment (see Chapter 2, section 2.3.10 for discussion).

<sup>32</sup> As discussed in Chapter 3 (section 3.7.2), it was not possible to model the effects of VPD as part of the light response analysis due to over-parameterisation. However, in addition to short-term effects on stomatal aperture, high VPD for sustained periods may also result in reduced leaf area, which is expected to be reflected in changes in light response parameters during summer.

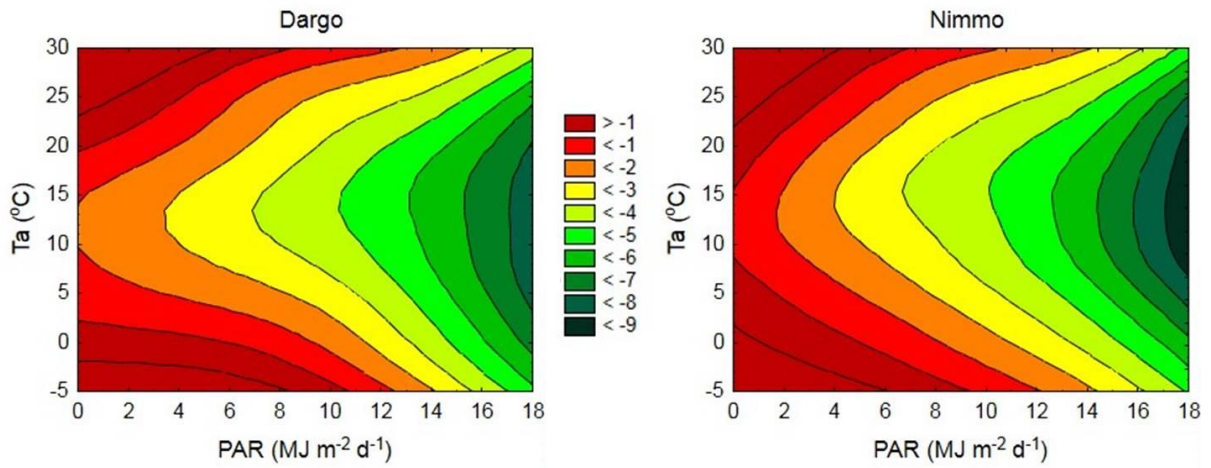


Figure 7.14: daily GPP as a function of air temperature ( $T_a$ ) and photosynthetically active radiation (PAR) for: a) Dargo, and; b) Nimmo.

Some indication of the relative effects of temperature and photoperiod can be gained from examination of phase consistency between  $A_{opt}$  and surface temperature and photoperiod (Figure 7.15). Temperature lagged photoperiod by approximately one month. At both sites, between April and October  $A_{opt}$  was generally in phase with temperature and out of phase with photoperiod. While it is not possible to assess the timing of the minimum value for  $A_{opt}$  at Dargo due to the presence of snow during winter, at Nimmo minimum  $A_{opt}$  approximately coincided with minimum temperature in July. In contrast, the photoperiod minimum occurs at the winter (June) solstice.



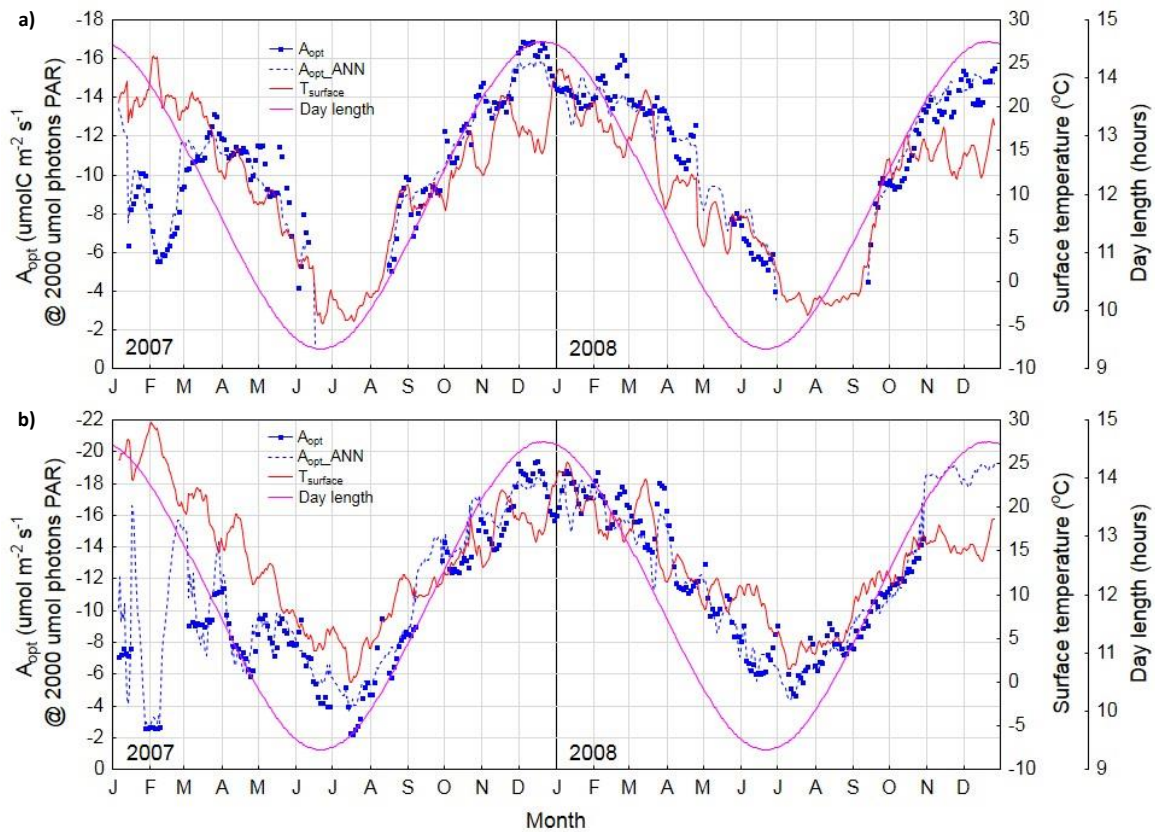


Figure 7.15: comparison of time series of  $A_{opt}$  with surface temperature and photoperiod for: a) Dargo and; b) Nimmo (note – dashed line represents artificial neural network [ANN] model output for  $A_{opt}$  with surface temperature, day length, soil moisture and vapour pressure deficit as input variables).

Accordingly, at Dargo surface temperature explained approximately 67% of the variance in  $A_{opt}$  below 15°C (Table 7.6). Above this threshold, temperature explained only 17% of the variance in  $A_{opt}$ . Photoperiod explained 44% of the variance in  $A_{opt}$  at temperatures below 15°C, and 10% at temperatures above 15°C. At Nimmo, similar results to those of Dargo were observed above 15°C (i.e. low correlation with both temperature and photoperiod), and below 15°C both temperature and photoperiod explained approximately 55% of the variance in  $A_{opt}$ .

**Table 7.6: coefficient of determination ( $r^2$ ) for regression of  $A_{opt}$  on driving variables above and below threshold temperature of 15°C (note: all correlations statistically significant at  $p < 0.05$  except soil moisture  $\leq 15^\circ\text{C}$  at Nimmo).**

	Dargo				Nimmo			
	$\leq 15^\circ\text{C}$			$> 15^\circ\text{C}$	$\leq 15^\circ\text{C}$			$> 15^\circ\text{C}$
	Month<7	All	Month>6		Month<7	All	Month>6	
Temperature	0.7	0.67	0.63	0.17	0.29	0.54	0.76	0.22
Photoperiod	0.82	0.59	0.84	0.10	0.66	0.56	0.83	0.17
VPD		0.13		0.04		0.3		0.13
Soil moisture		0.07		0.56		0.01		0.46

However, since photoperiod and temperature are closely correlated ( $r^2=0.68$  and  $0.65$  for Dargo and Nimmo, respectively), it is difficult to reliably assess their effects independently. Nonetheless, it is well documented that growth initiation is strongly tied to spring temperatures, whereas photoperiod is a more important control on down-regulation of growth during autumn (Ram *et al.*, 1988; Yi *et al.*, 2010; Migliavacca *et al.*, 2011). This is because the lag in phase of seasonal temperature dictates that during autumn, lower insolation occurs at a given temperature than during spring. Given that the system responds to the condition which is most limiting, it is expected that light levels are a more important constraint during autumn, and temperature more important during spring.

At Nimmo, in both years (but particularly during 2008), there were sustained periods during autumn / early winter during which temperatures temporarily stopped declining, thus degrading correlation between temperature and photoperiod ( $r^2 = 0.54$ ). During this period (confined to temperatures  $< 15^\circ\text{C}$  and the period preceding the beginning of July), there was much stronger correlation of  $A_{opt}$  with photoperiod ( $r^2 = 0.66$ ) than with temperature ( $r^2 = 0.29$ ). This is thus consistent with the expectation of autumn primary photoperiodic control of phenology as noted above.

On the other hand, during the subsequent midwinter / spring period when temperatures were increasing (confined to temperatures  $< 15^\circ\text{C}$  and the period succeeding the end of June), there was strong correlation of  $A_{opt}$  with temperature ( $r^2 = 0.76$ ). However, this does not confirm that temperature was the primary control, since correlation of  $A_{opt}$  with photoperiod during this period was even higher ( $r^2 = 0.83$ ). Thus some degree of photoperiodic control of phenological development of the canopy cannot be ruled out, since spring growth initiation is photoperiod-dependent in some alpine species (Keller and Körner, 2003). Moreover, following growth initiation in

spring, the sensitivity of canopy phenology to temperature may be photoperiod dependent (Keller and Körner, 2003). The data available here are however insufficient to tease out such complex relationships, and the observed correlations in spring may also simply reflect the strong correlation between temperature and photoperiod during this period ( $r^2 = 0.83$ ), in combination with the limited statistical sample available and chance effects of noise in the  $A_{opt}$  estimates (in turn propagated from the eddy covariance measurements).

At Dargo, the correlation of  $A_{opt}$  with temperature was similar between the late autumn temperature decline (using the same periods as defined above;  $r^2 = 0.69$ ) and early spring increase ( $r^2 = 0.63$ ) periods. The correlation between photoperiod and  $A_{opt}$  was also similar between these two periods, but substantially higher ( $r^2 = 0.82$  and  $0.84$ , respectively). However, the correlation between temperature and day length was lower ( $r^2 = 0.65$  and  $0.59$  for the two periods, respectively), making it less likely that the high correlation between photoperiod and  $A_{opt}$  is simply an artefact of the correlation between photoperiod and temperature. As noted above, growth initiation and subsequent temperature response during the early growing season may be photoperiod-dependent. This therefore implies that photoperiod may also be important in the phenological development of the canopy at Dargo during spring. However, as previously noted, there is insufficient data to explore these hypotheses in further detail.

But of key importance in this study is what controls the difference in  $A_{opt}$  between sites. In the discussion above, while there are conceivably cross-site differences in ecosystem response to photoperiod, differences in photoperiod itself are negligible (the sites are separated by less than  $1^\circ$  of latitude). In contrast, while daytime temperatures at the sites are highly correlated because of their close proximity, temperatures are systematically lower at Dargo, largely due to the adiabatic effects of higher altitude (5, section 5.3.1). However, the temperature response of  $A_{opt}$  across the range of mean daytime surface temperatures generally experienced at the sites was statistically indistinguishable (Figure 7.16). Specifically, the trend in the relationship is statistically significantly different from zero at both sites, but the difference in trend *between* sites is not statistically significant. The relationship between temperature and  $A_{opt}$  also appears to be largely confined to the interval  $0-15^\circ\text{C}$ , above which the relationship appears to break down. This reflects the effects of dry conditions (low soil moisture and / or high vapour pressure deficits) at higher temperatures, as also seen in Figure 7.14 (and see discussion below).

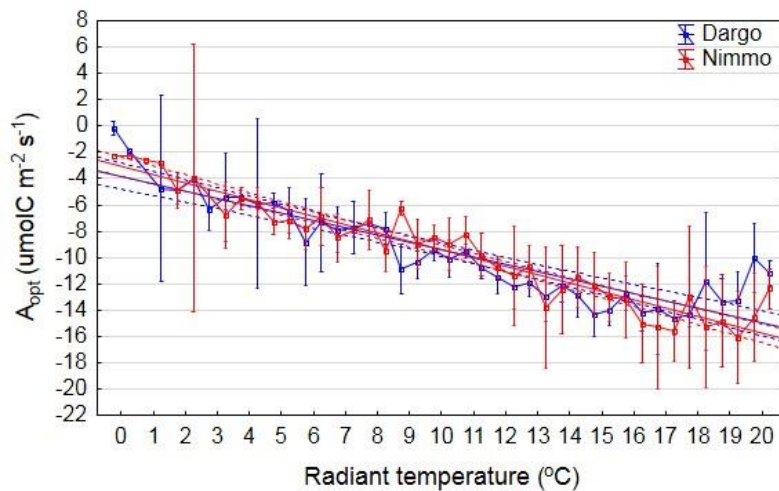


Figure 7.16: mean ( $\pm 95\text{CI}$ )  $A_{\text{opt}}$  binned by  $1^\circ\text{C}$  temperature increments for Dargo and Nimmo (solid line represents regression line, and dashed lines the  $95\text{CI}$  of the regression).

As such, this suggests that the difference in  $A_{\text{opt}}$  between sites during periods of the year when daily mean surface temperatures were below  $15^\circ\text{C}$  was largely determined by temperature. As detailed in section 7.3, cross-site differences in winter and spring carbon balance were responsible for the overwhelming majority of difference in annual carbon balance. In both cases temperature is implicated. In winter, low temperatures caused snow to be retained at Dargo, whereas at Nimmo daytime temperatures were too high for the snowpack to persist. Snow thus resulted in effective  $A_{\text{opt}}$  of zero because the canopy was not exposed to surface irradiance. In spring, when growth is more likely to be tied to temperature rather than photoperiod, the same temperature response at both sites resulted in higher  $A_{\text{opt}}$  at Nimmo due to higher temperatures. While cross-site  $A_{\text{opt}}$  differences were also large in summer, this did not manifest in large differences in NEE because, as previously discussed, the lag of the temperature phase relative to insolation results in a later peak in  $R_e$  that correspondingly reduces NEE. Moreover, the largest difference in temperature between sites also occurs in summer, which increases  $R_e$  at Nimmo and further erodes cross-site NEE differences. In autumn, differences in  $A_{\text{opt}}$  were small, and may reflect the fact that  $A_{\text{opt}}$  is tied more closely to photoperiod, which doesn't vary substantially across the sites.

The site responses to the remaining control variables were similar. VPD explained approximately 30% of the variance in  $A_{\text{opt}}$  below  $15^\circ\text{C}$  at both sites; however, at high temperatures there was only weak correlation with  $A_{\text{opt}}$ . This is the opposite of what might be expected in these ecosystems. Cross-correlation between temperature and VPD is thought to explain the observed correlation of VPD with  $A_{\text{opt}}$  at low temperatures, since seasonal variations in temperature are a strong driver of VPD. While high VPD is expected to induce progressive stomatal closure, rate

limitation of photosynthesis due to reduced stomatal conductance begins at approximately 1kPa, with non-linear declines to complete stomatal closure at approximately 4kPa (even where soils are moist) (Osonubi and Davies, 1980; Tenhunen *et al.*, 1982; Körner, 1995). At both sites, the number of days with mean VPD greater than this threshold for days below 15°C is zero (although on several days the *maximum* VPD exceeded 1.5kPa).

While VPD exceeded 1kPa regularly during the warmer months, since ecophysiologicaly-relevant VPD variations occur at much shorter time scales than the window used to fit the light response (10 days), it is unlikely that a meaningful correlation would be found with  $A_{opt}$ . Instead, the effects of VPD should be accounted for in the light response model itself; however, as noted in section 3.7.2, models that included a function to account for VPD performed poorly, and it was thus excluded from the light response analysis. The fact that this did not result in any clear distortion of  $R_e$  estimates relative to those estimated from nocturnal data suggests that the effects of VPD are limited in this study. This may relate to the fact that strong VPD effects (i.e. when VPD was substantially above the ecological threshold) would be confined to a limited period during the warmest months. Moreover, as noted previously, due to aerodynamic decoupling of the relatively smooth grassland surface from the atmosphere, VPD at the leaf surface may be substantially different to VPD measured at screen level, thereby degrading correlation when the latter is used. This therefore suggests that the proportion of variance in the data that may be explained by VPD does not rise above the noise.

On the other hand, soil moisture appears to be a much more important control of variations in  $A_{opt}$  at temperatures >15°C. At Dargo, soil moisture content explained approximately 56% of the variance in  $A_{opt}$ , and a slightly lower proportion (46%) at Nimmo. In contrast, below 15°C, variations in soil moisture were only weakly correlated with  $A_{opt}$  (and this correlation was only significant at  $p < 0.05$  at Dargo). This is also consistent with the expectation that soil moisture effects are only significant when soil moisture falls below a given threshold. The correlation at low temperatures at Dargo may simply be explained by the fact that the highest soil moistures were observed during winter (when  $A_{opt}$  was at a minimum) and progressively reduced with increasing temperature.

A linear regression model is also unlikely to be a strictly accurate model to describe the effects of control variables on plant phenology. Plants are generally sensitive to abiotic controls within certain ranges, but may be relatively insensitive outside these ranges. Given that the seasonal variation in  $A_{opt}$  can largely be explained by variations in LAI, a simple foliar phenology model may be able to capture variations in  $A_{opt}$  as a function of simple climatic indices known to influence foliar phenology (as manifest in LAI). The growing season index (GSI) model used here is a simplified

version of that used by Jolly *et al.* (2005), in which soil moisture is included but vapour pressure deficit is excluded<sup>33</sup> (see Chapter 3.7.33, section 3.7.3 for further description).

At Dargo, the GSI model using ramp functions for 3 variables - temperature, photoperiod and volumetric water content - explained 88% of the variance in  $A_{opt}$  (Figure 7.17; the inclusion of VPD increased the coefficient of determination by less than 1% - for this and the reasons noted above, VPD was thus excluded). The model suggests that during autumn, both temperature and photoperiod contributed to the reduction in  $A_{opt}$  (again, since this is a phenological model, it is hypothesised that changes in  $A_{opt}$  primarily reflect changes in LAI), whereas during spring, temperature was far more important; this is consistent with literature findings, as previously noted. This is particularly the case at Dargo, since snow cover remained in place for 1-2 months after the solstice, even as photoperiod increases.

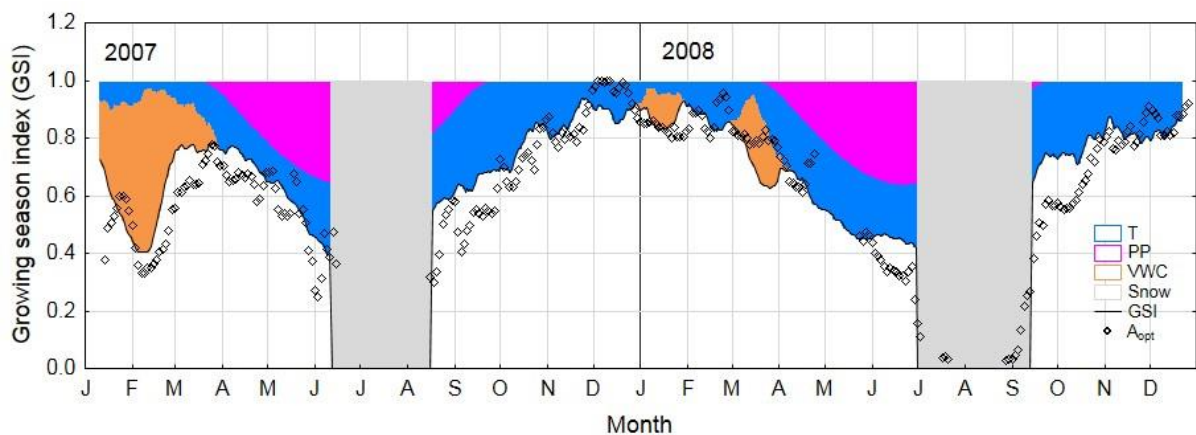


Figure 7.17: 2007/08 comparison of Dargo normalised  $A_{opt}$  ( $A_{opt} / A_{opt\_max}$ ) with growing season index and associated ramp function scalars (see Chapter 3, section 3.7.3) for temperature (T), photoperiod (PP), volumetric water content (VWC) and snow cover (Snow).

It is also clear from Figure 7.17 that there are particular periods when the simple phenological model fails to capture sub-seasonal variations in  $A_{opt}$ , particularly at the beginning and end of the snow season. The reasons for this are unknown, and most likely simply relate to the simplicity of the model - which nonetheless captures the seasonal dynamics of  $A_{opt}$  well - and potential errors or biases in the derivation of  $A_{opt}$ . There is also some evidence that the soil moisture response was overestimated in 2008 (and slightly underestimated in 2007), for example during

<sup>33</sup> Vapour pressure deficit was found to improve the coefficient of determination by less than 1%; however, it led to poorly constrained ramp function parameters, most likely because it is strongly correlated with temperature. For this reason, and for those reasons previously discussed, it was excluded from the analysis.

March when low soil moisture induces a downturn in GSI that is not reflected in the normalised value of  $A_{opt}$  (i.e. the value of  $A_{opt}$  as a proportion of its maximum value).

This soil moisture effect was more pronounced at Nimmo (Figure 7.18). When the entire two-year period was used to fit the ramp function parameters to estimate GSI, the result was substantial overestimation of the soil moisture response in 2008, and GSI was overall a substantially poorer estimator of  $A_{opt}$  ( $r^2 = 0.68$ ) relative to Dargo. This may be indicative of the fact that more severe drought during 2006 (because of the already drier nature of the site) accentuated the effect discussed above – antecedent conditions contributed to the subsequent ecosystem state with respect to live leaf area, such that this effect was artificially attributed to soil moisture due to the overly simplistic GSI model. This is most likely accentuated by the fact that there was less available data during the first 2 months of 2007 at Nimmo due to system malfunction.

Relative to Dargo, at Nimmo there was a much more substantial mismatch between GSI and normalised  $A_{opt}$  during spring of 2007. This indicates that the photosynthetic capacity of the ecosystem as observed was less than predicted on the basis of simple climate indices. This may also reflect the ongoing effects of prior drought, since drought effects at Nimmo were also prevalent during autumn. As such, it is possible that recovery of the photosynthetic capacity of the canopy – via new growth – occurred during spring, such that by the end of 2007, there was convergence between estimates of GSI and normalised  $A_{opt}$ .

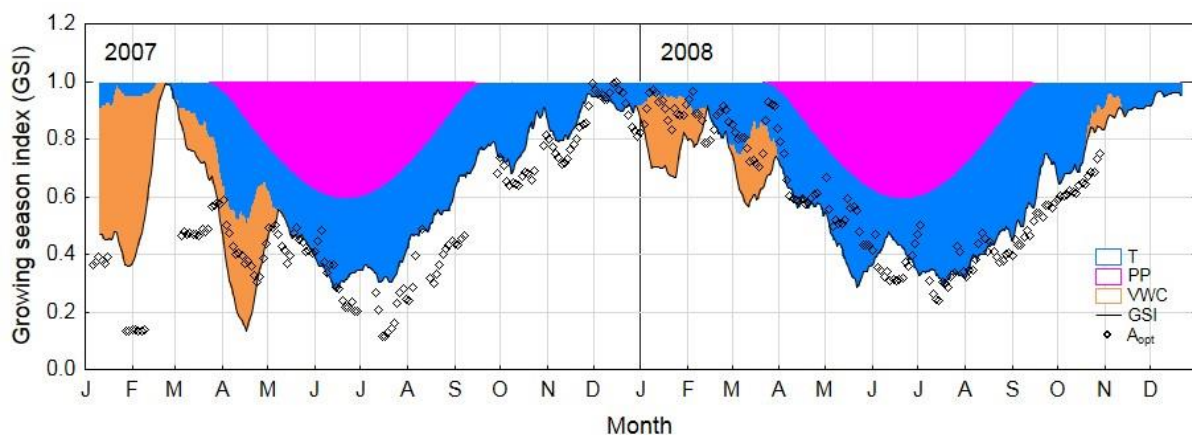


Figure 7.18: 2007/08 comparison of Nimmo normalised  $A_{opt}$  ( $A_{opt} / A_{opt\_max}$ ) with growing season index and associated ramp function scalars (see Chapter 3, section 3.7.3) for temperature (T), photoperiod (PP) and volumetric water content (VWC).

For both sites, soil moisture was largely superfluous in 2008. For example, a simplified model of GSI using only temperature and photoperiod and optimised using data from 2008 was able to explain 94% of the variance in  $A_{\text{opt}}$  at Dargo for that year (Figure 7.19). At Nimmo, the proportion of variance explained was lower but nonetheless large, at 85%. The addition of soil moisture had a very weak effect on the coefficient of determination ( $r^2$ ), which increased by 2% at Dargo and actually decreased by 1% at Nimmo. However, when the drivers for 2007 were used in conjunction with the parameters optimised for 2008, this model was a relatively poor predictor of  $A_{\text{opt}}$  in 2007, with  $r^2$  falling to 0.43 and 0.44 for Dargo and Nimmo, respectively. This was because there was little apparent response of  $A_{\text{opt}}$  to soil moisture in 2008, and thus the soil moisture response was underestimated during 2007.

A GSI model using only temperature and photoperiod optimised using 2007 data was only a marginally better predictor of  $A_{\text{opt}}$  in that year ( $r^2 = 0.37$  and  $0.43$  for Dargo and Nimmo, respectively), underscoring the greater importance of low soil moisture in 2007. Figure 7.19 also demonstrates the different soil moisture responses between years at the sites. At Dargo, a GSI model that includes temperature, photoperiod and soil moisture that was optimised using 2007 data ( $r^2 = 0.81$  for 2007) was also a good predictor of  $A_{\text{opt}}$  in 2008 ( $r^2 = 0.88$ ). This is because the soil moisture response was less pronounced during 2007, and soil moisture was generally higher, in 2008. At Nimmo, this was not the case; the model optimised for 2007 conditions ( $r^2 = 0.78$  for that year) was far too sensitive to soil moisture in 2008, such that  $r^2$  was reduced to 0.51. Again, this indicates a larger effect of dry conditions at Nimmo in 2007, although it should be reiterated that the soil moisture effect during 2007 at Nimmo is highly uncertain, due to the limited amount of data available during the driest period.



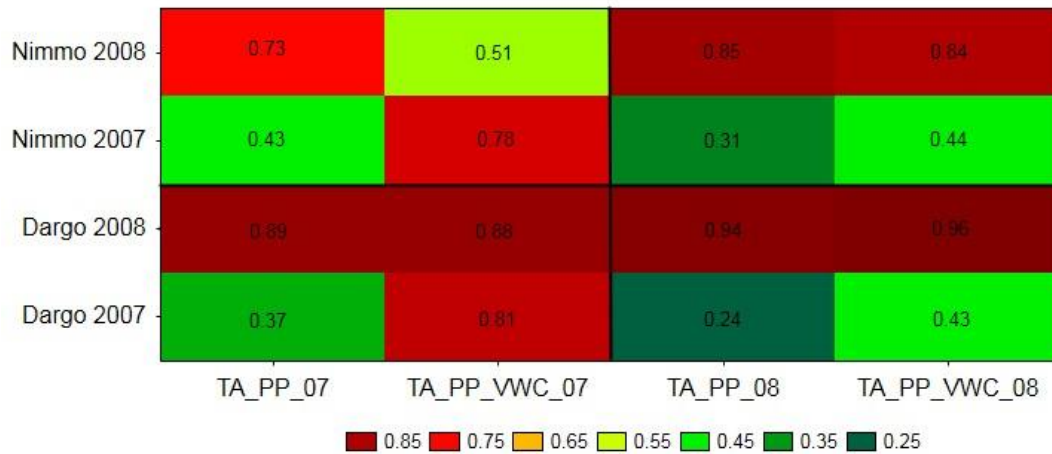


Figure 7.19: coefficient of determination ( $r^2$ ) between GSI and  $A_{opt}$  for model and data years. Text labels on the x axis represents the GSI model type and optimisation year: TA\_PP\_07 represent GSI models that use temperature and photoperiod as input variables and that were optimised using 2007 data, with TA\_PP\_VWC\_07 using volumetric water content as an additional variable and optimisation year 2007 etc.; text labels on the y axis represent the data year against which the relevant model output (forced using data from that year) was regressed. So, for example, the tile at  $x = \text{Ta\_PP\_07}$  and  $y = \text{Dargo 2008}$  represents the coefficient of determination for the  $A_{opt}$  estimates from 2008 regressed against the model output using 2008 climate drivers and 2007 parameters.

Due to this uncertainty, a robust comparison of cross-site soil moisture sensitivity of  $A_{opt}$  is not possible. At Dargo, the ramp function parameters yield a soil moisture response of  $A_{opt}$  almost identical to that for respiration (Figure 7.20). This is expected, given that a substantial component of respiration is underpinned by short-term assimilate supply provided by GPP, such that reductions in GPP are mirrored in  $R_e$  (see for example Bahn *et al.*, 2008). However, it is also the case that GPP is not measured by the eddy covariance system but is calculated by subtracting extrapolated daytime values of  $R_e$  from NEE. As such, any artefacts introduced when using response functions to estimate  $R_e$  necessarily map to GPP, so it is in principal possible that such agreement is simply an artefact of the analysis approach. Although the broader approach to modelling of respiration was independently validated in this study using chamber measurements (see Chapter 4, section 4.2.2.3), these measurements were not undertaken during a period of low soil moisture, and the accuracy of the soil moisture response function cannot be independently verified. Nonetheless, the results are consistent with theoretical expectation.

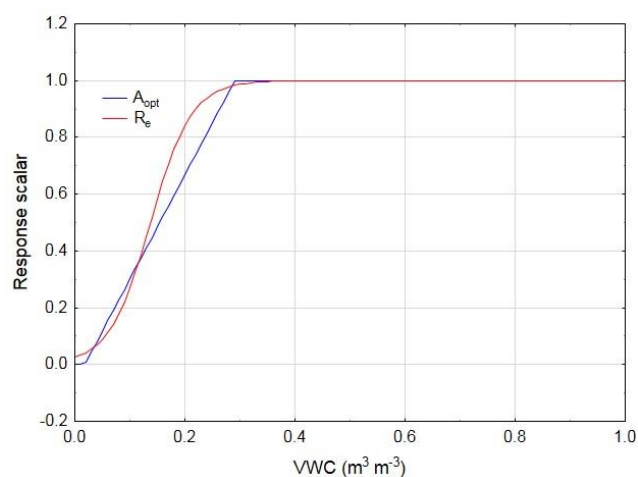


Figure 7.20: comparison of GSI model temperature response scalars for  $A_{opt}$  with sigmoid response scalar for  $R_e$  at Dargo.

With respect to temperature, the optimisation parameters (Table 7.7) and corresponding temperature responses defined by the GSI ramp function (Figure 7.21) were similar at the sites, further supporting the previous discussion noting that differences in  $A_{opt}$  are primarily a function of differences in temperature rather than differences in ecosystem response to temperature (note that these parameters are for the 2008 year, given that the effects of low soil moisture can largely be ignored for that year). While the absolute values for temperature are different, the GSI model uses minimum rather than mean temperatures and thus the optimum temperature is lower than the optimum temperature of 15°C indicated by the previous analysis.

Table 7.7: ramp function parameters for temperature ( $T$ , °C) and photoperiod (PP, hours) minima and maxima for simplified GSI model (optimised using 2008 data).

	Dargo	Nimmo
$T_{min}$	-7.9	-8.4
$T_{max}$	6.2	7.4
$PP_{min}$	7.0	8.1
$PP_{max}$	10.4	10.7

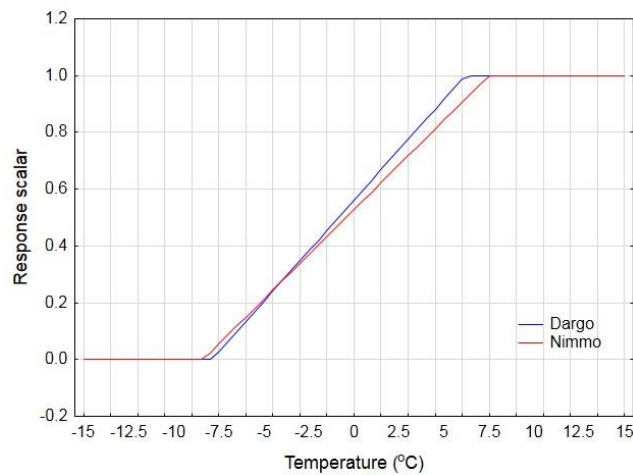


Figure 7.21: GSI model temperature response scalars for  $A_{opt}$  at Dargo and Nimmo derived from response parameters in Table 7.7.

#### 7.4.2.3 Discussion

The previous analysis demonstrates that cross-site GPP differences (in the absence of snow cover) were primarily associated with differences in light response; specifically, while the response to low light conditions was comparable across the sites, under higher light levels photosynthesis was generally higher at Nimmo. While insolation was very slightly lower at Dargo, this difference was inconsequential with respect to GPP differences – it was the *response* to insolation that was key in GPP differences. Seasonal variations in light response were strongly correlated with remotely-sensed estimates of LAI at Nimmo, suggesting that they largely reflect variations in foliar phenology. While it is considered probable that the observed cross-site systematic differences in light response are also explained by LAI differences, this cannot be rigorously tested given the uncertainties in the remotely-sensed data, which were clearly invalid at Dargo.

As noted above, this is thought to primarily reflect variations in leaf area, and a simple foliar phenology model proved highly successful in modelling seasonal variations in light response. Simple regression analysis suggests that temperature and photoperiod are the key controls of canopy light response at temperatures below approximately 15°C, although given the strong correlation between these variables, it is not possible given the limited data in this study to confidently extricate the precise relationships. Nonetheless, there is some evidence to suggest that – in common with findings in the literature – temperature is a more important control during spring, and photoperiod more important during autumn.

Most importantly, the relationship between light response and temperature was indistinguishable at the sites; this was clear both from the simple approach of comparing the linear trend in  $A_{opt}$  as a function of temperature, and the optimisation of the parameters in the growing season index (GSI) model to capture the seasonal variation in  $A_{opt}$ . Thus this suggests that GPP at the sites is effectively equivalent when the effects of temperature on  $A_{opt}$  (which is strongly correlated with and is therefore a useful approximator of LAI) are accounted for. Thus higher GPP at Nimmo is largely a function of higher temperatures.

In years with plentiful soil moisture, the GSI model indicates that most of the variance in  $A_{opt}$  (i.e. 85-95%) could be captured using only 2 parameters: minimum temperature and photoperiod. It has been concluded elsewhere that these parameters are the key controls on foliar phenology in the mid and high latitudes (Myneni *et al.*, 1997; White *et al.*, 1997). In dry years, however, soil moisture was required to accurately estimate light response parameters using the GSI model. At both sites, there was evidence to suggest that when a GSI model that included soil moisture was optimised using 2007 data, there was a tendency towards overestimation of the sensitivity of the ecosystem to soil moisture in 2008. This was far more pronounced at Nimmo.

Previously, the discussion touched on the fact that the low GPP at Nimmo in summer 2007 (the only time during which it was lower than at Dargo) may be associated not only with soil moisture conditions at the time, but the cumulative effects of antecedent drought on canopy foliar development (see section 7.3.1). As previously discussed, this drought was particularly severe in 2006 (see Chapter 5, section 5.4), and this may have either reduced growth or increased mortality during spring, thereby reducing the leaf area available to support photosynthesis. Thus if antecedent conditions impose lagged effects on LAI, these effects are artificially loaded onto the instantaneous effect of low soil moisture (as a result of the assumption implicit in the model that all soil moisture response is instantaneous), and following recovery of the canopy in subsequent growing seasons may result in overestimation of the physiological response to low soil moisture.

The fact that this effect appears to be more pronounced at Nimmo - the first 6 months of 2007 were the only time when the light response was less at than at Dargo - may reflect the fact that as an already drier site, plant growth at Nimmo is more likely to be affected by regional drought. As previously noted, plant growth and carbon balance are more sensitive to drought conditions in already dry ecosystems (Wohlfahrt *et al.*, 2008; Gilgen and Buchmann, 2009). This also supports the previous discussion with respect to ecosystem respiration ( $R_e$ ) at the sites (section 7.4.1.3). It was established that the relative reduction in  $R_e$  associated with low soil moisture was similar at the sites, and the lower  $R_e$  at Nimmo in 2007 was primarily due to the low  $R_e$  at higher temperatures i.e.

in the summer months at the start of the year. There it was argued that assimilate supply at Nimmo may be reduced because of the larger cumulative effects of antecedent drought on plant growth in the latter part of 2006, and subsequent effects on leaf area and corresponding canopy photosynthetic capacity carrying over into 2007.

Some caution is nonetheless required in the interpretation of soil moisture effects on ecosystem light response, because of the limited amount of data available at Nimmo in early 2007, in combination with the fact that GPP and  $R_e$  are not independent quantities. For example, systematic underestimation of  $R_e$  will result in corresponding underestimation of GPP, since GPP is calculated as the difference between NEE and  $R_e$ . Nonetheless, the uncertainty in estimation of  $R_e$  is likely far less than that for secondary quantities derived from GPP such as light response parameters, because the use of long time windows (in this case 10 days) to derive the latter drastically reduces the data available for parameter optimisation, whereas the response parameters applied to the respiration data were applied using half-hourly data, with a correspondingly much larger number of points available for model optimisation.

As such, between its indirect (snow cover) and direct (photosynthetic capacity) effects, temperature was the key control of cross-site differences in GPP – and thereby NEE, with soil moisture as a secondary, short term control that was only important in early 2007. While it is considered likely that in the longer-term, differences in soil moisture would contribute substantially to differences in interannual variability of NEE, a longer dataset would be required to establish whether this is the case.

## 7.5 Summary

Both Dargo and Nimmo were net carbon sinks during both years, but the magnitude of the carbon sink was larger at the warmer Nimmo site. The difference in NEE between sites was primarily due to differences in GPP rather than  $R_e$ . In turn this was primarily due to the winter cessation of photosynthesis at Dargo due to low temperatures. Even during the snow-free period, however, the bulk canopy photosynthetic capacity was slightly higher at Nimmo, resulting in higher GPP, particularly during spring (this was also the period of the highest GPP: $R_e$  at both sites, due to the phase lag of temperature relative to insolation). The relationship between photosynthetic capacity and temperature was indistinguishable between the sites, indicating that the observed difference in photosynthetic capacity was related to the cooler daytime temperatures at Dargo. In turn, the very

strong relationship between photosynthetic capacity and leaf area at Nimmo suggests that temperature primarily controls photosynthetic capacity via its effect on canopy phenological development (while photoperiod is also a well-established control on this development - and most likely contributed to regulation of photosynthetic capacity, particularly in autumn - the difference in photoperiod at the sites was negligible owing to their similar latitudes). Consistent with this, a simple phenological model was able to capture most of the seasonal variation in photosynthetic capacity of the canopy using only temperature, photoperiod and soil moisture as drivers.

Both sites were also sensitive to the effects of low soil moisture, with strong reductions in GPP in the early months of 2007 relative to 2008. As previously noted, the summer and early autumn months of 2007 were the driest observed during the study period. In comparison, there was relatively high summer rainfall during 2008. At Nimmo, the increased carbon uptake during summer 2008 translated to higher annual carbon uptake, since the carbon balance was comparable across years during the other seasons. There was evidence that GPP was more constrained by soil moisture at the drier Nimmo site in early 2007 than at Dargo, and that the lower photosynthetic capacity of the canopy during this time may be partly associated with prior effects of drought. Dry conditions also constrained GPP at Dargo during summer 2007, but enhanced summer carbon uptake during 2008 was offset by stronger winter carbon release, such that there was relatively little difference in annual carbon balance between years. This was due to a longer and later snow season in winter. In the following chapter, the discussion turns to reconciliation of the results of Chapter 6 (carbon storage) and those from the current chapter (carbon exchange).

## 8. Reconciling patterns of carbon storage and exchange

---

In Chapter 6 it was documented that the total carbon storage at Dargo was nearly 50% higher than at Nimmo (and over 95% of carbon storage was in the soil). It was also noted that globally, soil carbon storage is negatively correlated with temperature and positively correlated with rainfall. This is approximately consistent with the results documented here: the warmer, drier Nimmo stored far less soil carbon than the cooler, wetter Dargo.

In Chapter 7, while it was found that both sites were annual net carbon sinks, carbon uptake at Nimmo was twofold higher than at Dargo in 2007, and threefold higher in 2008. This was primarily due to the effects of higher temperatures on GPP at the sites. Higher daytime temperatures prevented the establishment of a sustained winter snowpack at Nimmo, and as outlined previously, available evidence suggests that higher temperatures also increased photosynthesis at Nimmo during the snow free period.

Thus the site with much lower soil carbon storage had much higher annual carbon uptake. This apparent discrepancy is most likely associated with the fact that the measurement period for this study was too short to capture the full range of climatic variability that in turn drives the carbon dynamics of these ecosystems i.e. a much longer measurement period is required to deduce the mean state of the system. Thus annual carbon balances must be interpreted in the context of this climatic variability, as discussed further below. Other possible explanations include: systematic measurement error and corresponding biasing of results; significant non-CO<sub>2</sub> atmospheric / non-atmospheric terms contributing to the carbon balance, and; observed changes in climate in recent decades that have begun to drive changes in ecosystem / atmosphere exchanges of carbon, while patterns of carbon storage still substantially reflect the dynamics of a quasi-stationary past. For reasons that will be discussed subsequently, these explanations are considered much less likely.

## 8.1 Effects of climate variability

As previously noted, the study period encompassed the end of a severe drought, and a comparatively non-limiting soil moisture environment in the following year (due to abundant 2007/08 summer rainfall). However, it is almost certainly the case that longer period would be required to adequately capture the mean behaviour of the carbon balance of the respective ecosystems, particularly given the strong effects of the quasi-decadal El Niño Southern Oscillation on interannual climatic variability in south-eastern Australia (Sturman and Tapper, 2005). In this respect, the stronger carbon uptake of the site at Nimmo may reflect the fact that the interannual amplitude of the carbon balance in response to climatic variability is larger at that site, and the study period represented a short window (in which the sites were exposed to the last stages of drought before the resumption of more moist conditions) within a longer oscillation.

The reasons why stronger interannual variability might be expected at Nimmo have been alluded to in the previous chapter. Mountain grasslands are often relatively unaffected by drought, because the combination of orographic rainfall and low evaporative demand - due to low temperatures - results in relatively moist ecosystems. Since stomatal conductance (and correspondingly photosynthetic capacity) in plants is relatively insensitive to soil moisture availability above a given threshold (Chapin *et al.*, 2002), the carbon balance may be unconstrained by low soil moisture even during summer if evaporative demand is low (due to lower temperatures at higher altitudes) and / or precipitation is high (due to orographic inducement). However, mountain grasslands in drier regions are more sensitive to the effects of drought (Wohlfahrt *et al.*, 2008; Gilgen and Buchmann, 2009). Specifically, since drought constrains GPP more than  $R_e$ , the result of drought conditions is generally to shift the ecosystem carbon balance towards net carbon efflux. As such, since lowland grasslands are primarily water limited (Sala, 2001), plant productivity (Knapp and Smith, 2001) and thus carbon balance (Yi *et al.*, 2012) among lowland grasslands is among the most interannually variable of all biomes (see, for example: Flanagan *et al.*, 2002; Suyker *et al.*, 2003; Jaksic *et al.*, 2006; Nagy *et al.*, 2007; Aires *et al.*, 2008). Thus whereas the range of variation of annual mountain grassland NEE uncovered in the literature was approximately +250 to -290gC m<sup>-2</sup> a<sup>-1</sup> (see Chapter 2, section 2.4.4), for grasslands generally Novick *et al.* (2004) report annual NEE of between +400 and -800gC m<sup>-2</sup> a<sup>-1</sup>, while Gilmanov *et al.* (2007) report a range of +160 to -650gC m<sup>-2</sup> a<sup>-1</sup>.

As detailed in Chapter 5, relative to Dargo, the climate of Nimmo is characterised by both higher temperatures (due to adiabatic altitude effects), resulting in higher evaporative demand, and



- in combination with lower rainfall (due to the rain shadow effects of the Australian Alps) - consequently lower soil moisture availability. If it is assumed that over a sufficient period of time, the carbon balance is in approximate equilibrium at both sites, periodic counterbalancing losses must also occur (since net carbon gains were documented in this study). Among water-limited grasslands, oscillation between net carbon sink and source status are routinely observed in response to periodic drought conditions (e.g. Meyers, 2001; Nagy *et al.*, 2007; Pereira *et al.*, 2007; Jongen *et al.*, 2011). Similarly, mass conservation dictates that periodic carbon losses would necessarily be larger at Nimmo (since net carbon gains were higher at that site, while carbon storage is lower). Such losses would be expected to occur during drought periods as experienced in 2006. Indeed, as documented previously (see section 7.4.2), at Nimmo, leaf area – which is strongly correlated with GPP – was much lower during the 2006-07 growing season than during the same period in 2007/08.

The sensitivity of Nimmo to drought is also demonstrated by the data in the summer period at the beginning of 2007, during which very dry conditions continued to prevail (see Chapter 7, section 7.3.1). The magnitude of GPP increased 74% from  $-315.6\text{gC m}^{-2}$  in 2007 to  $-549.8\text{gC m}^{-2}$  in 2008, with a more pronounced response relative to  $R_e$  (GPP: $R_e$  was 0.99 in summer 2007 and increased to 1.32 in 2008). Thus while the Nimmo grassland was a very weak carbon source during summer 2007 ( $4.7\text{gC m}^{-2}$ ), it switched to a sink of  $-131.6\text{gC m}^{-2}$  in 2008. In comparison, differences in carbon balance in the other seasons were relatively small between years. The dynamics of the summer season were therefore the key explanation for annual NEE differences between years at Nimmo; approximately 83% of the annual increase in GPP at Nimmo from 2007 to 2008 (an increase of 23% from  $1226.2$  to  $1507\text{gC m}^{-2}\text{a}^{-1}$ ) was accrued during summer (with a corresponding annual increase in GPP: $R_e$  from 1.2 to 1.27).

In comparison, at Dargo, summer GPP increased 49% from  $-345.2$  in 2007 to  $-515.2\text{gC m}^{-2}$  in 2008, with a corresponding change in GPP: $R_e$  from 1.05 to 1.28 (for 2007 and 2008, respectively). This translated to a change in summer NEE from  $-16.0\text{gC m}^{-2}$  to  $-112.4\text{gC m}^{-2}$ . However, in contrast to Nimmo, this was largely not reflected in changes in annual NEE because of compensating changes in winter carbon balance (see Chapter 07, section 7.3.3), with GPP decreasing from  $-93.9\text{gC m}^{-2}$  in 2007 to  $-46.0\text{gC m}^{-2}$  in 2008. Simultaneously,  $R_e$  increased from  $155.5\text{gC m}^{-2}$  in 2007 to  $180.7\text{gC m}^{-2}$  in 2008. The corresponding change in GPP: $R_e$  was from 0.6 to 0.25. This largely offset carbon gains accrued during the summer, such that there was only a small increase in carbon uptake at Dargo.

Thus the reason that there was limited change in NEE between years at Dargo was not primarily that the carbon balance was less sensitive to soil moisture variations than at Nimmo. The above analysis demonstrates that the sensitivity of Dargo to drought conditions – in terms of

changes in GPP and GPP: $R_e$  between years – appeared to be moderately less than that observed at Nimmo. But the primary reason that this did not translate to differences in annual NEE was the dynamics of winter carbon balance, which in turn was related to the fact that the snow pack persisted for longer and – critically – until later in 2008 relative to 2007. As previously detailed, changes in the date of establishment of the snowpack between years had limited effect because they occurred around the winter solstice, when insolation (and thus potential photosynthetic activity) is at a minimum. The corresponding increase in  $R_e$  may be related to increases in the labile carbon supply in the soil from 2007 to 2008 due to higher GPP in the preceding growing season (although this is necessarily speculative in the absence of information about partitioning between autotrophic and heterotrophic components).

While over the short study period it is certainly possible that drought conditions and earlier snowmelt were unrelated events, it is characteristic of the dominant driver of interannual climate variability – El Niño Southern Oscillation (ENSO) - that temperature and rainfall are generally inversely correlated. During El Niño years, on average, temperatures in south-eastern Australia are higher (Figure 8.1a), rainfall is lower (Figure 8.1b) and snow pack depth and season length are reduced (on average by approximately 35cm and 2.5 weeks, respectively) (BOM, 2014). Higher temperatures are moreover generally most pronounced during spring and summer, and spring temperatures are the main determinant of melt date of the snowpack (Murphy and Timbal, 2008).

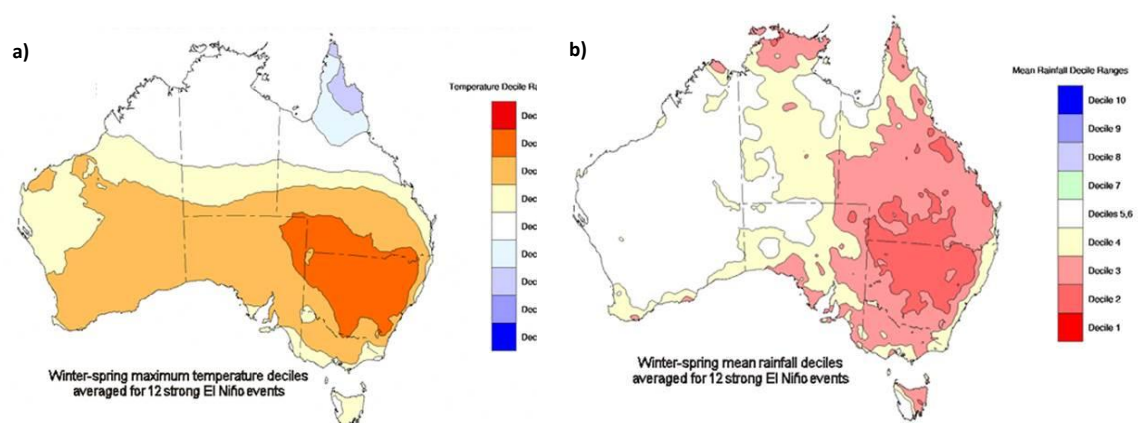


Figure 8.1: a) winter/spring mean temperature deciles for twelve El Niño events; b) winter/spring mean rainfall deciles for twelve El Niño events (BOM, 2014)

As such, this suggests an attenuating mechanism for interannual variations in the carbon balance at Dargo. As previously discussed, the snowpack had the effect of reducing annual GPP at Dargo; the degree of this reduction was more dependent on the melt date of the snowpack rather than the establishment date. This is because the seasonal temperature cycle – which largely determines these dates – is out of phase with the seasonal insolation cycle, lagging by 1-2 months (see Chapter 07, section 7.3.3 for further discussion). Since spring temperatures are the key determinant of melt timing, and higher spring temperatures occur during El Niño years, it is expected that late winter / spring GPP will be higher (as seen in 2007 in this study). In addition to the indirect effects of temperature on GPP at Dargo via snow cover, higher temperatures may also have the direct effect during spring of increasing photosynthetic capacity (Chapter 07, section 7.4.2.2). On the other hand, El Niño years are also likely to be typified by low soil moisture (i.e. drought conditions) during summer due to the combination of higher temperatures (therefore higher atmospheric demand), lower rainfall and the flow-on hydrological effects of early disintegration of the snow pack. As seen in early 2007 in this study, this is likely to strongly constrain GPP during summer, thereby potentially offsetting late winter / spring gains in GPP. The opposite counterbalancing dynamic (i.e. lower GPP during late winter/spring, higher GPP during summer) might be expected in La Nina years. The year 2008 in this study represents an appropriate analogue for such conditions.

A critical caveat with respect to effects on the summertime carbon balance is however the timing of rainfall, rather than simply the quantity, which profoundly affects growth and thus the ecosystem carbon balance (e.g. Chou *et al.*, 2008; Jongen *et al.*, 2011). As reported previously (Chapter 5, section 5.4.4), soil moisture was approximately equivalent between 2007 and 2008 and rainfall was actually lower at the sites (particularly at Dargo) in 2008. However, there was abundant rainfall during summer, thereby preventing depletion of soil moisture availability driven by high atmospheric demand.

Thus it is argued here that observed differences in annual carbon balance between sites are likely to reflect the fact that the current study captured a small window within the cycle of climatic – and corresponding carbon cycle – variability in which the amplitude of variability in annual NEE is higher at Nimmo than at Dargo, due both to the generally drier conditions at Nimmo and the counterbalancing effects of snow cover at Dargo. A longer time series would be required to confirm this, however, and other possible explanations are discussed below.

## 8.2 Systematic measurement error

While systematic measurement error cannot be comprehensively discounted with eddy covariance measurements (see Discussion in Chapter 2, section 2.5.4), as discussed in Chapter 4, passive indicators of data quality such as energy balance closure (4.2.1) and alternative methods of estimating carbon balance quantities (section 4.2.2) both suggest that the sites were not substantially affected by many of the documented problems that affect eddy covariance sites. The most serious source of potential systematic error in eddy covariance measurements is underestimation of nocturnal carbon fluxes, resulting in overestimation of ecosystem carbon uptake.

At both sites, respiratory response of the sites estimated from daytime light response analysis produced annual  $R_e$  estimates approximately 10% lower than estimates from nocturnal data (see Chapter 4, section 4.2.2), a difference quantitatively consistent with apparent effects of light inhibition of  $R_e$  in mountain grasslands (Wohlfahrt *et al.*, 2005b). This cross-method and cross-site consistency suggests that neither site was subject to systematic underestimation of  $R_e$ . Moreover, while it is generally observed that eddy covariance systems produce lower estimates of  $R_e$  relative to chamber systems (Goulden *et al.*, 1996a; Lavigne *et al.*, 1997; Wohlfahrt *et al.*, 2005a), in this study there was excellent agreement between these methods (Chapter 4, section 4.2.2.3), with the chamber system further verifying the accuracy of the empirical model used to estimate  $R_e$  at that site.

At Nimmo, while chamber measurements were not undertaken as part of this research project, it is more likely that advective effects at Nimmo would result in over- rather than underestimation of  $R_e$  due to the nature of the local terrain and vegetation. Specifically, its location in a broad valley floor plain means that the downslope flow of gravity currents would result in  $\text{CO}_2$ -enriched air being advected into rather than out of the control volume. Nonetheless, independent chamber-based estimates of annual  $R_e$  for Australian subalpine grasslands in the same region as Nimmo (Warren and Taranto, 2011) were within 5% of those calculated for the sites in this study. Taken together, these lines of evidence suggest that systematic measurement errors are unlikely to have been of a magnitude sufficient to significantly alter the conclusions drawn for the individual sites or for comparisons between them.

### 8.3 Unmeasured components of ecosystem carbon balance

It is also possible that unmeasured components of the carbon balance are important in determining its magnitude, such that NEE alone is not a sufficient approximation of net ecosystem production (NEP; see Chapter 2, section 2.4.1 for discussion and definition of these terms). Such components include ecosystem / atmosphere exchanges of non-CO<sub>2</sub> carbon species such as methane and volatile organic compounds, offsite transfer of carbon due to grazing by livestock, net lateral transfers of organic and inorganic carbon dissolved in water, and low-frequency / high-impact events such as fire. However, while not measured in this study, physical reasoning and literature estimates suggest that all of these quantities are likely to be small in comparison with the magnitudes of the measured carbon balance components reported here.

#### 8.3.1 Emission of non-CO<sub>2</sub> carbon species

No measurements were made of non-CO<sub>2</sub> carbon emissions from the ecosystems in this study, but the literature suggests that in a non-intensively grazed grassland, fluxes of methane (CH<sub>4</sub>) are unlikely to contribute significantly to the carbon mass balance. For example, growing season CH<sub>4</sub> emission was less than 0.5% of (respired) CO<sub>2</sub> during the growing season for a Tibetan alpine wetland, and a very small net growing season uptake of methane ( $-88.2 \mu\text{g m}^{-2} \text{ hr}^{-1}$ ) was reported for a Tibetan alpine grassland (He *et al.*, 2014). While volatile organic compound (VOC) emission may also contribute to the carbon balance of grasslands – particularly after cutting - they are generally at least one order of magnitude smaller than those associated with CO<sub>2</sub> (Wohlfahrt *et al.*, 2012).

#### 8.3.2 Non-atmospheric transfer

Non-atmospheric mechanisms for net transfers of carbon include leaching of dissolved organic / inorganic carbon (DOC / DIC) and – in periglacial environments - lateral transfer of carbon due to downslope flow of soils (solifluction). Given the relatively flat sites in this study, the latter is unlikely to be a relevant consideration. The former can however be approximated since both the annual runoff (difference between precipitation and transpiration) and DOC concentration in adjacent

streams<sup>34</sup> (during the peak of the growing season when DOC concentrations are expected to be high) were quantified. However, carbon losses via this pathway appear to be negligible – conservatively assuming that the peak growing season DOC concentration is representative of all times of year, leaching losses of carbon were less than 1% of NEE at either site (

Table 8.1). Moreover, the implicit assumption of the above is that grassland runoff contributes exclusively to the observed stream DOC, which, given the ecological heterogeneity of the local landscape (particularly the presence of *E. pauciflora* woodland patches), is unlikely to be strictly accurate. Hope *et al.* report generally higher DOC export from temperate forests than grasslands globally (1994). Given that the grasslands in this study were interspersed with woodland, this suggests that even the small quantities documented here may be overestimated.

**Table 8.1: estimated annual leaching C losses (note that only estimates of growing season peak 2008 were available, and are thus used for both years).**

	Dargo		Nimmo	
	2007	2008	2007	2008
Annual runoff (mm)	441	135	282	147
Peak growing season DOC (mgC L <sup>-1</sup> )	1.3	1.3	1.7	1.7
C leached (gC yr <sup>-1</sup> )	0.57	0.18	0.48	0.25

### 8.3.3 Grazing effects

Low-intensity livestock grazing was practised at the sites in the warmer months of the year, although precise figures were not available. The effects of grazing can contribute significantly to the ecosystem carbon balance (Cao *et al.*, 2004; Rogiers *et al.*, 2008), via changes in ecosystem / atmosphere carbon exchanges and also because carbon sequestered by livestock that consume vegetation is eventually transported offsite and thereby not accounted for. With respect to changes in ecosystem / atmosphere carbon exchanges, as noted in Chapter 2 (see section 2.4.5), no consistent effect of grazing has been reported across the literature. With respect to GPP, grazing inevitably affects leaf area, such that NEE may be initially reduced by the introduction of grazing; however, GPP often subsequently recovers because the continual removal of vegetation by grazing

<sup>34</sup> At experimental sites, streamflow DOC concentrations within an ecosystem have been shown to be similar to those collected directly from the soil column using lysimetry (Lajtha, 2000).

promotes regrowth when environmental conditions are non-limiting (Peichl *et al.*, 2012). As such, carbon uptake may actually be moderately enhanced by grazing. However, there is a second effect of livestock grazing on the carbon balance noted above: offsite transfer of carbon in meat and milk. Nonetheless, even in the case of intensive production on farm pastures, carbon sequestered in meat and milk transported out of the system is generally a minor component of the ecosystem carbon balance. For example, Byrne *et al.* (2007) report that across two farms with annual NEE of approximately  $300\text{gC m}^{-2}$ , the removal of carbon via meat and milk production was less than 10% of NEE. The moderate effects of even intensive livestock grazing on the carbon balance, in combination with the fact that there was minimal grazing at the sites in this study, therefore suggests that this is not likely to have contributed substantially to the respective carbon balances of the sites in this study, or to the observed differences in annual carbon balance between them.

#### 8.3.4 Low-frequency / high-impact events

Fire generally occurs infrequently in subalpine grasslands, but may be an important component of the carbon balance in the long term (i.e. decadal to centennial time scales). Fires transfer large quantities of carbon from ecosystem to atmosphere, thereby reducing ecosystem carbon storage, and carbon exchange may be in disequilibrium for long periods subsequently. This may take the form of additional net efflux in the short term, as dead organic matter is decomposed and carbon respired, and net influx in the longer term as vegetation and soil carbon pools are replenished (Knapp *et al.*, 1998). In ecosystems in which fire is suppressed, there is generally an increase in carbon storage (Tilman *et al.*, 2000). No fires occurred during the measurement period, but as noted previously, fires are part of the ecology of the High Country, albeit an infrequent one (Williams *et al.*, 2008a). While it is conceivable that historical fire may have contributed to differences in ecosystem carbon balance or storage as documented for the sites in this study, there is no evidence or specific site information indicating recent historical fire occurrence.

Some ecosystems are also subject to large variations in carbon balance due to the effects of insect attack (e.g. Van Gersel *et al.*, 2013). In the case of subalpine grasslands, grasses may be periodically attacked by moths (Williams and Ashton, 1987) but such effects are a regular occurrence and affect small patches of the ecosystem (Carr and Turner, 1959), and are thus more appropriately characterised as relatively high frequency, low impact events. As such, their effects on the carbon balance are unlikely to be large.

## 8.4 Climate change

The fourth possibility that may explain the divergent patterns of carbon storage and exchange is that the non-stationarity of the climate has already driven the carbon balance of the ecosystems away from quasi-equilibrium. In a qualitative sense this is true of the terrestrial biosphere as a whole, since both top-down and bottom-up measurements (see Chapter 02) confirm that it has been a persistent net sink for carbon in recent years. However, with respect to cross-site patterns of carbon exchange, it is considered unlikely that the higher carbon uptake observed at Nimmo relative to Dargo is sustained over longer time periods. If this was the case, the absorbed carbon would largely be stored in the soil reservoir, since there are clear structural limitations on the retention of additional standing biomass among grasslands. Since the uncertainties in the estimates of ecosystem carbon storage (95% confidence interval of slightly less than  $\pm 1.2 \text{ kgC m}^{-2}$  – see Chapter 6, section 6.4) are up to 10 times higher than estimates of annual NEE, a much longer period of time (and/or higher precision estimates of carbon storage) would be required to detect changes in storage. However, as previously detailed, approximately 50% more carbon was stored in the soil at the cooler, wetter Dargo site. This is consistent with the observed effects of climate on soil organic matter retention, which increases with increasing rainfall and decreasing temperature (Post *et al.*, 1982). Given these facts, it is difficult to identify plausible mechanisms whereby a greater quantity of carbon might be sequestered at Nimmo than at Dargo in response to a warming and – most likely - drying climate. Indeed, the observed global climate / soil carbon spatial relationships suggest that such changes would drive net carbon loss from the soil reservoir.

Nonetheless, this does not discount the possibility that changes in carbon balance are occurring in response to a changing climate. Even in the absence of snow,  $\text{GPP}:R_e$  was lower at Dargo. Jenkins and Adams (2010) report that there is a positive association between quantity of soil carbon and quantity of labile carbon for Australian alpine and subalpine ecosystems. Thus it is possible that warmer temperatures are already stimulating decomposition of soil organic matter at the sites. Given the warmer and drier conditions at Nimmo, there may be less labile soil carbon than at Dargo, such that an increased response to warmer temperatures may be detectable. This may possibly explain the fact that  $R_{\text{ref}}$  was higher at Dargo than at Nimmo. In the absence of knowledge of the carbon balance under long-term steady-state conditions, however, this is necessarily speculative, and further study would be required.



## 8.5 Summary

The most likely explanation for the larger carbon uptake observed at the site with lower carbon storage (Nimmo) is that the carbon balance is more interannually variable, due to the fact that the site is warmer and drier (and thus more likely to be subject to periodic water limitation) relative to Dargo. Thus whereas stronger carbon uptake may be expected in years with reduced soil moisture constraint, stronger carbon release may be expected in drought years. At Dargo on the other hand, variations in winter snow cover acted to attenuate carbon cycle variability caused by low summer soil moisture, thereby reducing variations in interannual carbon balance. It is suggested that this may be a more general pattern, given that the dominant mode of climatic variability on average induces either warm, dry or cool, wet conditions. Nonetheless, it is also possible that warmer temperatures may already be increasing  $R_e$  at Dargo – and thereby reducing net carbon uptake - since it is likely that the labile carbon supply in existing soil organic matter is higher at Dargo. As such, this may already be reducing carbon storage at Dargo, but a much longer time series and further investigation would be required to confirm this. Despite this limitation, the current study has yielded a number of valuable insights into the carbon dynamics of subalpine grassland ecosystems, which are discussed – along with implications for climate change - in the following chapter.

# 9. Conclusions

---

## 9.1 Recapitulation of objectives and findings

### Objective 1: Quantify carbon storage in soil and vegetation reservoirs

This study has established that Australian subalpine grasslands store substantial amounts of carbon. Dargo stored approximately  $20\text{kgC m}^{-2}$ , and Nimmo  $14\text{kgC m}^{-2}$ . This is almost certainly an underestimate, since soil carbon was only measured to a depth of 0.3m, and extrapolation of observed relationships to greater depth (assuming a soil mantle depth of approximately 1m) increased estimates by approximately 50%. Thus observed densities were comparable to or higher than observed for similar ecosystems in other parts of the world. The vast majority of this carbon (97%) is stored in the soil reservoir, and consistent with globally observed relationships, more carbon is stored at the cooler and wetter of the sites assessed, since these conditions constrain microbial decomposition of soil organic matter.

### Objective 2: Quantify net exchange of carbon between ecosystem and atmosphere

Both sites were also significant sinks for carbon during the study period (Dargo:  $-93$  and  $-111\text{gC m}^{-2} \text{a}^{-1}$  for 2007 and 2008, respectively; Nimmo:  $-204$  to  $-322\text{gC m}^{-2} \text{a}^{-1}$  for 2007 and 2008, respectively). In terms of magnitude, this was again approximately consistent with the literature for similar ecosystems globally, as was the fact that the more productive of the sites had higher carbon uptake. Both sites were affected by dry conditions in early 2007 (following on from severe regional drought in 2006). At Nimmo, the wetter summer conditions in 2008 translated to higher annual carbon uptake. While there was also stronger summer carbon uptake at Dargo in 2008, this was offset by enhanced winter carbon efflux associated with a longer, later snow season due to cooler temperatures. Higher carbon uptake during the study years at Nimmo does not necessarily reflect

higher uptake in general – instead, it is thought to reflect enhanced interannual variability in carbon balance at the drier Nimmo site generally.

Objective 3: Quantify assimilatory and respiratory components of net carbon exchange

In 2007:  $R_e$  at Dargo and Nimmo, respectively, was 1044 and 1022 gC m<sup>-2</sup> a<sup>-1</sup>; GPP, respectively, was -1133 and -1226 gC m<sup>-2</sup> a<sup>-1</sup>. In 2008:  $R_e$  at Dargo and Nimmo, respectively, was 1144 and 1185 gC m<sup>-2</sup> a<sup>-1</sup>; GPP, respectively, was -1256 and -1507 gC m<sup>-2</sup> a<sup>-1</sup>. The magnitude of these fluxes was intermediate with respect to published values internationally – similar ecosystems in colder environments generally had lower values, and higher values were observed for some intensively managed agricultural grasslands. The difference observed in NEE between sites was primarily due to differences in GPP. In turn, these differences primarily accrued during winter (the presence of snow cover at Dargo reduced GPP), and secondarily during spring (discussed below).

Objective 4: Quantify the effects of climatic controls on these components.

The effects of soil temperature and moisture availability on  $R_e$  differed between the sites; however, the ecosystem temperature and moisture responses attenuated the differences in the controls such that differences in  $R_e$  were relatively small (as described above). At Nimmo, despite drier conditions, the magnitude of  $R_e$  was less moisture-constrained (i.e. constraints became apparent at lower soil moisture levels for Nimmo), such that quantitative soil moisture limitation of  $R_e$  was approximately the same at both sites. This may partially reflect the evolution of the soil decomposer community to local conditions. A similar observation occurred with respect to temperature – higher average soil temperatures at Nimmo were largely counterbalanced by reduced  $R_e$  at a given temperature, thereby minimising differences in  $R_e$ . While the reasons for this are uncertain, it was noted that  $R_e$  was lower at Nimmo in 2007 and higher in 2008. This was associated with the much lower rates of respiration observed at Nimmo during the summer of early 2007. In turn, it is considered likely that this reflects the effects of reduced carbon supply to the soil associated with higher plant mortality / reduced growth during the drought conditions of 2006, extending into early 2007.

While the key driver of GPP is insolation, the small difference in insolation observed between sites did not materially contribute to the observed differences in GPP. As noted above, the main control on differences in GPP was the presence of the winter snowpack at Dargo. The winter snowpack was maintained by the cooler daytime temperatures observed at Dargo (due to its higher altitude). Lower GPP at Dargo in winter 2008 was related to the fact that snow cover persisted for approximately one month longer than during 2007, due to cooler daytime temperatures. As noted above, this reduction in winter GPP largely offset gains in summer GPP in 2008 relative to 2007, such that NEE did not change substantially between years at Dargo. This underscores the critical role of the snowpack – including its timing – in determining annual carbon balance in subalpine grasslands. GPP was also on average higher at Nimmo during spring, due to the higher photosynthetic capacity of the canopy at Nimmo. In turn, the temperature response of photosynthetic capacity was similar at the sites; thus the systematically lower temperatures at Dargo resulted in reduced photosynthetic capacity. The strong correlation between photosynthetic capacity and satellite-measured leaf area at Nimmo suggests that leaf area primarily determines the photosynthetic capacity of the canopy. Thus temperature-mediated differences in leaf area may explain differences in GPP between sites, but the lack of reliable estimates of leaf area for Dargo limit the confidence of this conclusion. A simple phenological model using only temperature, photoperiod and soil moisture was able to explain most of the variation in canopy photosynthetic capacity at both sites. Stronger soil moisture constraint of canopy photosynthetic capacity was evident at Nimmo in summer 2007, the only period during which it was lower than at Dargo. However, at Nimmo in particular, model parameters optimised using data including summer 2007 generally over-predicted the sensitivity of phenology to soil moisture in subsequent periods of low soil moisture. This may indicate the cumulative effects of prior drought on canopy development. However, the limited amount of data available for Nimmo during this period renders this conclusion uncertain.

## 9.2 Implications of future climate change

As previously noted, the higher soil carbon storage at the cooler, wetter Dargo site and lower soil carbon storage at the warmer, drier Nimmo site is consistent with global patterns of soil carbon storage in relation to climate. This pattern suggests that the expected warming and (possible) drying (see Chapter 1, section 1.2.4) of the Australian High Country in future will result in a reduction in soil carbon from these ecosystems. The results of this study however also suggest that warming may stimulate GPP, both through reductions in snow cover and direct stimulation of growth.

However, as this study has demonstrated, in Australian subalpine regions, dry conditions may also constrain GPP during summer. As noted previously, the presence of snow cover at Dargo had a modulating effect on GPP – in the warmer, drier year (2007), summer GPP was constrained by dry conditions but this was offset by increased winter / spring GPP due to earlier snowmelt. Thus while warming and drying are likely to affect the seasonal dynamics of GPP, the effect on annual GPP of seasonally snow-covered grasslands may be attenuated to some extent by the changing dynamics of the remaining snow cover.

Nimmo provides some indication of how the dynamics of carbon exchange may change with warmer and drier conditions (since it is approximately 2°C warmer and generally drier, this approximates the magnitude of change that might be expected in south-eastern Australia by mid-century 1.2.4) following elimination of snow cover. The much larger difference in annual carbon uptake between 2007 and 2008 relative to Dargo was associated with the fact that summer GPP was greatly constrained in early 2007 due to dry conditions, with no compensatory winter/spring increase in GPP as occurred at Dargo due to variations in snow cover. Moreover, there was also some evidence of substantial constraint on GPP during late 2006. Since variations in GPP were primarily responsible for variations in NEE at Nimmo between 2007 and 2008, this suggests that the carbon balance at snow-free sites is likely to be both variable and strongly responsive to moisture conditions, as observed for lowland grasslands more generally.

Thus warmer conditions and corresponding reductions in snow cover in the Australian High Country may be expected to have two effects. First, increased interannual variability of carbon exchange – as noted in chapter 7 (section 7.3.1), grasslands are among the most interannually variable ecosystems in terms of carbon dynamics. This is driven by soil moisture variability, to which GPP is generally more sensitive than  $R_e$ . As such, this brings us to the second potential effect - to the extent that the prevalence of drought conditions increases, carbon uptake may be expected to decline as GPP is more constrained than  $R_e$ . Indeed, this is thought to be a likely explanation for the

fact that carbon storage was much lower at Nimmo, despite higher carbon uptake in both study years – the drier site is more sensitive to drought, and may be a net source of carbon during drought years. This is expected to draw down the soil carbon reservoir because heterotrophic respiratory effluxes from the soil are less affected by drought than GPP, and reduced growth translates to reduced transfer of dead organic matter (and correspondingly carbon) to the soil.

But even in the absence of drought, warming and drying of the soil in the presence of large quantities of labile carbon is likely to result in loss of carbon from the soil. The net effect on ecosystem carbon storage will however also depend on the specific response of biomass amount to changing conditions. While further information would be required to translate the findings from this study into an understanding of climatically-mediated plant biomass variations (see section 9.3 below), as noted in Chapter 1 (section 1.2.3), in Europe alpine plant growth and biomass amount are both strongly tied to temperature and snow cover dynamics, and are thus expected to increase in future (Jonas *et al.*, 2008; Rammig *et al.*, 2010). This may potentially be further facilitated by mineralisation of nutrients associated with the decomposition of organic matter. However, the Australian context is one of periodic and variable water limitation, and thus changes in biomass will depend on the relative magnitudes of the competing effects of warming and drying. Moreover, the increase in biomass retention is clearly structurally limited in the case of herbaceous vegetation.

Nonetheless, over longer (e.g. centennial) time scales, successional transition to dominance by new functional groups may occur – as discussed in Chapter 2 (section 2.2.4), the advantages of prostrate growth forms in alpine regions are mainly due to decoupling from low ambient near-surface atmospheric temperatures (Körner, 1998), and thus warming is likely to diminish such advantages relative to shrubs and trees. Indeed, as noted in Chapter 1, altitudinal treelines in many regions are advancing (Harsch *et al.*, 2009). Losses of carbon from the soil reservoir may thus potentially be offset by increases in vegetation biomass. However, wholesale successional changes in response to warming are unlikely to occur quickly in Australia due to both the generally poor dispersal ability of the treeline tree species (*E. pauciflora*), and the requirement of initial disturbance to facilitate opportunistic establishment (Ferrar *et al.*, 1988; Green, 2009).

Two key agents of disturbance that are nevertheless likely to increase with warming and drying are drought and fire (Williams *et al.*, 2008a). Moreover, changes in fire frequency are likely to substantially affect carbon storage in soils, since layers of dried organic matter in the near surface soil are generally consumed (Turetsky *et al.*, 2015). While there is no documented history of fire for the sites in this study, given the already warmer, drier conditions at Nimmo, it is also possible that historical fire occurrence may have contributed to the lower soil carbon observed there.

In summary, warmer temperatures are likely to stimulate plant growth and possibly increase biomass across subalpine and alpine grasslands in future. However, the results of this study indicate that this may be partially counterbalanced by the inhibitory effects of dry summer conditions, which are expected to increase in frequency due to both higher evaporative demand associated with higher temperatures and likely decreases in rainfall. The results of this study also suggest that loss of soil carbon from the organic-rich soils of the alpine and subalpine grasslands is likely. In this study more than 95% of ecosystem carbon storage was in the soil reservoir. Moreover, there are phenotypic constraints on the potential increase of standing biomass in grassland ecosystems. Taken together, this suggests that even small relative reductions in soil organic carbon density are likely to result in net effluxes of carbon from ecosystem to atmosphere. In the much longer term (e.g. decadal to centennial timescales), however, this may be offset by increases in carbon fixation due to changes in plant functional groups (e.g. advancing treeline) spurred by warming.

### 9.3 **Relevance, limitations and scope for further investigation**

While a number of other studies have documented respiratory carbon exchanges between alpine soils and ecosystems and the atmosphere in Australia, this is the first study to document ecosystem-scale carbon balance – and its decomposition into respiratory and production processes – among the sod-tussock grasslands of the Australian High Country, and to do so on a continuous basis over multiple seasonal cycles. As well as providing a quantitative assessment of the annual carbon source-sink status of these ecosystems, the simultaneous capture of meteorological and other data over time has allowed quantification of plant responses to key environmental drivers. Understanding how the carbon balance responds to these drivers at present is key to understanding how it may change in response to ongoing climate change. And since the carbon balance is an aggregate measure of ecosystem function, it also provides an indication of critical ecological thresholds (for example, soil moisture thresholds) for the constituent species. This understanding is particularly important given the particular vulnerability of mountain ecosystems to climate change. This study thus represents an important contribution to the understanding of the functioning of these ecosystems both now and into the future.

Inevitably, given the time and resource constraints of research projects, there is much scope for furthering our understanding of these ecosystems. For example, this study was limited to an analysis of the key atmospheric processes of ecosystem carbon import / export, namely gross primary production and ecosystem respiration. However, further insight into ecosystem responses

to climate would be yielded if ecosystem respiration could be decomposed into autotrophic and heterotrophic components. This would allow an estimate of actual plant *growth* to be ascertained (i.e. net primary production, derived from the difference between gross primary production and autotrophic respiration – see Chapter 2, section 2.4.1). Moreover, with respect to carbon storage, it is standing phytomass rather than growth that is the critical quantity, and thus how phytomass varies with plant growth depends on rates of organic matter loss from above- (litterfall) and belowground plant tissue. Thus this additional information would yield insight into how the soil and vegetation reservoirs are likely to change with climate, disentangling the aggregate processes that were the subject of the current study. In practice, however, these are extremely demanding undertakings requiring a level of resources that put these questions beyond the scope of this investigation.

Soil nutrient status was also not addressed in any detail in this investigation. Yet given the fundamental physiological requirement of autotrophic and heterotrophic organisms for these nutrients, their cycles are intimately linked to and interdependent with that of carbon – for example, during uptake and assimilation in plant matter on the one hand, and remineralisation during microbial decomposition on the other. While their effects were not explicitly included here, their role in modulating ecosystem responses to climatic signals is implicit. Because nutrient cycles are also climatically controlled, what is characterised as ecosystem response to climate may arise partly due to interactions between carbon and nutrient cycles. For example, cold conditions may limit the availability of belowground resources and thus contribute to down-regulation of ecosystem productivity. As such, the mapping of whole ecosystem responses onto climate variables necessarily ignores what is in reality a complex chain of cause and effect relationships – to which nutrient availability is of central importance - within the ecosystem. For example, while the analysis largely framed GPP as a control of  $R_e$  via its effect on labile carbon supply, ultimately the relationship between production and decomposition is one of interdependence, since the decomposition process involves the mineralisation of organic matter to inorganic compounds that supply the nutritional needs of plants and thereby support photosynthesis. In making such simplifications however, this study provides an overarching context for ecosystem response into which these complex dynamics can be placed. Studies elucidating the role of nutrients in the regulation of ecosystem carbon balance would thus provide useful augmentation of the results reported here.

With respect to understanding future changes in carbon balance, a more complete understanding of the potential for successional change among High Country ecosystems – particularly at the level of plant functional type – is required. As noted, successional changes are



likely in the long term, but at present the carbon cycle consequences of such changes are necessarily speculative.

In terms of time, it would clearly be desirable to have a longer period of study than the two years available here. While those years were sufficiently climatologically contrasting to yield some insight into ecosystem responses to dry and wet, warm and cool conditions, ultimately the quasi-decadal nature of ENSO and the various frequencies of other contributing modes of internal climatic variability dictates that a longer period than two years is required to draw robust quantitative conclusions about the mean state of ecosystems, particular with respect to annual carbon balance estimates. A longer period of time would make it possible to link changes in carbon storage to changes in carbon balance; the uncertainty in storage measurements mean that the time scales required would be at least decadal. The current study was thus considered a preliminary one that established critical long-term ecological research infrastructure, and application of the tools developed here to a dataset accrued over the longer-term (both sites are still in operation) would consolidate and expand upon the findings reported here.

Similarly, an expansion of the spatial scope of the current investigation to include multiple additional sites would reduce the inherent uncertainties in the current study. For example, some proportion of the cross-site variability in carbon storage and fluxes observed in this study may be determined by local (e.g. geological, historical disturbance *etc.*) factors rather than purely by climate, and additional sites would provide some indication of the extent of such locally-induced variation.

# 10. References

---

Abramowitz, G. (2005). "Towards a benchmark for land surface models." Geophysical Research Letters **32**(L22702).

Adams, J. M., H. Faure, L. Faure-Denard, J. M. McGlade and F. I. Woodward (1990). "Increases in terrestrial carbon storage from the Last Glacial Maximum to the present." Nature **348**(6303): 711-714.

Aires, L. M. I., C. A. Pio and J. S. Pereira (2008). "Carbon dioxide exchange above a Mediterranean C3/C4 grassland during two climatologically contrasting years." Global Change Biology **14**(3): 539-555.

Aitken, S. N., S. Yeaman, J. A. Holliday, T. Wang and S. Curtis-McLane (2008). "Adaptation, migration or extirpation: climate change outcomes for tree populations." Evolutionary Applications **1**(1): 95-111.

Amiro, B. D. (1990). "Comparison of turbulence statistics within three boreal forest canopies." Boundary-Layer Meteorology **51**(1-2): 99-121.

Amthor, J. and D. D. Baldocchi (2001). Terrestrial higher plant respiration and net primary production. Terrestrial Global Productivity. J. Roy, B. Saugier and H. Mooney. San Diego, Academic Press.

Angert, A., S. Biraud, C. Bonfils, C. C. Henning, W. Buermann, J. Pinzon, C. J. Tucker and I. Fung (2005). "Drier summers cancel out the CO<sub>2</sub> uptake enhancement induced by warmer springs." Proceedings of the National Academy of Sciences of the United States of America **102**(31): 10823-10827.

Arya, S. (2001). Introduction to Micrometeorology. San Diego, Academic Press.

Ashton, D. H. and R. Williams (1989). Dynamics of the subalpine vegetation in the Victorian region. The Scientific Significance of the Australian Alps: The Proceedings of the First Fenner Conference. R. B. Good. Canberra, Australian Alps National Parks Liaison Committee.

Atkin, O. K., J. R. Evans and K. Siebke (1998). "Relationship between the inhibition of leaf respiration by light and enhancement of leaf dark respiration following light treatment." Functional Plant Biology **25**(4): 437-443.

Aubinet, M. (2008). "Eddy covariance CO<sub>2</sub> flux measurements in nocturnal conditions: an analysis of the problem." Ecological Applications **18**(6): 1368-1378.

Aubinet, M., C. Feigenwinter, B. Heinesch, C. Bernhofer, E. Canepa, A. Lindroth, L. Montagnani, C. Rebmann, P. Sedlak and E. Van Gorsel (2010). "Direct advection measurements do not help to solve the night-time CO<sub>2</sub> closure problem: Evidence from three different forests." Agricultural and Forest Meteorology **150**(5): 655-664.

Aubinet, M., C. Feigenwinter, B. Heinesch, Q. Laffineur, D. Papale, M. Reichstein, J. Rinne and E. Van Gorsel (2012a). Nighttime Flux Correction. Eddy Covariance: A Practical Guide to Measurement and Data Analysis. M. Aubinet, T. Vesala and D. Papale. Dordrecht, Springer.

Aubinet, M., A. Grelle, A. Ibrom, Ü. Rannik, J. Moncrieff, T. Foken, A. S. Kowalski, P. H. Martin, P. Berbigier, C. Bernhofer, R. Clement, J. Elbers, A. Granier, T. Grünwald, K. Morgenstern, K. Pilegaard, C. Rebmann, W. Snijders, R. Valentini, T. Vesala, A. H. Fitter and D. G. Raffaelli (1999). Estimates of the Annual Net Carbon and Water Exchange of Forests: The EUROFLUX Methodology. Advances in Ecological Research, Academic Press. **Volume 30**: 113-175.

Aubinet, M., B. Heinesch and M. Yernaux (2003). "Horizontal and Vertical CO<sub>2</sub> Advection In A Sloping Forest." Boundary-Layer Meteorology **108**(3): 397-417.

Aubinet, M., T. Vesala and D. Papale (2012b). Eddy Covariance: A Practical Guide to Measurement and Data Analysis. Dordrecht, Springer.

Bahn, M., M. Knapp, Z. Garajova, N. Pfahringer and A. Cernusca (2006). "Root respiration in temperate mountain grasslands differing in land use." Global Change Biology **12**(6): 995-1006.

Bahn, M., M. Rodeghiero, M. Anderson-Dunn, S. Dore, C. Gimeno, M. Drösler, M. Williams, C. Ammann, F. Berninger, C. Flechard, S. Jones, M. Balzarolo, S. Kumar, C. Newesely, T. Priwitzer, A. Raschi, R. Siegwolf, S. Susiluoto, J. Tenhunen, G. Wohlfahrt and A. Cernusca (2008). "Soil Respiration in European Grasslands in Relation to Climate and Assimilate Supply." Ecosystems **11**(8): 1352-1367.

Baldocchi, D. (2007). "Forward to Special Issue." Global Change Biology **13**(3): 547-547.

Baldocchi, D. (2008). "TURNER REVIEW No. 15. "Breathing" of the terrestrial biosphere: lessons learned from a global network of carbon dioxide flux measurement systems." Australian Journal of Botany **56**(1): 1-26.

Baldocchi, D., E. Falge, L. Gu, R. Olson, D. Hollinger, S. Running, P. Anthoni, C. Bernhofer, K. Davis, R. Evans, J. Fuentes, A. Goldstein, G. Katul, B. Law, X. Lee, Y. Malhi, T. Meyers, W. Munger, W. Oechel, K. T. Paw, K. Pilegaard, H. P. Schmid, R. Valentini, S. Verma, T. Vesala, K. Wilson and S. Wofsy (2001). "FLUXNET: A New Tool to Study the Temporal and Spatial Variability of Ecosystem Scale Carbon Dioxide, Water Vapor, and Energy Flux Densities." Bulletin of the American Meteorological Society **82**(11): 2415-2434.

Baldocchi, D. D. (2003). "Assessing the eddy covariance technique for evaluating carbon dioxide exchange rates of ecosystems: past, present and future." Global Change Biology **9**(4): 479-492.

Baldocchi, D. D. and R. Valentini (2004). Geographic and temporal variation of carbon exchange by ecosystems and their sensitivity to environmental perturbations. The Global Carbon Cycle: Integrating Humans, Climate and the Natural World. C. B. Field and M. R. Raupach. Washington, Island Press.

Barr, A. G., K. Morgenstern, T. A. Black, J. H. McCaughey and Z. Nesic (2006). "Surface energy balance closure by the eddy-covariance method above three boreal forest stands and implications for the measurement of the CO<sub>2</sub> flux." Agricultural and Forest Meteorology **140**(1-4): 322-337.

Barry, R. (2008). Mountain Weather and Climate. Cambridge, Cambridge University Press.

Barry, R. G. (1994). Past and potential future changes in mountain environments. Mountain Environments in Changing Climates. M. Beniston. London, Routledge.

Bear, R. and C. M. Pickering (2006). Recovery of subalpine grasslands from bushfire. Australian Journal of Botany. **54**: 451-458.

Beesley, C., A. Frost and J. Zajackowski (2009). A comparison of the BAWAP and SILO spatially interpolated daily rainfall datasets. 18th World IMACS / MODSIM Congress. Cairns, Australia: 3886:3892.

Beniston, M. (2003). "Climatic Change in Mountain Regions: A Review of Possible Impacts." Climatic Change **59**(1): 5-31.

Beniston, M., H. F. Diaz and R. S. Bradley (1997). "Climatic change at high elevation sites: an overview." Climatic Change **36**(3 - 4): 233-251.

Benson, J. (1994). "The native grasslands of the Monaro region: Southern Tablelands of NSW." Cunninghamia **3**(3): 609-650.

Billings, W. (1974a). Plant adaptations to cold summer climates. Arctic and Alpine Environments. J. Ives and R. Barry. London, Methuen and Co.

Billings, W. D. (1974b). "Adaptations and origins of alpine plants." Arctic and alpine research **6**(2): 129-142.

Bird, M. I., H. Santrůcková, J. Lloyd and E. M. Veenendaal (2001). The Global Soil Organic Carbon Pool. Global Biogeochemical Cycles in the Climate System. E. D. Schulze, S. Harrison, M. Heimann et al. San Diego, Academic Press.

Bishop, C. (1995). Neural Networks for Pattern Recognition. Oxford, Oxford University Press.

Blonquist Jr, J. M., B. D. Tanner and B. Bugbee (2009). "Evaluation of measurement accuracy and comparison of two new and three traditional net radiometers." Agricultural and Forest Meteorology **149**(10): 1709-1721.

BOM (2014). "What is El Niño and what might it mean for Australia?". Retrieved 16/12/2014, 2014, from <http://www.bom.gov.au/climate/updates/articles/a008-el-nino-and-australia.shtml>.

Bonan, G. (2002). Ecological Climatology: Concepts and Applications. Cambridge, Cambridge University Press.

Brady, N. and R. Weil (2002). The Nature and Properties of Soils. New Jersey, Prentice Hall.

Brooks, P. D., P. Grogan, P. H. Templer, P. Groffman, M. G. Öquist and J. Schimel (2011). "Carbon and Nitrogen Cycling in Snow-Covered Environments." Geography Compass **5**(9): 682-699.

Brooks, P. D., D. McKnight and K. Elder (2005). "Carbon limitation of soil respiration under winter snowpacks: potential feedbacks between growing season and winter carbon fluxes." Global Change Biology **11**(2): 231-238.

Brown, J. and F. Millner (1989). Aspects of the meteorology and hydrology of the Australian alps. The Scientific Significance of the Australian Alps: The Proceedings of the First Fenner Conference. R. B. Good. Canberra, Australian Alps National Parks Liaison Committee.

Burba, G. and D. Anderson (2010). A Brief Practical Guide to Eddy Covariance Flux Measurements: Principles and Workflow Examples for Scientific and Industrial Applications. Lincoln, LI-COR Biosciences.

Burba, G. G., D. K. McDermitt, A. Grelle, D. J. Anderson and L. Xu (2008). "Addressing the influence of instrument surface heat exchange on the measurements of CO<sub>2</sub> flux from open-path gas analyzers." Global Change Biology **14**(8): 1854-1876.

Byars, S. G., W. Papst and A. A. Hoffmann (2007). "Local adaptation and cogradients selection in the alpine plant, *Poa hiemata*, along a narrow altitudinal gradient." Evolution **61**(12): 2925-2941.

Byrne, K. A., G. Kiely and P. Leahy (2007). "Carbon sequestration determined using farm scale carbon balance and eddy covariance." Agriculture, Ecosystems & Environment **121**(4): 357-364.

Cai, T., L. B. Flanagan and K. H. Syed (2010). "Warmer and drier conditions stimulate respiration more than photosynthesis in a boreal peatland ecosystem: Analysis of automatic chambers and eddy covariance measurements." Plant, Cell & Environment **33**(3): 394-407.

Cai, W., D. Jones, K. Harle, T. Cowan, S. Power, I. Smith, J. Arblaster and D. Abbs (2007). Chapter 2: Past Climate Change. Climate Change in Australia. K. Pearce, P. Holper, M. Hopkinset al. Canberra, CSIRO.

Campbell, G. and J. Norman (1998). An Introduction to Environmental Biophysics. New York, Springer-Verlag.

Canadell, J. G., C. Le Quere, M. R. Raupach, C. B. Field, E. T. Buitenhuis, P. Ciais, T. J. Conway, N. P. Gillett, R. A. Houghton and G. Marland (2007). "Contributions to accelerating atmospheric CO<sub>2</sub> growth from economic activity, carbon intensity, and efficiency of natural sinks." Proceedings of the National Academy of Sciences **104**(47): 18866-18870.

Cao, G., Y. Tang, W. Mo, Y. Wang, Y. Li and X. Zhao (2004). "Grazing intensity alters soil respiration in an alpine meadow on the Tibetan plateau." Soil Biology and Biochemistry **36**(2): 237-243.

Cao, M. and F. I. Woodward (1998). "Net primary and ecosystem production and carbon stocks of terrestrial ecosystems and their responses to climate change." Global Change Biology **4**(2): 185-198.

Carr, S. and J. Turner (1959). "The ecology of the Bogong High Plains I: the environmental factors and the grassland communities." Australian Journal of Botany **7**: 12-33.

Cary, G., R. Bradstock, A. Gill and R. J. Williams (2012). Global change and fire regimes in Australia. Flammable Australia: Fire Regimes, Biodiversity and Ecosystems in a Changing World. R. Bradstock, A. Gill and R. J. Williams. Collingwood, CSIRO Publishing.

Chapin, F. (1978). Phosphate uptake and nutrient utilization by Barrow tundra vegetation. Vegetation and Production Ecology of an Alaskan Arctic Tundra. L. L. Tieszen. New York, Springer.

Chapin, F. S., III, P. Matson and H. Mooney (2002). Principles of Terrestrial Ecosystem Ecology. New York, Springer-Verlag.

Chapin, F. S., III, G. M. Woodwell, J. T. Randerson, E. B. Rastetter, G. M. Lovett, D. D. Baldocchi, D. A. Clark, M. E. Harmon, D. S. Schimel, R. Valentini, C. Wirth, J. D. Aber, J. J. Cole, M. L. Goulden, J. W. Harden, M. Heimann, R. W. Howarth, P. A. Matson, A. D. McGuire, J. M. Melillo, H. A. Mooney, J. C. Neff, R. A. Houghton, M. L. Pace, M. G. Ryan, S. W. Running, O. E. Sala, W. H. Schlesinger and E. D. Schulze (2006). "Reconciling Carbon-Cycle Concepts, Terminology, and Methods." Ecosystems **9**(7): 1041-1050.

Chen, J., M. Shen and T. Kato (2009). "Diurnal and seasonal light use efficiency in an alpine meadow ecosystem: causes and implications for remote sensing." Journal of Plant Ecology **2**(4): 173-185.

- Chimner, R. A. and J. M. Welker (2005). "Ecosystem respiration responses to experimental manipulations of winter and summer precipitation in a Mixedgrass Prairie, WY, USA." Biogeochemistry **73**(1): 257-270.
- Chou, W. W., W. L. Silver, R. D. Jackson, A. W. Thompson and B. Allen-Diaz (2008). "The sensitivity of annual grassland carbon cycling to the quantity and timing of rainfall." Global Change Biology **14**: 1-13.
- Ciais, P., M. Reichstein, N. Viovy, A. Granier, J. Ogee, V. Allard, M. Aubinet, N. Buchmann, C. Bernhofer, A. Carrara, F. Chevallier, N. De Noblet, A. D. Friend, P. Friedlingstein, T. Grunwald, B. Heinesch, P. Keronen, A. Knohl, G. Krinner, D. Loustau, G. Manca, G. Matteucci, F. Miglietta, J. M. Ourcival, D. Papale, K. Pilegaard, S. Rambal, G. Seufert, J. F. Soussana, M. J. Sanz, E. D. Schulze, T. Vesala and R. Valentini (2005). "Europe-wide reduction in primary productivity caused by the heat and drought in 2003." Nature **437**(7058): 529-533.
- Cobos, D. and J. Baker (2003). "In situ measurement of soil heat flux with the gradient method." Vadose Zone Journal **2**: 589-594.
- Costin, A. (1986). Genesis of Australian Alpine Soils. Flora and Fauna of Alpine Australasia. B. Barlow. Melbourne, CSIRO.
- Costin, A., M. Gray, C. Totterdell and D. Wimbush (2000). Kosciuszko Alpine Flora. Melbourne, CSIRO Publishing.
- Costin, A., E. Hallsworth and M. Woof (1952). "Studies in pedogenesis in New South Wales III: the alpine humus soils." Journal of Soil Science **3**(2): 190-218.
- Costin, A. B. (1983). Mountain lands in the Australian region: some basic principles of use and management. Mountain Ecology in the Australian Region. R. Purdie. Canberra, Canberra Times Print.
- Cox, P., R. Betts, C. Jones, S. Spall and I. Totterdell (2000). "Acceleration of global warming due to carbon cycle feedbacks in a coupled climate model." Nature **408**: 184-187.
- Crabb, P. (2003). Managing the Australian Alps: a History of Cooperative Management of the AUstralian Alps National Parks Canberra, Australian Alps Liaison Committee.
- Craine, J., D. Wedin and F. S. Chapin, III (1999). "Predominance of ecophysiological controls on soil CO<sub>2</sub> flux in a Minnesota grassland." Plant and Soil **207**(1): 77-86.
- CSI (2003). HFT3 Instruction Manual. Logan, Utah: 6.
- CSI (2007). CSAT3 Three Dimensional Sonic Anemometer. Logan, Campbell Scientific Instruments.

CSIRO (2010). Climate variability and change in south-eastern Australia: A synthesis of findings from Phase 1 of the South Eastern Australian Climate Initiative (SEACI).

DAAC), O. R. N. L. D. A. A. C. O. (2009). MODIS subsetting land products, Collection 5. 05/06/09. A. o.-l. [<http://daac.ornl.gov/MODIS/modis.html>].

Davidson, E. A. and I. A. Janssens (2006). "Temperature sensitivity of soil carbon decomposition and feedbacks to climate change." Science **440**(7081): 165-173.

Davidson, E. A., K. Savage, L. V. Verchot and R. Navarro (2002). "Minimizing artifacts and biases in chamber-based measurements of soil respiration." Agricultural and Forest Meteorology **113**(1-4): 21-37.

Desai, A. R., A. D. Richardson, A. M. Moffat, J. Kattge, D. Y. Hollinger, A. Barr, E. Falge, A. Noormets, D. Papale, M. Reichstein and V. J. Stauch (2008). "Cross-site evaluation of eddy covariance GPP and RE decomposition techniques." Agricultural and Forest Meteorology **148**(6-7): 821-838.

Djukic, I., F. Zehetner, M. Tatzber and M. Gerzabek (2010). "Soil organic matter stocks and characteristics along an alpine elevation gradient." Journal of Plant Nutrition and Soil Science **173**: 30-38.

Dragoni, D., H. Schmid, C. Grimmer and H. Loescher (2007). "Uncertainty of annual ecosystem productivity estimated using eddy covariance flux measurements." Journal of Geophysical Research-Biogeosciences **112**: D17102.

Edmonds, T., I. D. Lunt, D. A. Roshier and J. Louis (2006). "Annual variation in the distribution of summer snowdrifts in the Kosciuszko alpine area, Australia, and its effect on the composition and structure of alpine vegetation." Austral Ecology **31**(7): 837-848.

Edwards, A. and M. S. Cresser (1992). "Freezing and its effects on chemical and biological properties of soil." Advances in Soil Science **18**: 61-79.

Egli, M. (2004). "Experimental determination of climate-change effects on above-ground and below-ground organic matter in alpine grasslands by translocation of soil cores." Journal of plant nutrition and soil science **167**(4): 457-470.

Engler, R., C. F. Randin, W. Thuiller, S. Dullinger, N. E. Zimmermann, M. B. Araújo, P. B. Pearman, G. Le Lay, C. Piedallu, C. H. Albert, P. Choler, G. Coldea, X. De Lamo, T. Dirnböck, J.-C. Gégout, D. Gómez-García, J.-A. Grytnes, E. Heegaard, F. Høistad, D. Nogués-Bravo, S. Normand, M. Puşcaş, M.-T. Sebastià, A. Stanisci, J.-P. Theurillat, M. R. Trivedi, P. Vittoz and A. Guisan (2011). "21st century climate change threatens mountain flora unequally across Europe." Global Change Biology **17**(7): 2330-2341.



Falge, E., D. Baldocchi, R. Olson, P. Anthoni, M. Aubinet, C. Bernhofer, G. Burba, R. Ceulemans, R. Clement and H. Dolman (2001). "Gap filling strategies for defensible annual sums of net ecosystem exchange." Agricultural and Forest Meteorology **107**(1): 43-69.

Falge, E., D. Baldocchi, J. Tenhunen, M. Aubinet, P. Bakwin, P. Berbigier, C. Bernhofer, G. Burba, R. Clement and K. J. Davis (2002). "Seasonality of ecosystem respiration and gross primary production as derived from FLUXNET measurements." Agricultural and Forest Meteorology **113**(1-4): 53-74.

Fan, J., H. Zhong, W. Harris, G. Yu, S. Wang, Z. Hu and Y. Yue (2008). "Carbon storage in the grasslands of China based on field measurements of above- and below-ground biomass." Climatic Change **86**(3): 375-396.

Fang, C. and J. B. Moncrieff (2001). "The dependence of soil CO<sub>2</sub> efflux on temperature." Soil Biology and Biochemistry **33**(2): 155-165.

Fang, J. Y., Y. H. Yang, W. Ma, A. Mohammad and H. Shen (2010). "Ecosystem carbon stocks and their changes in China's grasslands." Science in China Series C: Life Sciences **53**(7): 757-765.

Feigenwinter, C., C. Bernhofer, U. Eichelmann, B. Heinesch, M. Hertel, D. Janous, O. Kolle, F. Lagergren, A. Lindroth, S. Minerbi, U. Moderow, M. Molder, L. Montagnani, R. Queck, C. Rebmann, P. Vestin, M. Yernaux, M. Zeri, W. Ziegler and M. Aubinet (2008). "Comparison of horizontal and vertical advective CO<sub>2</sub> fluxes at three forest sites." Agricultural and Forest Meteorology **148**(1): 12-24.

Ferrar, P., P. Cochrane and R. Slatyer (1988). "Factors influencing germination and establishment of *Eucalyptus pauciflora* near the alpine treeline." Tree Physiology **4**: 27-43.

Finnigan, J. (2008). "An introduction to flux measurements in difficult conditions." Ecological Applications **18**(6): 1340-1350.

Finnigan, J. J., R. Clement, Y. Malhi, R. Leuning and H. A. Cleugh (2003). "A Re-Evaluation of Long-Term Flux Measurement Techniques Part I: Averaging and Coordinate Rotation." Boundary-Layer Meteorology **107**(1): 1-48.

Fischlin, A., G. Midgley, J. Price, R. Leemans, B. Gopal, C. Turley, M. Rounsevell, O. Dube, J. Tarazona and A. Velichko (2007). Ecosystems, their properties, goods, and services. Climate Change 2007: Impacts, Adaptation and Vulnerability. Contribution of Working Group II to the Fourth Assessment Report of the Intergovernmental Panel on Climate Change. M. Parry, O. Canziani, J. Palutikof, P. van der Linden and C. Hanson. Cambridge, UK, Cambridge University Press.

Flanagan, L. B., L. A. Wever and P. J. Carlson (2002). "Seasonal and interannual variation in carbon dioxide exchange and carbon balance in a northern temperate grassland." Global Change Biology **8**(7): 599-615.

Foken, T. (2008). "The energy balance closure problem: an overview." Ecological Applications **18**(6): 1351-1367.

Foken, T., M. Aubinet and R. Leuning (2012a). The Eddy Covariance Method. Eddy Covariance. M. Aubinet, T. Vesala and D. Papale, Springer Netherlands: 1-19.

Foken, T., M. Gockede, M. Mauder, L. Mahrt, B. Amiro and W. Munger (2004). Post Field Data Quality Control. Handbook of Micrometeorology: A Guide for Surface Flux Measurement and Analysis. X. Lee, B. Massman and B. Law. Dordrecht, Netherlands, Kluwer Academic Publishers.

Foken, T., R. Leuning, S. R. Oncley, M. Mauder and M. Aubinet (2012b). Corrections and Data Quality Control

Eddy Covariance. M. Aubinet, T. Vesala and D. Papale, Springer Netherlands: 85-131.

Foken, T., M. Mauder, C. Liebethal, F. Wimmer, F. Beyrich, J.-P. Leps, S. Raasch, H. DeBruin, W. Meijninger and J. Bange (2010). "Energy balance closure for the LITFASS-2003 experiment." Theoretical and Applied Climatology **101**(1): 149-160.

Foken, T. and B. Wichura (1996). "Tools for quality assessment of surface-based flux measurements." Agricultural and Forest Meteorology **78**: 83-105.

Foken, T., F. Wimmer, M. Mauder, C. Thomas and C. Liebethal (2006). "Some aspects of the energy balance closure problem." Atmos. Chem. Phys. Discuss. **6**(2): 3381-3402.

Foley, J. and M. Ramankutty (2004). A primer on the terrestrial carbon cycle: what we don't know but should. The Global Carbon Cycle: Integrating Humans, Climate and the Natural World. C. Field and M. Raupach. Island Press, Washington, DC.

Fox, A. M., B. Huntley, C. R. Lloyd, M. Williams and R. Baxter (2008). "Net ecosystem exchange over heterogeneous Arctic tundra: Scaling between chamber and eddy covariance measurements." Global Biogeochem. Cycles **22**.

Franssen, H. J. H., R. Stöckli, I. Lehner, E. Rotenberg and S. I. Seneviratne (2010). "Energy balance closure of eddy-covariance data: A multisite analysis for European FLUXNET stations." Agricultural and Forest Meteorology **150**(12): 1553-1567.

Friedlingstein, P., P. Cox, R. Betts, L. Bopp, W. von Bloh, V. Brovkin, P. Cadule, S. Doney, M. Eby, I. Fung, G. Bala, J. John, C. Jones, F. Joos, T. Kato, M. Kawamiya, W. Knorr, K. Lindsay, H. D. Matthews, T. Raddatz, P. Rayner, C. Reick, E. Roeckner, K. G. Schnitzler, R. Schnur, K. Strassmann, A. J. Weaver, C. Yoshikawa and N. Zeng (2006). "Climate-Carbon Cycle Feedback Analysis: Results from the C4MIP Model Intercomparison." Journal of Climate **19**(14): 3337-3353.

Friend, A. D., A. Arneeth, N. Y. Kiang, M. Lomas, J. Og  , C. R  denbeck, S. W. Running, J.-D. Santaren, S. Sitch, N. Viovy, F. Ian Woodward and S. Zaehle (2007). "FLUXNET and modelling the global carbon cycle." Global Change Biology **13**(3): 610-633.

Fu, Y.-L., G.-R. Yu, X.-M. Sun, Y.-N. Li, X.-F. Wen, L.-M. Zhang, Z.-Q. Li, L. Zhao and Y.-B. Hao (2006). "Depression of net ecosystem CO<sub>2</sub> exchange in semi-arid *Leymus chinensis* steppe and alpine shrub." Agricultural and Forest Meteorology

Carbon Exchange Research in China **FLUX 137**(3-4): 234-244.

Fu, Y., Z. Zheng, G. Yu, Z. Hu, X. Sun, P. Shi, Y. Wang and X. Zhao (2009). "Environmental influences on carbon dioxide fluxes over three grassland ecosystems in China." Biogeosciences **6**: 2879-2893.

Fuchs, M. and C. Tanner (1968). "Calibration and field test of soil heat flux plates." Soil Science Society of America Proceedings **32**: 326-328.

Gallagher, R., L. Hughes and M. Leishman (2009). "Phenological trends among Australian alpine species: using herbarium records to identify climate change indicators." Australian Journal of Botany **57**: 1-9.

Galloway, R. (1989). Glacial and periglacial features of the Australian Alps. The Scientific Significance of the Australian Alps: The Proceedings of the First Fenner Conference. R. Good. Canberra, Australian Alps National Parks Liaison Committee.

Garcia-Pausas, J., P. Casals, L. Camarero, C. Hugu  t, M.-T. Sebasti  n, R. Thompson and J. Rom  ny   (2007). "Soil Organic Carbon Storage in Mountain Grasslands of the Pyrenees: Effects of Climate and Topography." Biogeochemistry **82**(3): 279-289.

Gentine, P., D. Entekhabi and B. Heusinkveld (2012). "Systematic errors in ground heat flux estimation from measurements and their correction." Water Resources Research **In Press**.

Gilgen, A. and N. Buchmann (2009). "Response of temperate grasslands at different altitudes to simulated summer drought differed but scaled with annual precipitation." Biogeosciences **6**(11): 2525-2539.

Gill, R. A., R. H. Kelly, W. J. Parton, K. A. Day, R. B. Jackson, J. A. Morgan, J. M. O. Scurlock, L. L. Tieszen, J. V. Castle, D. S. Ojima and X. S. Zhang (2002). "Using simple environmental variables to estimate below-ground productivity in grasslands." Global Ecology and Biogeography **11**(1): 79-86.

Gilmanov, T. G., J. F. Soussana, L. Aires, V. Allard, C. Ammann, M. Balzarolo, Z. Barcza, C. Bernhofer, C. L. Campbell, A. Cernusca, A. Cescatti, J. Clifton-Brown, B. O. M. Dirks, S. Dore, W. Eugster, J. Fuhrer, C. Gimeno, T. Gruenwald, L. Haszpra, A. Hensen, A. Ibrom, A. F. G. Jacobs, M. B. Jones, G. Lanigan, T. Laurila, A. Lohila, G. Manca, B. Marcolla, Z. Nagy, K. Pilegaard, K. Pinter, C. Pio, A. Raschi, N. Rogiers, M. J. Sanz, P. Stefani, M. Sutton, Z. Tuba, R. Valentini, M. L. Williams and G. Wohlfahrt

(2007). "Partitioning European grassland net ecosystem CO<sub>2</sub> exchange into gross primary productivity and ecosystem respiration using light response function analysis." Agriculture, Ecosystems & Environment **121**(1-2): 93-120.

Gilmanov, T. G., S. B. Verma, P. L. Sims, T. P. Meyers, J. A. Bradford, G. G. Burba and A. E. Suyker (2003). "Gross primary production and light response parameters of four Southern Plains ecosystems estimated using long-term CO<sub>2</sub>-flux tower measurements." Global Biogeochem. Cycles **17**(2): 1071.

Giorgi, F., J. W. Hurrell, M. R. Marinucci and M. Beniston (1997). "Elevation Dependency of the Surface Climate Change Signal: A Model Study." Journal of Climate **10**(2): 288-296.

Good, R. B. (1989). The Scientific Significance of the Australian Alps. Canberra, Australian Alps National Parks Liaison Committee / Australian Academy of Science.

Goulden, M., J. W. Munger, S.-M. Fan, B. Daube and S. Wofsy (1996a). "Exchange of carbon dioxide by a deciduous forest: response to interannual climate variability." Science **271**(1576-1578).

Goulden, M. L., B. C. Daube, S.-M. Fan, D. J. Sutton, A. Bazzaz, J. W. Munger and S. C. Wofsy (1997). "Physiological responses of a black spruce forest to weather." J. Geophys. Res. **102**(D24): 28987-28996.

Goulden, M. L., J. W. Munger, S.-M. Fan, B. C. Daube and S. C. Wofsy (1996b). "Measurements of carbon sequestration by long-term eddy covariance: methods and a critical evaluation of accuracy." Global Change Biology **2**(3): 169-182.

Grace, J. (1988). The functional significance of short stature in montane vegetation. Plant Form and Vegetation Structure. M. Werger, P. van der Art, H. During and J. Verhoeven. The Hague, SPB Academic Publishing.

Grant, I., D. Jones, W. Wang, R. Fawcett and D. Barratt (2008). Meteorological and Remotely Sensed Datasets for Hydrological Modelling: A Contribution to the Australian Water Availability Project. Catchment-scale Hydrological Modelling and Data Assimilation International Workshop (CAHMDA). Melbourne.

Green, K. (2009). "Causes of stability in the alpine treeline in the Snowy Mountains of Australia – a natural experiment." Australian Journal of Botany **57**(3): 171-179.

Green, K. (2010). "Alpine taxa exhibit differing responses to climate warming in the Snowy Mountains of Australia." Journal of Mountain Science **7**(2): 167-175.

Green, K. and C. M. Pickering (2009). "The Decline of Snowpatches in the Snowy Mountains of Australia: Importance of Climate Warming, Variable Snow, and Wind." Arctic, Antarctic, and Alpine Research **41**(2): 212-218.

Grieve, I. C. (2000). "Effects of human disturbance and cryoturbation on soil iron and organic matter distributions and on carbon storage at high elevations in the Cairngorm Mountains, Scotland." Geoderma **95**(1-2): 1-14.

Griffin, P. and A. Hoffmann (2011). "Mortality of Australian alpine grasses (*Poa* spp.) after drought: species differences and ecological patterns." Journal of Plant Ecology: doi:10.1093/jpe/rtr1010.

Griffis, T. J., T. A. Black, K. Morgenstern, A. G. Barr, Z. Nasic, G. B. Drewitt, D. Gaumont-Guay and J. H. McCaughey (2003). "Ecophysiological controls on the carbon balances of three southern boreal forests." Agricultural and Forest Meteorology **117**(1-2): 53-71.

Groffman, P., C. Driscoll, T. Fahey, J. Hardy, R. Fitzhugh and G. Tierney (2001). "Colder soils in a warmer world: A snow manipulation study in a northern hardwood forest ecosystem." Biogeochemistry **56**(2): 135-150.

Grogan, P., L. Illeris, A. Michelsen and S. Jonasson (2001). "Respiration of recently fixed carbon dominates mid-winter CO<sub>2</sub> production in sub-arctic heath tundra." Climatic change **50**: 129-142.

Gu, L., E. M. Falge, T. Boden, D. D. Baldocchi, T. A. Black, S. R. Saleska, T. Suni, S. B. Verma, T. Vesala, S. C. Wofsy and L. Xu (2005a). "Objective threshold determination for nighttime eddy flux filtering." Agricultural and Forest Meteorology **128**(3-4): 179-197.

Gu, S., Y. Tang, M. Du, X. Cui, T. Kato, Y. Li and X. Zhao (2005b). "Effects of temperature on CO<sub>2</sub> exchange between the atmosphere and an alpine meadow." Phyton **45**(4): 361-370.

Gu, S., Y. Tang, M. Du, T. Kato, Y. Li, X. Cui and X. Zhao (2003). "Short-term variation of CO<sub>2</sub> flux in relation to environmental controls in an alpine meadow on the Qinghai-Tibetan Plateau - art. no. 4670." Journal of geophysical research **108**(D21): 4670.

Hagedorn, F., M. Martin, C. Rixen, S. Rusch, P. Bebi, A. Zürcher, R. W. Siegwolf, S. Wipf, C. Escobar, J. Roy and S. Hättenschwiler (2010). "Short-term responses of ecosystem carbon fluxes to experimental soil warming at the Swiss alpine treeline." Biogeochemistry **97**(1): 7-19.

Hammerle, A., A. Haslwanter, M. Schmitt, M. Bahn, U. Tappeiner, A. Cernusca and G. Wohlfahrt (2007). "Eddy covariance measurements of carbon dioxide, latent and sensible energy fluxes above a meadow on a mountain slope." Boundary-Layer Meteorology **122**(2): 397-416.

Hardy, J., P. Groffman, R. Fitzhugh, K. Henry, A. Welman, J. Demers, T. Fahey, C. Driscoll, G. Tierney and S. Nolan (2001). "Snow depth manipulation and its influence on soil frost and water dynamics in a northern hardwood forest." Biogeochemistry **56**(2): 151-174.

Harsch, M., P. Hulme, M. McGlone and R. Duncan (2009). "Are treelines advancing? A global meta-analysis of treeline response to global warming." Ecology Letters **12**(10): 1040-1049.

Haverd, V., M. Cuntz, R. Leuning and H. Keith (2007). "Air and biomass heat storage fluxes in a forest canopy: Calculation within a soil vegetation atmosphere transfer model." Agricultural and Forest Meteorology **147**(3-4): 125-139.

Hayhoe, K., C. Wake, B. Anderson, X.-Z. Liang, E. Maurer, J. Zhu, J. Bradbury, A. DeGaetano, A. Stoner and D. Wuebbles (2008). "Regional climate change projections for the Northeast USA." Mitigation and Adaptation Strategies for Global Change **13**(5-6): 425-436.

He, G., K. Li, X. Liu, Y. Gong and Y. Hu (2014). "Fluxes of methane, carbon dioxide and nitrous oxide in an alpine wetland and an alpine grassland of the Tianshan Mountains, China." Journal of Arid Land **6**(6): 717-724.

Heimann, M. and M. Reichstein (2008). "Terrestrial ecosystem carbon dynamics and climate feedbacks." Nature **451**(7176): 289-292.

Hennessy, K., C. Lucas, N. Nicholls, J. Bathols, R. Suppiah and J. Ricketts (2005). *Climate Change Impacts on Fire Weather in South-east Australia*. Melbourne, CSIRO.

Hennessy, K., P. Whetton, K. Walsh, I. Smith, J. Bathols, M. Hutchinson and J. Sharples (2008). "Climate change effects on snow conditions in mainland Australia and adaptation at ski resorts through snowmaking." Climate Research **35**: 255-270.

Henseler, J. (1995). *Back Propagation. Artificial Neural Networks: An Introduction to ANN Theory and Practice*. P. Braspenning, F. Thuijsman and A. Weijters. Berlin, Springer-Verlag.

Heusinkveld, B. G., A. F. G. Jacobs, A. A. M. Holtslag and S. M. Berkowicz (2004). "Surface energy balance closure in an arid region: role of soil heat flux." Agricultural and Forest Meteorology **122**(1-2): 21-37.

Hiller, R., M. Zeeman and W. Eugster (2008). "Eddy-Covariance Flux Measurements in the Complex Terrain of an Alpine Valley in Switzerland." Boundary-Layer Meteorology **127**(3): 449-467.

Hobbie, S. E., J. P. Schimel, S. E. Trumbore and J. R. Randerson (2000). "Controls over carbon storage and turnover in high-latitude soils." Global Change Biology **6**(S1): 196-210.

Hoefnagel, M. H. N., O. K. Atkin and J. T. Wiskich (1998). "Interdependence between chloroplasts and mitochondria in the light and the dark." Biochimica et Biophysica Acta (BBA) - Bioenergetics **1366**(3): 235-255.

Hofstede, R., E. Chilito and P. Sandovals (1995). "Vegetative structure, microclimate and leaf growth of a páramo tussock grass species in undisturbed, burned and grazed conditions." Vegetatio **119**: 53-65.

Hogberg, P., A. Nordgren, N. Buchmann, A. F. S. Taylor, A. Ekblad, M. N. Hogberg, G. Nyberg, M. Ottosson-Lofvenius and D. J. Read (2001). "Large-scale forest girdling shows that current photosynthesis drives soil respiration." Nature **411**(6839): 789-792.

Holdridge, L. (1947). "Determination of world plant formations from simple climatic data." Science **105**: 367-368.

Hollinger, D. Y. and A. D. Richardson (2005). "Uncertainty in eddy covariance measurements and its application to physiological models." Tree Physiology **25**: 873-885.

Hope, D., M. F. Billett and M. S. Cresser (1994). "A review of the export of carbon in river water: Fluxes and processes." Environmental Pollution **84**(3): 301-324.

Hu, Q.-W., Q. Wu, G.-M. Cao, D. Li, R.-J. Long and Y.-S. Wang (2008). "Growing Season Ecosystem Respirations and Associated Component Fluxes in Two Alpine Meadows on the Tibetan Plateau." Journal of Integrative Plant Biology **50**(3): 271-279.

Huber, E., T. L. Bell, R. R. Simpson and M. A. Adams (2011). "Relationships among microclimate, edaphic conditions, vegetation distribution and soil nitrogen dynamics on the Bogong High Plains, Australia." Austral Ecology **36**(2): 142-152.

Hughes, L. (2003). "Climate change and Australia: Trends, projections and impacts." Austral Ecology **28**(4): 423-443.

Hukseflux (2009). HFP01 Heat Flux Plate. Delft, Hukseflux.

Hunt, J., F. Kelliher, T. Mcseveney, D. Ross and D. Whitehead (2004). "Long-term carbon exchange in a sparse, seasonally dry tussock grassland." Global Change Biology **10**: 1785-1800.

Huntingford, C., J. A. Lowe, B. B. Booth, C. D. Jones, G. R. Harris, L. K. Gohar and P. Meir (2009). "Contributions of carbon cycle uncertainty to future climate projection spread." Tellus B **61**(2): 355-360.

Hurry, V., A. Igamberdiev, O. Keerberg, T. Pärnik, O. Atkin, J. Zaragoza-Castells and P. Gardeström (2005). Respiration in photosynthetic cells: gas exchange components, interactions with

photorespiration and the operation of mitochondria in the light. Plant Respiration From Cell to Ecosystem. H. Lambers and M. Ribas-Carbo. Dordrecht, Springer. **18**.

Hussain, M. Z., T. Grünwald, J. D. Tenhunen, Y. L. Li, H. Mirzae, C. Bernhofer, D. Otieno, N. Q. Dinh, M. Schmidt, M. Wartinger and K. Owen (2011). "Summer drought influence on CO<sub>2</sub> and water fluxes of extensively managed grassland in Germany." Agriculture, Ecosystems & Environment **141**(1–2): 67-76.

Jackson, R. B., J. G. Canadell, J. Ehleringer, H. Mooney, O. Sala and E. D. Schulze (1996). "A global analysis of root distributions for terrestrial biomes." Oecologia **108**: 389-411.

Jacobs, A., B. Heusinkveld and A. Holtslag (2008). "Towards Closing the Surface Energy Budget of a Mid-latitude Grassland." Boundary-Layer Meteorology **126**(1): 125-136.

Jaksic, V., G. Kiely, J. Albertson, R. Oren, G. Katul, P. Leahy and K. A. Byrne (2006). "Net ecosystem exchange of grassland in contrasting wet and dry years." Agricultural and Forest Meteorology **139**: 323-334.

Janssens, I. A., S. Dore, D. Epron, H. Lankreijer, N. Buchmann, B. Longdoz, J. Brossaud and L. Montagnani (2003). Climatic influences on seasonal and spatial differences in soil CO<sub>2</sub> efflux. Fluxes of Carbon, Water and Energy of European Forests. R. Valentini. Berlin, Springer.

Janssens, I. A., A. S. Kowalski, B. Longdoz and R. Ceulemans (2000). "Assessing forest soil CO<sub>2</sub> efflux: an in situ comparison of four techniques." Tree Physiology **20**(23-32).

Janssens, I. A., H. Lankreijer, G. Matteucci, A. S. Kowalski, N. Buchmann, D. Epron, K. Pilegaard, W. Kutsch, B. Longdoz, T. Grünwald, L. Montagnani, S. Dore, C. Rebmann, E. J. Moors, A. Grelle, Ü. Rannik, K. Morgenstern, S. Oltchev, R. Clement, J. Guðmundsson, S. Minerbi, P. Berbigier, A. Ibrom, J. Moncrieff, M. Aubinet, C. Bernhofer, N. O. Jensen, T. Vesala, A. Granier, E. D. Schulze, A. Lindroth, A. J. Dolman, P. G. Jarvis, R. Ceulemans and R. Valentini (2001). "Productivity overshadows temperature in determining soil and ecosystem respiration across European forests." Global Change Biology **7**(3): 269-278.

Jarrad, F., C.-H. Wahren, R. Williams and M. Burgman (2008). "Impacts of experimental warming and fire on phenology of subalpine open-heath species." Australian Journal of Botany **56**: 617-629.

Jarrad, F., C. H. Wahren, R. Williams and M. Burgman (2009). "Subalpine plants show short-term positive growth responses to experimental warming and fire." Australian Journal of Botany **57**: 465-473.

Jeffrey, S. J., J. O. Carter, K. B. Moodie and A. R. Beswick (2001). "Using spatial interpolation to construct a comprehensive archive of Australian climate data." Environmental Modelling & Software **16**(4): 309-330.



- Jenkins, M. and M. Adams (2010). "Vegetation type determines heterotrophic respiration in subalpine Australian ecosystems." Global Change Biology **16**: 209-219.
- Jobbágy, E. G. and R. B. Jackson (2000). "The Vertical Distribution of Soil Organic Carbon and Its Relation to Climate and Vegetation." Ecological Applications **10**(2): 423-436.
- Jolly, W. M., R. Nemani and S. W. Running (2005). "A generalized, bioclimatic index to predict foliar phenology in response to climate." Global Change Biology **11**(4): 619-632.
- Jonas, T., C. Rixen, M. Sturm and V. Stoeckli (2008). "How alpine plant growth is linked to snow cover and climate variability." Journal of Geophysical Research-Biogeosciences **113**(G3): 3013-3013.
- Jones, H. (1992). Plants and Microclimate: a Quantitative Approach to Environmental Plant Physiology. Cambridge, Cambridge University Press.
- Jones, M. B. and A. Donnelly (2004). "Carbon sequestration in temperate grassland ecosystems and the influence of management, climate and elevated CO<sub>2</sub>." New Phytologist **164**(3): 423-439.
- Jongen, M., J. S. Pereira, L. M. I. Aires and C. A. Pio (2011). "The effects of drought and timing of precipitation on the inter-annual variation in ecosystem-atmosphere exchange in a Mediterranean grassland." Agricultural and Forest Meteorology **151**(5): 595-606.
- Kabwe, L. K., R. E. Farrell, S. K. Carey, M. J. Hendry and G. W. Wilson (2005). "Characterizing spatial and temporal variations in CO<sub>2</sub> fluxes from ground surface using three complimentary measurement techniques." Journal of Hydrology **311**(1-4): 80-90.
- Kaimal, J. and J. Finnigan (1994). Atmospheric Boundary Layer Flows: Their Structure and Measurement. New York, Oxford University Press.
- Kaimal, J. C., J. C. Wyngaard, Y. Izumi and O. R. Coté (1972). "Spectral characteristics of surface-layer turbulence." Quarterly Journal of the Royal Meteorological Society **98**(417): 563-589.
- Kanda, M., A. Inagaki, M. O. Letzel, S. Raasch and T. Watanabe (2004). "LES Study of the Energy Imbalance Problem with Eddy Covariance Fluxes." Boundary-Layer Meteorology **110**(3): 381-404.
- Kato, T., Y. Tang, S. Gu, X. Cui, M. Hirota, M. Du, Y. Li, X. Zhao and T. Oikawa (2004). "Carbon dioxide exchange between the atmosphere and an alpine meadow ecosystem on the Qinghai-Tibetan Plateau, China." Agricultural and forest meteorology **124**(1-2): 121-134.
- Kato, T., Y. Tang, S. Gu, M. Hirota, M. Du, Y. Li and X. Zhao (2006). "Temperature and biomass influences on interannual changes in CO<sub>2</sub> exchange in an alpine meadow on the Qinghai-Tibetan Plateau." Global Change Biology **12**(7): 1285-1298.

Katul, G., J. Finnigan, D. Poggi, R. Leuning and S. Belcher (2006). "The Influence of Hilly Terrain on Canopy-Atmosphere Carbon Dioxide Exchange." Boundary-Layer Meteorology **118**(1): 189-216.

Keller, F. and C. Körner (2003). "The Role of Photoperiodism in Alpine Plant Development." Arctic, Antarctic, and Alpine Research **35**(3): 361-368.

Kipp and Zonen (2002). CNR1 Instruction Manual. Delft, Netherlands, Kipp & Zonen.

Kirschbaum, M. U. F. (1995). "The temperature dependence of soil organic matter decomposition, and the effect of global warming on soil organic C storage." Soil Biology and Biochemistry **27**(6): 753-760.

Kirschbaum, M. U. F. (2000). "Will changes in soil organic carbon act as a positive or negative feedback on global warming?" Biogeochemistry **48**(1): 21-51.

Knapp, A. K., S. L. Conard and J. M. Blair (1998). "Determinants of Soil CO<sub>2</sub> Flux from a Sub-Humid Grassland: Effect of Fire and Fire History." Ecological Applications **8**(3): 760-770.

Knapp, A. K. and M. D. Smith (2001). "Variation Among Biomes in Temporal Dynamics of Aboveground Primary Production." Science **291**(5503): 481-484.

Koch, O., D. Tscherko, M. Küppers and E. Kandeler (2008). "Interannual Ecosystem CO<sub>2</sub> Dynamics in The Alpine Zone of The Eastern Alps, Austria." Arctic, Antarctic, and Alpine Research **40**(3): 487-496.

Kohsiek, W., C. Liebethal, T. Foken, R. Vogt, S. Oncley, C. Bernhofer and H. Debruin (2007). "The Energy Balance Experiment EBEX-2000. Part III: Behaviour and quality of the radiation measurements." Boundary-Layer Meteorology **123**(1): 55-75.

Körner, C. (1995). Leaf diffusive conductances in the major vegetation types of the globe. Ecophysiology of photosynthesis. E. D. Schulze and M. Caldwell. Berlin, Springer Verlag: 463-490.

Körner, C. (1998). "A re-assessment of high elevation treeline positions and their explanation." Oecologia **115**(4): 445-459.

Körner, C. (2003). Alpine Plant Life: Functional Plant Ecology of High Mountain Ecosystems (2nd ed.). Heidelberg, Springer-Verlag.

Körner, C. (2005). The green cover of mountains in a changing environment. Global Change and Mountain Regions. U. Huber, H. K. M. Bugmann and M. A. Reasoner. Dordrecht, Springer.

Körner, C. (2007). "Climatic Treelines: Conventions, Global Patterns, Causes." Erdkunde **61**(4): 316-324.

Körner, C., M. Diemer, B. Schappi, P. Niklaus and J. Arnone lii (1997). "The responses of alpine grassland to four seasons of CO<sub>2</sub> enrichment: a synthesis." Acta Oecologica **18**(3): 165-175.

Körner, C., J. A. Morgan and R. J. Norby (2007). CO<sub>2</sub> Fertilization: When, Where and How Much? Terrestrial Ecosystems in a Changing World. J. G. Canadell, D. Pataki and L. Pitelka. Berlin, Springer-Verlag.

Körner, C., M. Ohsawa, E. Spehn, E. Berge, H. Bugmann, B. Groombridge, L. Hamilton, T. Hofer, J. Ives, N. Jodha, B. Messerli, J. Pratt, M. Price, M. Reasoner, A. Rodgers, J. Thonell and M. Yoshino (2005). Mountain Systems. Millenium Ecosystem Assessment: Current State and Trends. R. Hassan, R. Scholes and N. Ash. New York, Island Press. **1**.

Kump, L., J. Kasting and R. Crane (2004). The Earth System. New Jersey, Pearson.

Lajtha, K. (2000). Ecosystem Nutrient Balance and Dynamics. Methods in Ecosystem Science. O. Sala, R. B. Jackson, H. Mooney and R. Howarth. New York, Springer Verlag.

Labbers, H., F. Chapin and T. Pons (2008). Plant Physiological Ecology, Springer.

Lamp, C., S. Forbes and J. Cade (2001). Grasses of Temperate Australia: A Field Guide. Melbourne, Bloomings Books.

Larcher, W. (2012). Bioclimatic Temperatures in the High Alps

Plants in Alpine Regions. C. Lütz, Springer Vienna: 21-27.

Larsen, K. S., P. Grogan, S. Jonasson and A. Michelsen (2007). "Respiration and Microbial Dynamics in Two Subarctic Ecosystems during Winter and Spring Thaw: Effects of Increased Snow Depth." Arctic, Antarctic, and Alpine Research **39**(2): 268-276.

Lasslop, G., M. Reichstein, D. Papale, A. D. Richardson, A. Arneeth, A. Barr, P. Stoy and G. Wohlfahrt (2010). "Separation of net ecosystem exchange into assimilation and respiration using a light response curve approach: critical issues and global evaluation." Global Change Biology **16**(1): 187-208.

Lauenroth, W. K. and O. E. Sala (1992). "Long-Term Forage Production of North American Shortgrass Steppe." Ecological Applications **2**(4): 397-403.

Laurance, W. F., B. Dell, S. M. Turton, M. J. Lawes, L. B. Hutley, H. McCallum, P. Dale, M. Bird, G. Hardy, G. Prideaux, B. Gawne, C. R. McMahon, R. Yu, J.-M. Hero, L. Schwarzkopf, A. Krockenberger,

M. Douglas, E. Silvester, M. Mahony, K. Vella, U. Saikia, C.-H. Wahren, Z. Xu, B. Smith and C. Cocklin (2011). "The 10 Australian ecosystems most vulnerable to tipping points." Biological Conservation **144**(5): 1472-1480.

Lavigne, M. B., M. G. Ryan, D. E. Anderson, D. D. Baldocchi, P. M. Crill, D. R. Fitzjarrald, M. L. Goulden, S. T. Gower, J. M. Massheder, J. H. McCaughey, M. Rayment and R. G. Striegl (1997). "Comparing nocturnal eddy covariance measurements to estimates of ecosystem respiration made by scaling chamber measurements at six coniferous boreal sites." Journal of Geophysical Research: Atmospheres **102**(D24): 28977-28985.

Law, B. E., E. Falge, L. Gu, D. D. Baldocchi, P. Bakwin, P. Berbigier, K. Davis, A. J. Dolman, M. Falk and J. D. Fuentes (2002). "Environmental controls over carbon dioxide and water vapor exchange of terrestrial vegetation." Agricultural and Forest Meteorology **113**(1-4): 97-120.

Law, B. E., M. G. Ryan and P. M. Anthoni (1999). "Seasonal and annual respiration of a ponderosa pine ecosystem." Global Change Biology **5**(2): 169-182.

Lee, X., J. Finnigan and K. Paw U (2004a). Coordinate Systems and Flux Bias Error. Handbook of Micrometeorology: A Guide for Surface Flux Measurement and Analysis. X. Lee, B. Massman and B. Law. Dordrecht, Netherlands, Kluwer Academic Publishing.

Lee, X., J. D. Fuentes, R. M. Staebler and H. H. Neumann (1999). "Long-term observation of the atmospheric exchange of CO<sub>2</sub> with a temperate deciduous forest in southern Ontario, Canada." J. Geophys. Res. **104**(D13): 15975-15984.

Lee, X., B. Massman and B. Law (2004b). "Handbook of Micrometeorology: A Guide for Surface Flux Measurement and Analysis."

Lee, X., W. J. Massman and B. Law (2004c). Handbook of Micrometeorology: A Guide for Surface Flux Measurement and Analysis. Dordrecht, Kluwer Academic publishers.

Leifeld, J., M. Zimmermann, J. Fuhrer and F. Conen (2009). "Storage and turnover of carbon in grassland soils along an elevation gradient in the Swiss Alps." Global Change Biology **15**(3): 668-679.

Lennon, J. (1999). The International Significance of the Cultural Values of the Australian Alps, Australian Alps Liaison Committee.

Lenschow, D. (1995). Micrometeorological techniques for measuring biosphere-atmosphere trace gas exchange. Biogenic Trace Gases: Measuring Emissions from Soil and Water. P. Matson and R. Harris. New York, Blackwell.

Leuning, R., H. A. Cleugh, S. J. Ziegler and D. Hughes (2005). "Carbon and water fluxes over a temperate Eucalyptus forest and a tropical wet/dry savanna in Australia: measurements and

comparison with MODIS remote sensing estimates." Agricultural and Forest Meteorology **129**(3-4): 151-173.

Leuning, R., E. Van Gorsel, B. Massman and P. Isaac (2012). "Reflections on the surface energy imbalance problem." Agricultural and Forest Meteorology **152**: 65-74.

Leuning, R., S. J. Zegelin, K. Jones, H. Keith and D. Hughes (2008). "Measurement of horizontal and vertical advection of CO<sub>2</sub> within a forest canopy." Agricultural and Forest Meteorology **148**(11): 1777-1797.

Li, H.-j., J.-x. Yan, X.-f. Yue and M.-b. Wang (2008). "Significance of soil temperature and moisture for soil respiration in a Chinese mountain area." Agricultural and Forest Meteorology **148**(3): 490-503.

Liang, N., T. Nakadai, T. Hirano, L. Qu, T. Koike, Y. Fujinuma and G. Inoue (2004). "In situ comparison of four approaches to estimating soil CO<sub>2</sub> efflux in a northern larch (*Larix kaempferi* Sarg.) forest." Agricultural and Forest Meteorology **123**(1-2): 97-117.

Lin, X., Z. Zhang, S. Wang, Y. Hu, G. Xu, C. Luo, X. Chang, J. Duan, Q. Lin, B. Xu, Y. Wang, X. Zhao and Z. Xie (2011). "Response of ecosystem respiration to warming and grazing during the growing seasons in the alpine meadow on the Tibetan plateau." Agricultural and Forest Meteorology **151**(7): 792-802.

Linderholm, H. W. (2006). "Growing season changes in the last century." Agricultural and Forest Meteorology **137**(1-2): 1-14.

Lindroth, A., M. Mauder and F. Lagergren (2010). "Heat storage in forest biomass improves energy balance closure." Biogeosciences **7**(1): 301-313.

Liu, H., J. Randerson, J. Lindfors, W. Massman and T. Foken (2006). "Consequences of Incomplete Surface Energy Balance Closure for CO<sub>2</sub> Fluxes from Open-Path CO<sub>2</sub>/H<sub>2</sub>O Infrared Gas Analysers." Boundary-Layer Meteorology **120**(1): 65-85.

Livingston, G. and G. Hutchinson (1995). Enclosure based measurements of trace gas exchanges: applications and sources of error. Biogenic Trace Gases: Measuring Emissions from Soil and Water. P. Matson and R. Harriss. Oxford, Blackwell Science.

Lloyd, J. and J. Taylor (1994). "On the temperature dependence of soil respiration." Functional Ecology **8**: 315-323.

Loescher, H. W., B. E. Law, L. Mahrt, D. Y. Hollinger, J. Campbell and S. C. Wofsy (2006). "Uncertainties in, and interpretation of, carbon flux estimates using the eddy covariance technique." J. Geophys. Res. **111**.

Ma, W., J. Y. Fang, Y. H. Yang and A. Mohammad (2010a). "Biomass carbon stocks and their changes in northern China's grasslands during 1982-2006." Science in China Series C: Life Sciences **53**(7): 841-850.

Ma, W., P. Shi, W. Li, Y. He, X. Zhang, Z. Shen and S. Chai (2010b). "Changes in individual plant traits and biomass allocation in alpine meadow with elevation variation on the Qinghai-Tibetan Plateau." SCIENCE CHINA Life Sciences **53**(9): 1142-1151.

Mahrt, L. (2010). "Computing turbulent fluxes near the surface: Needed improvements." Agricultural and Forest Meteorology **150**(4): 501-509.

Malhi, Y., K. McNaughton and C. von Randow (2004). Low Frequency Atmospheric Transport and Surface Flux Measurements. Handbook of Micrometeorology. X. Lee, B. Massman and B. Law. Dordrecht, Kluwer Academic Publishers.

Marcolla, B. and A. Cescatti (2005). "Experimental analysis of flux footprint for varying stability conditions in an alpine meadow." Agricultural and Forest Meteorology **135**: 291-301.

Marcolla, B., A. Cescatti, G. Manca, R. Zorer, M. Cavagna, A. Fiora, D. Gianelle, M. Sottocornola and R. Zampedri (2011). "Climatic controls and ecosystem responses drive the inter-annual variability of the net ecosystem exchange of an alpine meadow." Agricultural and Forest Meteorology **151**(9): 1233-1243.

Mason, R. and J. Williams (2008a). Soils of the Australian Alps, Australian Alps National Parks.

Mason, R. and J. Williams (2008b). Vegetation in the Australian Alps, Australian Alps National Parks.

Massman, B. (1992). "Correcting errors associated with soil heat flux measurements and estimating soil thermal properties from soil temperature and heat flux plate data." Agricultural and Forest Meteorology **59**: 249-266.

Massman, B. and R. Clement (2004). Uncertainty in eddy covariance flux estimates resulting from spectral attenuation. Handbook of Micrometeorology. X. Lee, B. Massman and B. Law. Dordrecht, Kluwer Academic Publishers: 67-99.

Massman, W. J. (2004). Concerning the measurement of atmospheric trace gas fluxes with open- and closed-path eddy covariance systems: the WPL terms and spectral attenuation. Handbook of Micrometeorology. X. Lee, B. Massman and B. Law. Dordrecht, Kluwer Academic Publishing.

Matthews, H. D., M. Eby, T. Ewen, P. Friedlingstein and B. Hawkins (2007). "What determines the magnitude of the carbon cycle feedback?" Global Biogeochemical Cycles **21**: GB2012, doi:10.1029/2006GB002733.

Mauder, M., T. Foken, R. Clement, J. A. Elbers, W. Eugster, T. Grünwald, B. Heusinkveld and O. Kolle (2008). "Quality control of CarboEurope flux data Part 2: Inter-comparison of eddy-covariance software." Biogeosciences **5**(2): 451-462.

Mauder, M., C. Liebethal, M. Göckede, J.-P. Leps, F. Beyrich and T. Foken (2006). "Processing and quality control of flux data during LITFASS-2003." Boundary-Layer Meteorology **121**(1): 67-88.

McGuire, A. D., L. G. Anderson, T. R. Christensen, S. Dallimore, L. Guo, D. J. Hayes, M. Heimann, T. D. Lorenson, R. W. Macdonald and N. Roulet (2009). "Sensitivity of the carbon cycle in the Arctic to climate change." Ecological Monographs **79**(4): 523-555.

Meehl, G. A., T. F. Stocker, W. D. Collins, P. Friedlingstein, A. T. Gaye, J. M. Gregory, A. Kitoh, R. Knutti, J. M. Murphy, A. Noda, S. C. B. Raper, I. G. Watterson, A. J. Weaver and Z.-C. Zhao (2007). Global Climate Projections. Climate Change 2007: The Physical Science Basis. Contribution of Working Group I to the Fourth Assessment Report of the Intergovernmental Panel on Climate Change. S. Solomon, D. Qin, M. Manning et al. Cambridge UK, Cambridge University Press.

Meyers, T. P. (2001). "A comparison of summertime water and CO<sub>2</sub> fluxes over rangeland for well watered and drought conditions." Agricultural and Forest Meteorology **106**(3): 205-214.

Meyers, T. P. and S. E. Hollinger (2004). "An assessment of storage terms in the surface energy balance of maize and soybean." Agricultural and Forest Meteorology **125**(1-2): 105-115.

Migliavacca, M., M. Galvagno, E. Cremonese, M. Rossini, M. Meroni, O. Sonnentag, S. Cogliati, G. Manca, F. Diotri, L. Busetto, A. Cescatti, R. Colombo, F. Fava, U. Morra di Cella, E. Pari, C. Siniscalco and A. D. Richardson (2011). "Using digital repeat photography and eddy covariance data to model grassland phenology and photosynthetic CO<sub>2</sub> uptake." Agricultural and Forest Meteorology **151**(10): 1325-1337.

Moffat, A. M., C. Beckstein, G. Churkina, M. Mund and M. Heimann (2010). "Characterization of ecosystem responses to climatic controls using artificial neural networks." Global Change Biology **16**(10): 2737-2749.

Moffat, A. M., D. Papale, M. Reichstein, D. Y. Hollinger, A. D. Richardson, A. G. Barr, C. Beckstein, B. H. Braswell, G. Churkina, A. R. Desai, E. Falge, J. H. Gove, M. Heimann, D. Hui, A. J. Jarvis, J. Kattge, A. Noormets and V. J. Stauch (2007). "Comprehensive comparison of gap-filling techniques for eddy covariance net carbon fluxes." Agricultural and Forest Meteorology **147**(3-4): 209-232.

Mokany, K., R. J. Raison and A. S. Prokushkin (2006). "Critical analysis of root : shoot ratios in terrestrial biomes." Global Change Biology **12**(1): 84-96.

Moncrieff, J., R. Clement, J. Finnigan and T. Meyers (2004). Averaging, detrending and filtering of eddy covariance time series. Handbook of Micrometeorology. X. Lee, B. Massman and B. Law. Dordrecht, Kluwer Academic Publishers.

Moncrieff, J., P. Jarvis and R. Valentini (2000). Canopy fluxes. Methods in Ecosystem Science. O. Sala, R. B. Jackson, H. Mooney and R. Howarth. New York, Springer.

Moncrieff, J. B., Y. Malhi and R. Leuning (1996). "The propagation of errors in long-term measurements of land-atmosphere fluxes of carbon and water." Global Change Biology **2**(3): 231-240.

Monson, R. K., D. L. Lipson, S. P. Burns, A. A. Turnipseed, A. C. Delany, M. W. Williams and S. K. Schmidt (2006). "Winter forest soil respiration controlled by climate and microbial community composition." Nature **439**(7077): 711-714.

Monteith, J. and M. Unsworth (2008). Principles of Environmental Physics. London, Academic Press.

Moore, C. J. (1986). "Frequency response corrections for eddy correlation systems." Boundary-Layer Meteorology **37**(1): 17-35.

Moore, R. and J. Williams (1976). "A study of a subalpine woodland-grassland boundary." Australian Journal of Ecology **1**: 145-153.

Morgenstern, K., T. Andrew Black, E. R. Humphreys, T. J. Griffis, G. B. Drewitt, T. Cai, Z. Nesic, D. L. Spittlehouse and N. J. Livingston (2004). "Sensitivity and uncertainty of the carbon balance of a Pacific Northwest Douglas-fir forest during an El Niño/La Niña cycle." Agricultural and Forest Meteorology **123**(3-4): 201-219.

Mules, T., P. Faulks, N. Stoeckl and M. Cegielski (2005). The Economic Value of Tourism in the Australian Alps. C. Cooper, C. De Lacy and L. Jago. Canberra, Cooperative Research Centre for Sustainable Tourism.

Murphy, B. F. and B. Timbal (2008). "A review of recent climate variability and climate change in southeastern Australia." International Journal of Climatology **28**(7): 859-879.

Myklebust, M. C., L. E. Hipps and R. J. Ryel (2008). "Comparison of eddy covariance, chamber, and gradient methods of measuring soil CO<sub>2</sub> efflux in an annual semi-arid grass, *Bromus tectorum*." Agricultural and Forest Meteorology **148**(11): 1894-1907.

Myneni, R., C. Keeling, C. Tucker, G. Asrar and R. Nemani (1997). "Increased plant growth in the northern latitudes from 1981 to 1991." Nature **386**: 698-702.

Nagy, Z., K. Pinter, S. Czobel, J. Balogh, L. Horvath, S. Foti, Z. Barcza, T. Weidinger, Z. Csintalan, N. Q. Dinh, B. Grosz and Z. Tuba (2007). "The carbon budget of semi-arid grassland in a wet and a dry year in Hungary." Agriculture, Ecosystems & Environment **121**(1-2): 21-29.



- Nemani, R. R., C. D. Keeling, H. Hashimoto, W. M. Jolly, S. C. Piper, C. J. Tucker, R. B. Myneni and S. W. Running (2003). "Climate-Driven Increases in Global Terrestrial Net Primary Production from 1982 to 1999." Science **300**(5625): 1560-1563.
- Ni, J. (2002). "Carbon storage in grasslands of China." Journal of Arid Environments **50**(2): 205-218.
- Ni, J. (2004). "Forage Yield-Based Carbon Storage in Grasslands of China." Climatic Change **67**(2): 237-246.
- Nicholls, N. (2004). "The Changing Nature of Australian Droughts." Climatic Change **63**(3): 323-336.
- Nicholls, N. (2005). "Climate variability, climate change and the Australian snow season." Australian Meteorological Magazine **54**: 177-185.
- Nobel, P. (1983). Biophysical Plant Physiology and Ecology. San Francisco, W.H Freeman and Company.
- Nobrega, S. and P. Grogan (2007). "Deeper snow enhances winter respiration from both plant-associated and bulk soil carbon pools in birch hummock tundra." Ecosystems **10**(419:431).
- Novick, K. A., P. C. Stoy, G. G. Katul, D. S. Ellsworth, M. B. S. Siqueira, J. Juang and R. Oren (2004). "Carbon dioxide and water vapor exchange in a warm temperate grassland." Oecologia **138**(2): 259-274.
- NRC (2010). Advancing the Science of Climate Change, The National Academies Press.
- Ohtsuka, T., M. Hirota, X. Zhang, A. Shimono, Y. Senga, M. Du, S. Yonemura, S. Kawashima and Y. Tang (2008). "Soil organic carbon pools in alpine to nival zones along an altitudinal gradient (4400-5300 m) on the Tibetan Plateau." Polar Science **2**(4): 277-285.
- Oke, T. (1987). Boundary Layer Climates. Cambridge, Routledge.
- Olson, J., J. Watts and L. Allison (1983). Carbon in live vegetation of major world ecosystems. Environmental Sciences Division Publication number 1997, Oak Ridge National Laboratory.
- Ooba, M., T. Hirano, J.-I. Mogami, R. Hirata and Y. Fujinuma (2006). "Comparisons of gap-filling methods for carbon flux dataset: A combination of a genetic algorithm and an artificial neural network." Ecological Modelling **198**(3-4): 473-486.
- Orchard, V. A. and F. J. Cook (1983). "Relationship between soil respiration and soil moisture." Soil Biology and Biochemistry **15**(4): 447-453.

Osonubi, O. and W. Davies (1980). "The influence of plant water stress on stomatal control of gas exchange at different levels of atmospheric humidity." Oecologia **46**: 1-6.

Papale, D. (2012). Data Gap Filling. Eddy Covariance: A Practical Guide to Measurement and Data Analysis. M. Aubinet, T. Vesala and D. Papale, Springer Netherlands: 159-172.

Papale, D., M. Reichstein, M. Aubinet, E. Canfora, C. Bernhofer, W. Kutsch, B. Longdoz, S. Rambal, R. Valentini, T. Vesala and D. Yakir (2006). "Towards a standardized processing of net ecosystem exchange measured with eddy covariance technique: algorithms and uncertainty estimation." Biogeosciences **3**: 571-583.

Peichl, M., O. Carton and G. Kiely (2012). "Management and climate effects on carbon dioxide and energy exchanges in a maritime grassland." Agriculture, Ecosystems & Environment **158**(0): 132-146.

Pepin, N. C. and J. D. Lundquist (2008). "Temperature trends at high elevations: Patterns across the globe." Geophys. Res. Lett. **35**.

Pereira, J. S., J. Mateus, L. Aires, G. Pita, C. Pio, V. Andrade, J. Banza, T. David, A. Rodrigues and J. David (2007). "Effects of drought - altered seasonality and low rainfall - in net ecosystem carbon exchange of three contrasting Mediterranean ecosystems." Biogeosciences Discussions **4**: 1703-1736.

Pickering, C. (2004). Potential effects of global warming on the biota of the Australian Alps : a report for the Australian Greenhouse Office / by Catherine Pickering, Roger Good, Ken Green. Canberra, A.C.T. :, Australian Greenhouse Office.

Pickering, C., W. Hill and K. Green (2008). "Vascular plant diversity and climate change in the alpine zone of the Snowy Mountains, Australia." Biodiversity and Conservation **17**(1627-1644).

Pinelli, P. and F. Loreto (2003). "12CO<sub>2</sub> emission from different metabolic pathways measured in illuminated and darkened C3 and C4 leaves at low, atmospheric and elevated CO<sub>2</sub> concentration." Journal of Experimental Botany **54**(388): 1761-1769.

Pittock, B. (2009). Climate Change: The Science, Impacts and Solutions. Melbourne, CSIRO Publishing.

Post, W. M., W. R. Emanuel, P. J. Zinke and A. G. Stangenberger (1982). "Soil carbon pools and world life zones." Nature **298**(5870): 156-159.

Poulenard, J. and P. Podwojewski (2006). Alpine Soils. Encyclopedia of Soil Science: Second Edition. R. Lal. London, Taylor & Francis: 75 - 79.

- Prichard, S., D. Peterson and R. Hammer (2000). "Carbon distribution in subalpine forests and meadows of the Olympic Mountains, Washington." Soil Science Society of America Journal **64**(5): 1834-1845.
- Pumpanen, J., P. Kolari, H. Ilvesniemi, K. Minkkinen, T. Vesala, S. Niinistö, A. Lohila, T. Larmola, M. Morero, M. Pihlatie, I. Janssens, J. C. Yuste, J. M. Grünzweig, S. Reth, J.-A. Subke, K. Savage, W. Kutsch, G. Østreg, W. Ziegler, P. Anthoni, A. Lindroth and P. Hari (2004). "Comparison of different chamber techniques for measuring soil CO<sub>2</sub> efflux." Agricultural and Forest Meteorology **123**(3-4): 159-176.
- Ram, J., S. P. Singh and J. S. Singh (1988). "Community Level Phenology of Grassland above Treeline in Central Himalaya, India." Arctic and Alpine Research **20**(3): 325-332.
- Rammig, A., T. Jonas and N. Zimmermann (2010). "Changes in alpine plant growth under future climate conditions." Biogeosciences **7**(6): 2013-2024.
- Rao, M. and J. Srinivas (2003). Neural Networks: Algorithms and Applications. UK, Alpha Science International Ltd.
- Raupach, M., P. Briggs, V. Haverd, E. King, M. Paget and C. Trudinger (2008). Australian Water Availability Project. CSIRO Marine and Atmospheric Research Component: Final Report for Phase 3. Canberra, CSIRO.
- Raupach, M. R. (1995). "Vegetation-atmosphere interaction and surface conductance at leaf, canopy and regional scales." Agricultural and Forest Meteorology **73**(3-4): 151-179.
- Raupach, M. R. and J. G. Canadell (2010). "Carbon and the Anthropocene." Current Opinion in Environmental Sustainability **2**(4): 210-218.
- Rebmann, C., O. Kolle, B. Heinesch, R. Queck, A. Ibrom and M. Aubinet (2012). Data Acquisition and Flux Calculations. Eddy Covariance. M. Aubinet, T. Vesala and D. Papale, Springer Netherlands: 59-83.
- Reichstein, M., P. Ciais, D. Papale, R. Valentini, S. Running, N. Viovy, W. Cramer, A. Granier, J. OgÉE, V. Allard, M. Aubinet, C. Bernhofer, N. Buchmann, A. Carrara, T. GrÜNwald, M. Heimann, B. Heinesch, A. Knohl, W. Kutsch, D. Loustau, G. Manca, G. Matteucci, F. Miglietta, J. M. Ourcival, K. Pilegaard, J. Pumpanen, S. Rambal, S. Schaphoff, G. Seufert, J. F. Soussana, M. J. Sanz, T. Vesala and M. Zhao (2007). "Reduction of ecosystem productivity and respiration during the European summer 2003 climate anomaly: a joint flux tower, remote sensing and modelling analysis." Global Change Biology **13**(3): 634-651.
- Reichstein, M., E. Falge, D. Baldocchi, D. Papale, M. Aubinet, P. Berbigier, C. Bernhofer, N. Buchmann, T. Gilmanov, A. Granier, T. Grünwald, K. Havránková, H. Ilvesniemi, D. Janous, A. Knohl, T. Laurila, A. Lohila, D. Loustau, G. Matteucci, T. Meyers, F. Miglietta, J.-M. Ourcival, J. Pumpanen, S.

Rambal, E. Rotenberg, M. Sanz, J. Tenhunen, G. Seufert, F. Vaccari, T. Vesala, D. Yakir and R. Valentini (2005). "On the separation of net ecosystem exchange into assimilation and ecosystem respiration: review and improved algorithm." Global Change Biology **11**(9): 1424-1439.

Reichstein, M., A. Rey, A. Freibauer, J. Tenhunen, R. Valentini, J. Banza, P. Casals, Y. Cheng, J. M. Grünzweig, J. Irvine, R. Joffre, B. E. Law, D. Loustau, F. Miglietta, W. Oechel, J.-M. Ourcival, J. S. Pereira, A. Peressotti, F. Ponti, Y. Qi, S. Rambal, M. Rayment, J. Romanya, F. Rossi, V. Tedeschi, G. Tirone, M. Xu and D. Yakir (2003). "Modeling temporal and large-scale spatial variability of soil respiration from soil water availability, temperature and vegetation productivity indices." Global Biogeochemical Cycles **17**(4): 1104.

Richardson, A. D., B. H. Braswell, D. Y. Hollinger, P. Burman, E. A. Davidson, R. S. Evans, L. B. Flanagan, J. W. Munger, K. Savage, S. P. Urbanski and S. C. Wofsy (2006a). "Comparing simple respiration models for eddy flux and dynamic chamber data." Agricultural and Forest Meteorology **141**(2-4): 219-234.

Richardson, A. D. and D. Y. Hollinger (2005). "Statistical modeling of ecosystem respiration using eddy covariance data: Maximum likelihood parameter estimation, and Monte Carlo simulation of model and parameter uncertainty, applied to three simple models." Agricultural and Forest Meteorology **131**(3-4): 191-208.

Richardson, A. D. and D. Y. Hollinger (2007). "A method to estimate the additional uncertainty in gap-filled NEE resulting from long gaps in the CO<sub>2</sub> flux record." Agricultural and Forest Meteorology **147**(3-4): 199-208.

Richardson, A. D., D. Y. Hollinger, J. Aber, S. Ollinger and B. Braswell (2007). "Environmental variation is responsible for short- but not long-term variation in forest-atmosphere carbon exchange." Global Change Biology **13**: 788-803.

Richardson, A. D., D. Y. Hollinger, G. Burba, K. Davis, L. B. Flanagan, G. Katul, J. W. Munger, D. Ricciuto, P. C. Stoy, A. Suyker, S. Verma and S. C. Wofsy (2006b). "A multi-site analysis of random error in tower-based measurements of carbon and energy fluxes." Agricultural and Forest Meteorology **136**: 1-18.

Rodeghiero, M. and A. Cescatti (2005). "Main determinants of forest soil respiration along an elevation/temperature gradient in the Italian Alps." Global Change Biology **11**(7): 1024-1041.

Rödenbeck, C., S. Houweling, M. Gloor and M. Heimann (2003). "CO<sub>2</sub> flux history 1982–2001 inferred from atmospheric data using a global inversion of atmospheric transport." Atmospheric Chemistry and Physics **3**: 1919-1964.

Rogiers, N., F. Conen, M. Furger, R. Stöckli and W. Eugster (2008). "Impact of past and present land-management on the C-balance of a grassland in the Swiss Alps." Global Change Biology **14**(11): 2613-2625.

Rosenzweig, C., D. Karoly, M. Vicarelli, P. Neofotis, Q. Wu, G. Casassa, A. Menzel, T. L. Root, N. Estrella, B. Seguin, P. Tryjanowski, C. Liu, S. Rawlins and A. Imeson (2008). "Attributing physical and biological impacts to anthropogenic climate change." Nature **453**(7193): 353-357.

Ruimy, A., P. Jarvis and D. D. Baldocchi (1995). "CO<sub>2</sub> fluxes over plant canopies and solar radiation: a review. ." Advances in Ecological Research **26**: 1-68.

Runyuan, W. and Z. Qiang (2011). "An assessment of storage terms in the surface energy balance of a subalpine meadow in northwest China." Advances in Atmospheric Sciences **28**(3): 691-698.

Saito, M., T. Kato and Y. Tang (2009). "Temperature controls ecosystem CO<sub>2</sub> exchange of an alpine meadow on the northeastern Tibetan Plateau." Global Change Biology **15**(1): 221-228.

Sala, O. (2001). Temperate Grasslands. Global Biodiversity in a Changing Environment: Scenarios for the 21st Century. F. S. Chapin, O. Sala and E. Huber-Sannwald. New York, Springer-Verlag.

Sala, O., R. B. Jackson, H. Mooney and R. Howarth (2000). Methods in Ecosystem Science. New York, Springer-Verlag.

Sauer, T. (2005). Soil Heat Flux. Micrometeorology in Agricultural Systems. J. Hatfield and J. Baker. Madison, Wisconsin, American Society of Agronomy

Crop Science Society of America

Soil Science Society of America. **Agronomy Monograph 47**.

Sauer, T., T. Ochsner and R. Horton (2007). "Soil heat flux plates: heat flow distortion and thermal contact resistance." Agronomy Journal **99**: 304-310.

Scherrer, P. and C. M. Pickering (2005). "Recovery of Alpine Vegetation from Grazing and Drought: Data from Long-term Photoquadrats in Kosciuszko National Park, Australia." Arctic, Antarctic, and Alpine Research **37**(4): 574-584.

Schimel, D. (1995). "Terrestrial ecosystems and the carbon cycle." Global Change Biology **1**: 77-91.

Schimel, D. S., B. H. Braswell, E. A. Holland, R. McKeown, D. S. Ojima, T. H. Painter, W. J. Parton and A. R. Townsend (1994). "Climatic, edaphic, and biotic controls over storage and turnover of carbon in soils." Global Biogeochem. Cycles **8**(3): 279-293.

Schimel, D. S., T. Kittel, S. Running, R. Monson, A. Turnipseed and D. Anderson (2002). "Carbon sequestration studies in western US mountains." EOS: Transactions of the American Geophysical Union **83**(40): 445-449.

Schlesinger, W. (1977). "Carbon balance in terrestrial detritus." Annual Review of Ecological Systems **8**: 51-81.

Schlesinger, W. (1997). Biogeochemistry: An Analysis of Global Change. San Diego, Academic Press.

Schmid, H. P. (1997). "Experimental design for flux measurements: matching scales of observations and fluxes." Agricultural and Forest Meteorology **87**(2-3): 179-200.

Schmitt, M., M. Bahn, G. Wohlfahrt, U. Tappeiner and A. Cernusca (2010). "Land use affects the net CO<sub>2</sub> exchange and its components in mountain grasslands." Biogeosciences **7**(8): 2297-2309.

Schrier-Uijl, A. P., P. S. Kroon, A. Hensen, P. A. Leffelaar, F. Berendse and E. M. Veenendaal (2010). "Comparison of chamber and eddy covariance-based CO<sub>2</sub> and CH<sub>4</sub> emission estimates in a heterogeneous grass ecosystem on peat." Agricultural and Forest Meteorology **150**(6): 825-831.

Schuur, E. A. G., J. Bockheim, J. G. Canadell, E. S. Euskirchen, C. Field, S. Goryachkin, S. Hagemann, P. Kuhry, P. Lafleur, H. Lee, G. Mazhitova, F. Nelson, A. Rinke, V. Romanovsky, N. Shiklomanov, C. Tarnocai, S. Venevsky, J. Vogel and S. Zimov (2008). "Vulnerability of permafrost carbon to climate change: implications for the global carbon cycle." Bioscience **58**(8): 701-714.

Schwalm, C. R., C. Williams, K. Schaefer, A. Arneth, D. Bonals, N. Buchmann, J. Chen, B. Law, A. Lindroth, S. Luyssaert, M. Reichstein and A. D. Richardson (2010). "Assimilation exceeds respiration sensitivity to drought: a Fluxnet synthesis." Global Change Biology **16**: 657-670.

Sevruk, B. and L. Zahlavova (1994). "Classification system of precipitation gauge site exposure: evaluation and application." International Journal of Climatology **14**: 681-689.

Slatyer, R. (1978). "Altitudinal variation in the photosynthetic characteristics of snow gum, *Eucalyptus pauciflora*." Australian Journal of Botany **26**: 111-121.

Slatyer, R. (1989). Alpine and valley bottom treelines. The Scientific Significance of the Australian Alps: The Proceedings of the First Fenner Conference. R. B. Good. Canberra, Australian Alps National Parks Liaison Committee.

Slatyer, R., P. Cochrane and R. Galloway (1985). "Duration and extent of snow cover in the Snowy Mountains and a comparison with Switzerland." Search **15**(11-12): 327-331.

Sommerfeld, R. A., A. R. Mosier and R. C. Musselman (1993). "CO<sub>2</sub>, CH<sub>4</sub> and N<sub>2</sub>O flux through a Wyoming snowpack and implications for global budgets." Nature **361**(6408): 140-142.

Spain, A., R. Isbell and M. Probert (1983). Soil Organic Matter. Soils: An Australian Viewpoint. D. o. Soils. London, Melbourne / Academic Press.

Starr, G. and S. F. Oberbauer (2003). "Photosynthesis of arctic evergreens under snow: implications for tundra ecosystem carbon balance." Ecology **84**(6): 1415-1420.

Stern, H., G. de Hoedt and J. Ernst (2000). "Objective classification of Australian climates." Australian Meteorological Magazine **49**: 87-96.

Stull, R. (1997). An Introduction to Boundary Layer Meteorology. Dordrecht, Kluwer Academic Publishers.

Sturman, A. and N. Tapper (2005). The Weather and Climate of Australia and New Zealand. Melbourne, Oxford University Press.

Suh, S., E. Lee and J. Lee (2009). "Temperature and moisture sensitivities of CO<sub>2</sub> efflux from lowland and alpine meadow soils." Journal of Plant Ecology **2**(4): 225-231.

Sun, X.-M., Z.-L. Zhu, X.-F. Wen, G.-F. Yuan and G.-R. Yu (2006). "The impact of averaging period on eddy fluxes observed at ChinaFLUX sites." Agricultural and Forest Meteorology **137**(3-4): 188-193.

Suppiah, R., K. Hennessy, P. Whetton, K. McInnes, I. Macadam, J. Bathols, J. Ricketts and C. Page (2007). "Australian climate change projections derived from simulations performed for the IPCC 4th Assessment Report." Australian Meteorological Magazine **56**: 131-152.

Suyker, A. E. and S. B. Verma (2001). "Year-round observations of the net ecosystem exchange of carbon dioxide in a native tallgrass prairie." Global Change Biology **7**(3): 279-289.

Suyker, A. E., S. B. Verma and G. G. Burba (2003). "Interannual variability in net CO<sub>2</sub> exchange of a native tallgrass prairie." Global Change Biology **9**(2): 255-265.

Tappeiner, U., E. Tasser, G. Leitinger, A. Cernusca and G. Tappeiner (2008). "Effects of Historical and Likely Future Scenarios of Land Use on Above- and Belowground Vegetation Carbon Stocks of an Alpine Valley." Ecosystems **11**(8): 1383-1400.

Tarnocai, C., J. G. Canadell, E. A. G. Schuur, P. Kuhry, G. Mazhitova and S. Zimov (2009). "Soil organic carbon pools in the northern circumpolar permafrost region." Global Biogeochem. Cycles **23**.

Tate, K., N. Scott, D. Ross, A. Parshotam and J. Claydon (2000). "Plant effects on soil carbon storage and turnover in a montane beech (*Nothofagus*) forest and adjacent tussock grassland in New Zealand." Australian Journal of Soil Research **38**: 685-697.

Tenhunen, J. D., O. L. Lange and D. Jahner (1982). "The Control by Atmospheric Factors and Water Stress of Midday Stomatal Closure in *Arbutus unedo* Growing in a Natural Macchia." Oecologia **55**(2): 165-169.

Theurillat, J.-P., F. Felber, P. Geissler, J.-M. Gobat, M. Fierz, A. Fischlin, F. Kupfer, A. Schlusser, C. Velluti, G.-F. Zhao and J. Williams (1998). Sensitivity of plant and soil ecosystems of the Alps to climate change. Views From the Alps: Regional Perspectives on Climate Change. P. Cebon, U. Dahinden, H. Davies, D. Imboden and C. Jaeger. Boston, USA, Massachusetts Institute of Technology.

Thompson, L. G., T. Yao, E. Mosley-Thompson, M. E. Davis, K. A. Henderson and P. N. Lin (2000). "A High-Resolution Millennial Record of the South Asian Monsoon from Himalayan Ice Cores." Science **289**(5486): 1916-1919.

Thuiller, W., S. Lavorel, M. B. Araújo, M. T. Sykes and I. C. Prentice (2005). "Climate change threats to plant diversity in Europe." Proceedings of the National Academy of Sciences of the United States of America **102**(23): 8245-8250.

Tilman, D., P. Reich, H. Phillips, M. Menton, A. Patel, E. Vos, D. Peterson and J. Knops (2000). "Fire suppression and ecosystem carbon storage." Ecology **81**(10): 2680-2685.

Torn, M. S., C. W. Swanston, C. Castanha and S. E. Trumbore (2009). Storage and Turnover of Organic Matter in Soil. Biophysico-Chemical Processes Involving Natural Nonliving Organic Matter in Environmental Systems. N. Senesi, B. Xing and P.-M. Huang, John Wiley & Sons, Inc.: 219-272.

Trenberth, K. E., P. D. Jones, P. Ambenje, R. Bojariu, D. Easterling, A. Klein Tank, D. Parker, F. Rahimzadeh, J. A. Renwick, M. Rusticucci, B. Soden and P. Zhai (2007). Observations: Surface and Atmospheric Climate Change Contribution of Working Group I to the Fourth Assessment Report of the Intergovernmental Panel on Climate Change. S. Solomon, D. Qin, M. Manning et al. Cambridge, Cambridge University Press.

Trumbore, S. E. and C. I. Czimczik (2008). "An uncertain future for soil carbon." Science **321**: 1455-1456.

Turetsky, M. R., B. Benscoter, S. Page, G. Rein, G. R. van der Werf and A. Watts (2015). "Global vulnerability of peatlands to fire and carbon loss." Nature Geosci **8**(1): 11-14.

Twine, T. E., W. P. Kustas, J. M. Norman, D. R. Cook, P. R. Houser, T. P. Meyers, J. H. Prueger, P. J. Starks and M. L. Wesely (2000). "Correcting eddy-covariance flux underestimates over a grassland." Agricultural and Forest Meteorology **103**(3): 279-300.

van der Molen, M. K., A. J. Dolman, P. Ciais, T. Eglin, N. Gobron, B. E. Law, P. Meir, W. Peters, O. L. Phillips, M. Reichstein, T. Chen, S. C. Dekker, M. Doubková, M. A. Friedl, M. Jung, B. J. J. M. van den Hurk, R. A. M. de Jeu, B. Kruijt, T. Ohta, K. T. Rebel, S. Plummer, S. I. Seneviratne, S. Sitch, A. J. Teuling, G. R. van der Werf and G. Wang (2011). "Drought and ecosystem carbon cycling." Agricultural and Forest Meteorology **151**(7): 765-773.



Van Gorsel, E., J. Berni, P. Briggs, A. Cabello-Leblic, L. Chasmer, H. A. H. Cleugh, J. S. Hantson, V. Haverd, D. Hughes, C. Hopkinson, H. Keith, N. Kljun, R. Leuning, M. Yebra and S. J. Zegelin (2013). "Primary and secondary effects of climate variability on net ecosystem carbon exchange in an evergreen Eucalyptus forest." Agricultural and Forest Meteorology **182-183**: 248-256.

van Gorsel, E., N. Delapierre, R. Leuning, A. Black, J. W. Munger, S. Wofsy, M. Aubinet, C. Feigenwinter, J. Beringer, D. Bonal, B. Chen, J. Chen, R. Clement, K. J. Davis, A. R. Desai, D. Dragoni, S. Etzold, T. Grünwald, L. Gu, B. Heinesch, L. R. Hutya, W. W. P. Jans, W. Kutsch, B. E. Law, M. Y. Leclerc, I. Mammarella, L. Montagnani, A. Noormets, C. Rebmann and S. Wharton (2009). "Estimating nocturnal ecosystem respiration from the vertical turbulent flux and change in storage of CO<sub>2</sub>." Agricultural and Forest Meteorology **149**(11): 1919-1930.

Van Wijk, M. T. and M. Williams (2003). "Interannual variability of plant phenology in tussock tundra: modelling interactions of plant productivity, plant phenology, snowmelt and soil thaw." Global Change Biology **9**(5): 743-758.

von Lütow, M. and I. Kögel-Knabner (2009). "Temperature sensitivity of soil organic matter decomposition—what do we know?" Biology and Fertility of Soils **46**(1): 1-15.

Wahren, C.-H. A., W. Papst and R. J. Williams (1994). "Long-term vegetation change in relation to cattle grazing in subalpine grassland and heathland on the Bogong High Plains: an analysis of vegetation records from 1945 to 1994." Australian Journal of Botany **42**: 607-639.

Walker, B., W. Steffen and J. Langridge (1999a). Interactive and integrated effects of global change on terrestrial ecosystems. The Terrestrial Biosphere and Global Change. B. Walker, W. Steffen, J. G. Canadell and J. Ingram. Cambridge, UK, Cambridge University Press.

Walker, M., D. Walker, J. Welker, A. Arft, T. Bardsley, P. Brooks, J. T. Fahnestock, M. Jones, M. Losleben, A. Parsons, T. Seastedt and P. Turner (1999b). "Long-term experimental manipulation of winter snow regime and summer temperature in arctic and alpine tundra." Hydrological Processes **13**: 2315-2330.

Walther, G.-R., S. Beißner and R. Pott (2005). Climate change and high mountain vegetation shifts. Mountain Ecosystems: Studies in Treeline Ecology. G. Broll and B. Keplin. Berlin, Springer-Verlag.

Wang, S., H. Tian, J. Liu and S. Pan (2003). "Pattern and change of soil organic carbon storage in China: 1960s–1980s." Tellus B **55**(2): 416-427.

Warren, C. R. and M. T. Taranto (2011). "Ecosystem Respiration in a Seasonally Snow-Covered Subalpine Grassland." Arctic, Antarctic, and Alpine Research **43**(1): 137-146.

Webb, E., G. Pearman and R. Leuning (1980). "Correction of flux measurements for density effects due to heat and water vapour transfer." Quarterly Journal of the Royal Meteorological Society **106**(447): 85-100.

Welker, J., Clare (2004). "Alpine grassland CO<sub>2</sub> exchange and nitrogen cycling: Grazing history effects, medicine bow range, Wyoming, USA." Arctic, antarctic, and alpine research **36**(1): 11-20.

White, M. A., P. E. Thornton and S. W. Running (1997). "A continental phenology model for monitoring vegetation responses to interannual climatic variability." Global Biogeochemical Cycles **11**(2): 217-234.

Whiteman, C. (2000). Mountain Meteorology: Fundamentals and Applications. New York, Oxford University Press.

Whiteman, C. and S. Zhong (2008). "Downslope flows on a low angle slope and their interactions with valley inversions. Part I: observations." Journal of Applied Meteorology and Climatology **47**(7): 2023-2038.

Wieser, G., A. Hammerle and G. Wohlfahrt (2008). "The Water Balance of Grassland Ecosystems in the Austrian Alps." Arctic, Antarctic, and Alpine Research **40**(2): 439-445.

Wilczak, J., S. Oncley and S. Stage (2001). "Sonic Anemometer Tilt Correction Algorithms." Boundary-Layer Meteorology **99**(1): 127-150.

Williams, R. (1987). "Patterns of air temperature and accumulation of snow in subalpine heathlands and grasslands on the Bogong High Plains, Victoria." Australian Journal of Ecology **12**: 153-163.

Williams, R. and D. H. Ashton (1987). "Effects of disturbance and grazing by cattle on the dynamics of heathland and grassland communities on the Bogong high Plains, Victoria." Australian Journal of Botany **35**: 413-431.

Williams, R., I. Mansergh, C.-H. Wahren, N. Rosengren and W. Papst (2003). Alpine Landscapes. Ecology: An Australian Perspective. P. Attiwill and B. Wilson. Melbourne, Oxford University Press.

Williams, R. and C.-H. Wahren (2005). Potential Impacts of Global Change on Vegetation in Australian Alpine Landscapes: Climate Change, Landuse, Vegetation Dynamics and Biodiversity Conservation. Global Change and Mountain Regions. U. M. Huber, H. K. M. Bugmann and M. A. Reasoner, Springer Netherlands. **23**: 401-408.

Williams, R., C.-H. Wahren, A. Tolsma, G. Sanecki, W. Papst, B. Myers, K. McDougall, D. Heinze and K. Green (2008a). "Large fires in Australian alpine landscapes: their part in the historical fire regime and their impacts on alpine biodiversity." International Journal of Wildland Fire **17**: 793-808.

Williams, R. J. (1990). "Growth of subalpine shrubs and snow grass following a rare occurrence of frost and drought in south-eastern Australia." Arctic and Alpine Research **22**: 412-422.

Williams, R. J., R. Bradstock, D. Barrett, J. Beringer, M. Boer, G. Cary, G. Cook, A. Gill, L. Hutley, H. Keith, S. Maier, C. Meyer, O. Price, S. Roxburgh and J. Russell-Smith (2012). Fire regimes and carbon in Australian vegetation. Flammable Australia: Fire Regimes, Biodiversity and Ecosystems in a Changing World. R. Bradstock, A. Gill and R. J. Williams. Collingwood, CSIRO Publishing.

Williams, R. J. and A. B. Costin (1994). Alpine and subalpine vegetation. Australian Vegetation (2nd ed.). R. H. Groves. Melbourne, Cambridge University Press: 467-500.

Williams, R. J., C. Wahren, A. D. Tolsma, G. M. Sanecki, W. A. Papst, B. A. Myers, K. L. McDougall, D. A. Heinze and K. Green (2008b). "Large fires in Australian alpine landscapes: their part in the historical fire regime and their impacts on alpine biodiversity." International Journal of Wildland Fire **17**(6): 793-808.

Wilson, K., A. Goldstein, E. Falge, M. Aubinet, D. Baldocchi, P. Berbigier, C. Bernhofer, R. Ceulemans, H. Dolman, C. Field, A. Grelle, A. Ibrom, B. E. Law, A. Kowalski, T. Meyers, J. Moncrieff, R. Monson, W. Oechel, J. Tenhunen, R. Valentini and S. Verma (2002). "Energy balance closure at FLUXNET sites." Agricultural and Forest Meteorology **113**(1-4): 223-243.

Wohlfahrt, G., M. Anderson-Dunn, M. Bahn, M. Balzarolo, F. Berninger, C. Campbell, A. Carrara, A. Cescatti, T. Christensen, S. Dore, W. Eugster, T. Friborg, M. Furger, D. Gianelle, C. Gimeno, K. Hargreaves, P. Hari, A. Haslwanter, T. Johansson, B. Marcolla, C. Milford, Z. Nagy, E. Nemitz, N. Rogiers, M. Sanz, R. Siegwolf, S. Susiluoto, M. Sutton, Z. Tuba, F. Ugolini, R. Valentini, R. Zorer and A. Cernusca (2008). "Biotic, abiotic, and management controls on the net ecosystem CO<sub>2</sub> exchange of European mountain grassland ecosystems." Ecosystems **11**(8): 1338-1351.

Wohlfahrt, G., C. Anfang, M. Bahn, A. Haslwanter, C. Newesely, M. Schmitt, M. Drösler, J. Pfadenhauer and A. Cernusca (2005a). "Quantifying nighttime ecosystem respiration of a meadow using eddy covariance, chambers and modelling." Agricultural and Forest Meteorology **128**(3-4): 141-162.

Wohlfahrt, G., M. Bahn, A. Haslwanter, C. Newesely and A. Cernusca (2005b). "Estimation of daytime ecosystem respiration to determine gross primary production of a mountain meadow." Agricultural and Forest Meteorology **130**(1-2): 13-25.

Wohlfahrt, G., K. Klumpp and J.-F. Soussana (2012). Eddy Covariance Measurements over Grasslands. Eddy Covariance. M. Aubinet, T. Vesala and D. Papale, Springer Netherlands: 333-344.

Wookey, P., P. Aerts, R. Bardgett, F. Baptists, K. Brathen, J. Cornelissen, L. Gough, I. Hartley, D. Hopkins, S. Lavorel and G. Shaver (2009). "Ecosystem feedbacks and cascade processes: understanding their role in the responses of Arctic and alpine ecosystems to environmental change." Global Change Biology **15**: 1153-1172.

Wu, H., Z. Guo and C. Peng (2003). "Distribution and storage of soil organic carbon in China." Global Biogeochemical Cycles **17**(2): doi: 10.1029/2001GB001844.

Xie, Z., J. Zhu, G. Liu, G. Cadisch, T. Hasegawa, C. Chen, H. Sun, H. Tang and Q. Zeng (2007). "Soil organic carbon stocks in China and changes from 1980s to 2000s." Global Change Biology **13**(9): 1989-2007.

Xu, L. and D. D. Baldocchi (2004). "Seasonal variation in carbon dioxide exchange over a Mediterranean annual grassland in California." Agricultural and Forest Meteorology **123**(1–2): 79-96.

Yahdjian, L. and O. E. Sala (2006). "Vegetation structure constrains primary production response to water availability in the Patagonian steppe." Ecology **87**(4): 952-962.

Yang, Y., J. Fang, D. Guo, C. Ji and W. Ma (2010a). "Vertical patterns of soil carbon, nitrogen and carbon:nitrogen stoichiometry in Tibetan grasslands." Biogeosciences Discussion **7**: 1-24.

Yang, Y., J. Fang, W. Ma, P. Smith, A. Mohammad, S. Wang and W. E. I. Wang (2010b). "Soil carbon stock and its changes in northern China's grasslands from 1980s to 2000s." Global Change Biology **16**(11): 3036-3047.

Yang, Y., J. Fang, P. Smith, Y. Tang, A. Chen, C. Ji, H. Hu, S. Rao, K. U. N. Tan and J.-S. He (2009). "Changes in topsoil carbon stock in the Tibetan grasslands between the 1980s and 2004." Global Change Biology **15**(11): 2723-2729.

Yang, Y., J. Fang, Y. Tang, C. Ji, C. Zheng, J. He and B. Zhu (2008). "Storage, patterns and controls of soil organic carbon in the Tibetan grasslands." Global Change Biology **14**: 1592-1599.

Yi, C., D. Ricciuto, R. Li, J. Wolbeck, X. Xu, M. Nilsson, L. Aires, J. Albertson, C. Ammann, M. Arain, A. de Araujo, M. Aubinet, M. Aurela, Z. Barcza, A. Barr, P. Berbigier, J. Beringer, C. Bernhofer, A. Black, P. Bolstad, F. Bosveld, M. Broadmeadow, N. Buchmann, S. Burns, P. Cellier, J. Chen, J. Chen, P. Ciais, R. Clement, B. Cook, P. Curtis, D. Dail, E. Dellwik, N. Delpierre, A. Desai, S. Dore, D. Dragoni, B. Drake, E. Dufrêne, A. Dunn, J. Elbers, W. Eugster, M. Falk, C. Feigenwinter, L. Flanagan, T. Foken, J. Frank, J. Fuhrer, D. Gianelle, A. Goldstein, M. Goulden, A. Granier, T. Grünwald, L. Gu, H. Guo, A. Hammerle, S. Han, S. Hanan, L. Haszpra, B. Heinesch, C. Helfter, D. Hendriks, L. Hutley, A. Ibrom, C. Jacobs, T. Johansson, M. Jongen, G. Katul, G. Kiely, K. Klumpp, A. Knohl, T. Kolb, W. Kutsch, P. Lafleur, T. Laurila, R. Leuning, A. Lindroth, H. Liu, B. Loubet, G. Manca, M. Marek, H. Margolis, T. Martin, W. Massman, R. Matamala, G. Matteucci, H. McCaughey, L. Merbold, T. Meyers, M. Migliavacca, F. Miglietta, L. Misson, M. Mölder, J. Moncrieff, R. Monson, L. Montagnani, M. Montes-Helu, E. Moors, C. Moureaux, M. Mukelabai, J. Munger, M. Myklebust, Z. Nagy, A. Noormets, W. Oechel, R. Oren, S. Pallardy, K. Paw U, J. Pereira, K. Pilegaard, K. Pintér, C. Pio, G. Pita, T. Powell, S. Rambal, J. Randerson, C. von Randow, C. Rebmann, J. Rinne, F. Rossi, N. Roulet, R. Ryel, J. Sagerfors, N. Saigusa, M. Sanz, G.-S. Mugnozza, H. Schmid, G. Seufert, M. Siqueira, J.-F. Soussana, G. Starr, M. Sutton, J. Tenhunen, Z. Tuba, J.-P. Tuovinen, R. Valentini, C. Vogel, J. Wang, S. Wang, W. Wang, L. Welp, X. Wen, S. Wharton, M. Wilkinson, C. Williams, G. Wohlfahrt, S. Yamamoto, G. Yu, R. Zampedri, B. Zhao and X. Zhao (2010). "Climate control of terrestrial carbon exchange across biomes and continents." Environmental Research Letters **5**(3): 034007.

Yi, C., G. Rustic, X. Xiyan, J. Wang, A. Dookie, S. Wei, G. Hendrey, D. Ricciuto, T. Meyers, Z. Nagy and K. Pinter (2012). "Climate extremes and grassland potential productivity." Environmental Research Letters **7**(3): 035703.

Zeeman, M., R. Hiller, A. Gilgen, P. Michna, P. Pluss, N. Buchmann and W. Eugster (2010). "Management and climate impacts on net CO<sub>2</sub> fluxes and carbon budgets of three grasslands along an elevational gradient in Switzerland." Agricultural and Forest Meteorology **150**: 519-530.

Zhang, P., M. Hirota, H. Shen, A. Yamamoto, S. Mariko and Y. Tang (2009). "Characterization of CO<sub>2</sub> flux in three Kobresia meadows differing in dominant species." Journal of Plant Ecology **2**(4): 187-196.

Zhao, L., Y. Li, X. Zhao, S. Xu, Y. Tang, G. Yu, S. Gu, M. Du and Q. Wang (2005). "Comparative study of the net exchange of CO<sub>2</sub> in 3 types of vegetation ecosystems on the Qinghai-Tibetan Plateau." Chinese Science Bulletin **50**(16): 1767-1774.

Zheng, D., E. Hunt and S. Running (1993). "A daily soil temperature model based on air temperature and precipitation for continental applications." Climate Research **2**: 183-191.

Zhengquan, L., Y. Guirui, W. Xuefa, Z. Leiming, R. Chuanyou and F. Yuling (2005). "Energy balance closure at Chinaflux sites." Science in China Series D: Earth Sciences **48**: 51-62.

Zimov, S., G. Zimova, S. Davidov, A. Davidova, Y. Voropaev, Z. Voropaeva, S. Prosiannikov, O. Prosiannikova, I. Semiletova and I. Semiletov (1993). "Winter biotic activity and production of CO<sub>2</sub> in Siberian soils - a factor in the greenhouse effect." Journal of Geophysical Research - Atmospheres **98**: 5017-5023.

Ziska, L. H. and J. A. Bunce (2007). Plant Responses to Rising Atmospheric Carbon Dioxide. Plant Growth and Climate Change. J. Morison and M. Morecroft. Oxford, Blackwell Publishing Ltd: 17-47.